NUCLEAR ASTROPHYSICS

NUCLEAR ASTROPHYSICS

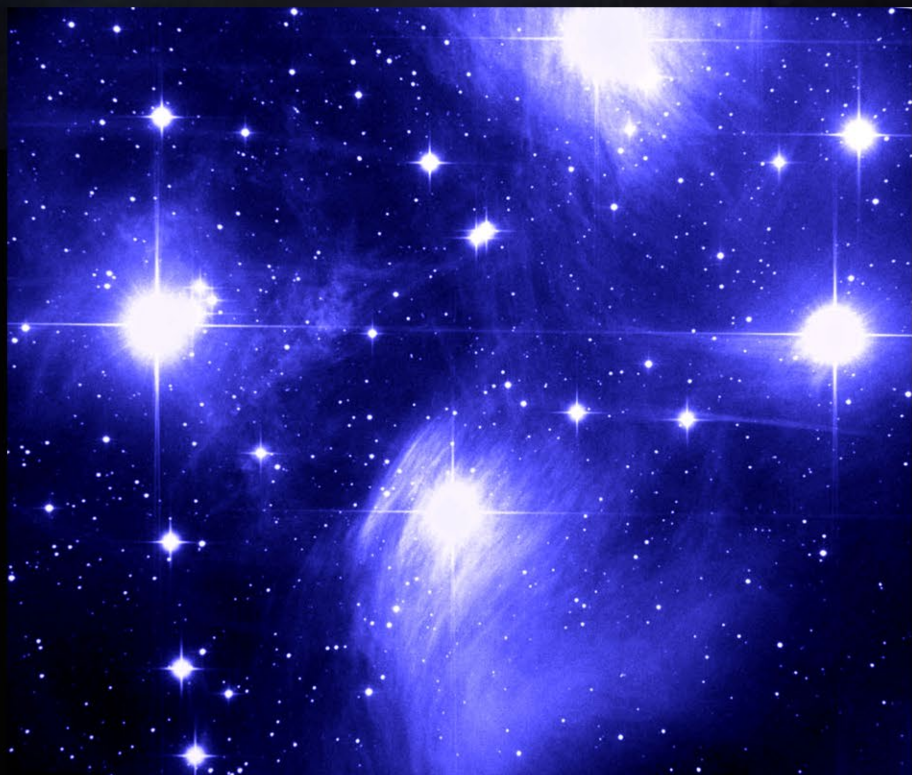

NUCLEAR ASTROPHYSICS

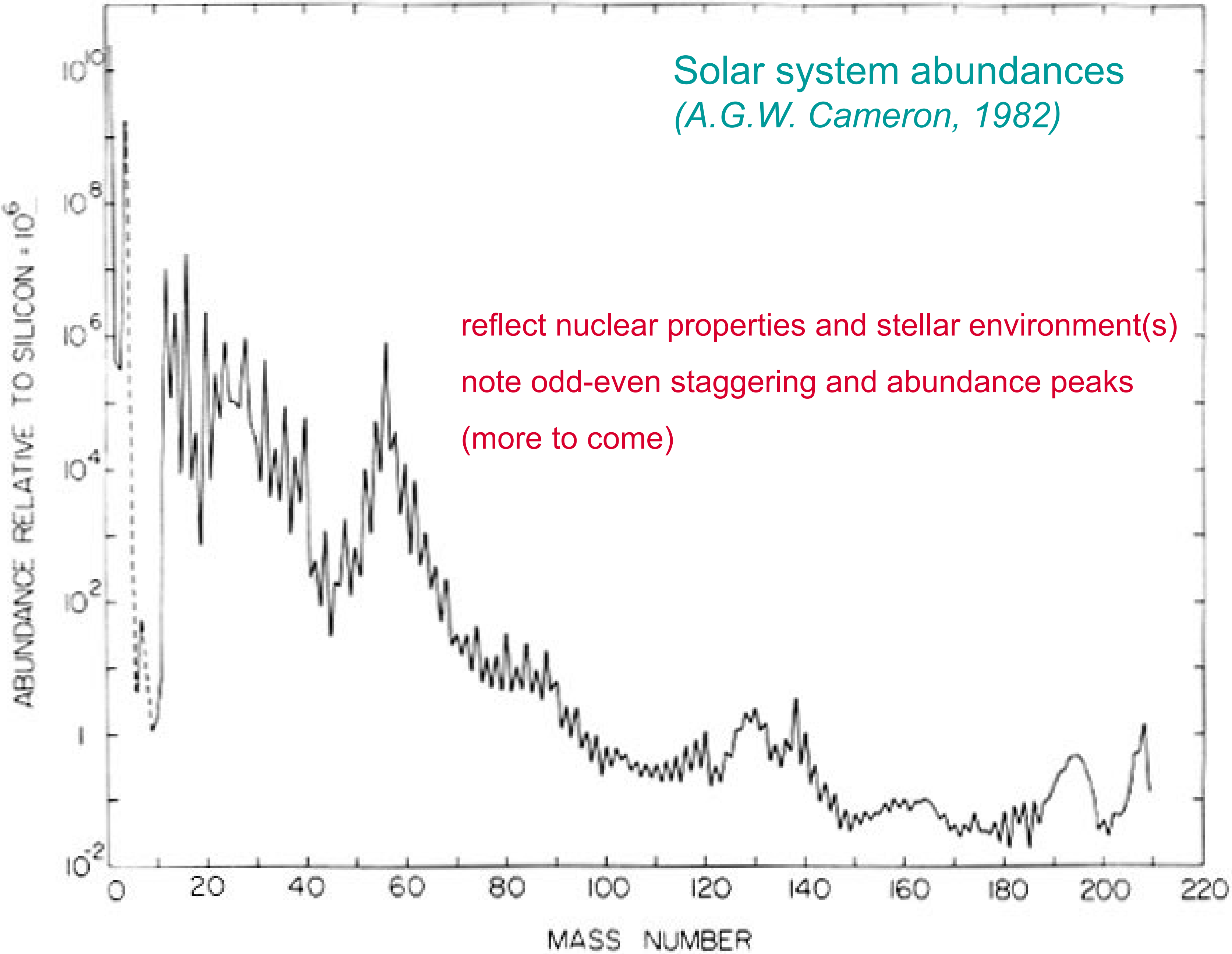
Solar system abundances
(A.G.W. Cameron, 1982)
reflect nuclear properties and stellar environment(s)
note odd-even staggering and abundance peaks
(more to come)
ABUNDANCE RELATIVE TO SILICON = 10^6
MASS NUMBER
0
20
40
60
80
100
120
140
160
180
200
220

A blanket statement:

1. Almost all problems in astrophysics ultimately reduce to stars, stellar structure or stellar evolution

2. Stars evolve because of changes in their chemical composition

Basic approach:

1. Identify the astrophysical problem

2. Find an observable whose attributes depend upon a nuclear process

3. Develop a strategy for acquiring the needed nuclear information

Stars

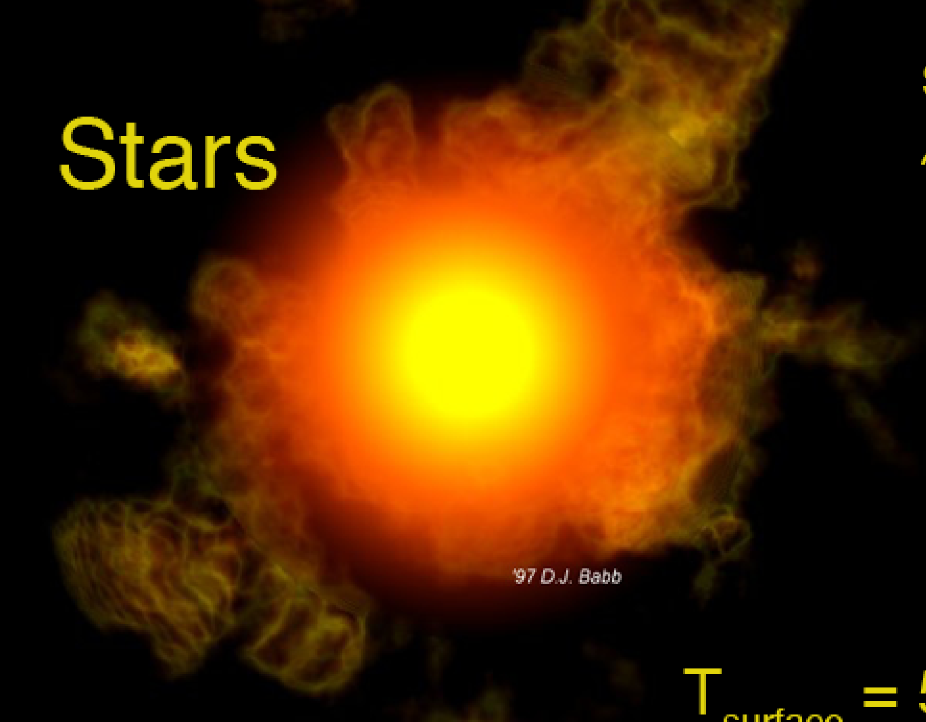

sun:

~ 75% H, 25% He by mass

$M_\odot = 1.99 \times 10^{30}$ kg

$(0.1 M_\odot \leq M_{star} \leq 100\ M_\odot)$

$R_\odot = 6.96 \times 10^{8}$ m

$T_{surface} = 5800$ K $\quad (2500\ K \leq T_{star} \leq 25000\ K)$

$L_\odot = 3.83 \times 10^{26}$ W $\quad (10^{-4}\ L_\odot \leq L_{star} \leq 10^{5}\ L_\odot)$

[sun has ~ 9×10^{56} protons so L/proton (L_p) ~ 2.8×10^{-18} MeV/s
E/proton (E_p) = $L_p \tau$, where $\tau = 5 \times 10^{9}$ y

E_p ~ 450 keV $\longrightarrow$ nuclear force]

Equations of stellar structure

1. structure

$$\frac{\partial r}{\partial m} = \frac{1}{4\pi r^2 \rho(m)}$$

(defines mass as an independent variable)

$$\frac{\partial P}{\partial m} = -\frac{Gm}{4\pi r^4} - \frac{1}{4\pi r^2}\frac{\partial^2 r}{\partial t^2}$$

sets hydrodynamic timescale
= 0 for *"hydrostatic equilibrium"*

see: Prialnik: "An Introduction to the Theory of Stellar Structure and Evolution", Kippenhahn & Weigert: "Stellar Structure and Evolution", etc.

2. thermodynamics and chemistry

$$\frac{\partial T}{\partial m} = -\frac{GmT}{4\pi r^4 P}\nabla, \text{ where } \nabla = \left(\frac{\partial \ln T}{\partial \ln P}\right) = \nabla_{ad}, \nabla_{rad} \ldots$$

adiabatic gradient

radiation

reactions and decays

$$\frac{\partial L}{\partial m} = \epsilon_n - \epsilon_\nu - C_p \frac{\partial T}{\partial t} - \frac{1}{\rho}\left(\frac{\partial \ln \rho}{\partial \ln T}\right)_p$$

neutrino losses

gravitational part (sets thermal timescale)
dU + P dV

mass fraction of species i

$$\frac{\partial X_i}{\partial t} = \frac{\rho}{m_i}\left(\sum_j r_{ji} - \sum_k r_{ik}\right)$$

sets nuclear timescale

production rates

destruction rates

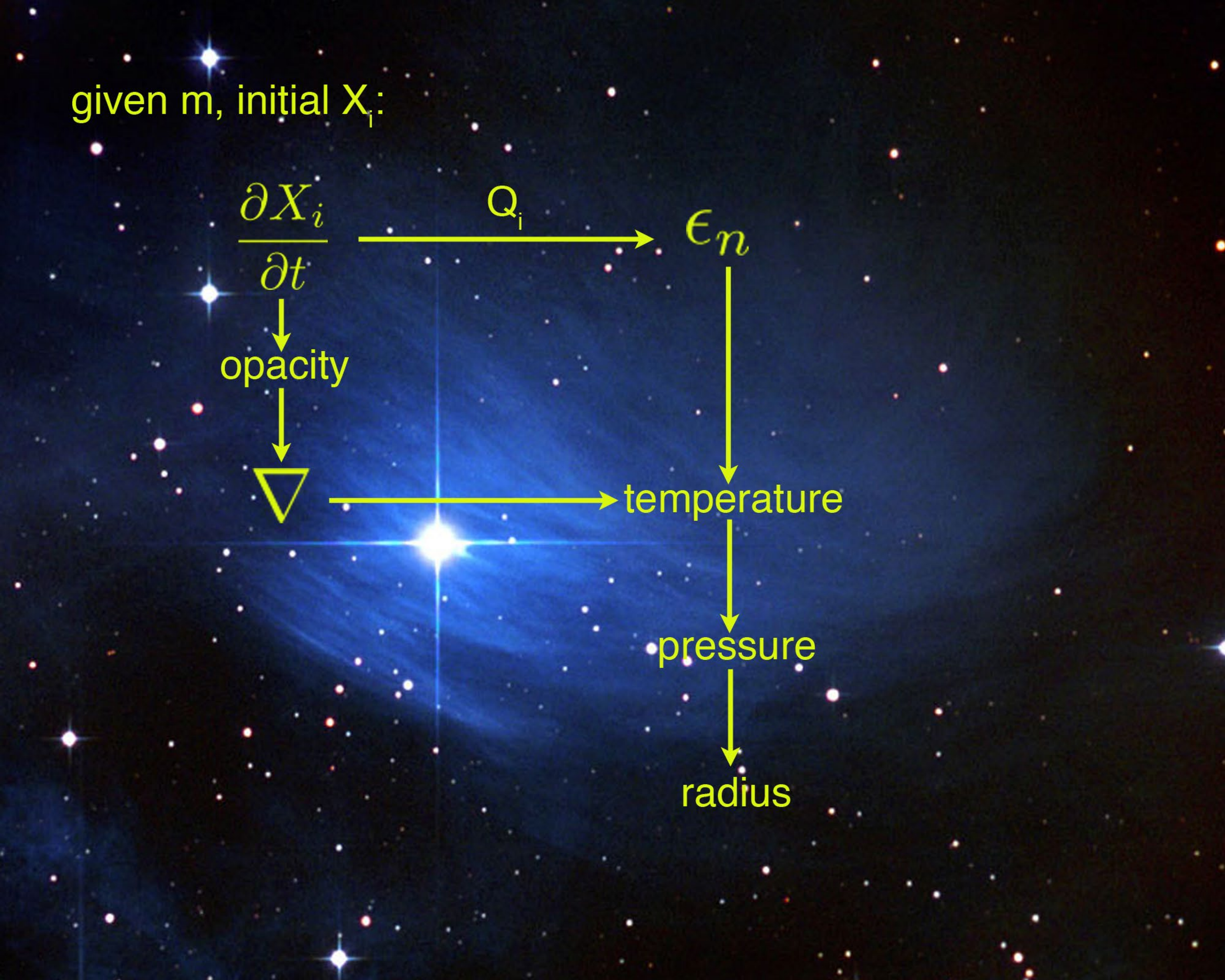
given m, initial X_i:
$\frac{\partial X_i}{\partial t}$
Q_i
ϵ_n
opacity
∇
temperature
pressure
radius

Thermonuclear reaction rate

reaction a + b with number densities N_a and N_b

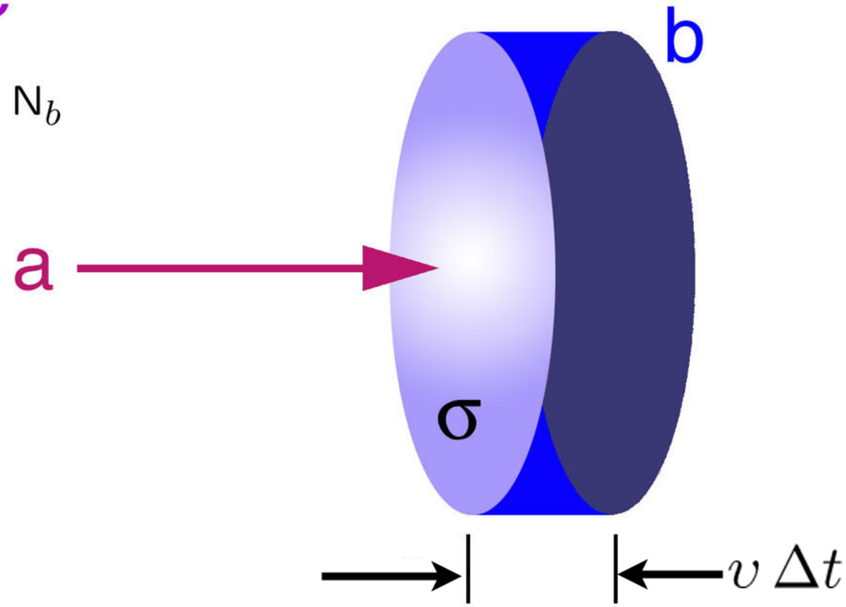

number of nuclei reacting in time Δt is

$$N_b \times \sigma v \times \Delta t$$

$$\text{Rate} = N_b \times \sigma v$$

$$\frac{\text{Rate}}{\text{unit volume of gas}} = \frac{N_a N_b \cdot \sigma v}{1+\delta_{ab}}$$

(prevents double counting if a = b)

but there is a distribution of relative velocities

so $R_{ab} = N_a N_b \langle \sigma v \rangle, \qquad \langle \sigma v \rangle = \int_0^\infty \sigma(v)\, v\, \phi(v)\, dv$

at thermal equilibrium*

$$\phi(v) = 4\pi v^2 \sqrt{\frac{\mu}{2\pi kT}}\, exp\left(-\frac{\mu v^2}{2kT}\right)$$

$$\langle \sigma v \rangle = \sqrt{\frac{8}{\mu \pi k^3 T^3}} \int_0^\infty \sigma(E)\, exp\left(-\frac{E}{kT}\right) dE$$

reaction time: in general, $N_i = \rho\, N_A \frac{X_i}{A_i}$, N_A = Avogadro's number
X_i = mass fraction of i
A_i = atomic number of i

$$\frac{dN_b}{dt} = -\lambda\, N_b = \frac{N_b}{\tau_b}$$

$$R_{ab} = \frac{N_a\, N_b\, \langle \sigma v \rangle_{ab}}{1 + \delta_{ab}} = \frac{N_b}{\tau_b}$$

so $\tau_b = \left(N_a\, \langle \sigma v \rangle_{ab}\right)^{-1}$

(no δ_{ab} ! if a = b, then 2 particles are destroyed)

*Yes, this is a good asssumption. The mean-free path for a photon in the center of the sun is ~10^{-3} cm

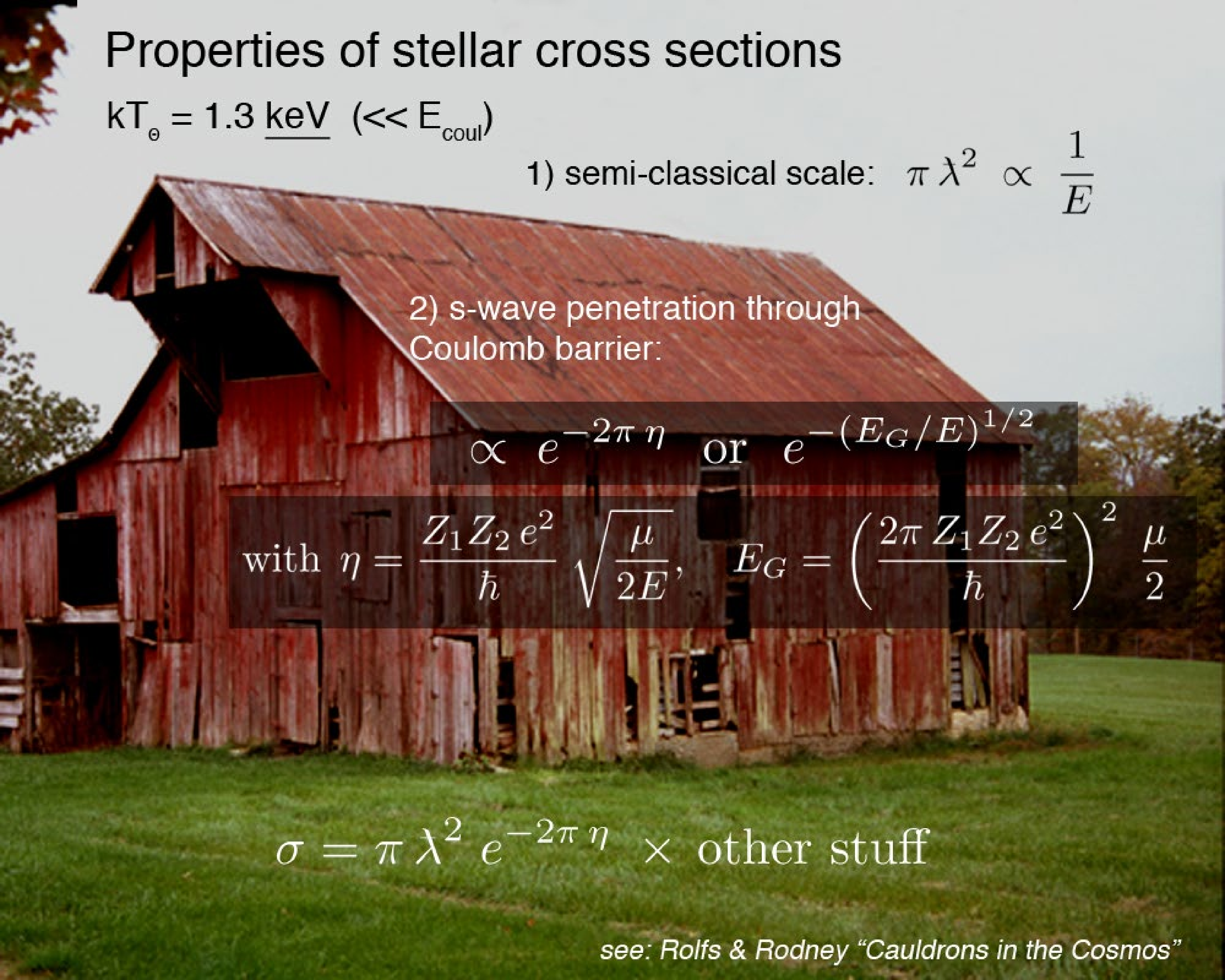

Properties of stellar cross sections

$kT_\odot = 1.3$ keV ($\ll E_{coul}$)

1) semi-classical scale: $\pi \lambda^2 \propto \frac{1}{E}$

2) s-wave penetration through Coulomb barrier:

$$\propto e^{-2\pi\eta} \quad \text{or} \quad e^{-(E_G/E)^{1/2}}$$

$$\text{with } \eta = \frac{Z_1 Z_2 e^2}{\hbar}\sqrt{\frac{\mu}{2E}}, \quad E_G = \left(\frac{2\pi Z_1 Z_2 e^2}{\hbar}\right)^2 \frac{\mu}{2}$$

$$\sigma = \pi \lambda^2 e^{-2\pi\eta} \times \text{other stuff}$$

see: Rolfs & Rodney "Cauldrons in the Cosmos"

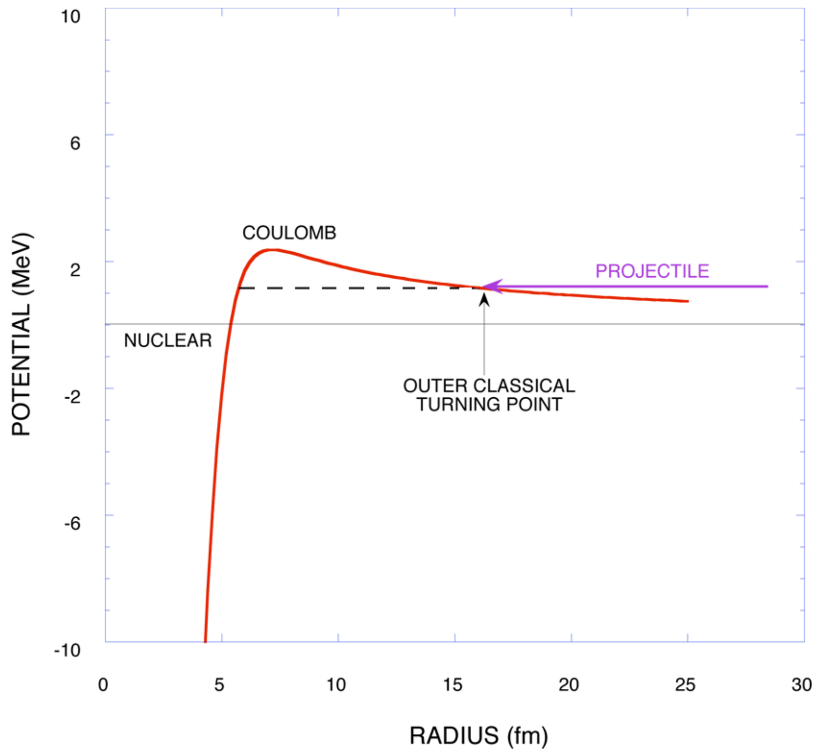

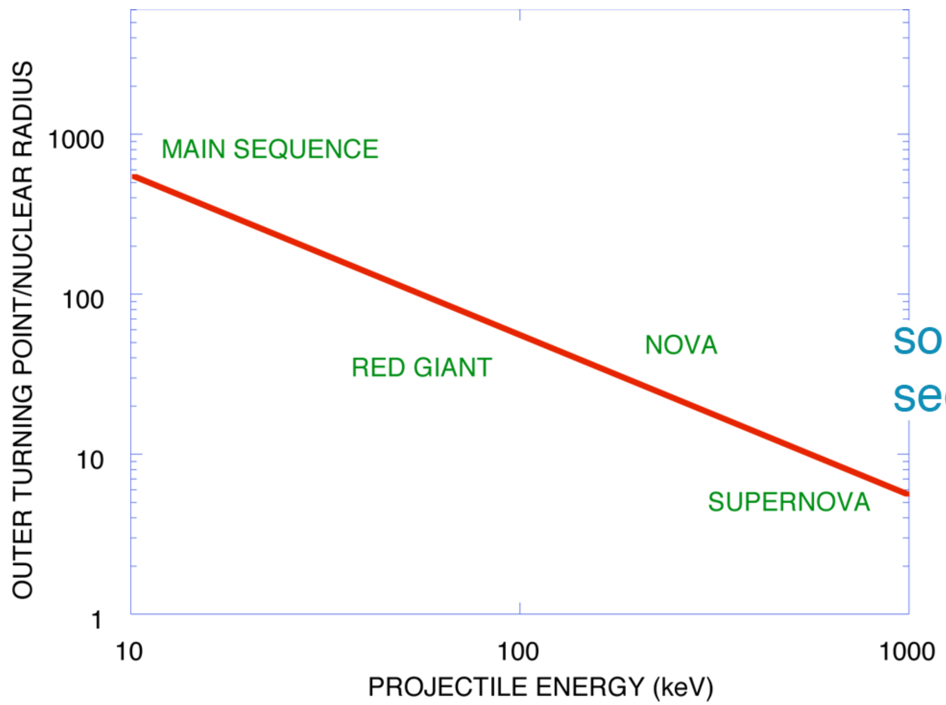

so these approximations seem appropriate

parameterize: $\sigma(E) = \frac{1}{E}\, e^{-2\pi\eta}\, S(E)$ "S-factor" S(E) contains: nuclear interaction
nuclear structure
finite-size effects
other partial waves
final-state phase space, etc.

recall that: $$\langle \sigma v \rangle = \sqrt{\frac{8}{\mu \pi k^3 T^3}} \int_0^\infty \sigma(E)\, exp\left(-\frac{E}{kT}\right) dE$$

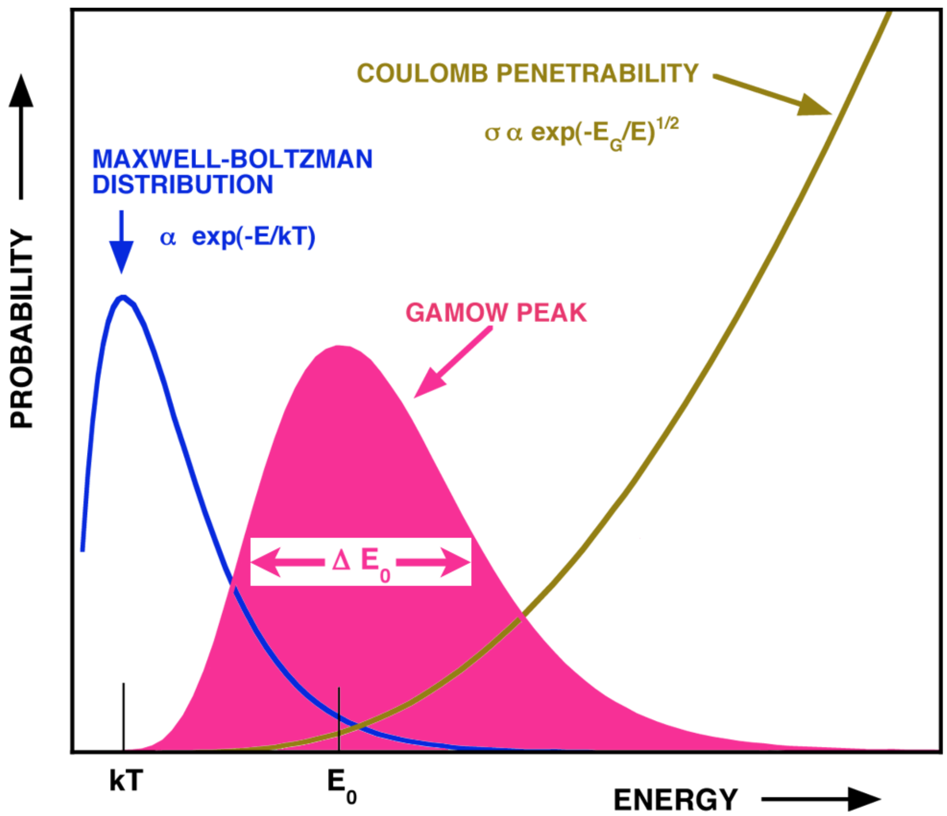

$$\langle \sigma v \rangle = \sqrt{\frac{8}{\pi \mu\, k^3 T^3}} \times$$

$$\int_0^\infty S(E)\, exp\left[-\frac{E}{kT} - \left(\frac{E_G}{E}\right)^{1/2}\right] dE$$

$$E_0 = \left(\frac{E_G^{1/2}\, kT}{2}\right)^{2/3} \qquad \Delta E_0 = 4\left(\frac{E_0\, kT}{3}\right)^{1/2}$$

Careful! - the Gamow peak is a useful concept, but it really pertains to non-resonant reactions. However, we tend to use it indiscriminantly. For resonances at high temp., the most effective energy may be less than E_0!

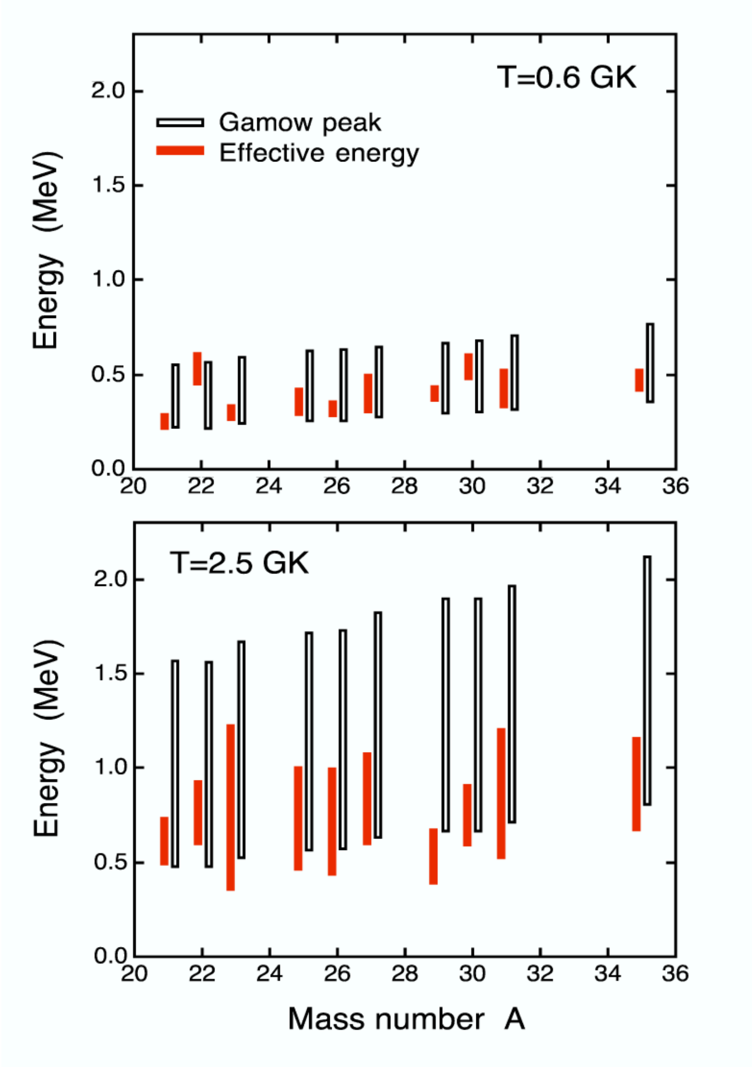

from experimental data

*[J.R. Newton et al. Phys. Rev. C **75**, 045801 (2007)]*

reaction	place	T_6	E_0 (keV)
p + p	sun	15	6
p + ^{14}N	3 $M_\odot$	30	42
α + ^{12}C	red giant	190	300
p + ^{17}F	nova	300	232
α + ^{30}S	x-ray burst	1000	1793

note: 1) reactions occur in a narrow window around E_0

2) strong temperature dependence

($<\sigma\upsilon> \alpha\ T^{(E_0/kT\ -\ 2/3)}$)

3) small cross sections @ E_0

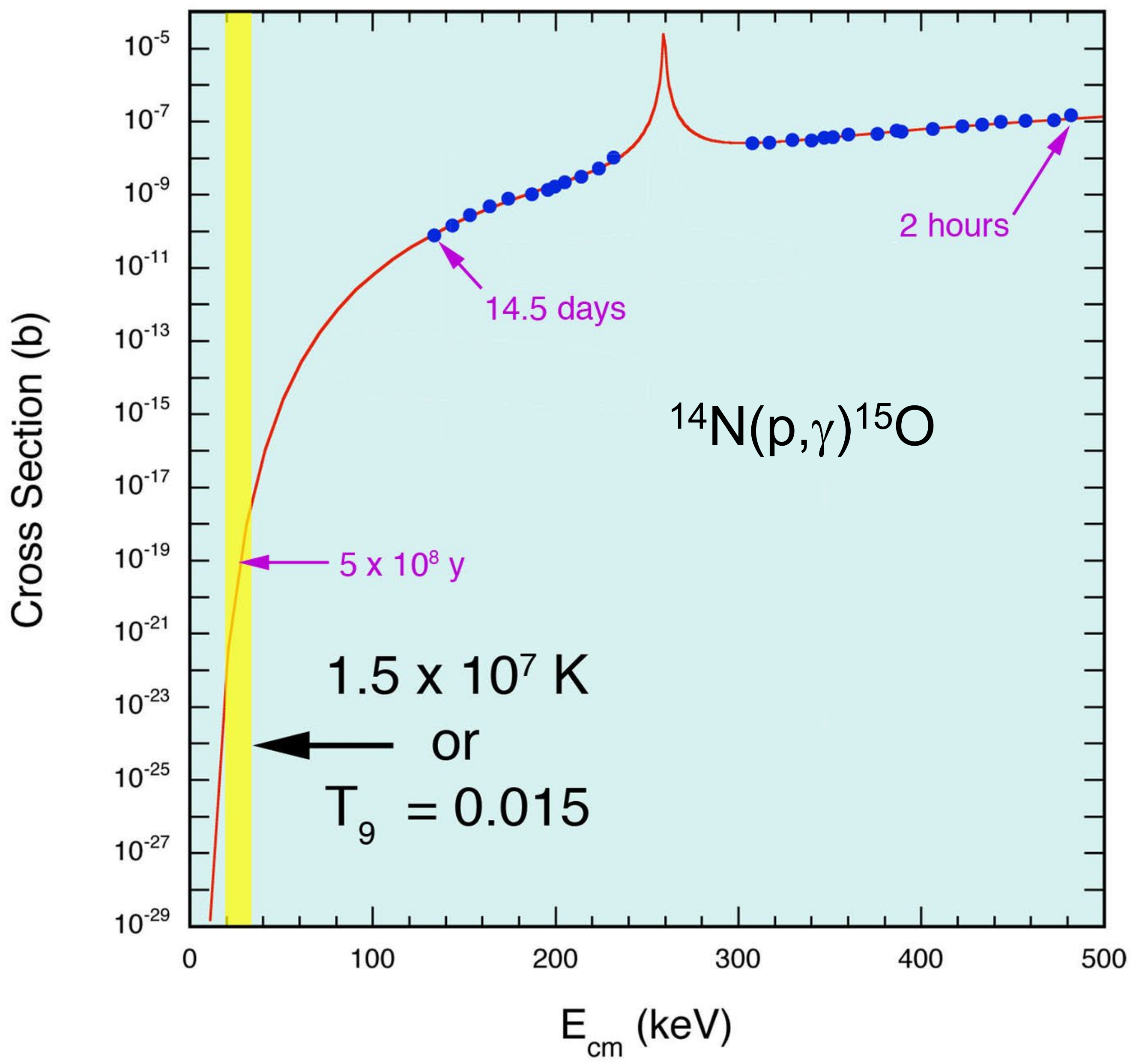

Cross Section (b)
10^-5
10^-7
10^-9
10^-11
10^-13
10^-15
10^-17
10^-19
10^-21
10^-23
10^-25
10^-27
10^-29
0
100
200
300
400
500
E_cm (keV)
14.5 days
2 hours
14N(p,γ)15O
5 x 10^8 y
1.5 x 10^7 K
or
T_9 = 0.015

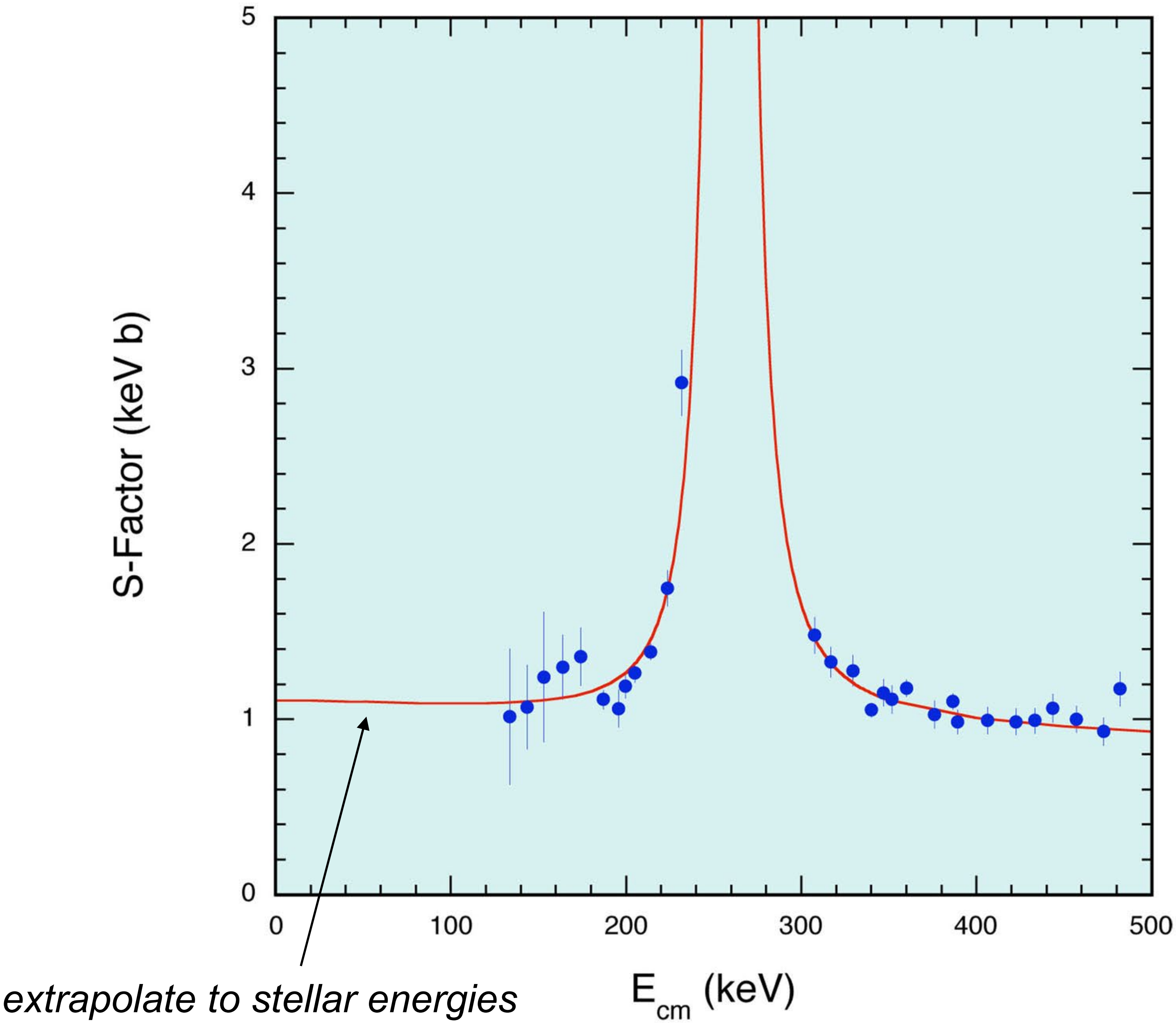
S-Factor (keV b)
0
1
2
3
4
5
0
100
200
300
400
500
E_{cm} (keV)
extrapolate to stellar energies

Rough outline of nuclear reactions

1) compound-nuclear

$$\sigma(\alpha,\beta) = \sigma_{CN}(\alpha) \times P(\beta)$$

cross section for forming compound system from entrance channel α

probability of exit channel β

$$P(\beta) = \frac{\Gamma_\beta}{\Gamma}, \quad \Gamma = \sum_\beta \Gamma_\beta$$

a simple model for Γ_β:

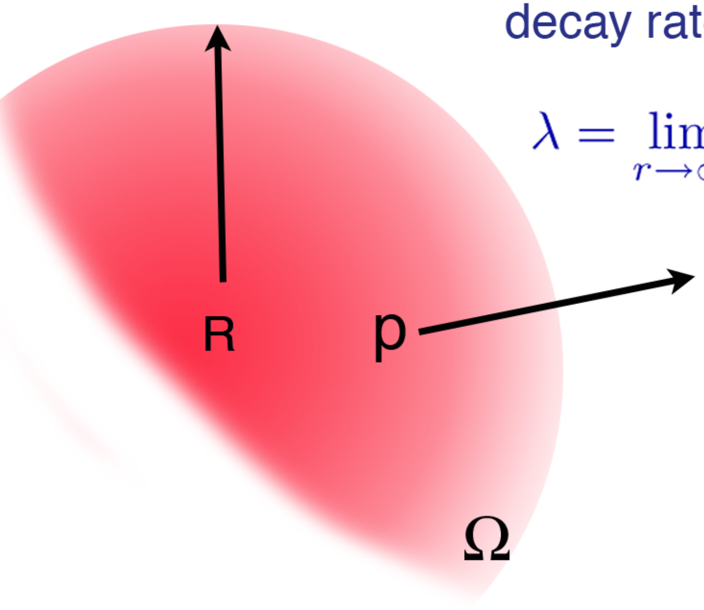

decay rate = flux x emitting area

$$\lambda = \lim_{r\to\infty} v \int_\Omega |\Psi(\vec{r})|^2 \, r^2 \, d\Omega$$

where $\Psi(\vec{r}) = \frac{U_\ell(kr)}{r} Y_{\ell m}(\theta,\phi)$

$$\lambda = \lim_{r\to\infty} v \, |U_\ell(kr)|^2 \int |Y_{\ell m}(\theta,\phi)|^2 \, d\Omega$$

$$= v\, |U_\ell(\infty)|^2 = \sqrt{\frac{2E}{\mu}}\, |U_\ell(\infty)|^2$$

define “penetrability” $P_\ell(E) \equiv kR_{nuc} \left| \frac{U_\ell(\infty)}{U_\ell(kR_{nuc})} \right|^2$

$$(= kR_{nuc} \text{ for s} - \text{wave neutrons}; \; = \frac{kR_{nuc}}{F_\ell^2(kR_{nuc}) + G_\ell^2(kR_{nuc})} \text{ for charged particles})$$

$$\Gamma_\beta = \lambda\hbar = \hbar\sqrt{\frac{2E}{\mu}}\; |U_\ell(\infty)|^2$$

$$= \frac{\hbar^2}{\mu R_{nuc}}\; |U_\ell(kR_{nuc})|^2\; P_\ell(E)$$

$$\equiv 2\,\gamma_p^2\, P_\ell(E) \text{ where } \gamma_p^2 = \frac{\hbar^2}{2\mu R_{nuc}}\; |U_\ell(kR_{nuc})|^2$$ "reduced width"

what about $\sigma_{CN}(\alpha)$? (come back to it later)

$\ell = 0$ asymptotic wavefunction: $U_0 = e^{-\imath kr} - S_0\, e^{\imath kr}, \quad S_0 = e^{2\imath\delta_0}$

now equate logarithmic derivatives at r = R:

$S_0 = \frac{L^I + \imath kR}{L^I - \imath kR}\, e^{-2\imath kR}$ and suppose that $L^I = a - \imath b$ (inner logarithmic deriv.)

$$S_0 = -\left[\frac{(kR - b) - \imath a}{(kR + b) + \imath a}\right] e^{-2\imath kR} \longrightarrow \sigma_{reaction} = \frac{4\pi}{k^2}\left(1 - |S_0|^2\right)$$

see e.g. Bertulani & Danielewicz "Introduction to Nuclear Reactions" *if you like this so far, you won't mind:*

what happens if a = 0 at E = E_r? (this is equivalent to matching wavefunctions with zero slope @ r = R)

near E = E_r: $a(E) \simeq \left.\frac{\partial a(E)}{\partial E}\right|_{E=E_r} (E - E_r)$ so $\frac{a}{a'} = E - E_r$

$\frac{a}{a'} = E - E_r$ and $\Gamma_{scat} \equiv -\frac{2kR}{a'(E_r)}$, $\Gamma_b \equiv -\frac{2b}{a'(E_r)}$, $\Gamma = \Gamma_{scat} + \Gamma_b$

$$\sigma_{res} = \frac{\pi}{k^2} \frac{\Gamma_{scat} \quad \Gamma_b}{(E - E_r)^2 + \Gamma^2/4}$$

a.k.a. Breit-Wigner

for a (p,γ) reaction $\Gamma_{scat} = \Gamma_p, \quad \Gamma_b = \Gamma_\gamma$

$$\sigma_{res} = \frac{\pi}{k^2} \underbrace{\frac{2J_f + 1}{(2J_i + 1)(2J_p + 1)}}_{\omega} \frac{\Gamma_p \Gamma_\gamma}{(E - E_r)^2 + \Gamma^2/4}$$

(spin and higher partial waves included) some comments:

1) Believe it of not, these (seemingly arbitrary) definitions of partial widths are equivalent to the earlier parameterization.

2) There's no nuclear potential anywhere in sight so this is not a calculation of the cross section, but a parameterization in terms of (hopefully) observable quantities.

3) If Γ << E_r:

$$\langle \sigma v \rangle = \left(\frac{2\pi}{\mu k T} \right)^{3/2} \hbar^2 \, \omega\gamma \, e^{-E_r/kT}, \quad \text{where } \gamma = \frac{\Gamma_p \Gamma_\gamma}{\Gamma}$$

"resonance strength"

4) If temperatures (energies) are high enough, then resonances are no longer isolated and narrow. Here, it's better to go back to our initial idea of a compound-nuclear cross section, but suitably averaged.

$$\sigma^J_{CN,\ell}(\alpha) = \frac{\pi}{k_\alpha^2}\,(2\ell+1)\,T^J_{\alpha\ell\jmath}\;|\langle \jmath m \ell 0 | JM\rangle|^2$$

transmission coeff. $= \dfrac{16\mu^2}{\pi^2\hbar^4}\left|\int \vec{r}\, j_\ell(kr)\, V_\ell(\vec{r})\, U_\ell(k,\vec{r})\, d^3r\right|^2$

optical potential

from reciprocity: $P(\beta) = \dfrac{T^J_{\beta\ell'\jmath'}}{\sum_{\alpha\ell\jmath} T^J_{\alpha\ell\jmath}}\;|\langle \jmath' m' \ell' (M-m') | JM\rangle|^2$

$$\sigma(\alpha\beta) = \frac{\pi}{k_\alpha^2}\sum_J \frac{2J+1}{(2\jmath+1)(2\jmath'+1)}\,\frac{T^J_{\alpha\ell\jmath}\,T^J_{\beta\ell'\jmath'}}{\sum_{\alpha\ell\jmath} T^J_{\alpha\ell\jmath}}$$

this is the “Hauser-Feshbach” cross section and it’s no bargain as written
$\sum_{\alpha\ell\jmath} T^J_{\alpha\ell\jmath}$ can contain thousands of terms (so it must be modeled)

2. direct reactions

Treat (p,γ) in perturbation theory: $$\frac{d\sigma}{d\Omega} = \frac{E_\gamma}{2\pi\hbar^2 c v_i} \, |V_{fi}|^2$$

wavefunctions? initial state: target x incident distorted wave
final state: target x single-particle
(photon is contained in H_{int})

helicity = ±1

rotate into $\theta_\gamma, \phi_\gamma$

$$H_{int}(E1) = \sum_m (-\imath) \left(\frac{4\pi}{3}\right)^{1/2} \frac{E_\gamma}{\hbar c} P \frac{m_1 m_2}{m_1 + m_2} e \left(\frac{Z_1}{m_1} - \frac{Z_1}{m_1}\right) \times D^{(1)*}_{mP} \, \mathcal{O}_{E1}(r) \, Y^*_{\ell m}(\theta\phi)$$

recoil correction

E1 radial operator

left with radial integral: $$\mathcal{R}_{fi} = \int_0^\infty R_f(r) \, \mathcal{O}_{E1}(r) \, R_i(r) \, r^2 \, dr$$

"direct capture" $$\sigma_{DC}(exp) = \sum_{\ell f} C^2 S_{\ell f} \, \sigma_{DC}(th)$$

$C^2 S_{\ell f}$ is a "spectroscopic factor". Final state wavefunction asssumes a pure single-particle state. Multiply this by spectroscopic amplitude θ for the "real" state. $S = n\theta^2$, where n arises when antisymmetrized wavefunctions are used. C^2 is an isospin C.G. coeff.

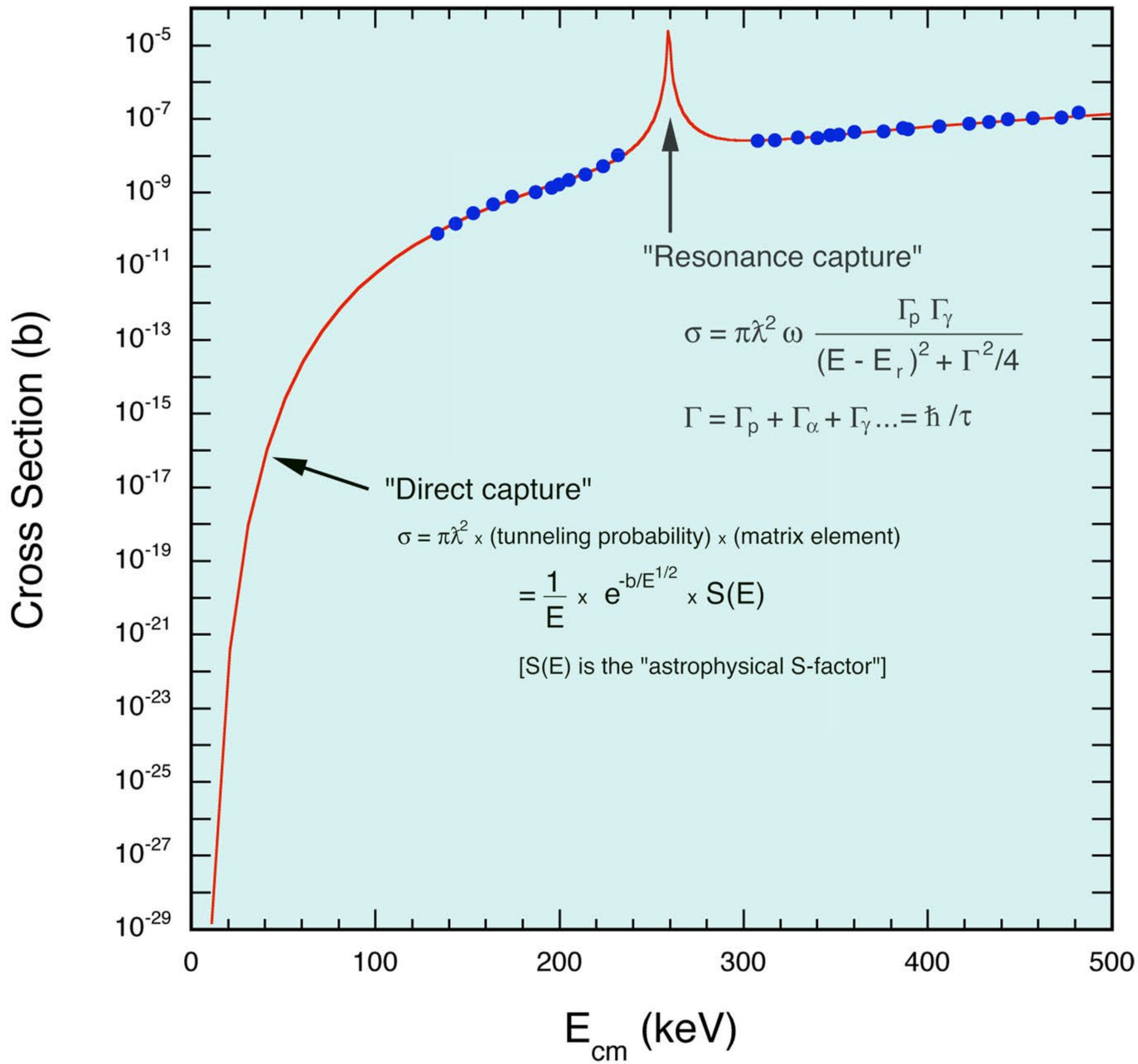

Cross Section (b)
E_{cm} (keV)
10^{-5}
10^{-7}
10^{-9}
10^{-11}
10^{-13}
10^{-15}
10^{-17}
10^{-19}
10^{-21}
10^{-23}
10^{-25}
10^{-27}
10^{-29}
0
100
200
300
400
500
"Resonance capture"
$\sigma = \pi\lambda\!\!\!^{-2}\,\omega\,\frac{\Gamma_p\,\Gamma_\gamma}{(E - E_r)^2 + \Gamma^2/4}$
$\Gamma = \Gamma_p + \Gamma_\alpha + \Gamma_\gamma \ldots = \hbar/\tau$
"Direct capture"
$\sigma = \pi\lambda\!\!\!^{-2}$ x (tunneling probability) x (matrix element)
$= \frac{1}{E} \times e^{-b/E^{1/2}} \times S(E)$
[S(E) is the "astrophysical S-factor"]

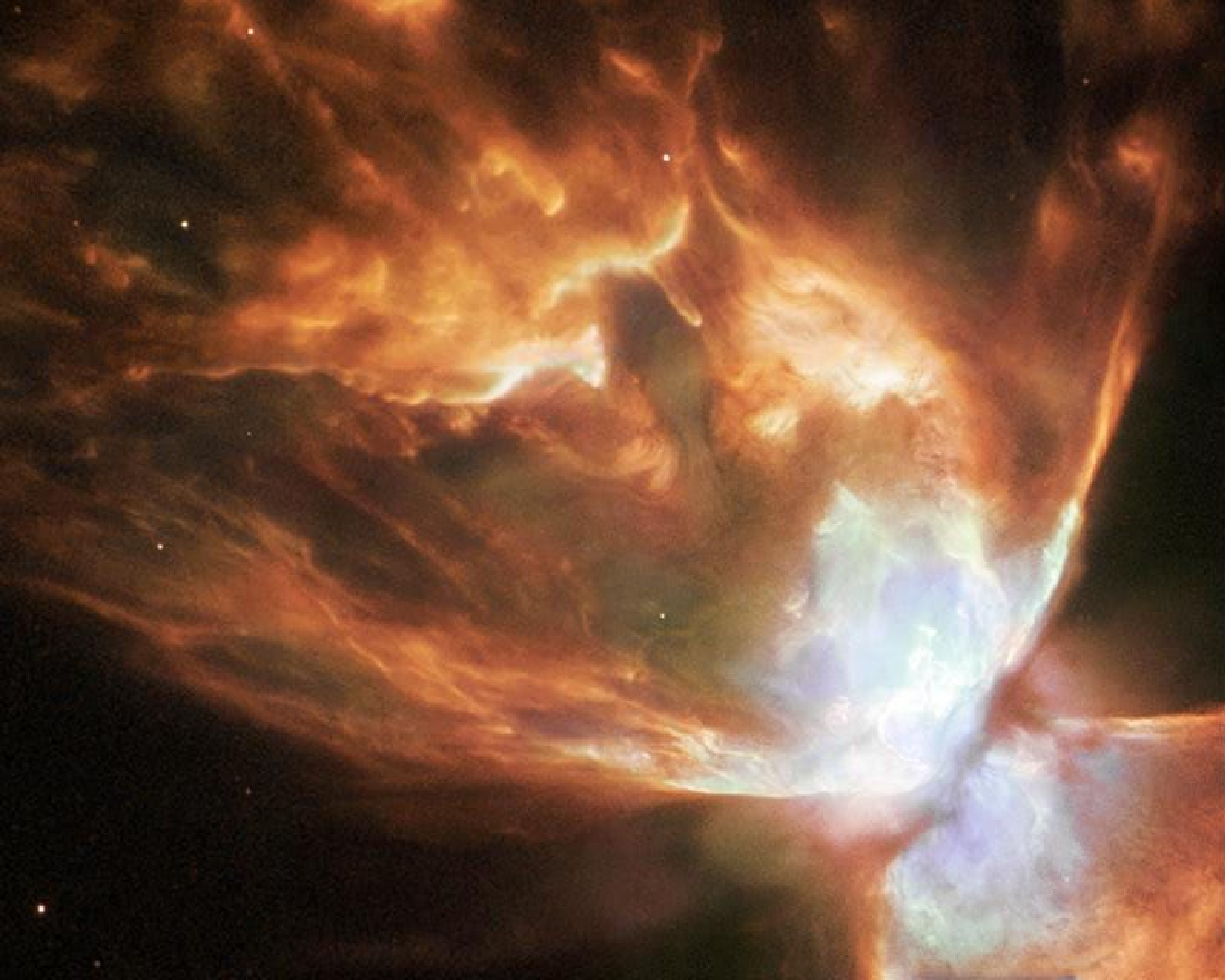

inverse reactions!

$$1 + 2 \leftrightarrow 3 + 4$$

$$\frac{\sigma_{12}}{\sigma_{34}} = \frac{\mu_{12}}{\mu_{34}} \frac{E_{34}}{E_{12}} \frac{(2J_3+1)(2J_4+1)}{(2J_1+1)(2J_2+1)}$$

$$\frac{\langle \sigma v \rangle_{34}}{\langle \sigma v \rangle_{12}} = \left(\frac{\mu_{12}}{\mu_{34}} \right)^{1/2} \frac{\int_0^\infty \sigma_{34} \, E_{34} \; exp(-E_{34}/kT) \; dE_{34}}{\int_0^\infty \sigma_{12} \, E_{12} \; exp(-E_{12}/kT) \; dE_{12}}$$

$$E_{34} = E_{12} + Q$$

$$= \left(\frac{\mu_{12}}{\mu_{34}} \right)^{3/2} \frac{(2J_1+1)(2J_2+1)}{(2J_3+1)(2J_4+1)} \, e^{-Q/kT}$$

Electron screening: electron cloud shields projectile from nuclear charge in external region

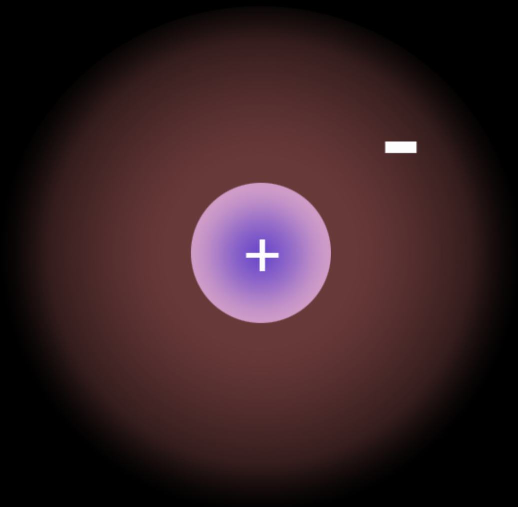

reaction takes place at higher effective energy than for bare nucleus (in star and in lab)

extreme example: d+p

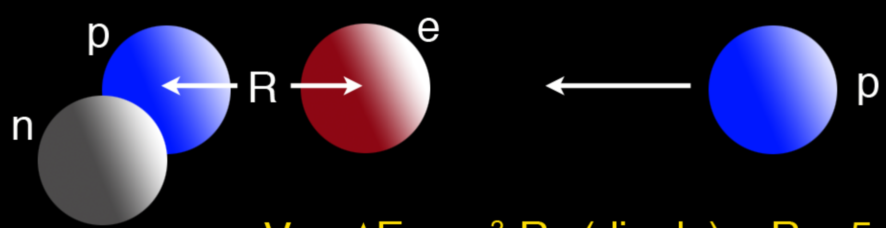

$V_Z = \Delta E = -\frac{e^2 R}{r^2}$ (dipole), $R \sim 5 \times 10^{-11}$ m

from $r = \infty$ to R, $\Delta E = 29$ eV

a bit more realistic:

initial:

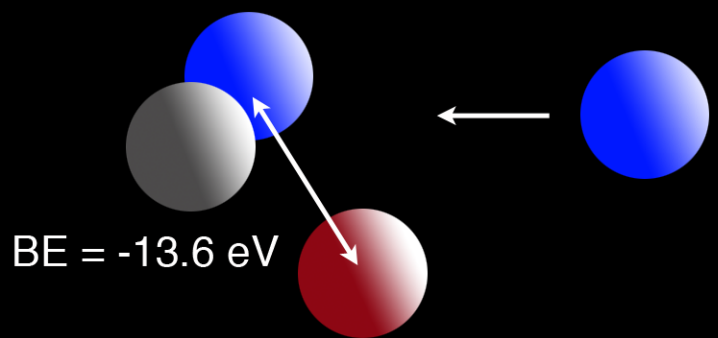

final:

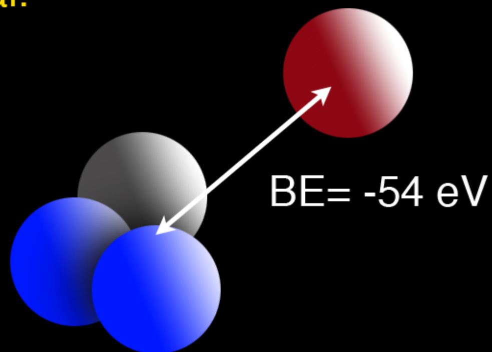

(see e.g. D.D. Clayton "Principles of Stellar Evolution & Nucleosynthesis" or Rolfs & Rodney "Cauldrons in the Cosmos")

Adiabatic approx:
Δ(binding energy) = 40.4 eV, which should be an upper limit on ΔE

$$<\sigma\upsilon>_{exp} = f(E) <\sigma\upsilon>_{nuc} \sim \exp(-\Delta E/kT)<\sigma\upsilon>_{nuc}$$

in a star, the situation is different: $V(r) = \frac{Z_1 Z_2 e^2}{r} e^{-r/R_D}$, where R_D is the *Debye-Hückel* radius

$$f_{star} = \exp(Z_1 Z_2 e^2/R_D kT)$$

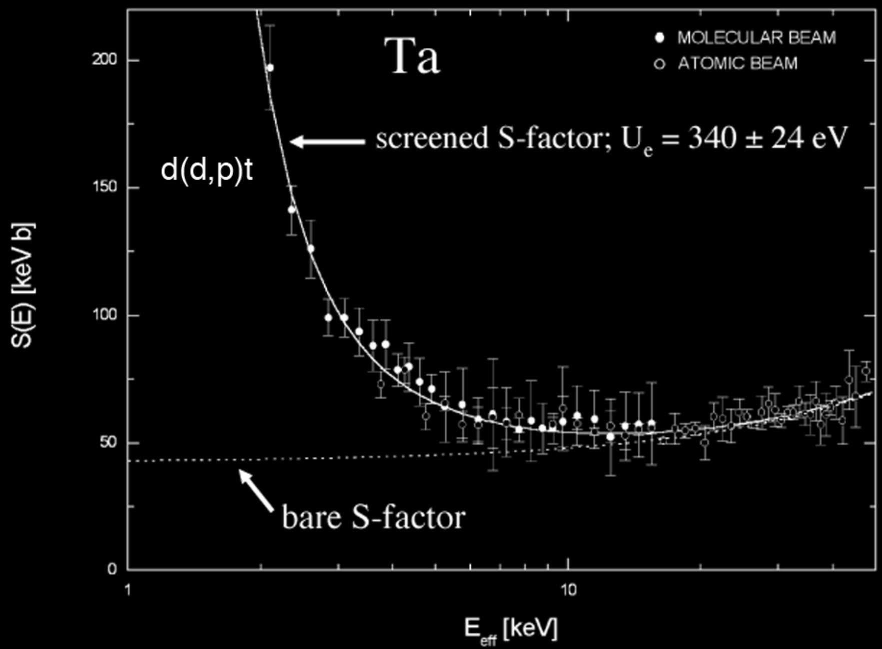

expect $\Delta E \leq 52$ eV (hmm..)
[see F. Raiola et al., Phys. lett. ***B547****, 193 (2002)]*

when do we care?

reaction	T_6	ρ(g/cm^3)	R_D(fm)	f
d+p	15	140	2.24e+4	1.05
$p+^{12}C$	15	140	2.24e+4	1.35
$p+^{17}F$	300	1000	3.75e+4	1.01
$\alpha+^{30}S$	1000	1e+6	2.17e+3	1.26

Other things that we sometimes ignore:

thermal population of excited states

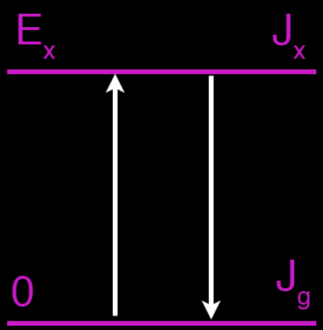

in equilibrium: $N_x \, \langle \sigma v \rangle_{x \to g} = N_g \, \langle \sigma v \rangle_{g \to x}$

$$\frac{N_x}{N_g} = \frac{\langle \sigma v \rangle_{g \to x}}{\langle \sigma v \rangle_{x \to g}} = \frac{2J_x + 1}{2J_g + 1} \, e^{-E_x/kT}$$

this will affect e.g. proton-capture rate: $\Gamma_p = 2\gamma_p^2 \, P_\ell(E)$

different core potential (γ_p^2)

different ℓ, E_r ($P_\ell(E)$)

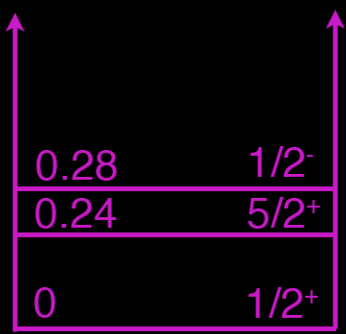

^{19}Ne

for ^{19}Ne(p,γ):

		$T_9 = 0.5$	1.5
N(%)	0	98.6	62.5
	1	1.2	30.0
	2	0.2	7.5

this must be calculated!

An interesting case (and my favorite nucleus) - ^{26}Al

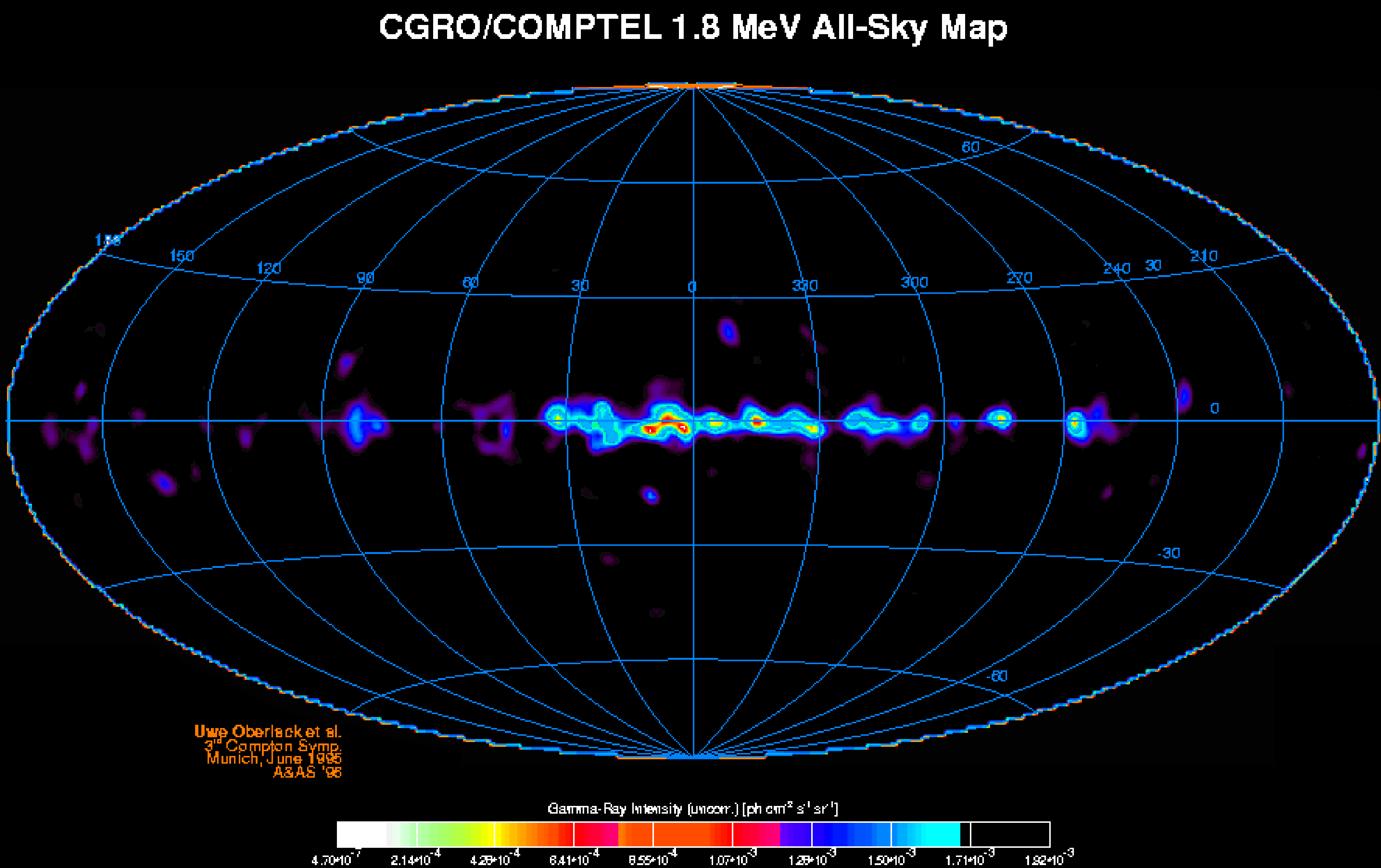

(check out Roland Diehl's web page)

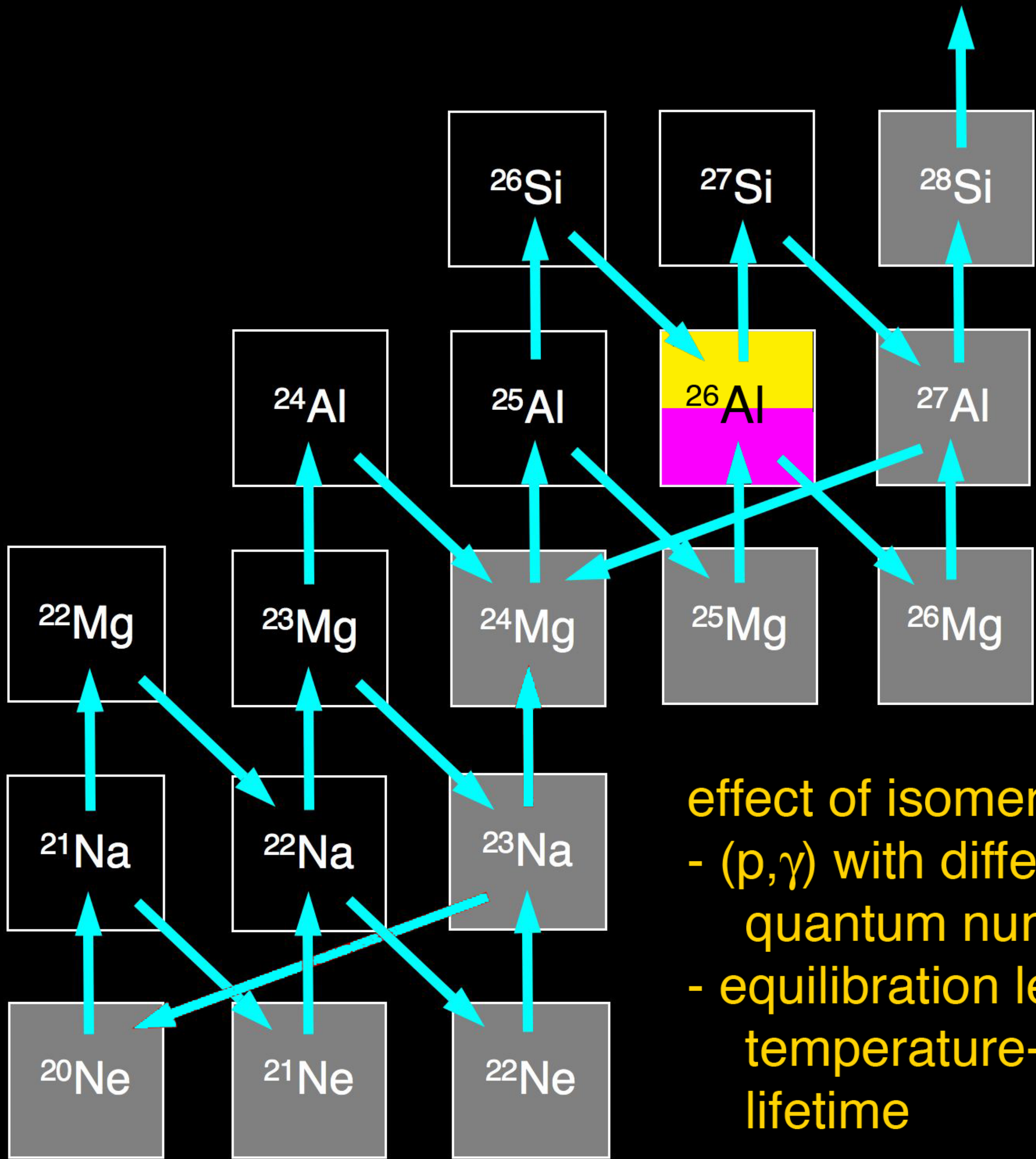

effect of isomer:

- (p,γ) with different Q-value, quantum numbers
- equilibration leads to temperature-dependent lifetime

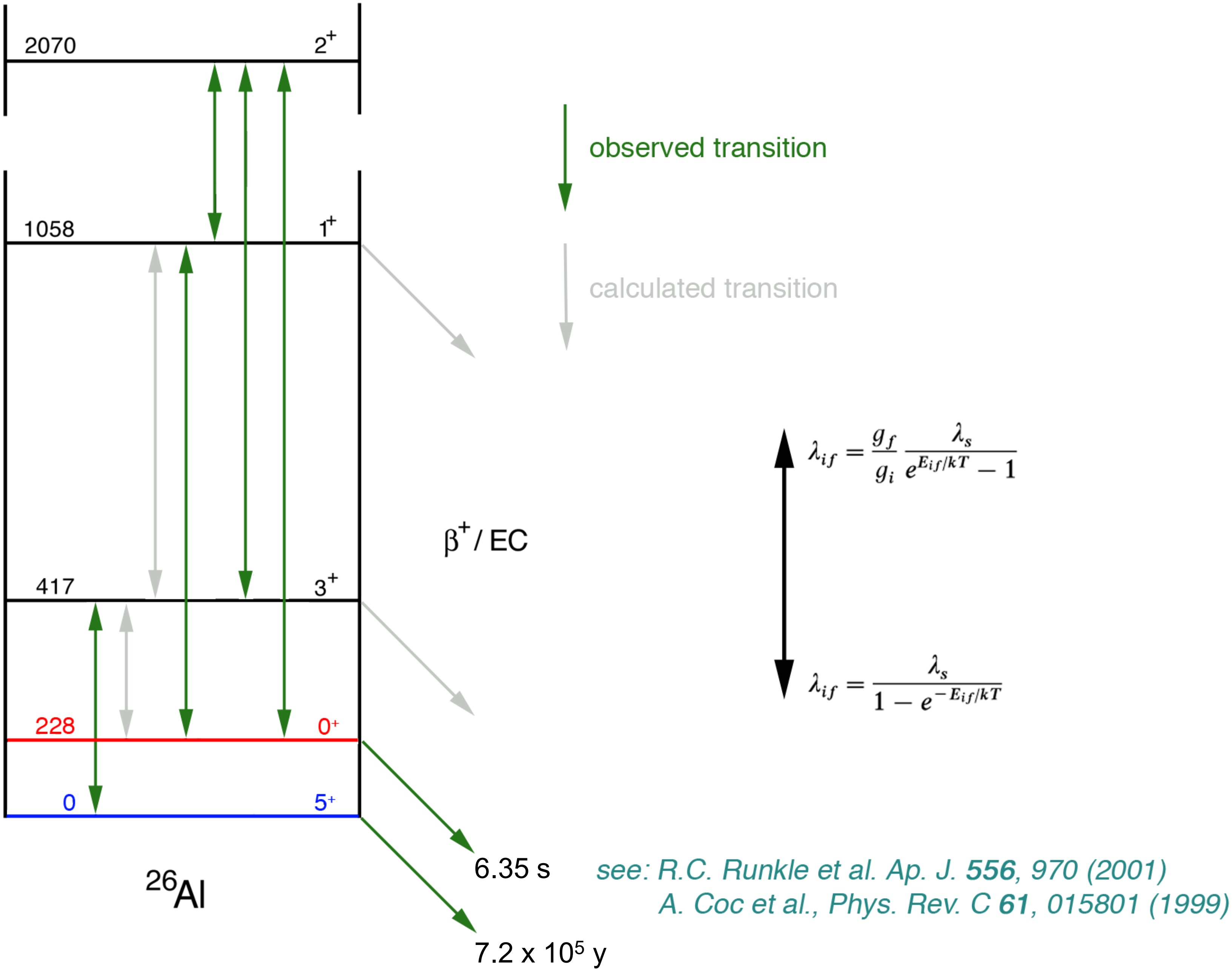
2070
2^+
1058
1^+
417
3^+
228
0^+
0
5^+
^{26}Al
observed transition
calculated transition
β^+ / EC
$\lambda_{if} = \frac{g_f}{g_i} \frac{\lambda_s}{e^{E_{if}/kT} - 1}$
$\lambda_{if} = \frac{\lambda_s}{1 - e^{-E_{if}/kT}}$
6.35 s
7.2×10^5 y
see: R.C. Runkle et al. Ap. J. **556**, 970 (2001)
A. Coc et al., Phys. Rev. C **61**, 015801 (1999)

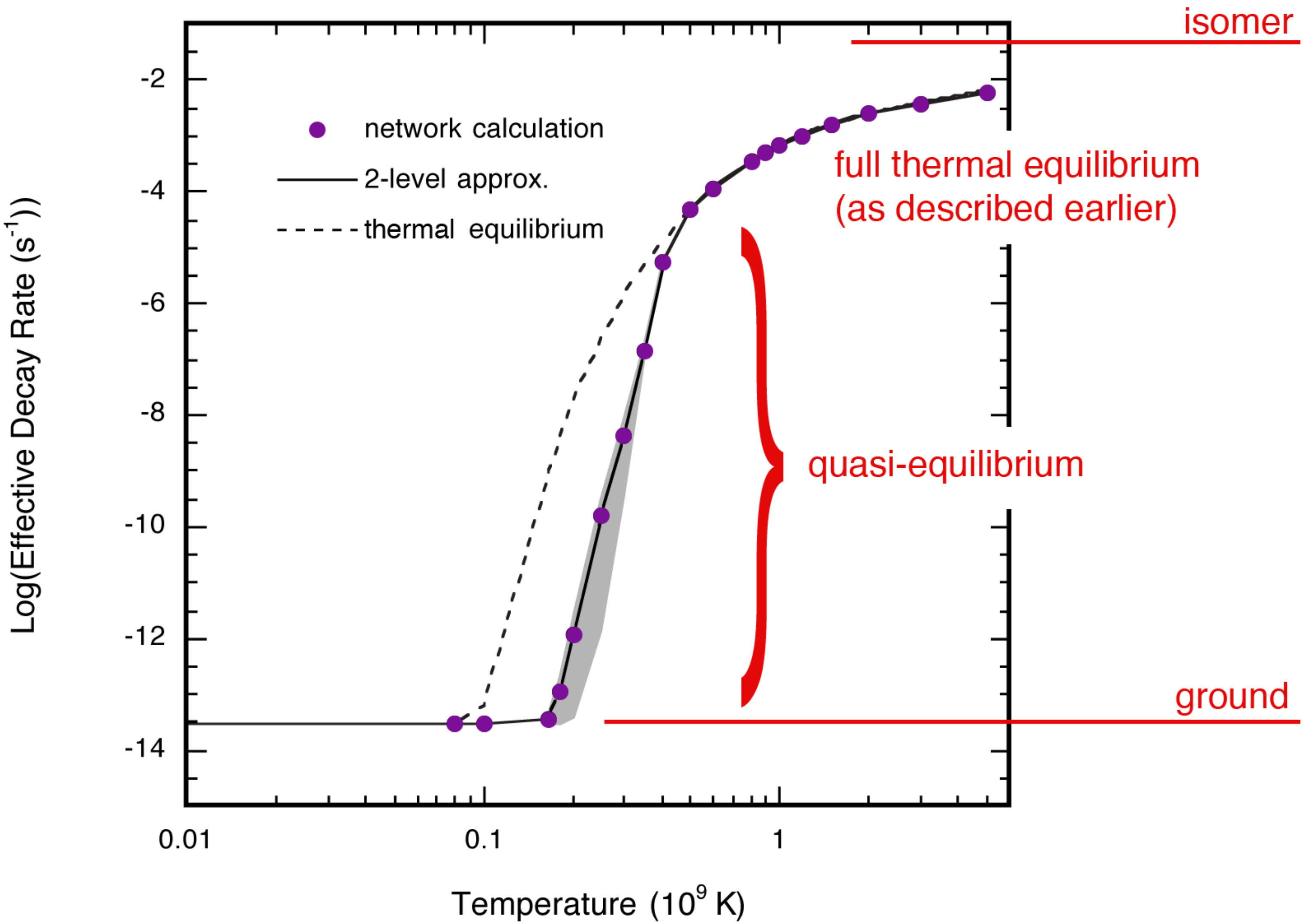
isomer
full thermal equilibrium
(as described earlier)
quasi-equilibrium
ground
network calculation
2-level approx.
thermal equilibrium
Log(Effective Decay Rate (s-1))
Temperature (10^9 K)
-2
-4
-6
-8
-10
-12
-14
0.01
0.1
1

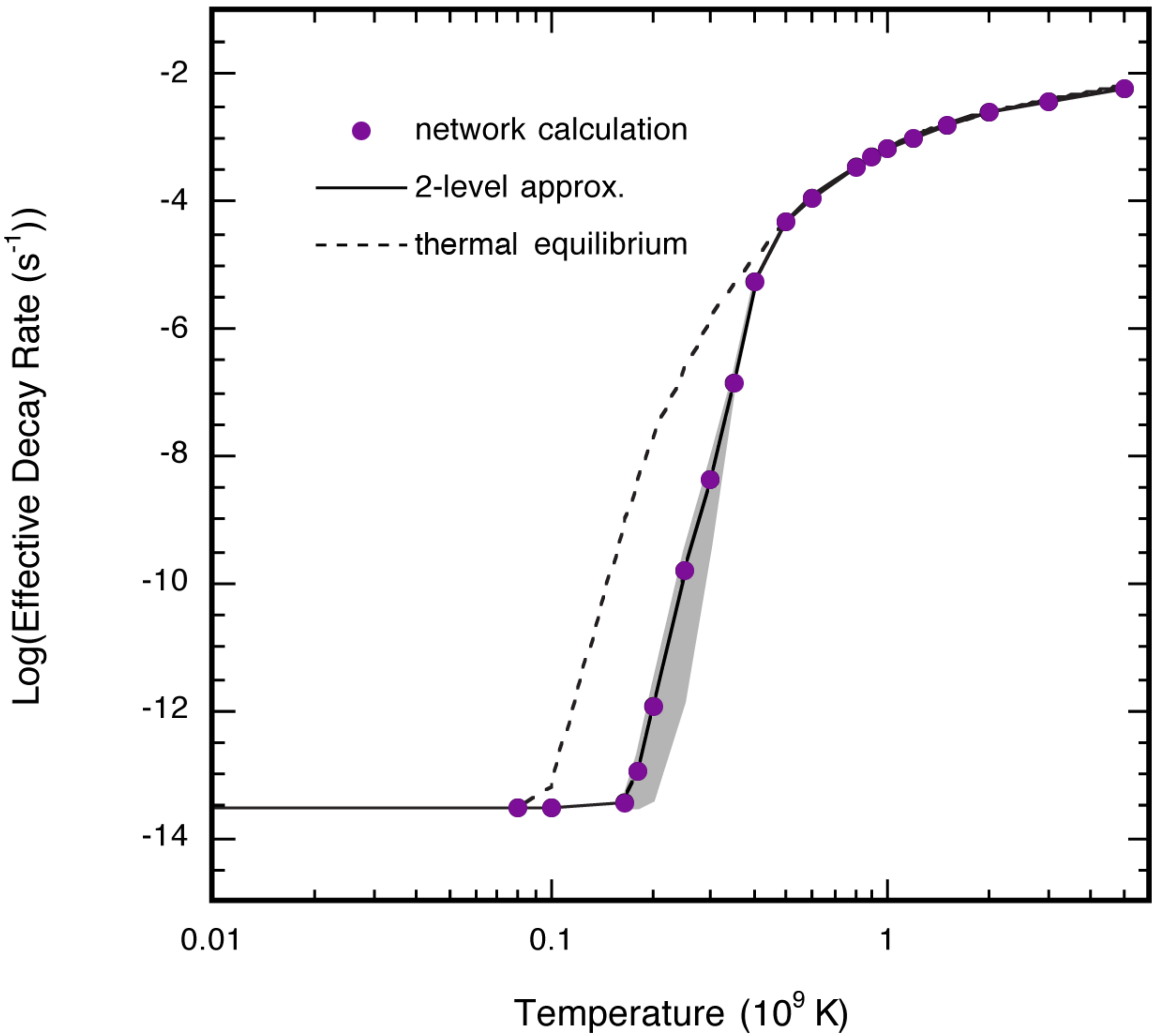

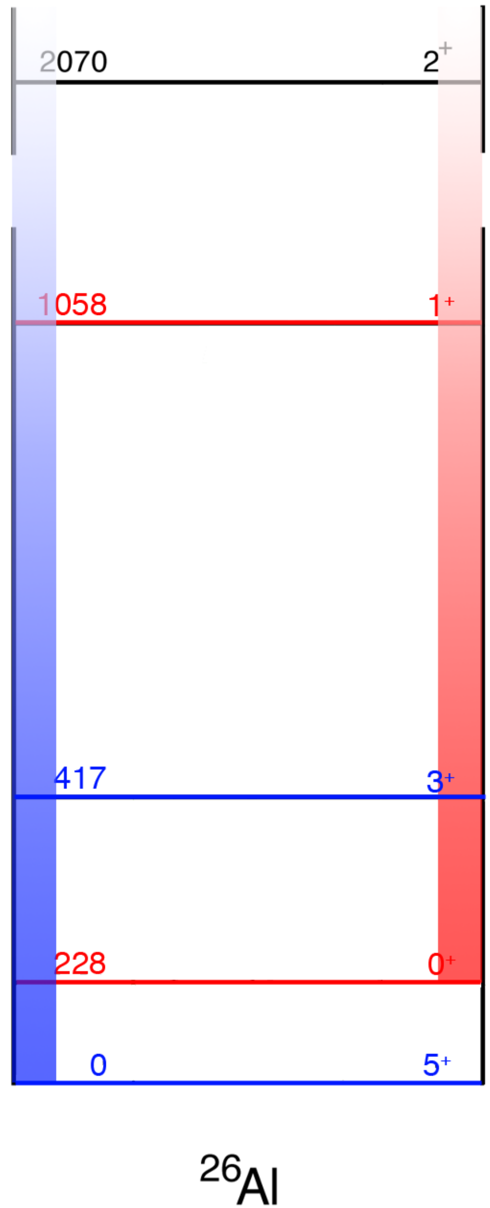

Quasi-equilibrium clusters and approach to equilibrium

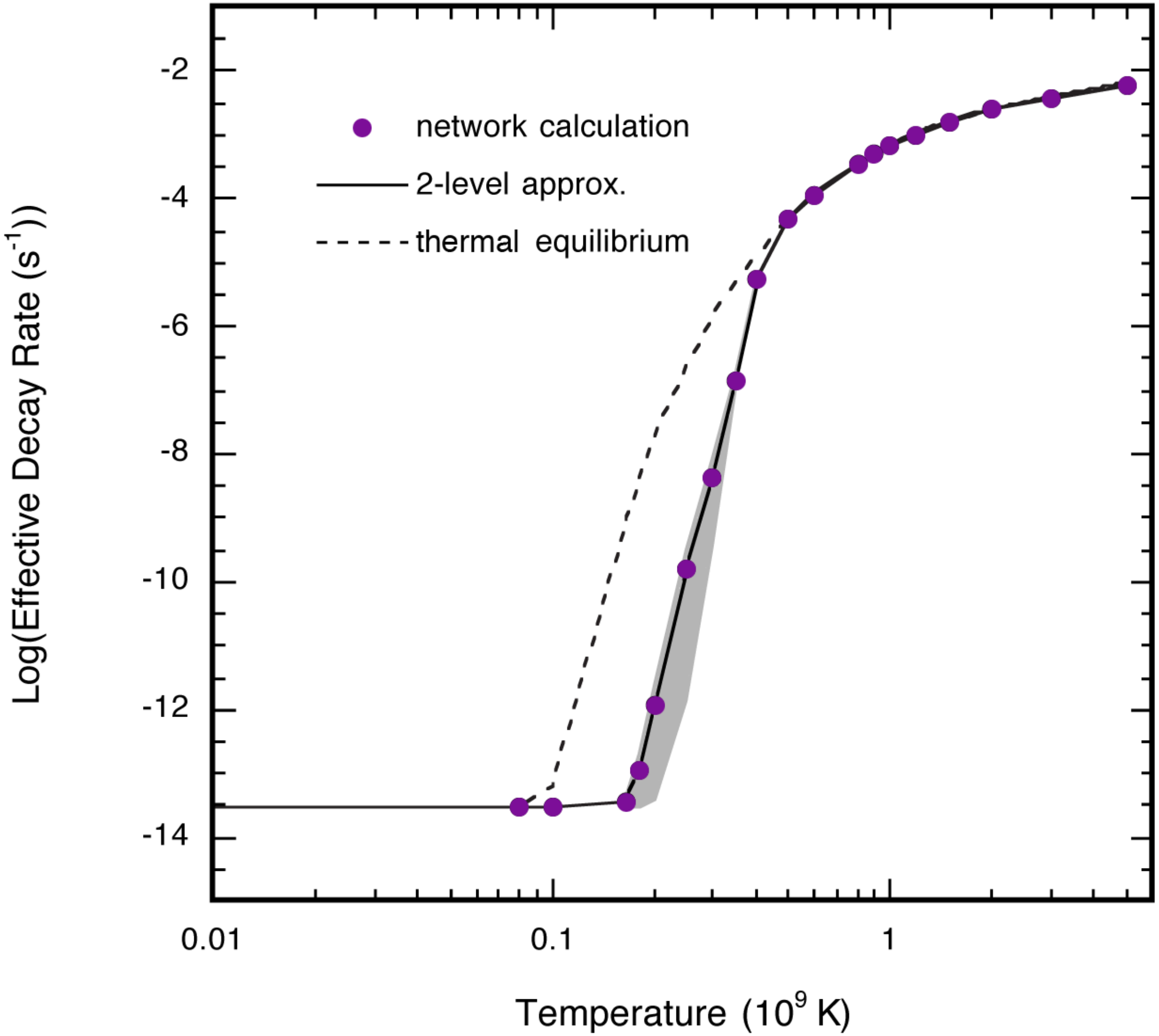

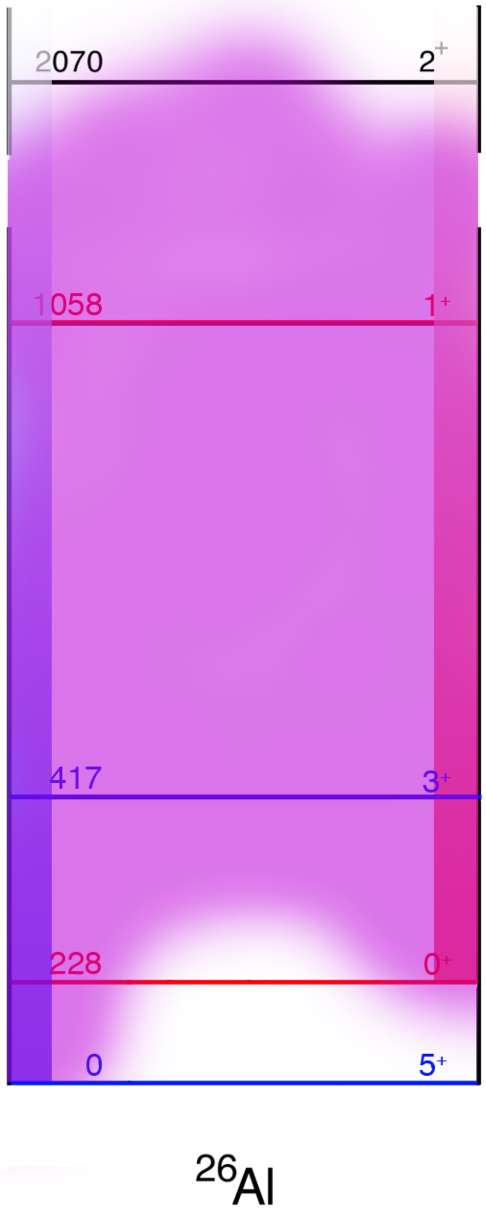

Important feature is interplay of timescales:

$\tau_{burning}$ vs. $\tau_{nuclear}$ vs. τ_{equil}

β- decay in stellar plasmas:

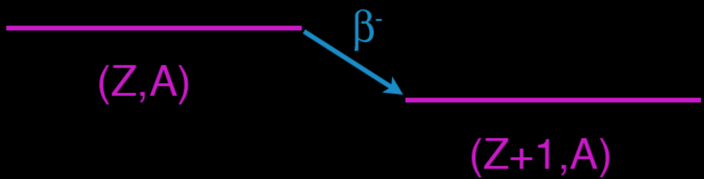

in a star, electron phase space depends on ρ and degree of ionization; β^--decay is "turned off" under degenerate conditions

electron capture can be favored:

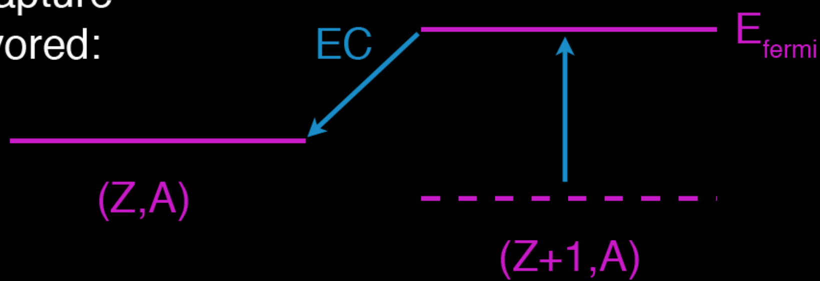

$$\frac{T_{1/2}^{*}}{T_{1/2}^{lab}} \sim \frac{10\mu_e Z^3}{\rho F[Z,w(T)]}$$

(however, removal of inner-shell electrons will suppress EC)

$$Q_{\beta^-} = [M(Z,A) - M(Z+1,A)]c^2 + [B_Z - B_{Z+1}]$$

$$Q_{\beta^+} = [M(Z,A) - M(Z-1,A)]c^2 - 2\, m_e c^2 + [B_Z - B_{Z-1}]$$

atomic masses — usually ignored

so $\left\{ \begin{array}{l} Q_{\beta^-} \downarrow \text{ as ionization } \uparrow \\ Q_{\beta^+} \uparrow \text{ as ionization } \uparrow \end{array} \right.$

*[see e.g. J.N. Bahcall, Ap. J. **139**, 318 (1964); G.M. Fuller et al., Ap. J. Supp. **42**, 447 (1980) and 48, 279 (1982); T. Kajino et al., Nucl. Phys. **A480**, 175 (1988)]*

on the other hand, ionization can allow "bound-state β-decay" to occur:

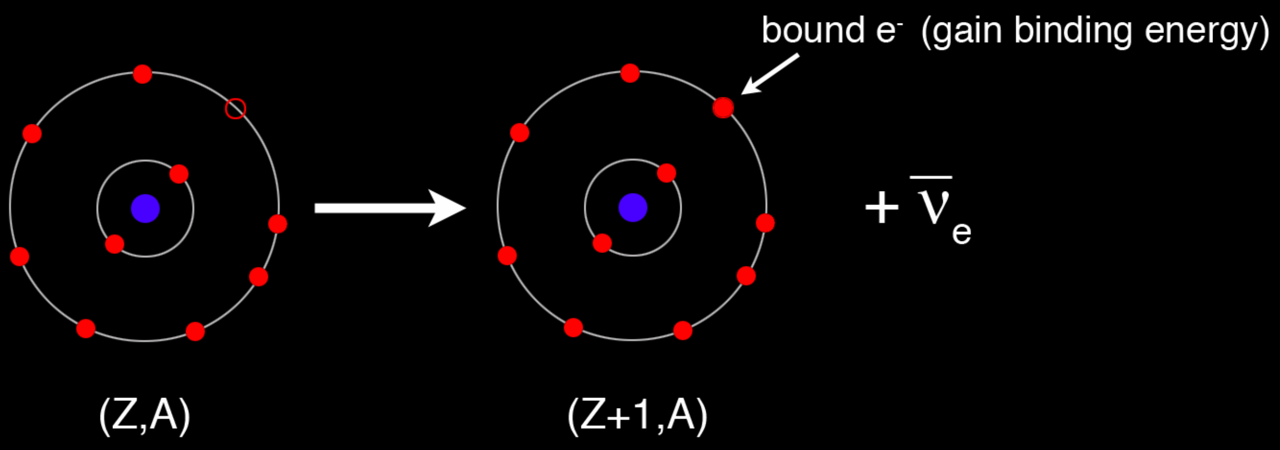

^{163}Dy, ^{187}Re, ^{193}Ir, ^{205}Tl are stable (or nearly so) as neutral atoms, but undergo bound-state decay when fully ionized

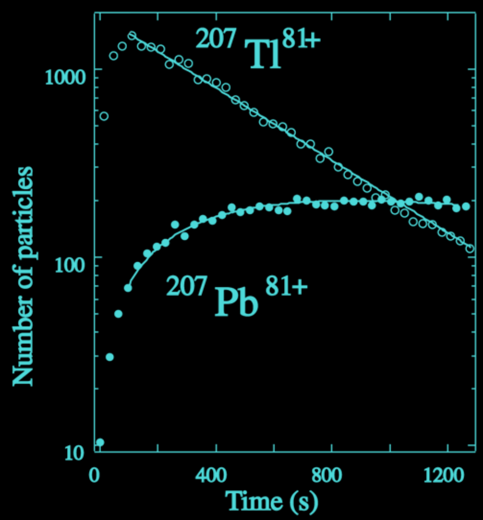

FIG. 3. Number of stored bare $^{207}Tl^{81+}$ ions and their β_b daughters $^{207}Pb^{81+}$ as a function of the storage time in the ESR. The statistical errors for most data points are smaller than the size of the symbols.

$T_{1/2}$(bound + continuum) = 264(10) s
vs. $T_{1/2}$(EC) = 286(2) s

T. Ohtsubo et al., Phys. Rev. Lett. 95, 052501 (2005)

Exotica: the "Urca" process*

simplest form:

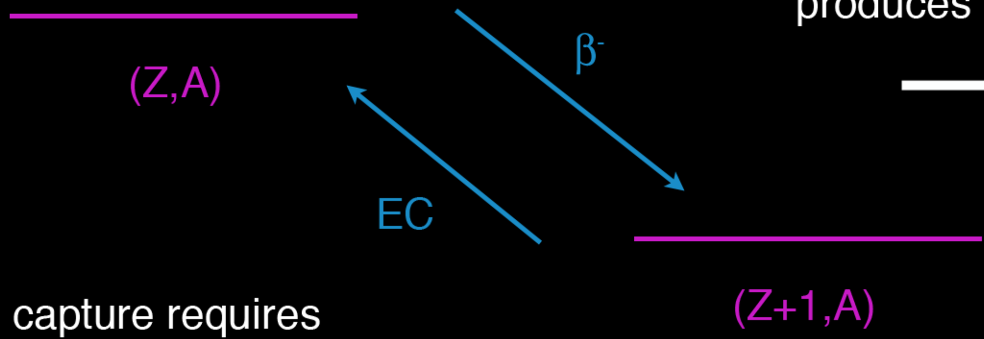

produces $\bar{\nu}_e$, ν_e per cycle

⟶ net cooling

upward electron capture requires energy from (~ degenerate) electron gas

e.g. for ^{23}Ne ⟷ ^{23}Na pair, $\rho \geq 1.7 \times 10^9$ g/cm^3 (important in cores of massive stars)

[see e.g., D. Arnett, "Supernovae and Nucleosynthesis", ch. 11]

*named for a Rio de Janeiro casino

calculating nucleosynthesis

have relative isotopic abundances $Y_i = X_i / A_i$

and reaction rates $N_A \langle \sigma v \rangle \quad (cm^3 s^{-1} mole^{-1})$

+ = production
- = destruction

number of particles of type i

$$\frac{dY_i}{dt} = \sum_j (\pm) N_i \, \lambda_j \, Y_j \; + \sum_{j,k} \frac{(\pm) N_i}{N_j! N_k!} \rho N_A \langle \sigma v \rangle_{j,k} \; Y_j Y_k$$

decays

2-body reactions

$N_j! N_k! = (1 + \delta_{jk})$

$$+ \sum_{j,kl} \frac{(\pm) N_i}{N_j! N_k! N_l!} \rho^2 N_A^2 \langle \sigma v \rangle_{j,k,l} \; Y_j Y_k Y_l \quad (\text{reactions/s})$$

3-body reactions

net flow $F_{i,j} = \int \left[\frac{dY_i}{dt}_{(i \to j)} - \frac{dY_j}{dt}_{(j \to i)} \right] dt$

energy released $\epsilon = \sum_{i,j} F_{i,j} \, Q_{i,j}$

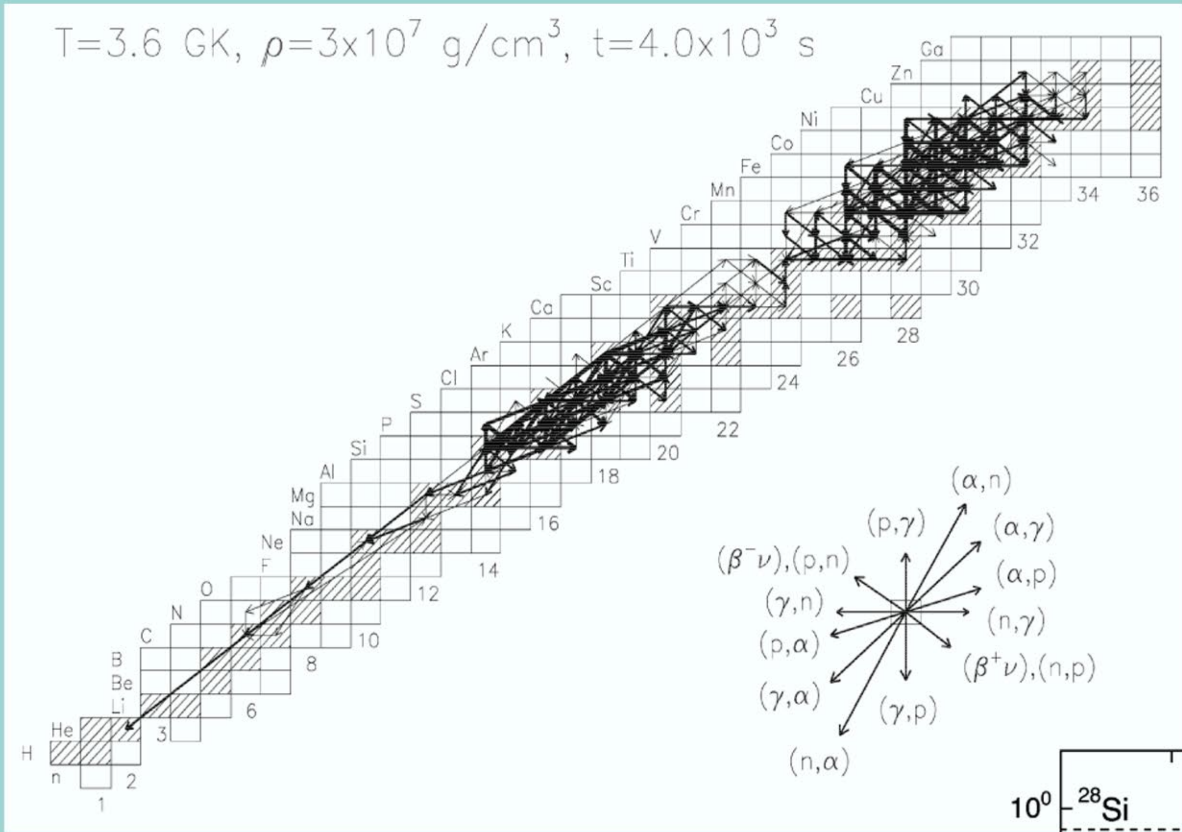

Core Si-burning

25 $M_\odot$

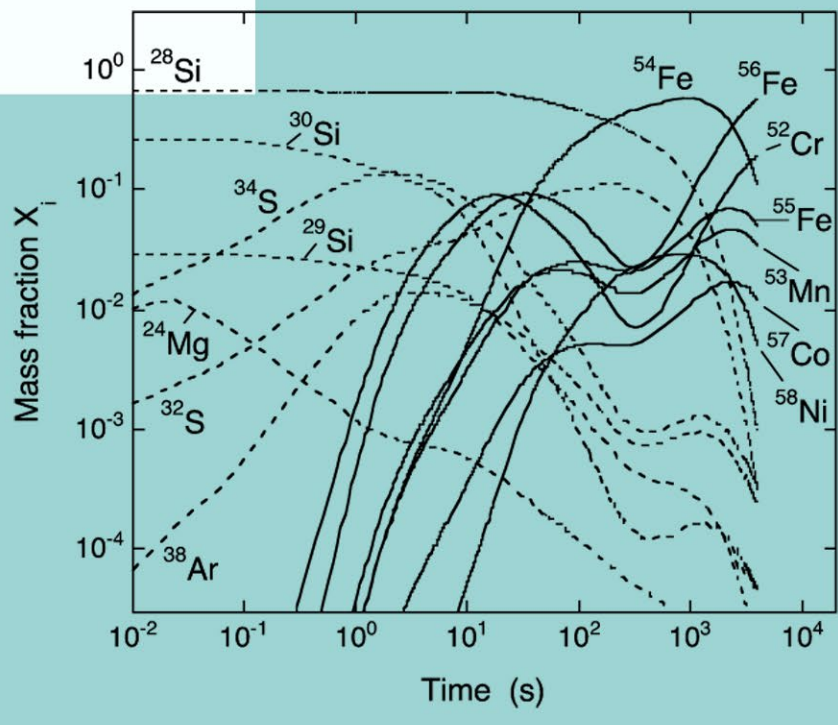

(courtesy of C. Iliadis)

Nucleosynthesis and galactic evolution

Sombrero Galaxy • M104

NASA and The Hubble Heritage Team (STScI/AURA) • Hubble Space Telescope ACS • STScI-PRC03-28

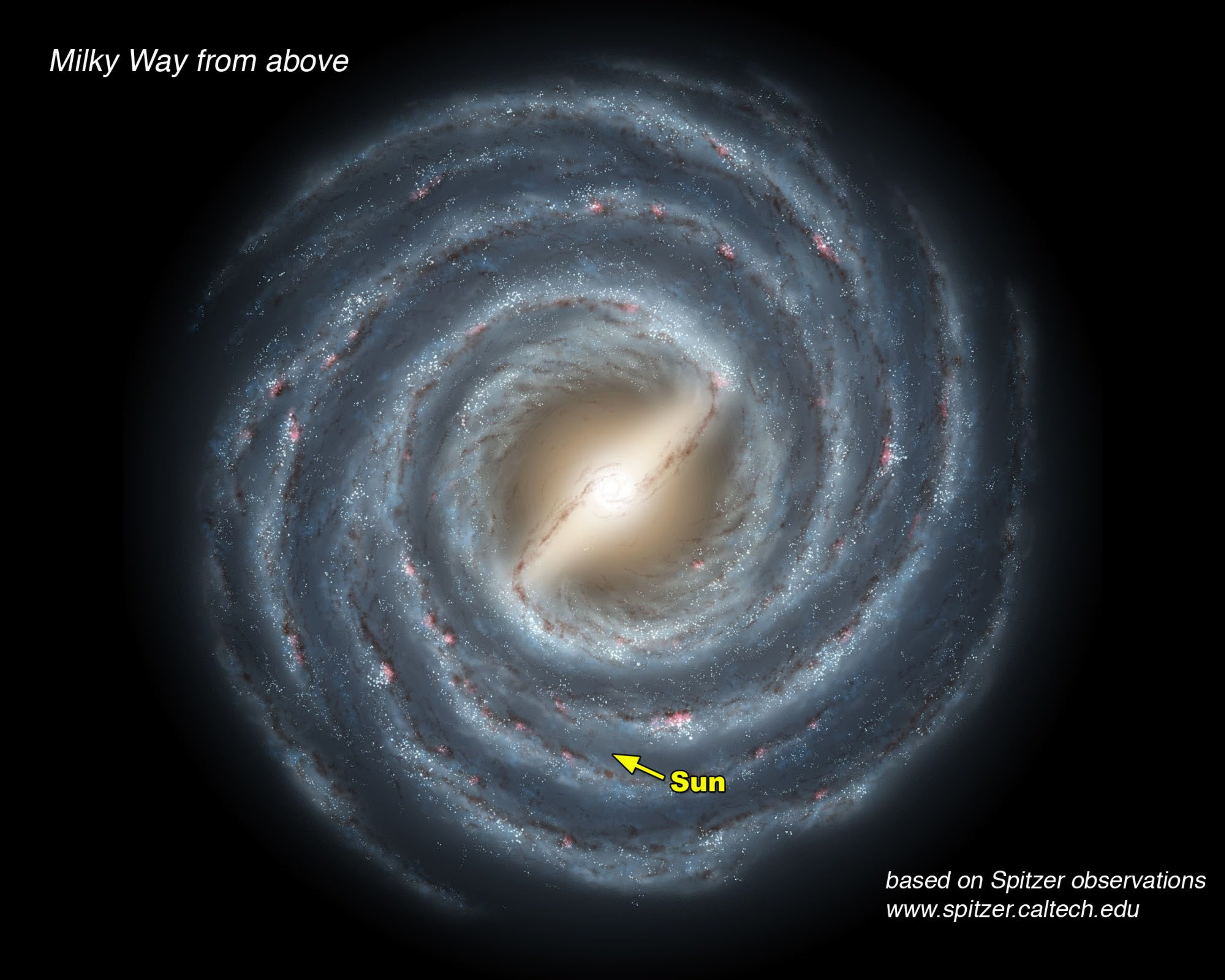
Milky Way from above
Sun
based on Spitzer observations
www.spitzer.caltech.edu

side view:

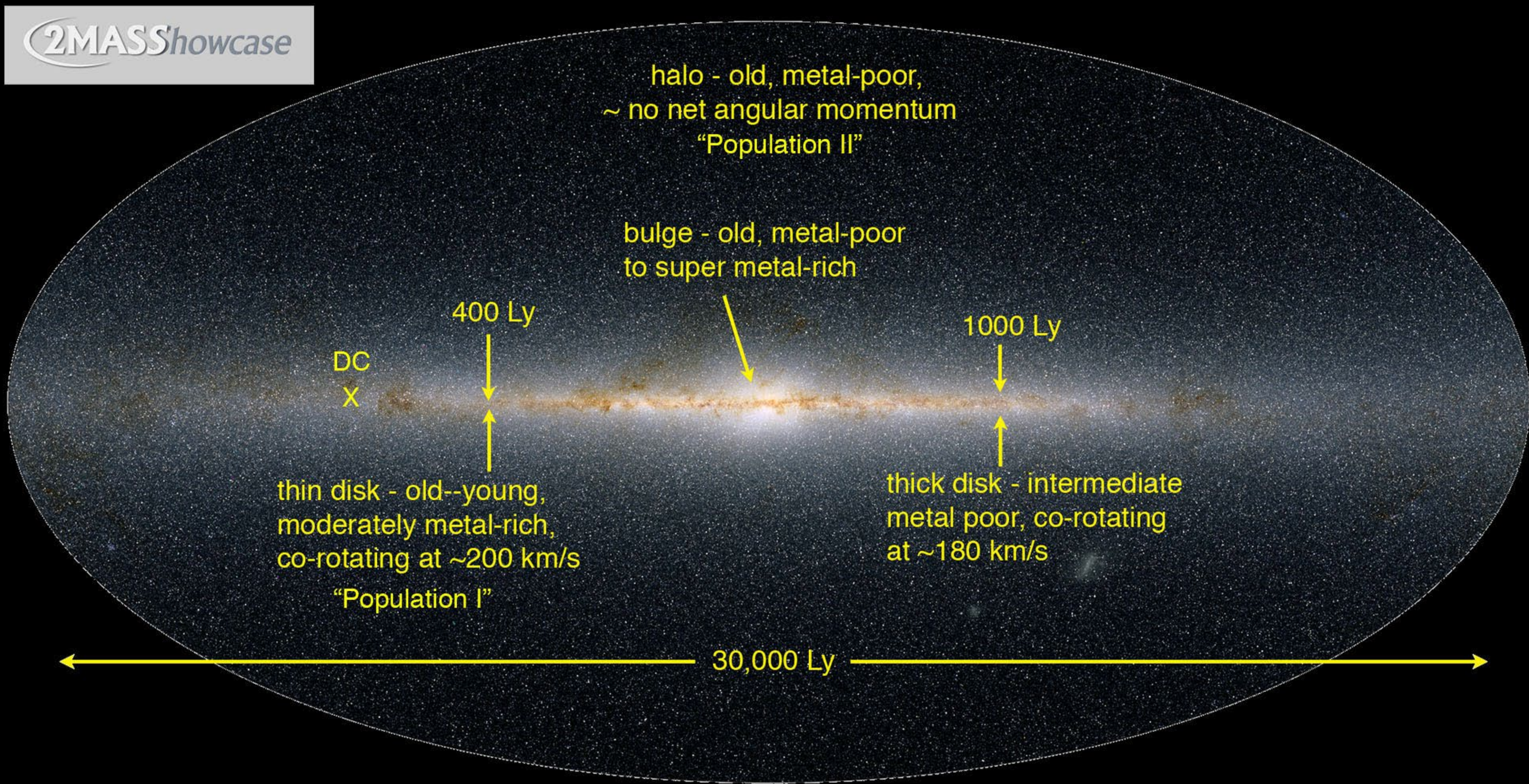
2MASS Showcase
halo - old, metal-poor,
~ no net angular momentum
"Population II"
bulge - old, metal-poor
to super metal-rich
400 Ly
1000 Ly
DC
X
thin disk - old--young,
moderately metal-rich,
co-rotating at ~200 km/s
"Population I"
thick disk - intermediate
metal poor, co-rotating
at ~180 km/s
30,000 Ly

some interesting questions

when did the galaxy form?
how? rapid collapse of halo followed by relaxation into disk?
2 collapse episodes?
mergers?
did the first stars form before the galaxy?
what is the relationship between the thin/thick disks, bulge and halo?
etc.

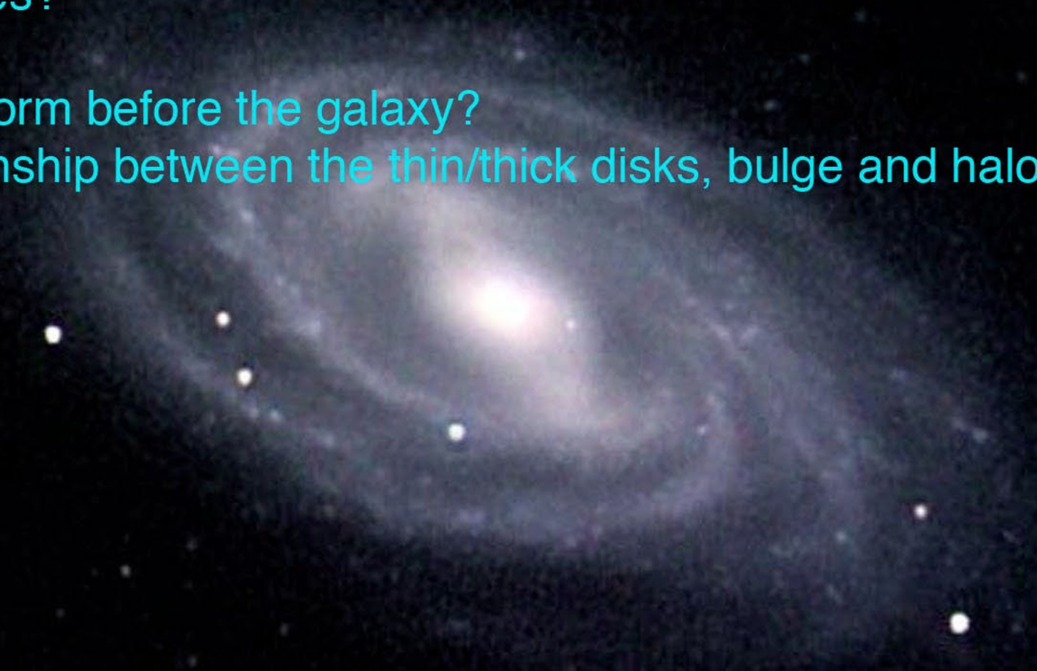

some clues from stellar evolution and nucleosynthesis
(as well as populations, kinematics, etc.)

disk:

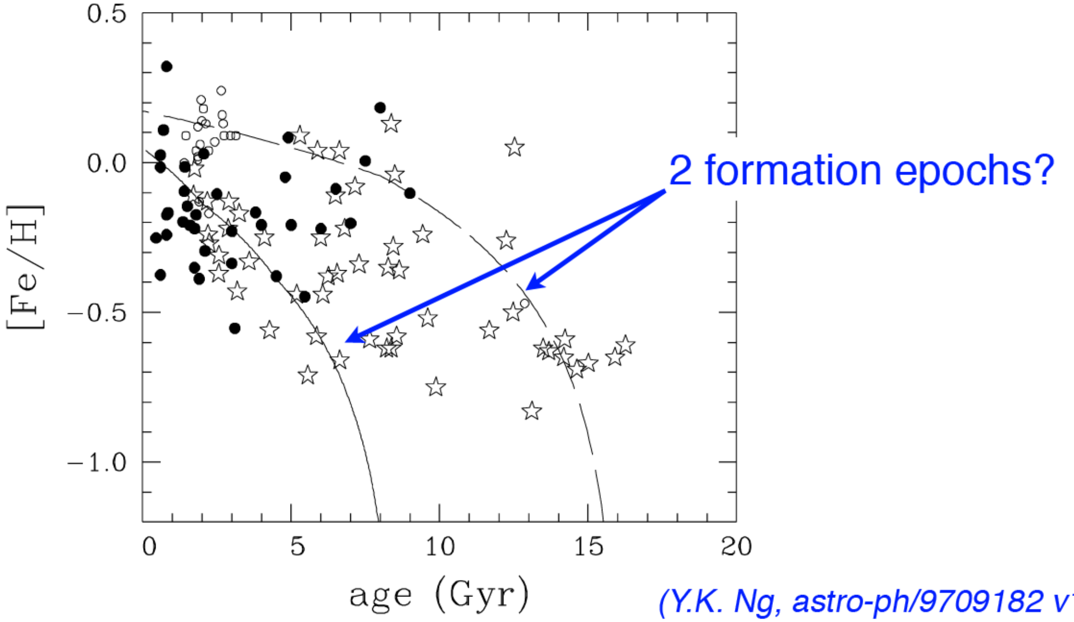

(Y.K. Ng, astro-ph/9709182 v1)

O from short-lived, massive stars (SNII);
Fe from longer-lived, lower-mass (SNIa)

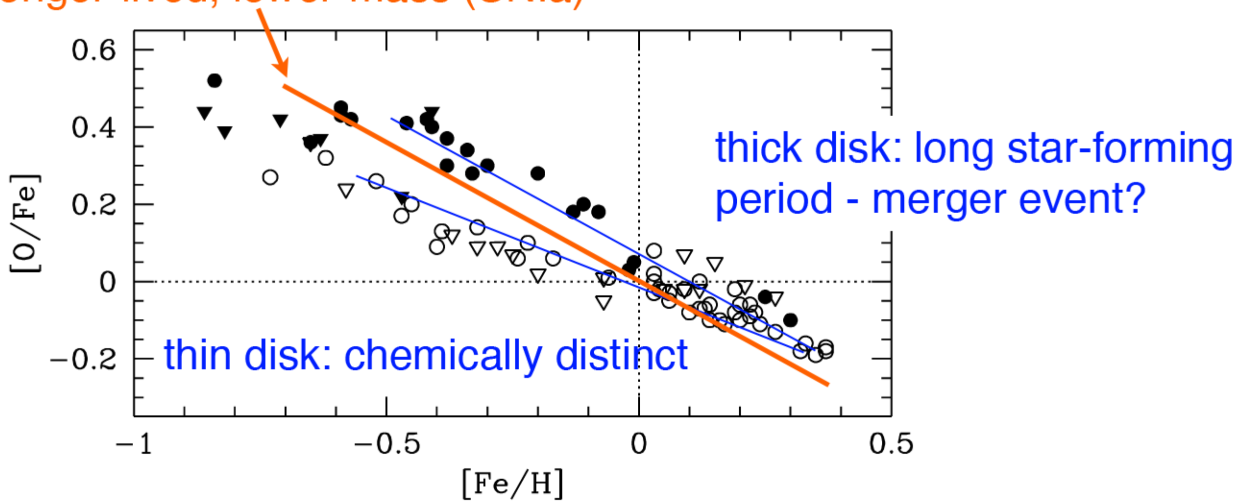

*[T. Bensby et al., Astron. Astrophys., **421**, 969 (2004)]*

halo observations:

Sloan Digital Sky Survey Scan
[H.J. Newberg and B. Yanny, astro-ph0507671 v1 (2005)]

star density for
spheroidal halo (model)

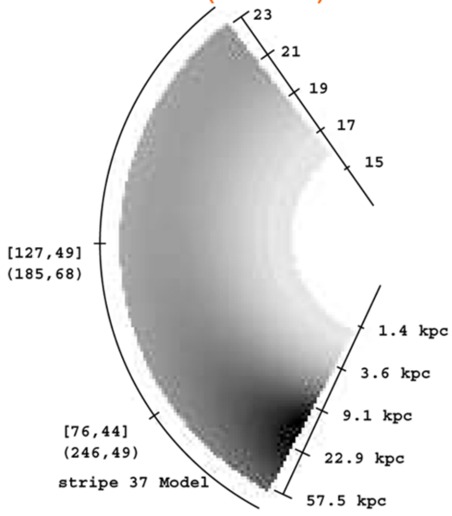

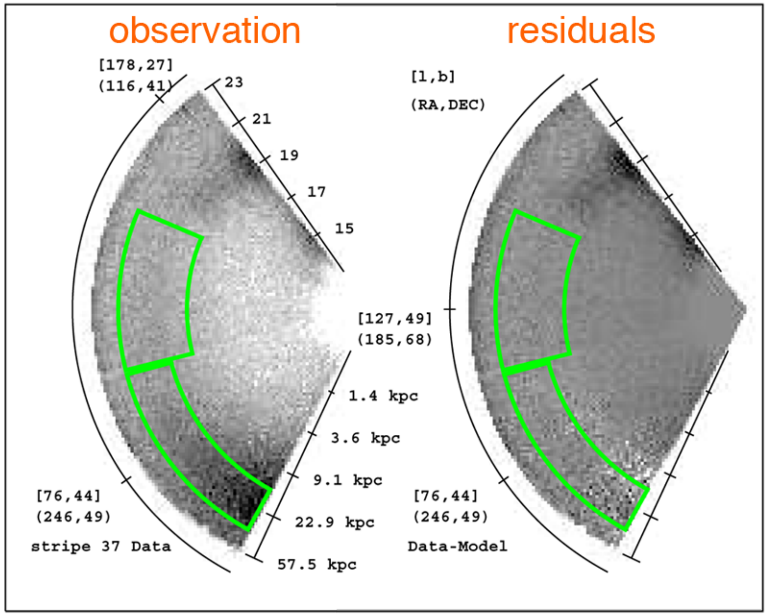

clumps and tidal streams
consistent with mergers

but:

ages of 55 globular clusters:
*M. Salaris and A. Weiss, Astron & Astrophys. **388**, 492 (2002)]*

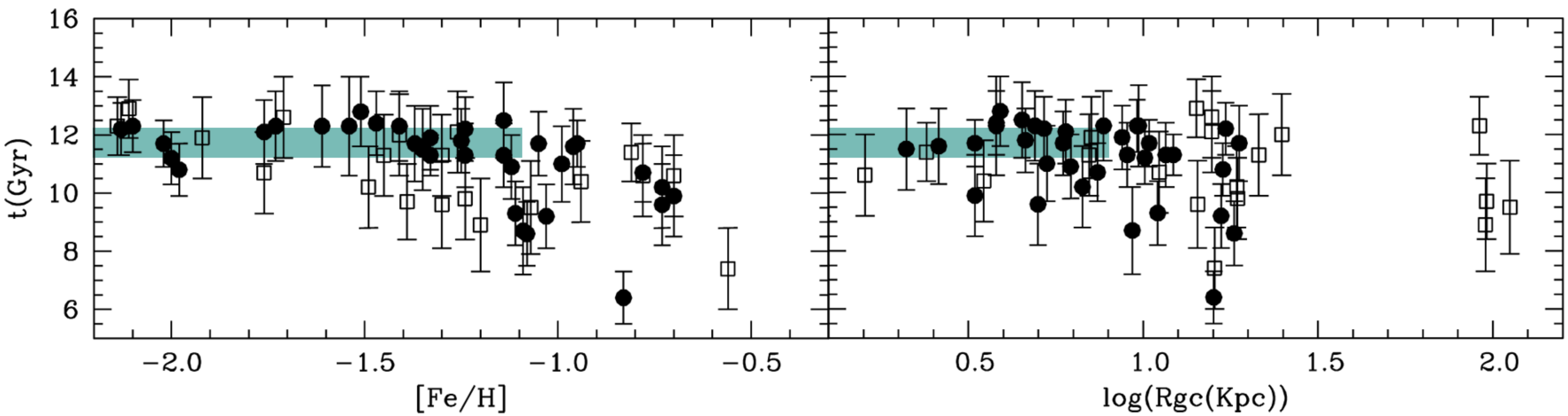

clusters with [Fe/h] <-1.2 and r< 8 kpc formed
at the same time, throughout the halo

how to measure the age of the galaxy and/or galactic timescales:

1. globular clusters
2. r-process abundances in metal-poor halo stars
3. white dwarf cooling curves

} more to come (items 1 and 2)

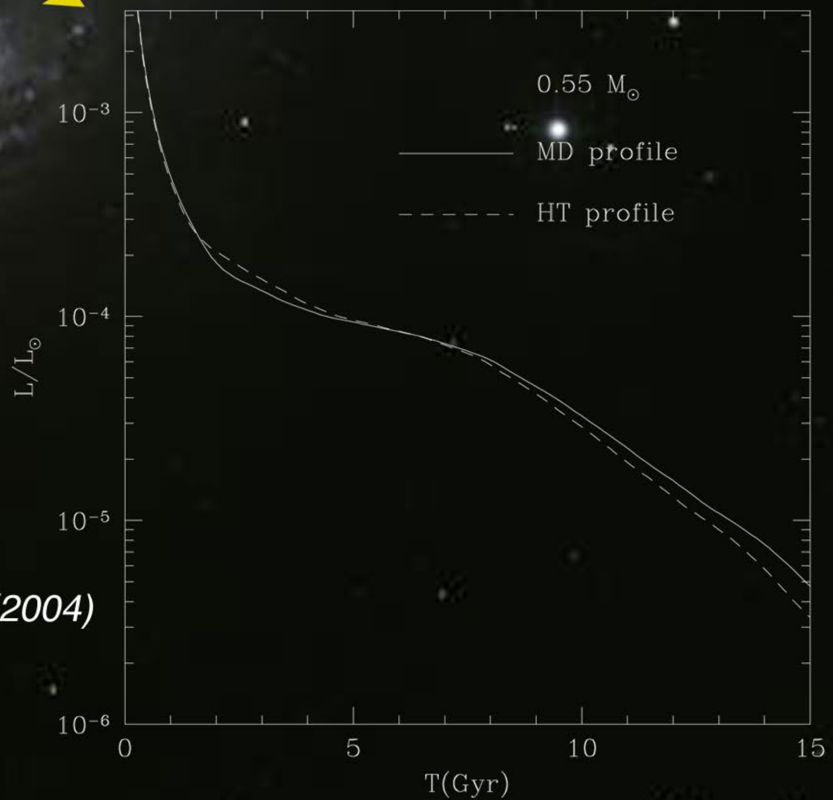

see B.M.S. Meyer et al., astro-ph/0401443 v1 (2004)

Quick tour of stellar evolution:

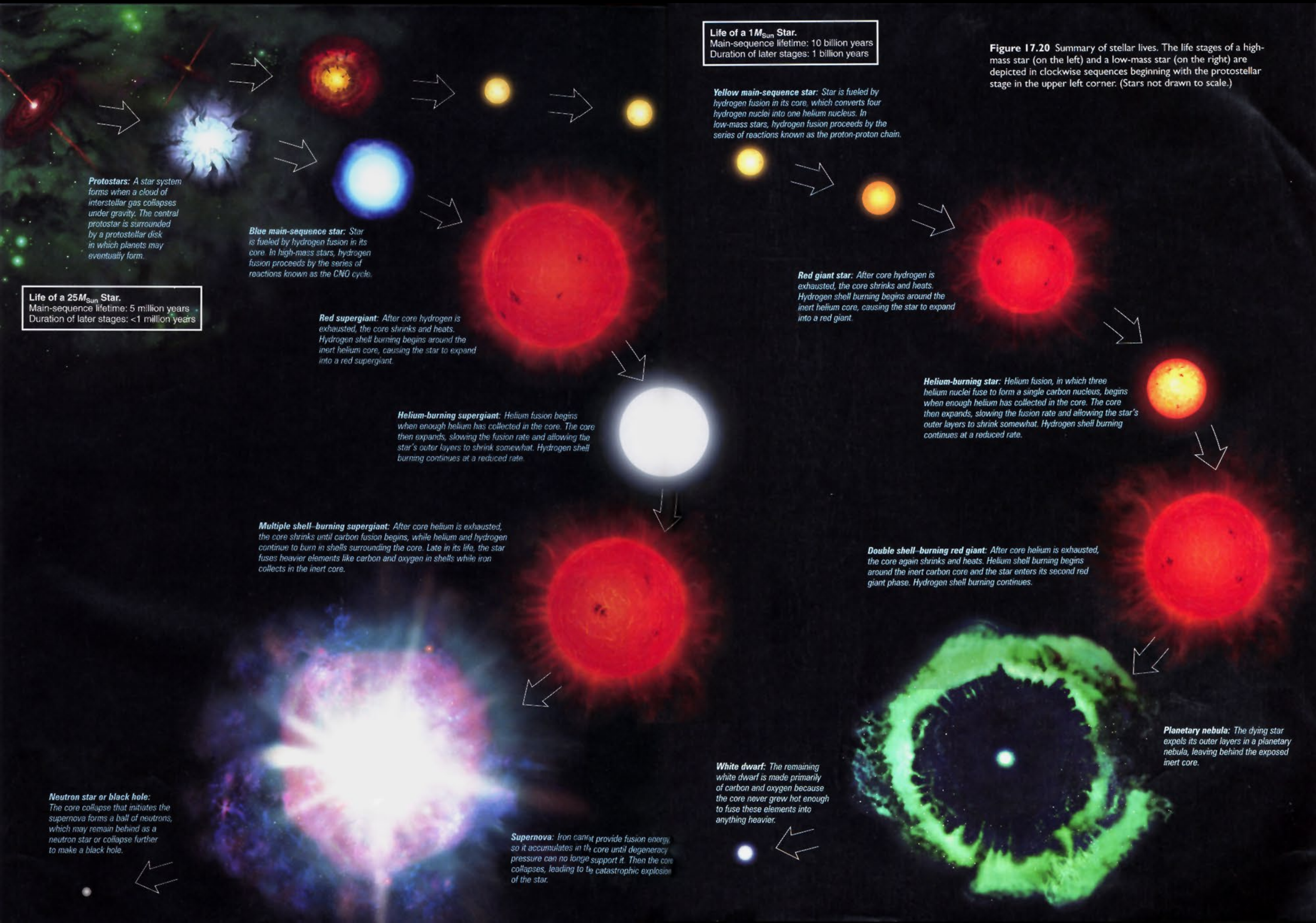

Figure 17.20 Summary of stellar lives. The life stages of a high-mass star (on the left) and a low-mass star (on the right) are depicted in clockwise sequences beginning with the protostellar stage in the upper left corner. (Stars not drawn to scale.)

visualizing stellar evolution

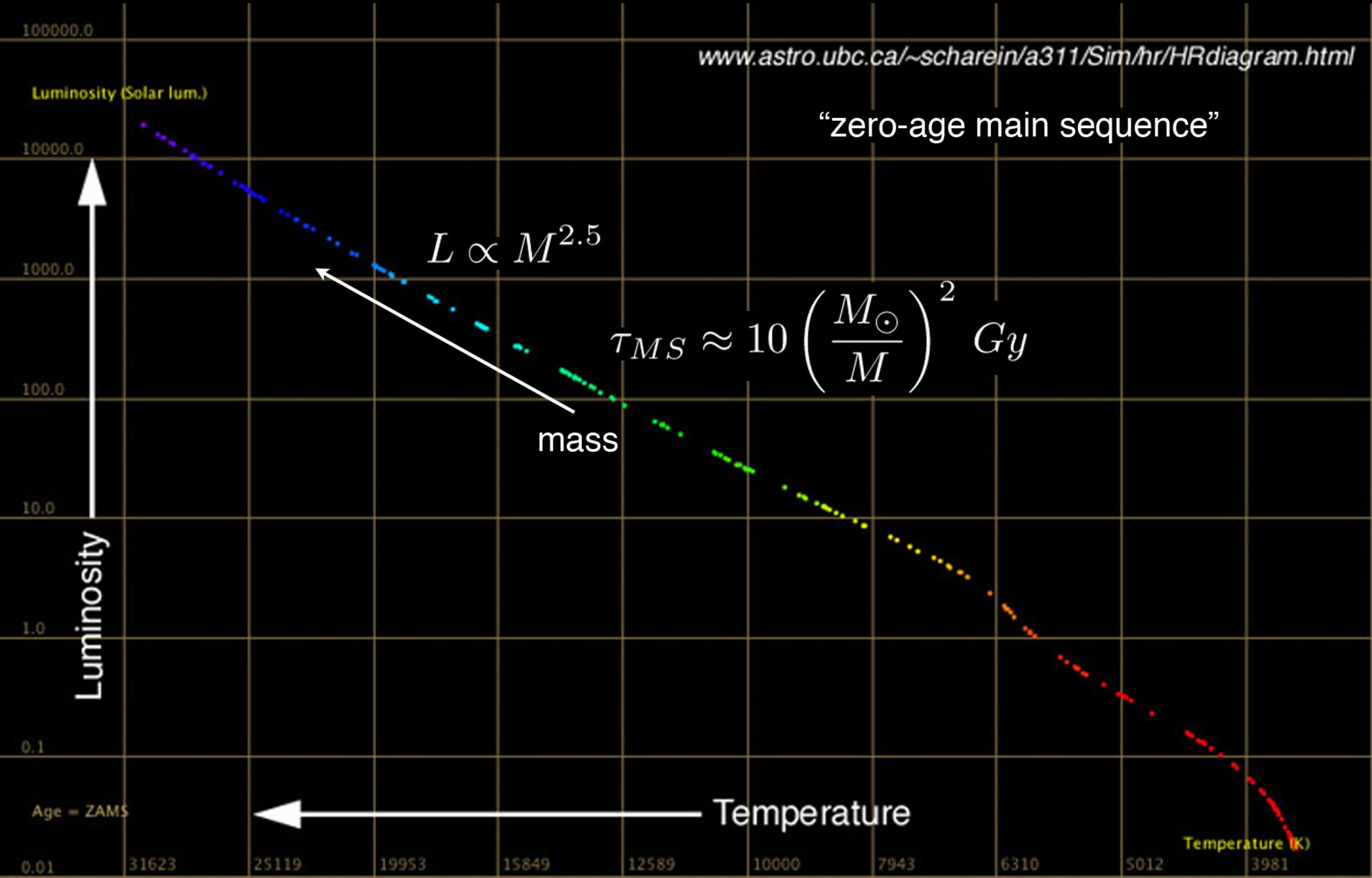

visualizing stellar evolution

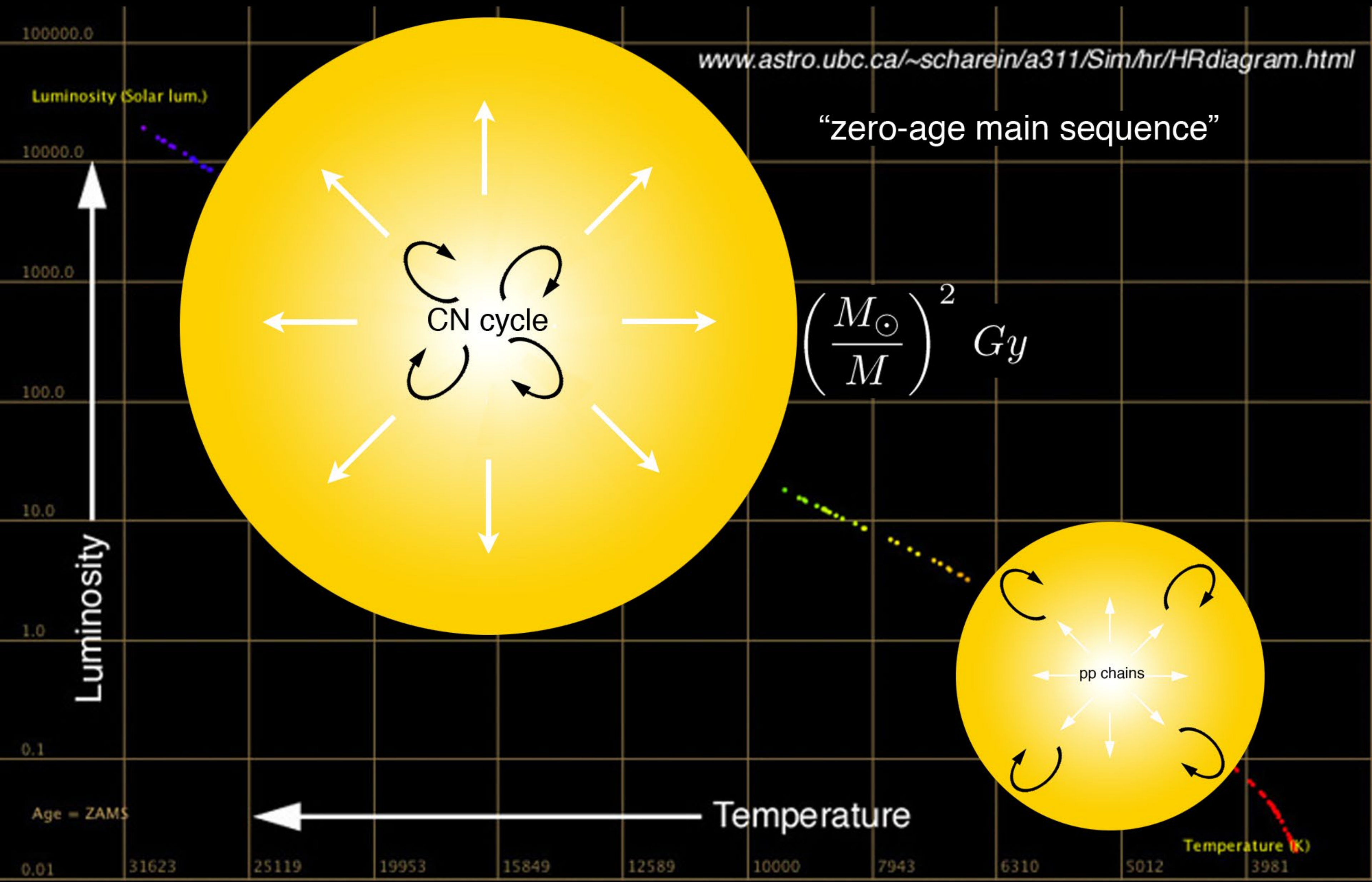

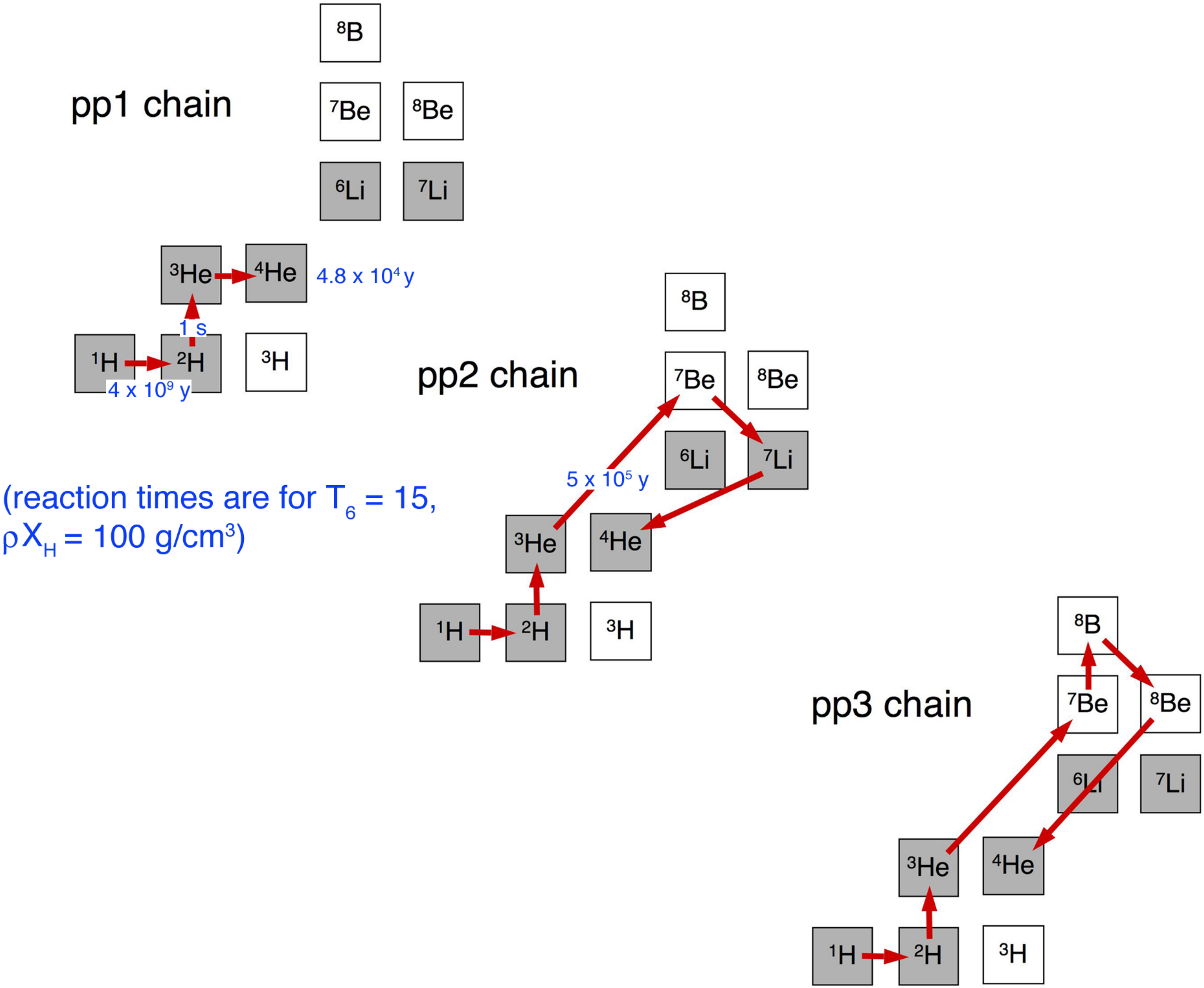
pp1 chain
8B
7Be
8Be
6Li
7Li
3He
4He
4.8 x 10^4 y
1 s
1H
2H
3H
4 x 10^9 y
pp2 chain
8B
7Be
8Be
6Li
7Li
5 x 10^5 y
3He
4He
1H
2H
3H
(reaction times are for T_6 = 15,
ρX_H = 100 g/cm^3)
pp3 chain
8B
7Be
8Be
6Li
7Li
3He
4He
1H
2H
3H

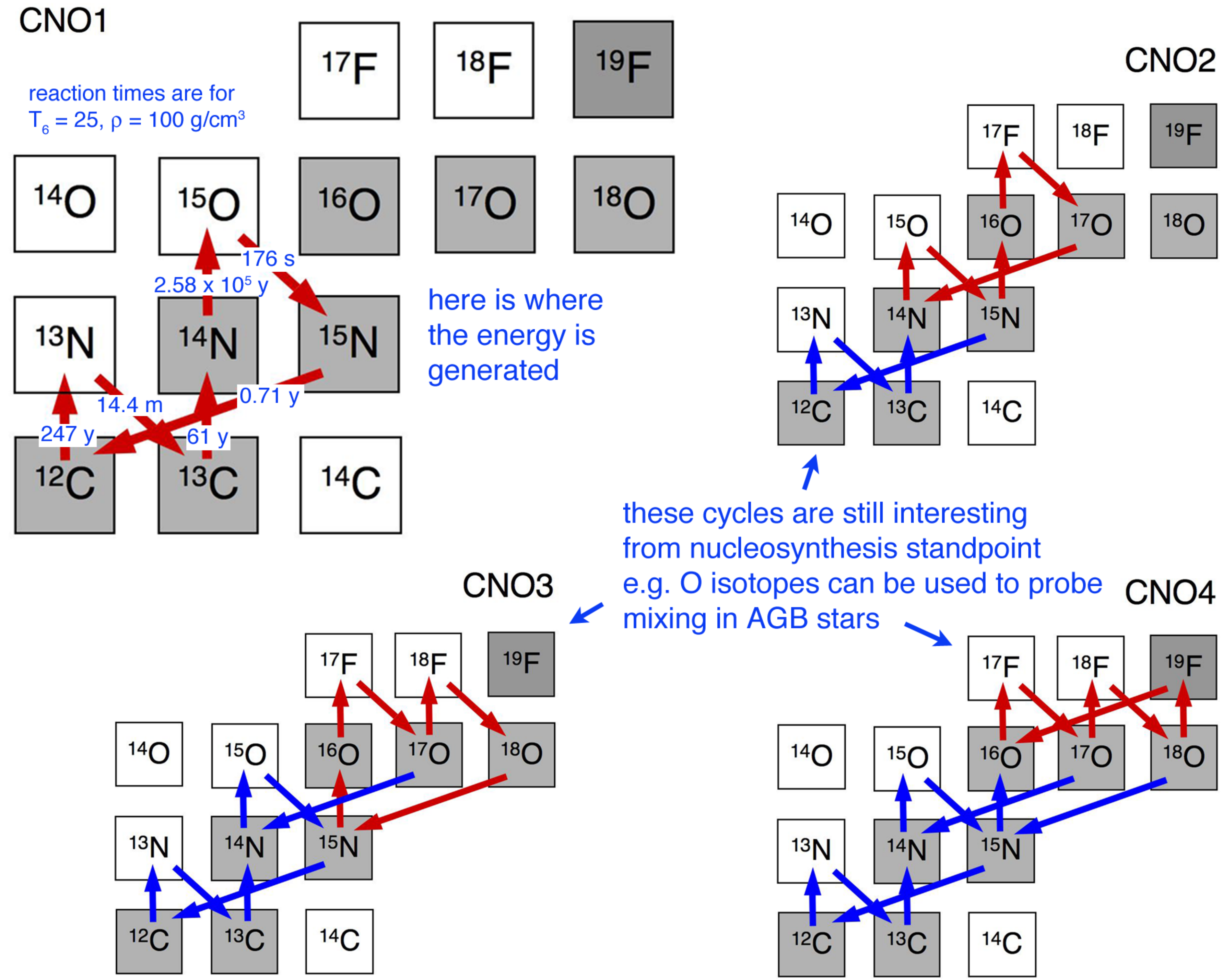
CNO1
reaction times are for
T_6 = 25, ρ = 100 g/cm^3
^{17}F
^{18}F
^{19}F
^{14}O
^{15}O
^{16}O
^{17}O
^{18}O
176 s
2.58 x 10^5 y
^{13}N
^{14}N
^{15}N
14.4 m
0.71 y
247 y
61 y
^{12}C
^{13}C
^{14}C
here is where
the energy is
generated
CNO2
these cycles are still interesting
from nucleosynthesis standpoint
e.g. O isotopes can be used to probe
mixing in AGB stars
CNO3
CNO4

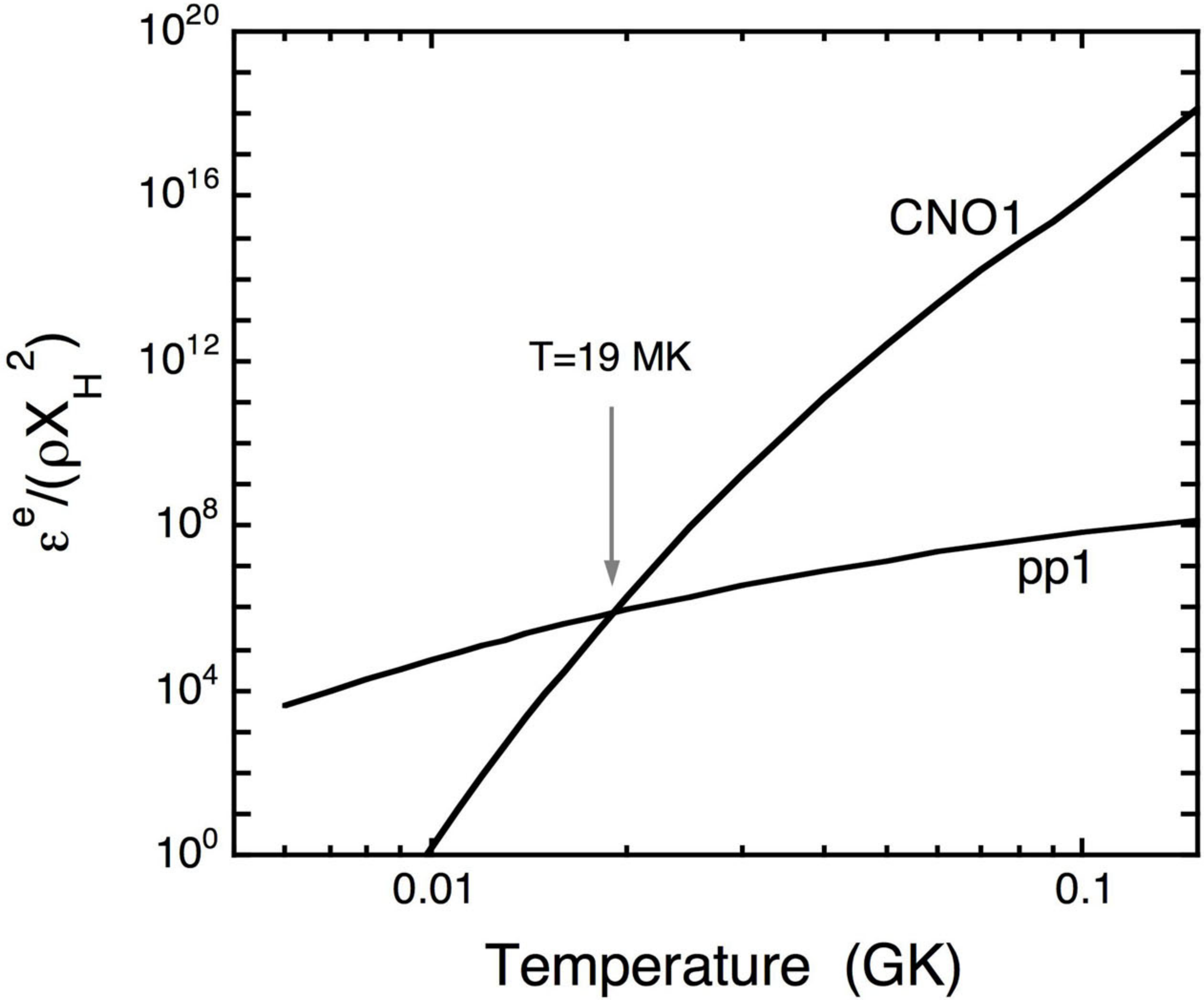

10^{20}
10^{16}
10^{12}
10^{8}
10^{4}
10^{0}
$\varepsilon^e/(\rho X_H^2)$
CNO1
T=19 MK
pp1
0.01
0.1
Temperature (GK)

later:

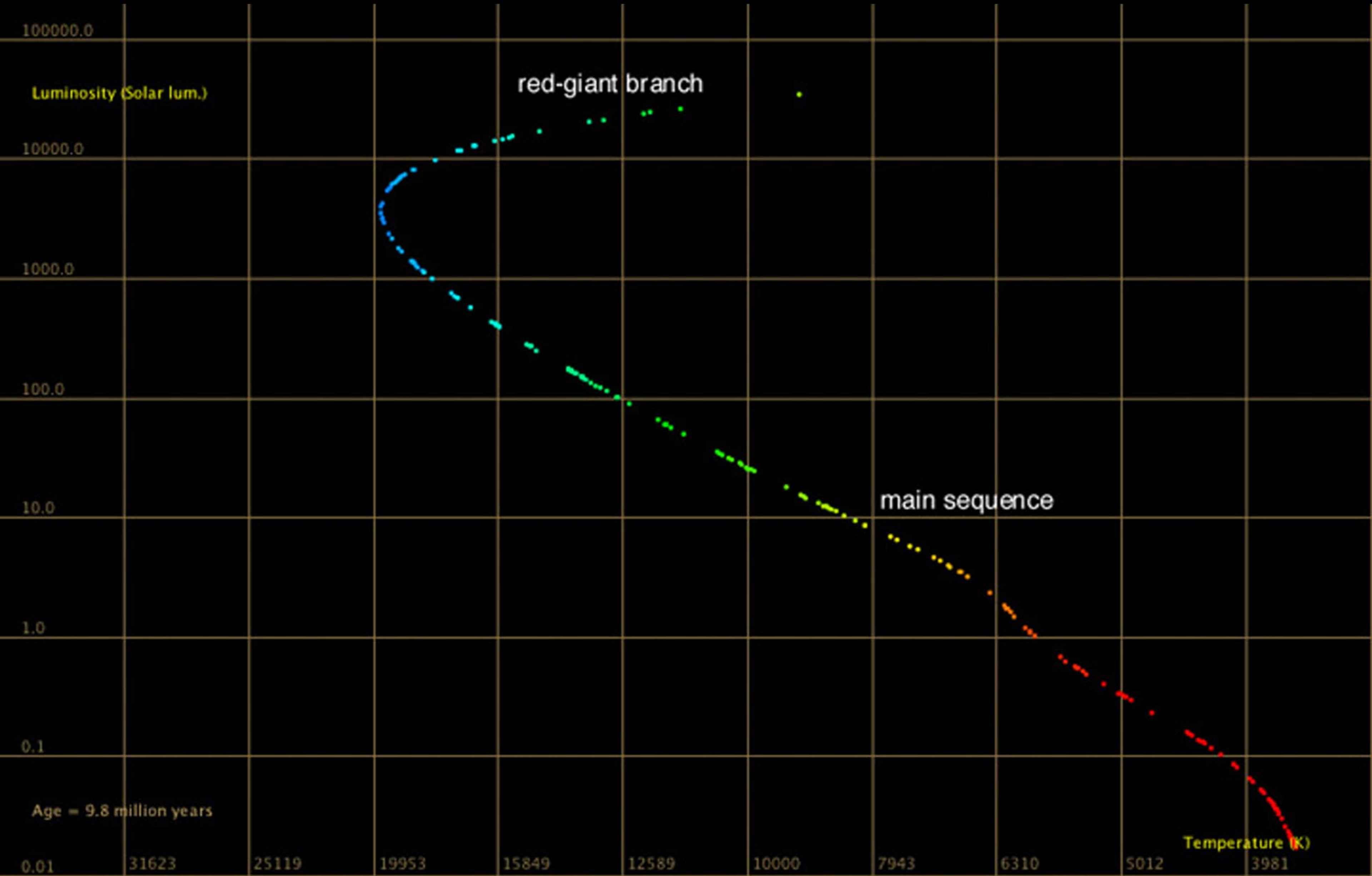
100000.0
Luminosity (Solar lum.)
red-giant branch
10000.0
1000.0
100.0
main sequence
10.0
1.0
0.1
Age = 9.8 million years
Temperature (K)
0.01
31623
25119
19953
15849
12589
10000
7943
6310
5012
3981

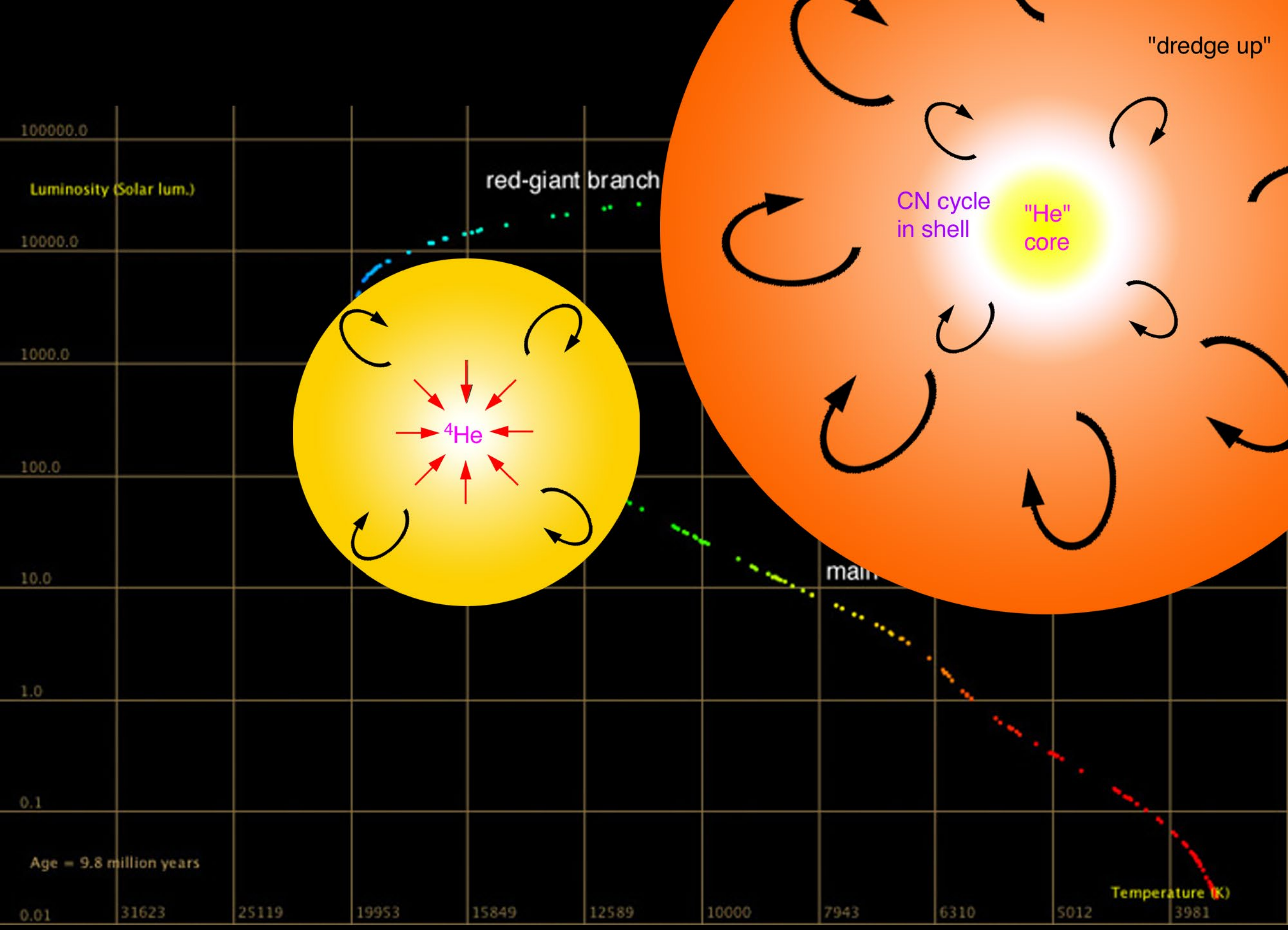
"dredge up"
100000.0
Luminosity (Solar lum.)
red-giant branch
10000.0
CN cycle
in shell
"He"
core
1000.0
100.0
^{4}He
10.0
main
1.0
0.1
Age = 9.8 million years
Temperature (K)
0.01
31623
25119
19953
15849
12589
10000
7943
6310
5012
3981


100000.0
Luminosity (Solar lum.)
10000.0
1000.0
100.0
10.0
main-sequence
turnoff
1.0
0.1
Age = 1983.7 million years
Temperature (K)
0.01
31623
25119
19953
15849
12589
10000
7943
6310
5012
3981

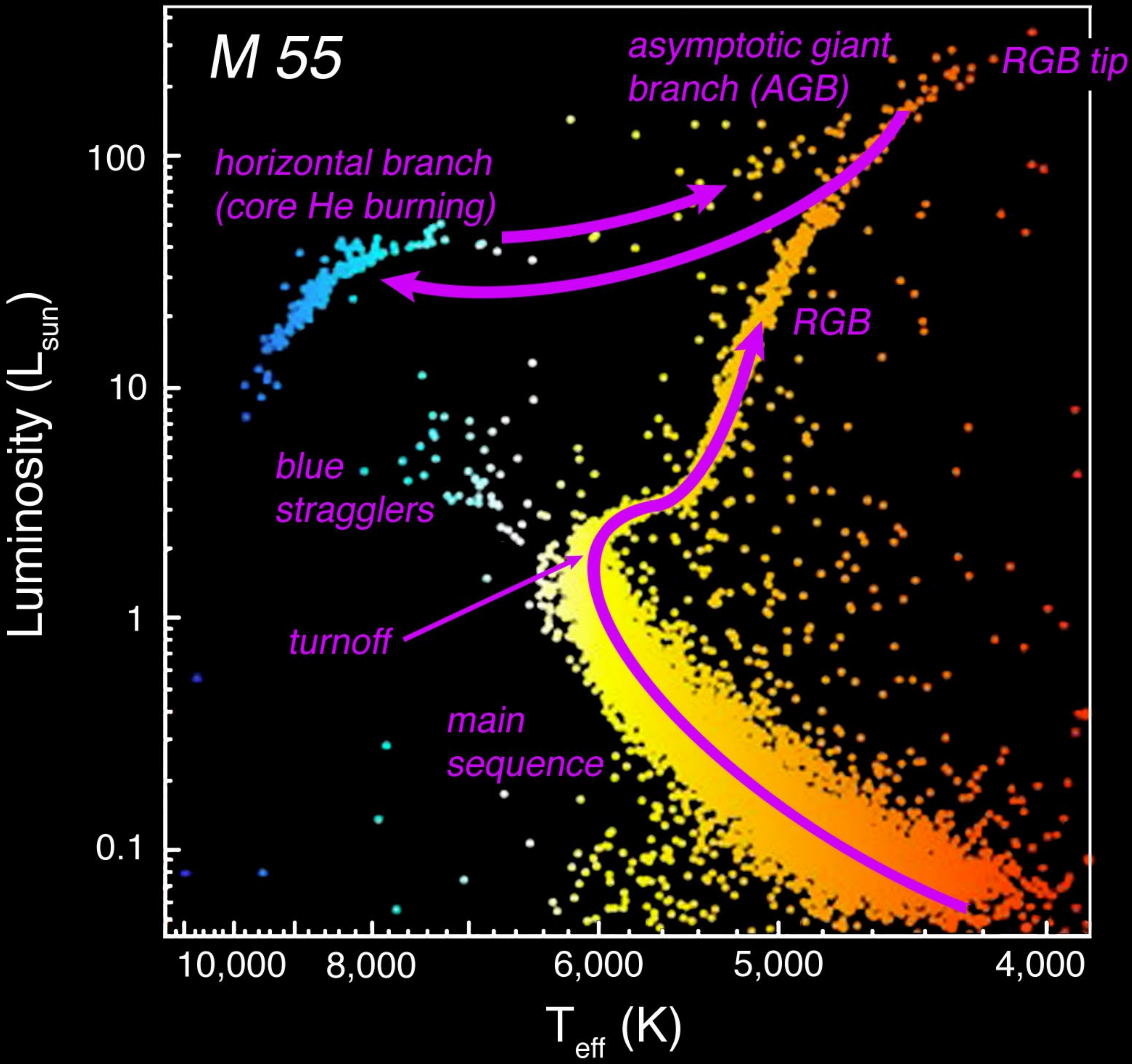
adapted from B.J. Mochejska, J. Kaluzny (CAMK), 1m Swope Telescope
M 55
asymptotic giant branch (AGB)
RGB tip
horizontal branch (core He burning)
RGB
blue stragglers
turnoff
main sequence
Luminosity (L_{sun})
100
10
1
0.1
10,000
8,000
6,000
5,000
4,000
T_{eff} (K)

the sun

red-giant
phase

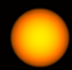

horizontal branch

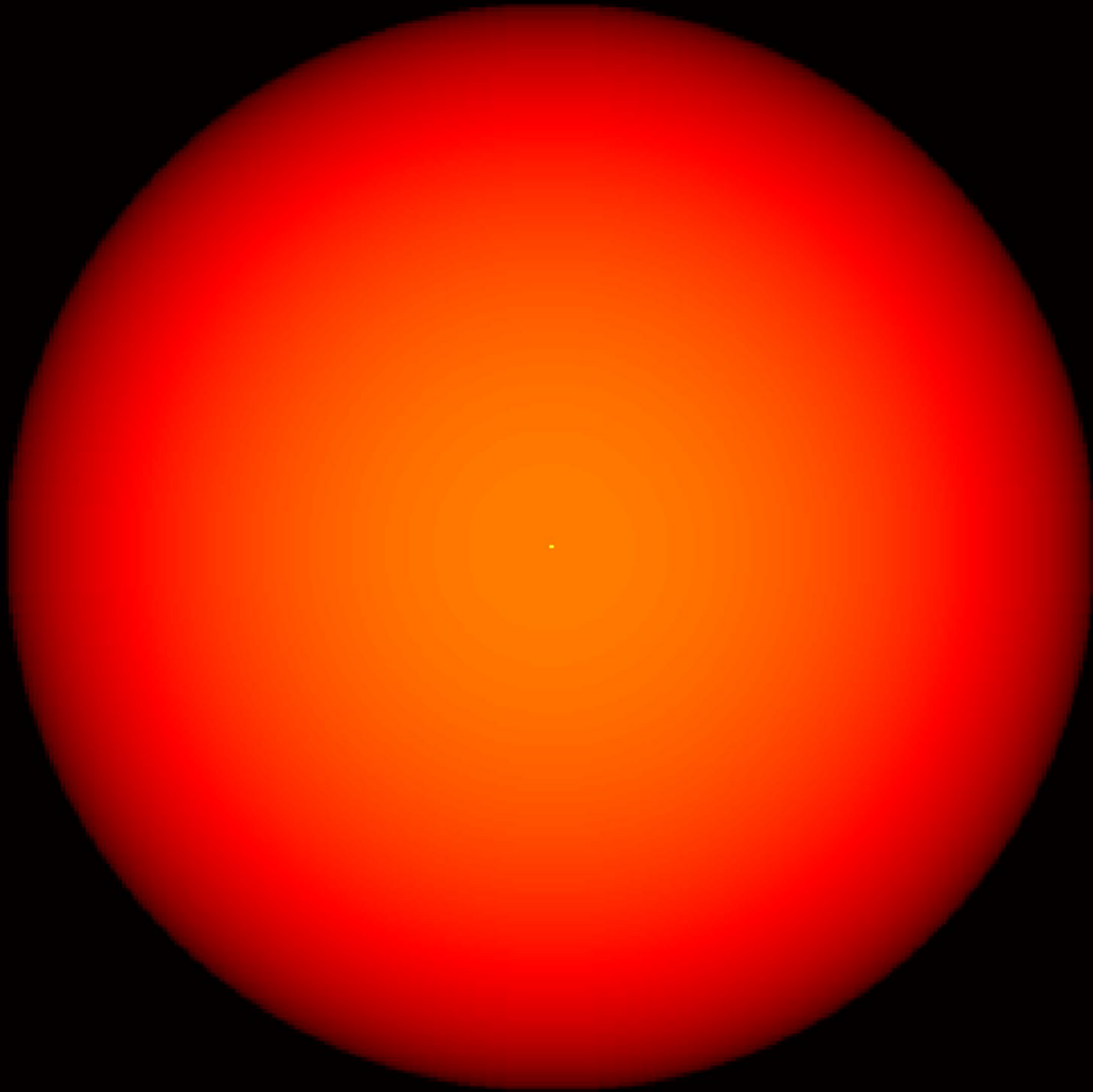

AGB

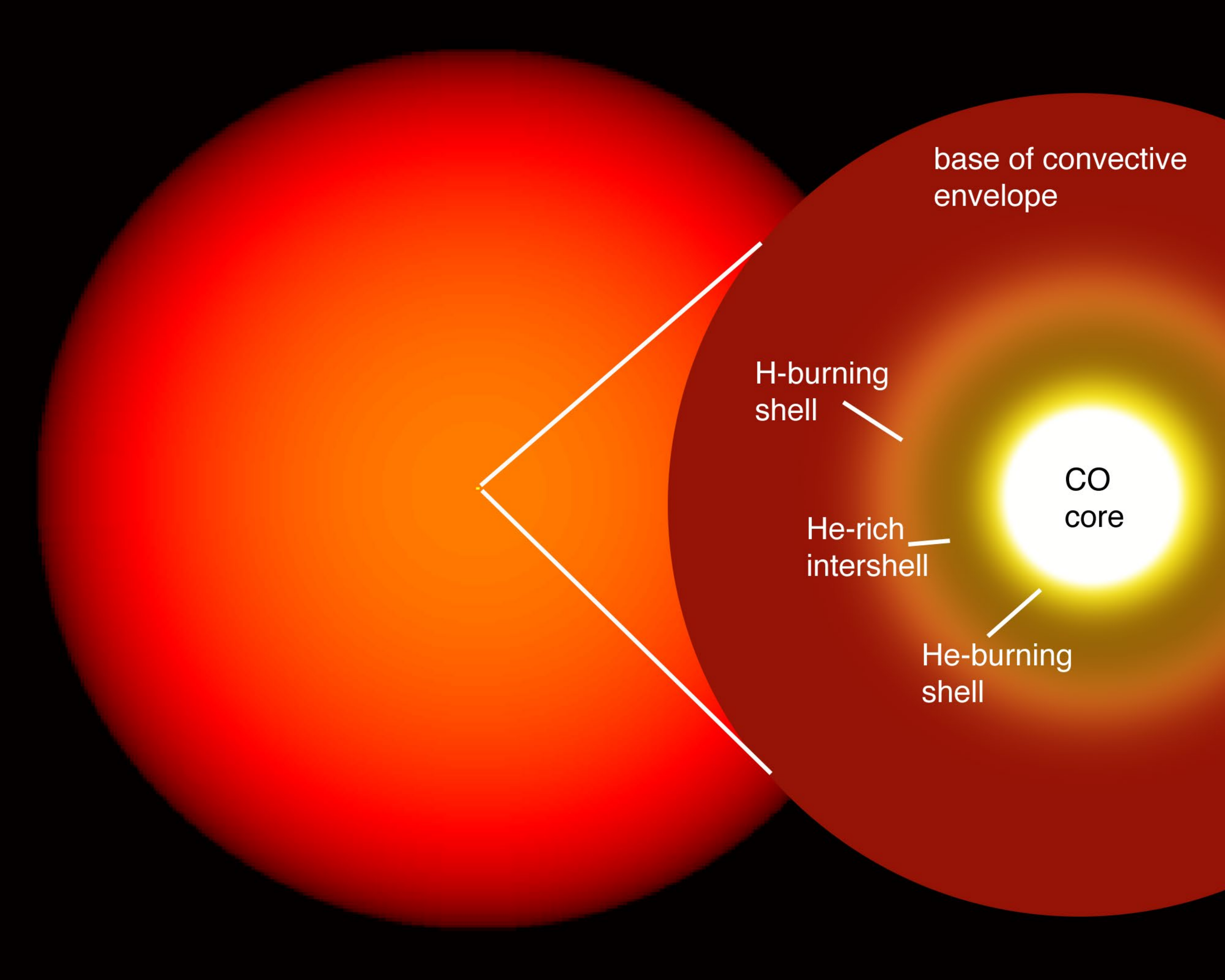
base of convective envelope
H-burning shell
He-rich intershell
CO core
He-burning shell

Planetary Nebula Mz 3

Hubble Heritage

NASA, ESA, and The Hubble Heritage Team (STScI/AURA) • Hubble Space Telescope WFPC2 • STScI-PRC01-05


ages of globular clusters
(this is M53)

Globular clusters are coeval, chemically homogeneous groups of 10^3 - 10^6 stars

They provide an integrated sequence of stellar evolution

Their kinematics and ages trace out the evolution of structure in the galaxy

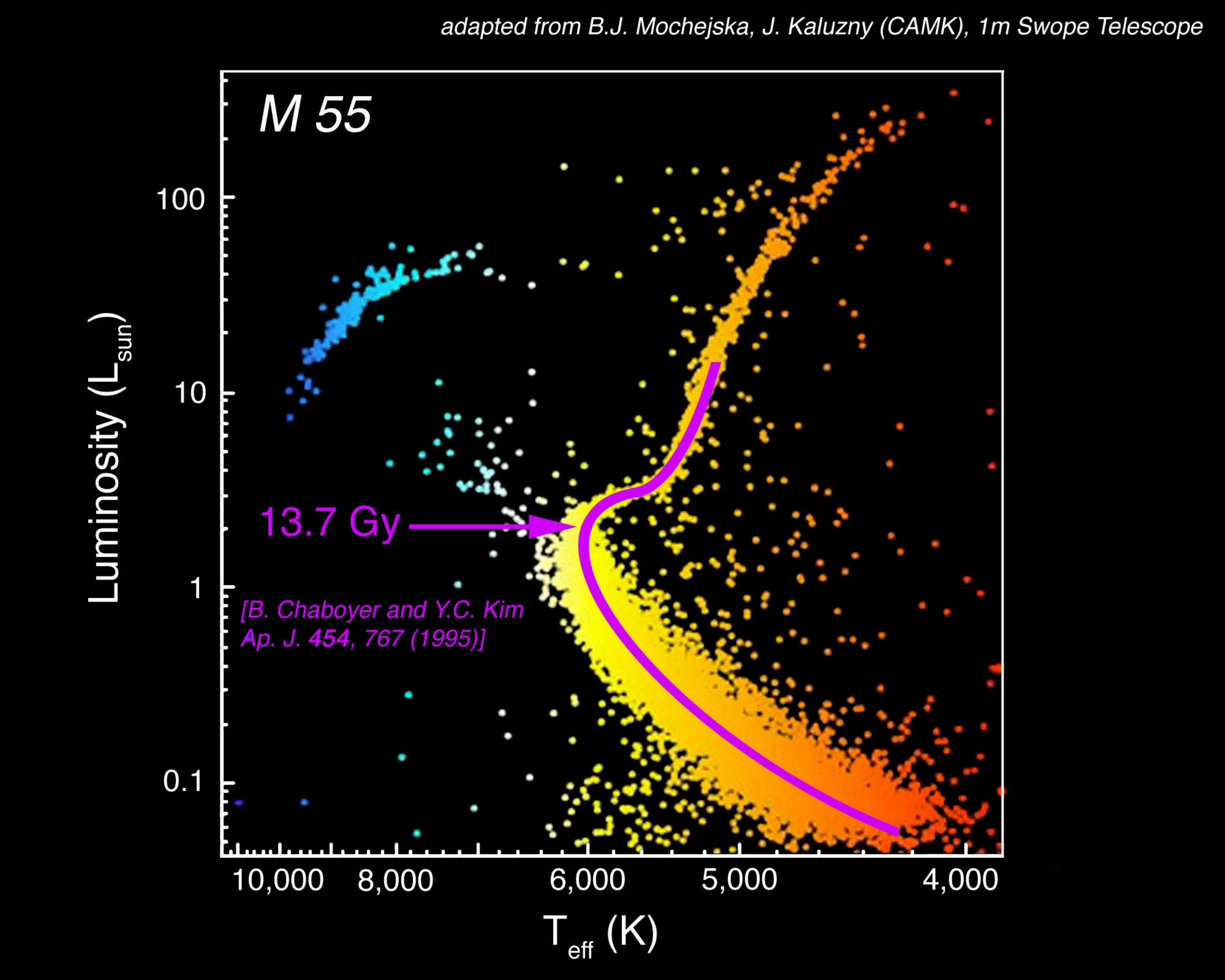
adapted from B.J. Mochejska, J. Kaluzny (CAMK), 1m Swope Telescope
M 55
100
10
1
0.1
Luminosity (L_{sun})
13.7 Gy
[B. Chaboyer and Y.C. Kim
Ap. J. 454, 767 (1995)]
10,000
8,000
6,000
5,000
4,000
T_{eff} (K)

distance scale: affects absolute luminosity - only a few parallax measurements, t/L relationship for RR-Lyraes...

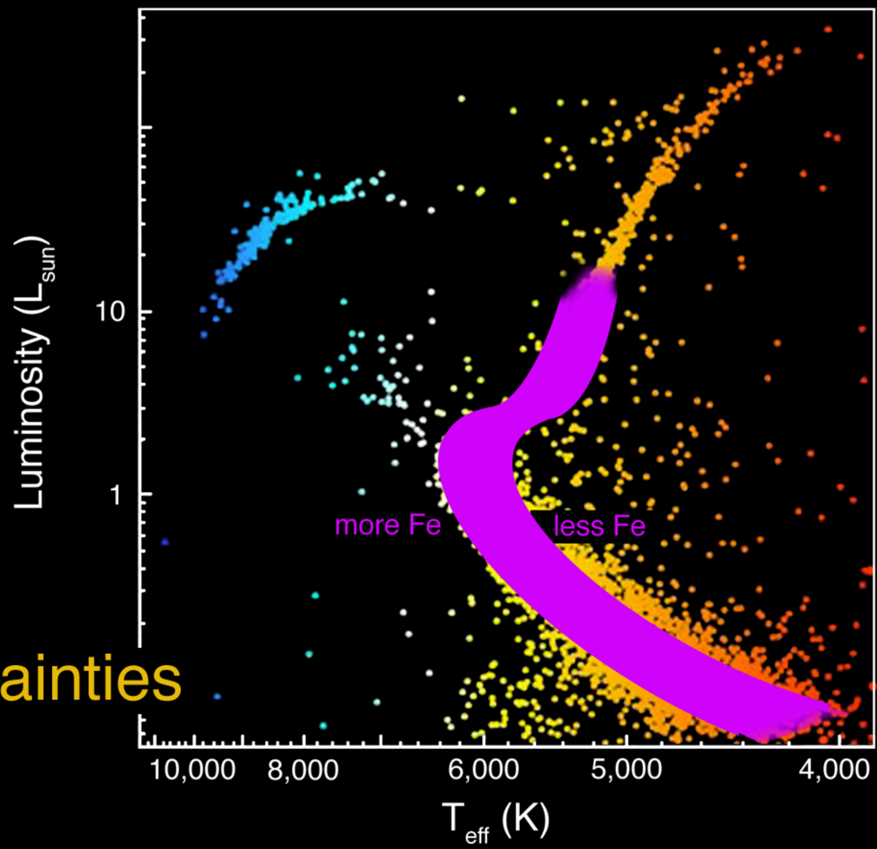

He abundance: more He, less H; when does CN cycle take over?

convection: use mixing-length theory; if dT/dr increases, then radius decreases and T_{eff} goes up

uncertainties

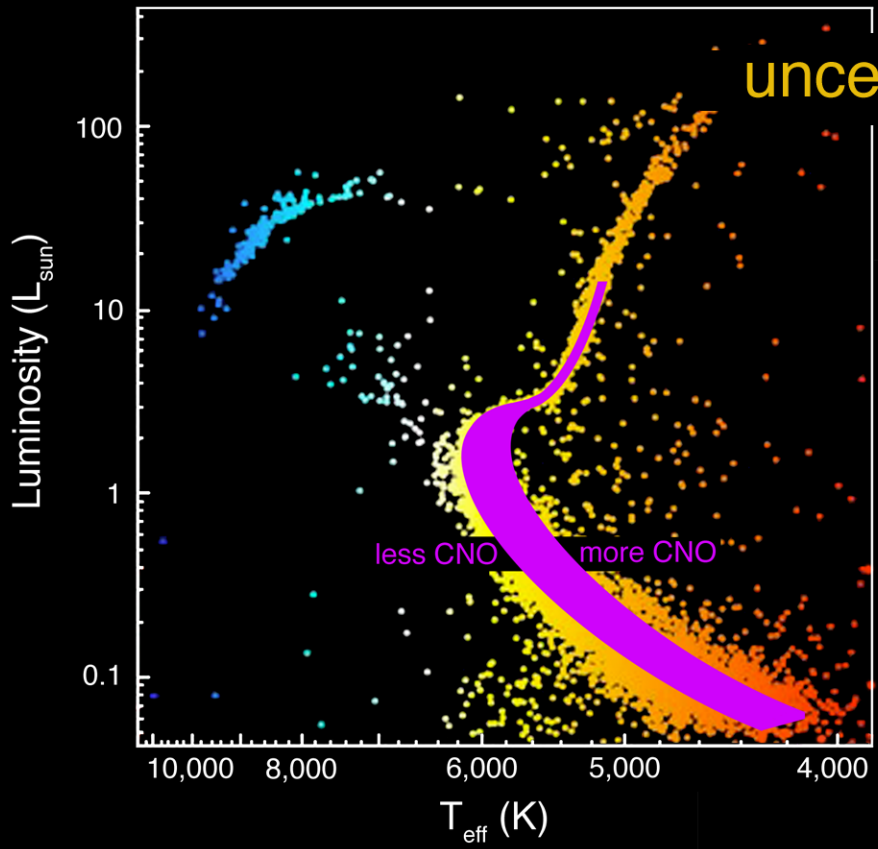

opacity: affects size of envelope, T_{eff}

diffusion: decreases H abundance, reduces τ_{ms}

$^{14}N(p,\gamma)^{15}O$: regulates power in CN cycle, affects L_{TO}

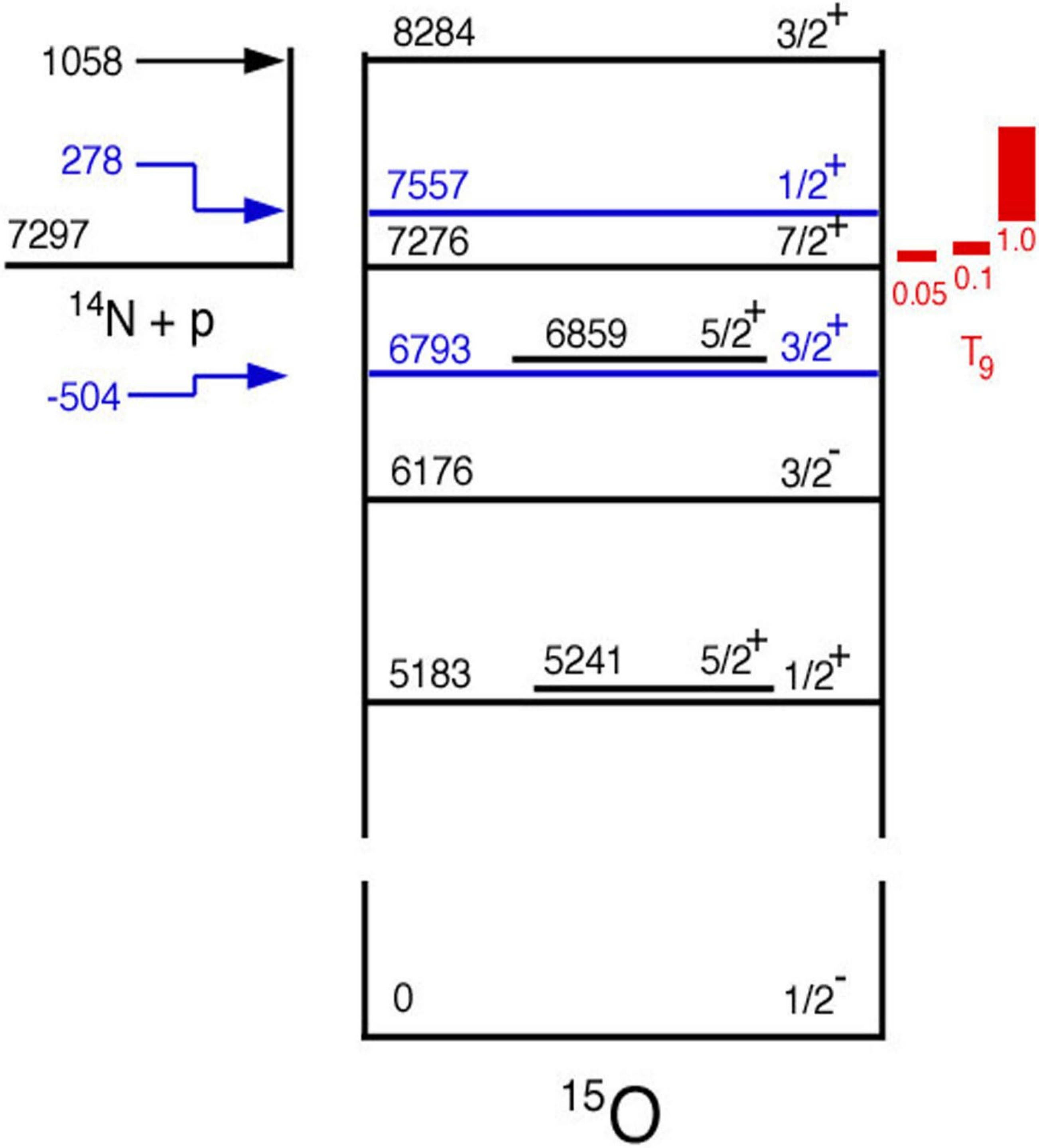

8284 3/2+
1058
278
7557 1/2+
7297
7276 7/2+
1.0
0.05
0.1
14N + p
6793
6859 5/2+
3/2+
T9
-504
6176 3/2-
5183
5241 5/2+
1/2+
0 1/2-
15O

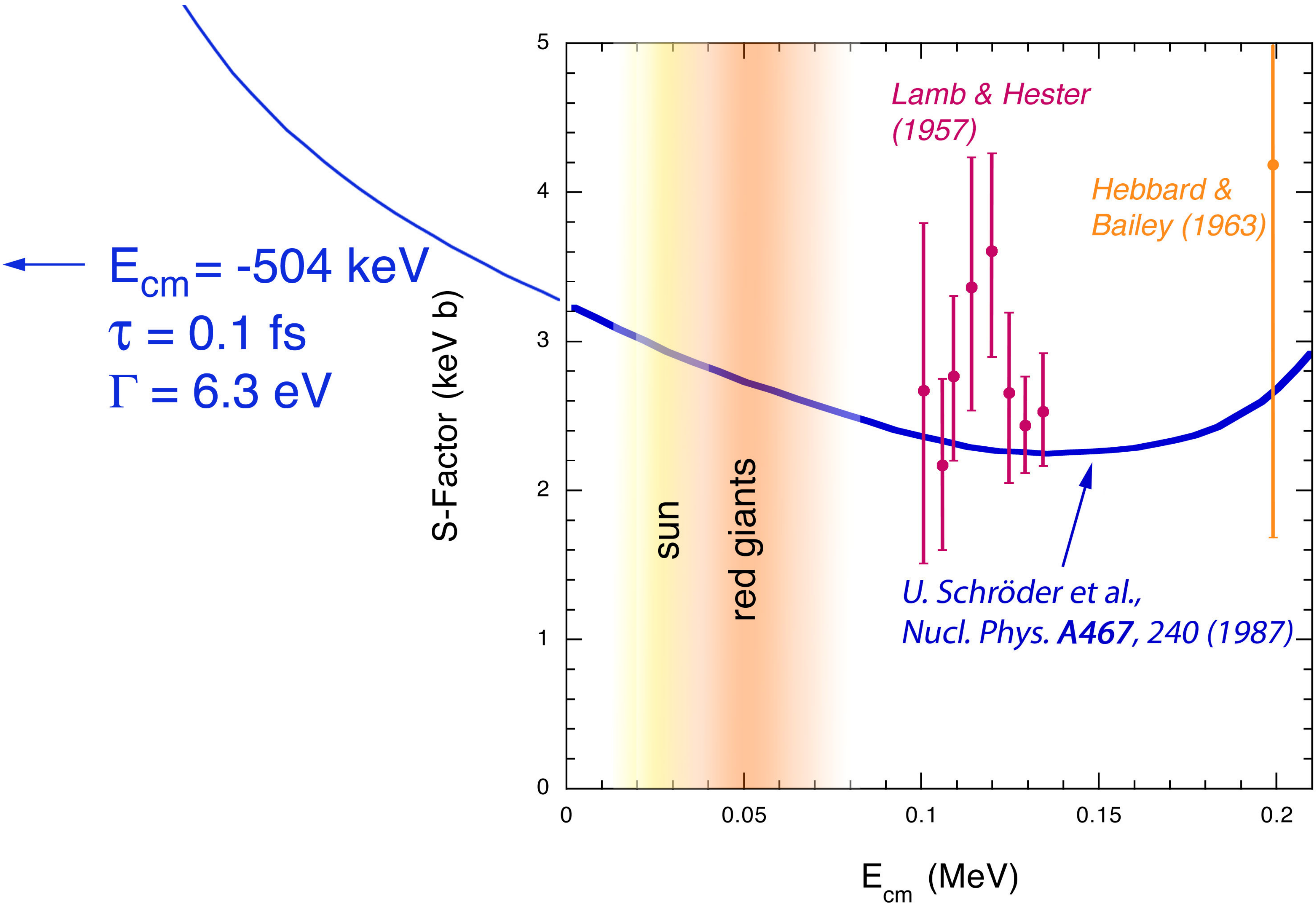

E_cm = -504 keV
τ = 0.1 fs
Γ = 6.3 eV
S-Factor (keV b)
sun
red giants
Lamb & Hester (1957)
Hebbard & Bailey (1963)
U. Schröder et al., Nucl. Phys. A467, 240 (1987)
E_cm (MeV)
0
0.05
0.1
0.15
0.2
1
2
3
4
5

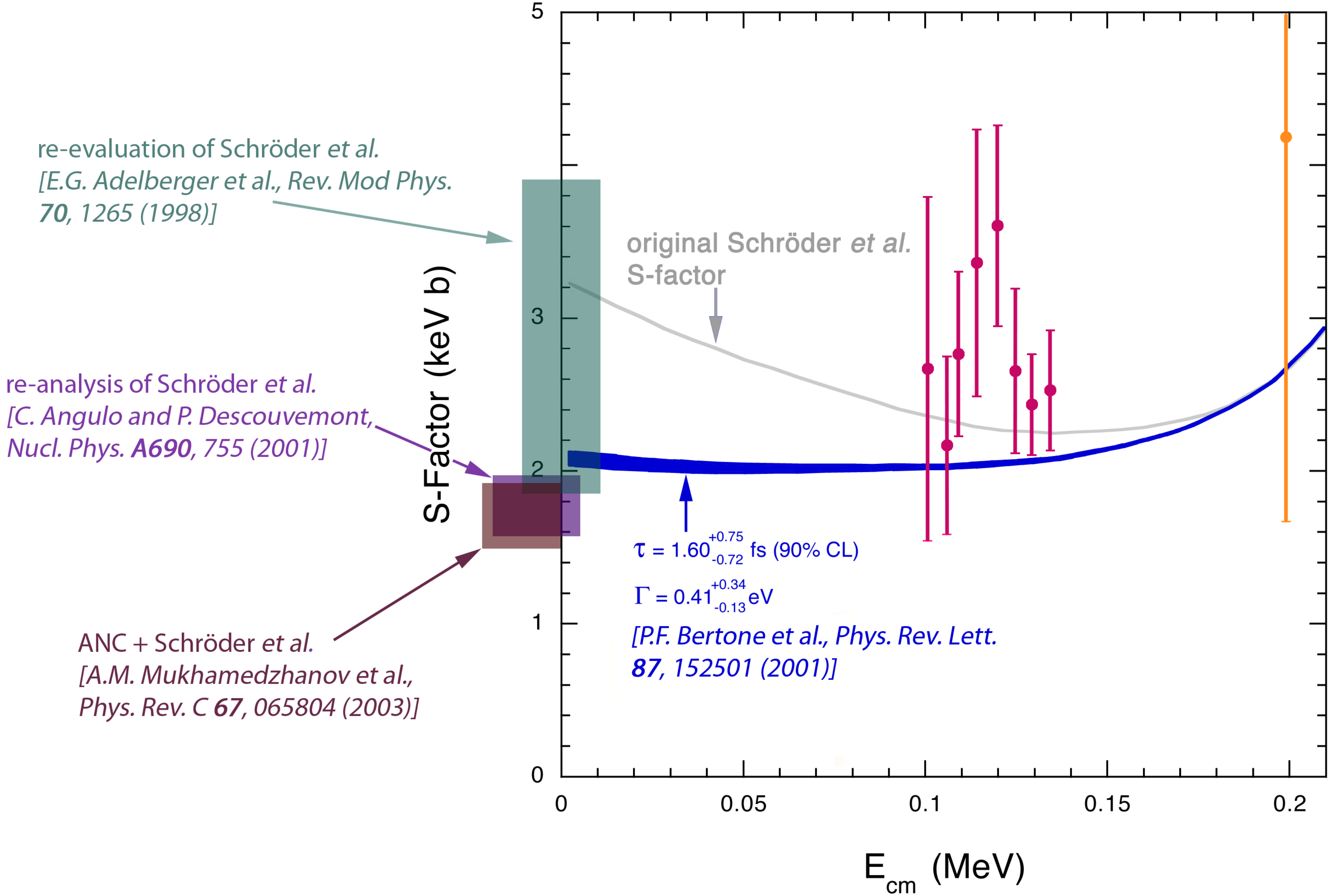
re-evaluation of Schröder et al.
[E.G. Adelberger et al., Rev. Mod Phys. 70, 1265 (1998)]
original Schröder et al. S-factor
re-analysis of Schröder et al.
[C. Angulo and P. Descouvemont, Nucl. Phys. A690, 755 (2001)]
ANC + Schröder et al.
[A.M. Mukhamedzhanov et al., Phys. Rev. C 67, 065804 (2003)]
τ = 1.60 +0.75 -0.72 fs (90% CL)
Γ = 0.41 +0.34 -0.13 eV
[P.F. Bertone et al., Phys. Rev. Lett. 87, 152501 (2001)]
S-Factor (keV b)
E cm (MeV)
0
1
2
3
5
0.05
0.1
0.15
0.2

LUNA2 (400 kV)

Voltage Range :
50 - 400 kV

Output Current: 1 mA 75% H
(@ 400 kV) 25% H_2
: 500 μA ^{4}He

Beam energy spread:
76 eV

Long term stability (1 h) :
10 eV

Terminal Voltage ripple:
10 Vpp

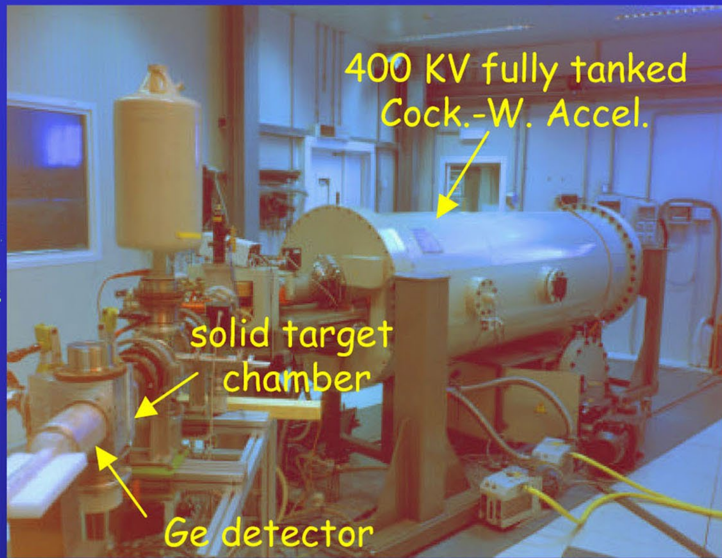

200-kV ECR

1-MV van de Graaff

LENA

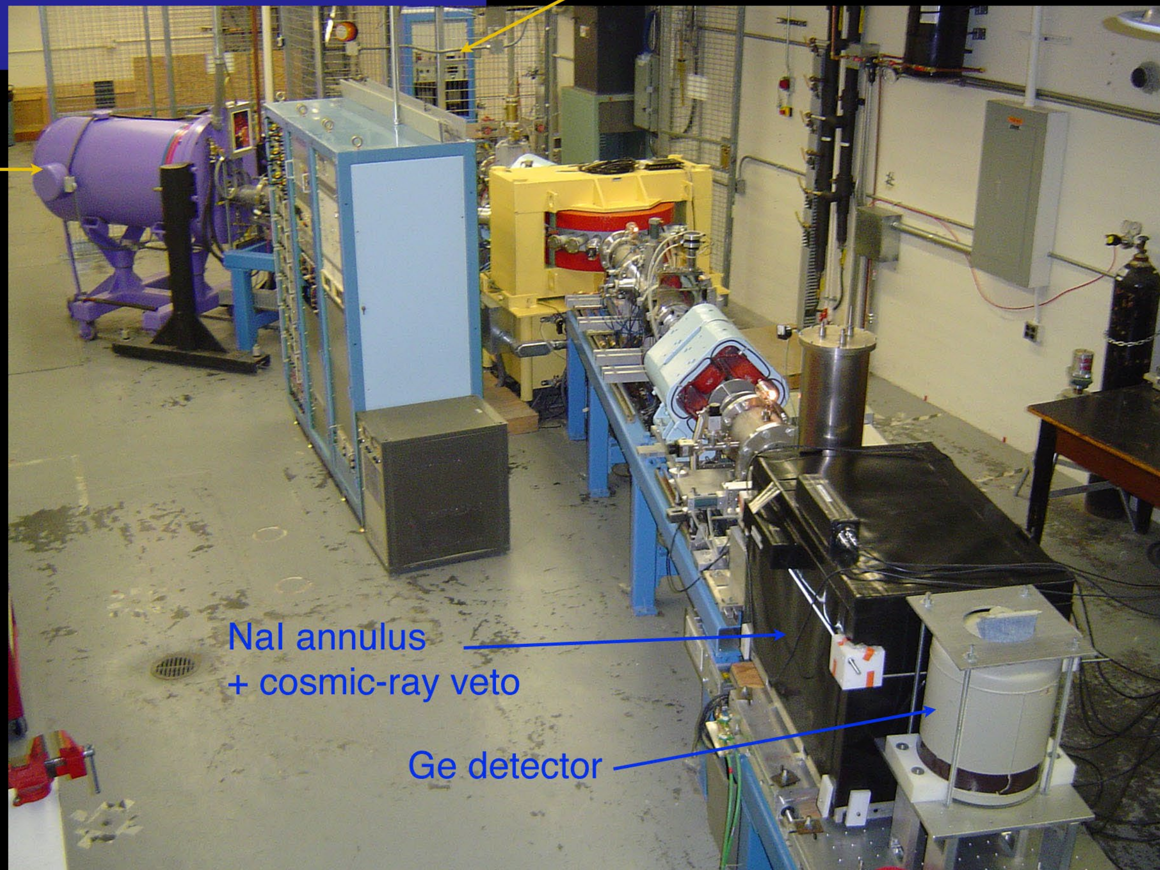

classical approach:

$$\text{figure of merit} = \frac{\text{signal rate}}{\sqrt{\text{background rate}}}$$

sources of background:

1. beam (always present at some level)

2. natural radioactivity (up to ~3 MeV; suppress with passive shielding)

3. cosmic rays (direct interactions of muons, neutrons, muon-induced bremsstrahlung, etc. ; suppress with active shield or move underground)

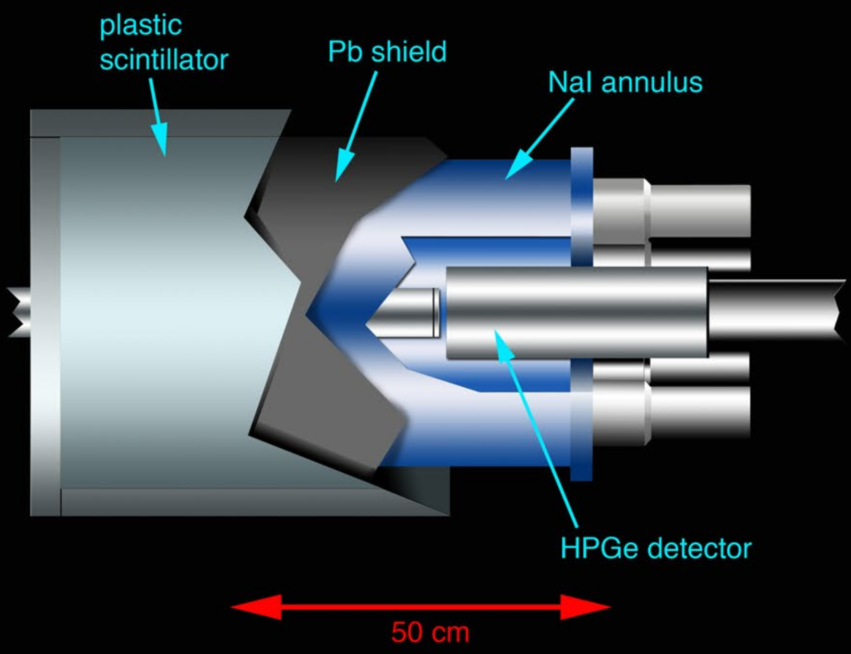

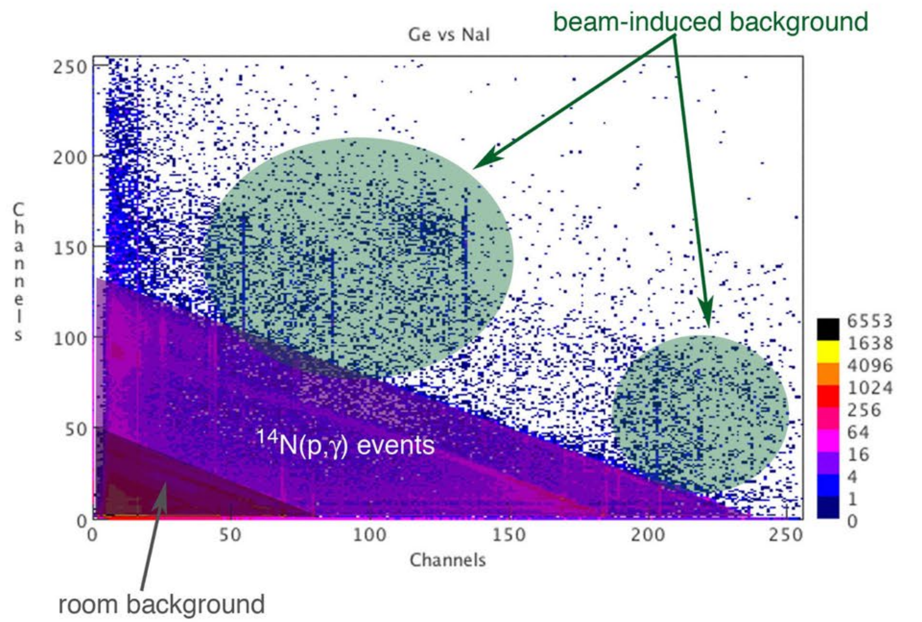

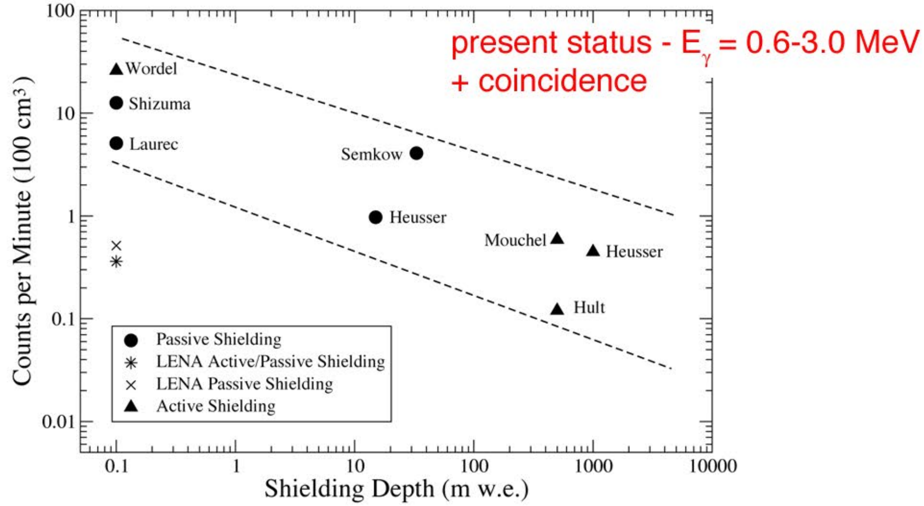

future improvements:

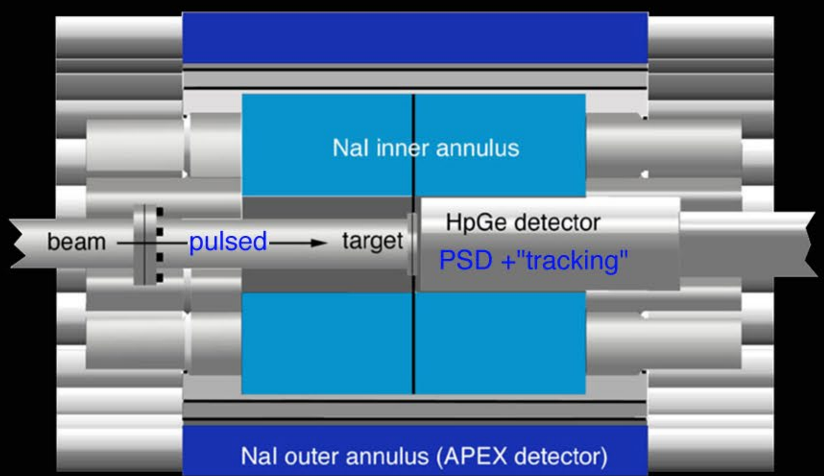

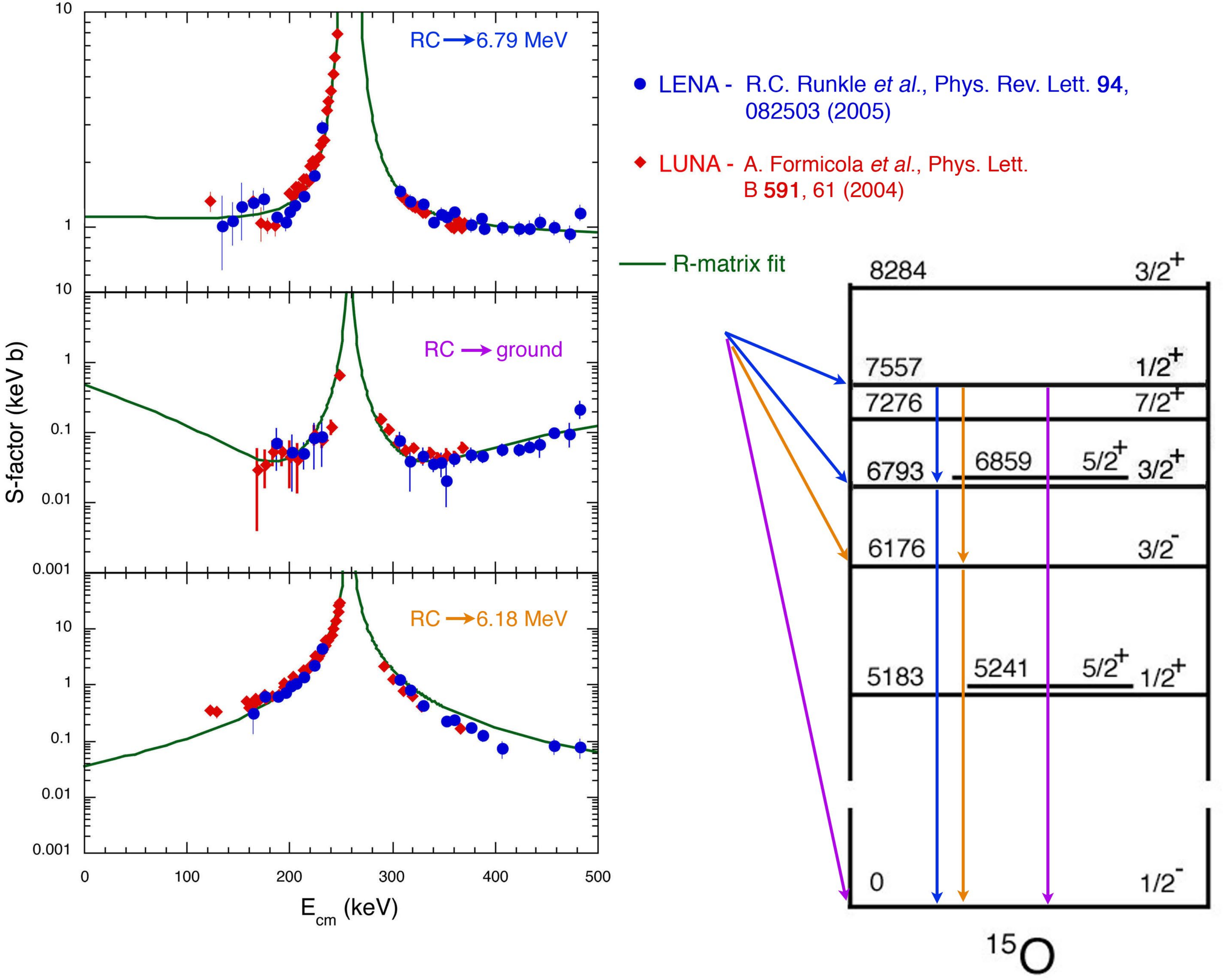

RC → 6.79 MeV
RC → ground
RC → 6.18 MeV
S-factor (keV b)
E_cm (keV)
LENA - R.C. Runkle et al., Phys. Rev. Lett. 94, 082503 (2005)
LUNA - A. Formicola et al., Phys. Lett. B 591, 61 (2004)
R-matrix fit
8284 3/2+
7557 1/2+
7276 7/2+
6793 6859 5/2+ 3/2+
6176 3/2-
5183 5241 5/2+ 1/2+
0 1/2-
15O

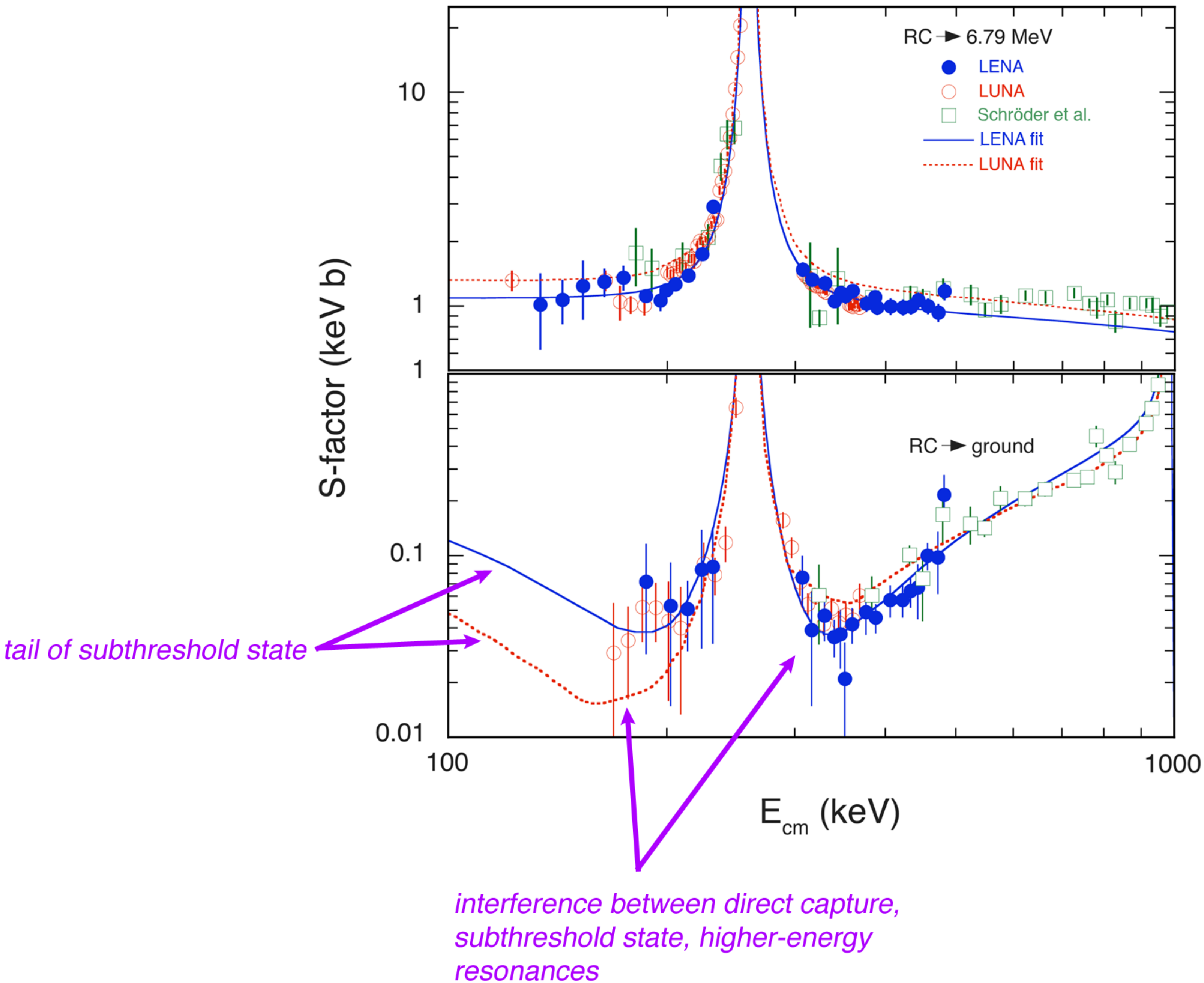

RC → 6.79 MeV
LENA
LUNA
Schröder et al.
LENA fit
LUNA fit
RC → ground
S-factor (keV b)
10
1
1
0.1
0.01
100
1000
E_cm (keV)
tail of subthreshold state
interference between direct capture,
subthreshold state, higher-energy
resonances

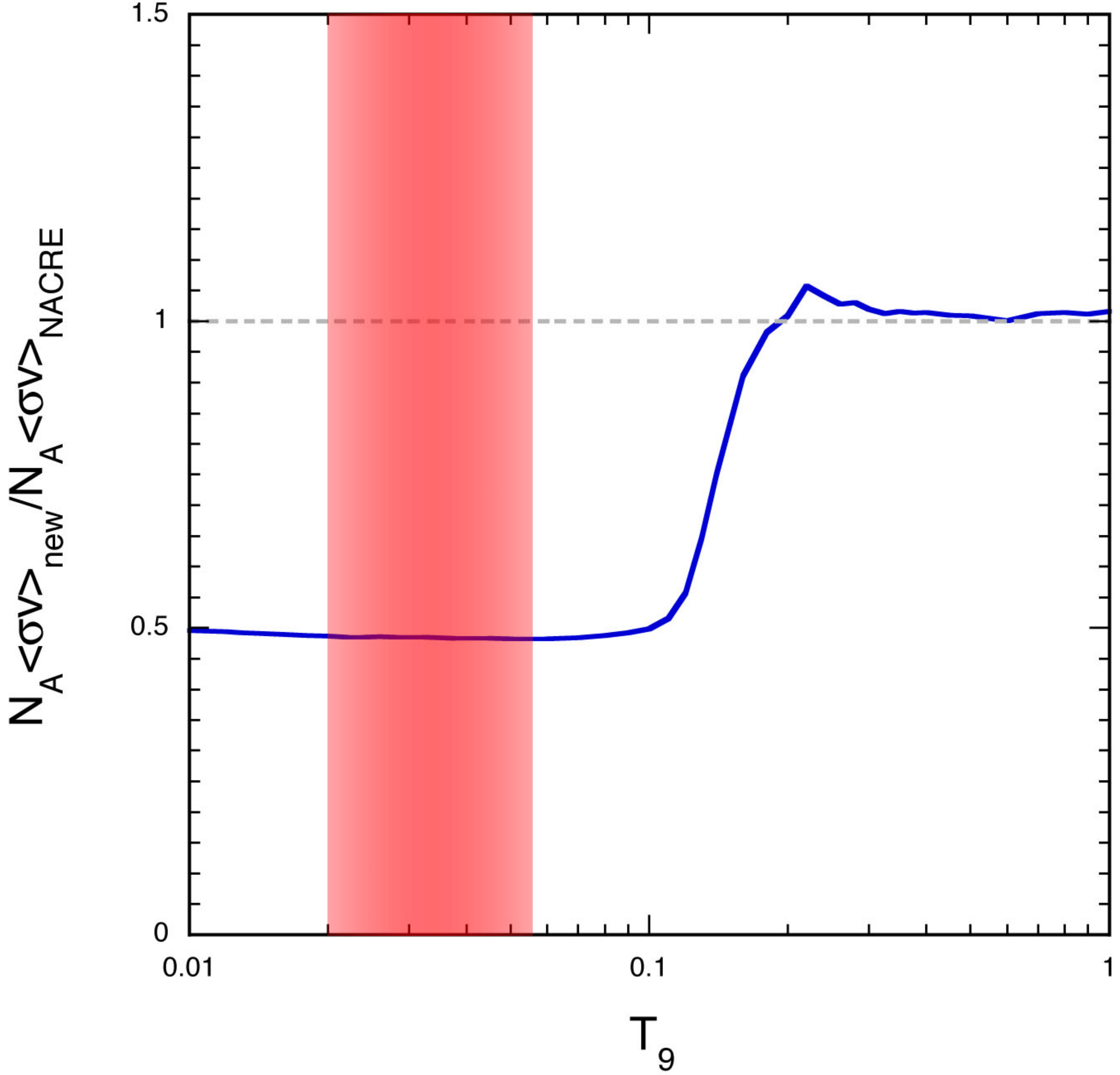

1.5
1
0.5
0
0.01
0.1
1
$N_A\langle\sigma v\rangle_{new}/N_A\langle\sigma v\rangle_{NACRE}$
T_9

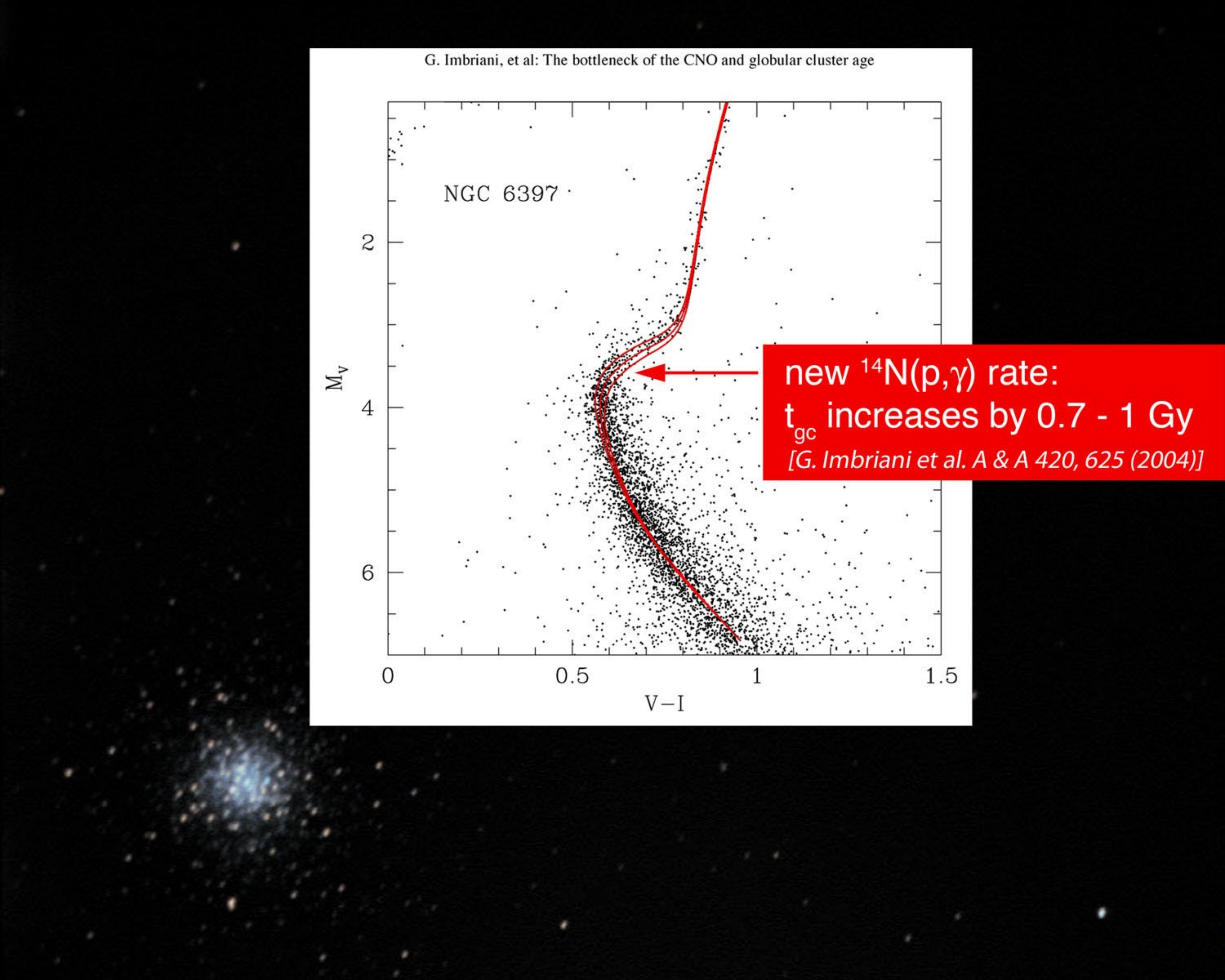
G. Imbriani, et al: The bottleneck of the CNO and globular cluster age
NGC 6397
M_V
2
4
6
0
0.5
1
1.5
V−I
new ¹⁴N(p,γ) rate:
t_gc increases by 0.7 - 1 Gy
[G. Imbriani et al. A & A 420, 625 (2004)]

L.M. Krauss & B. Chaboyer, *Science* **299**, 65 (2003)

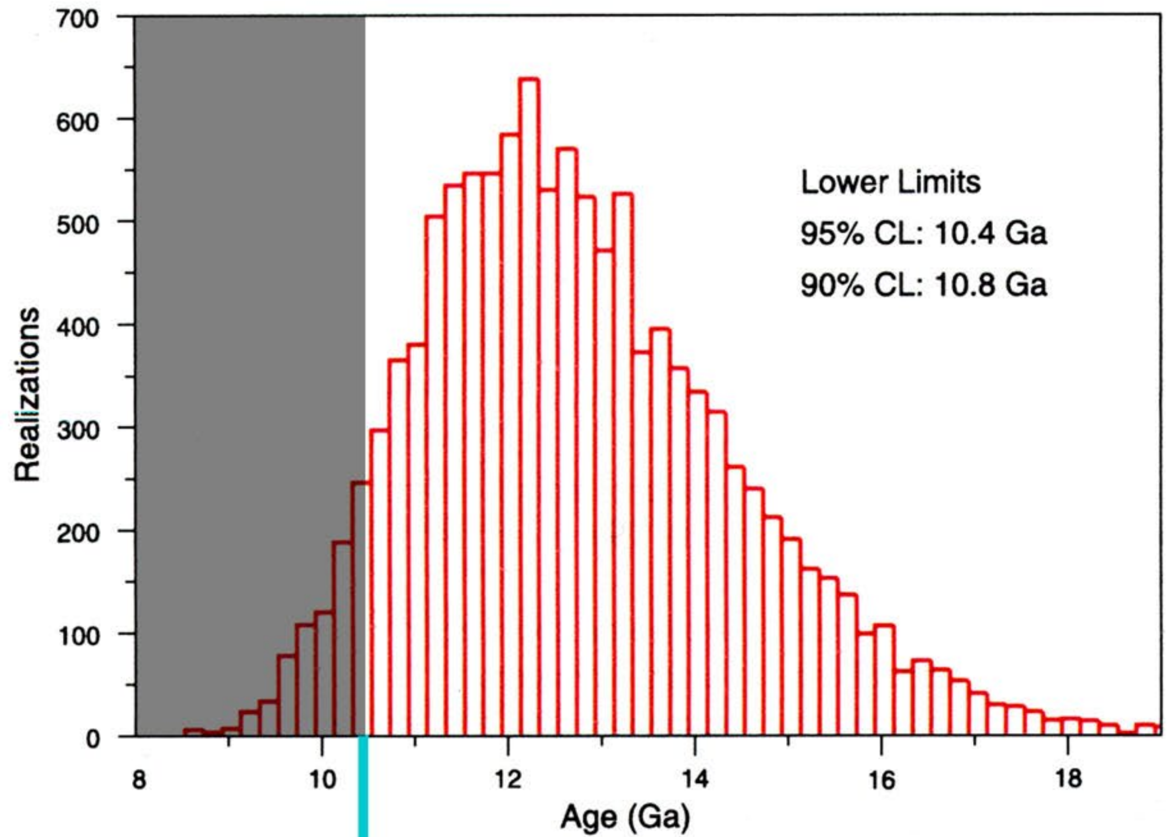

$t_{gc} \gtrsim 11.2$ Gy

best-fit age ≈ 13.4 Gy

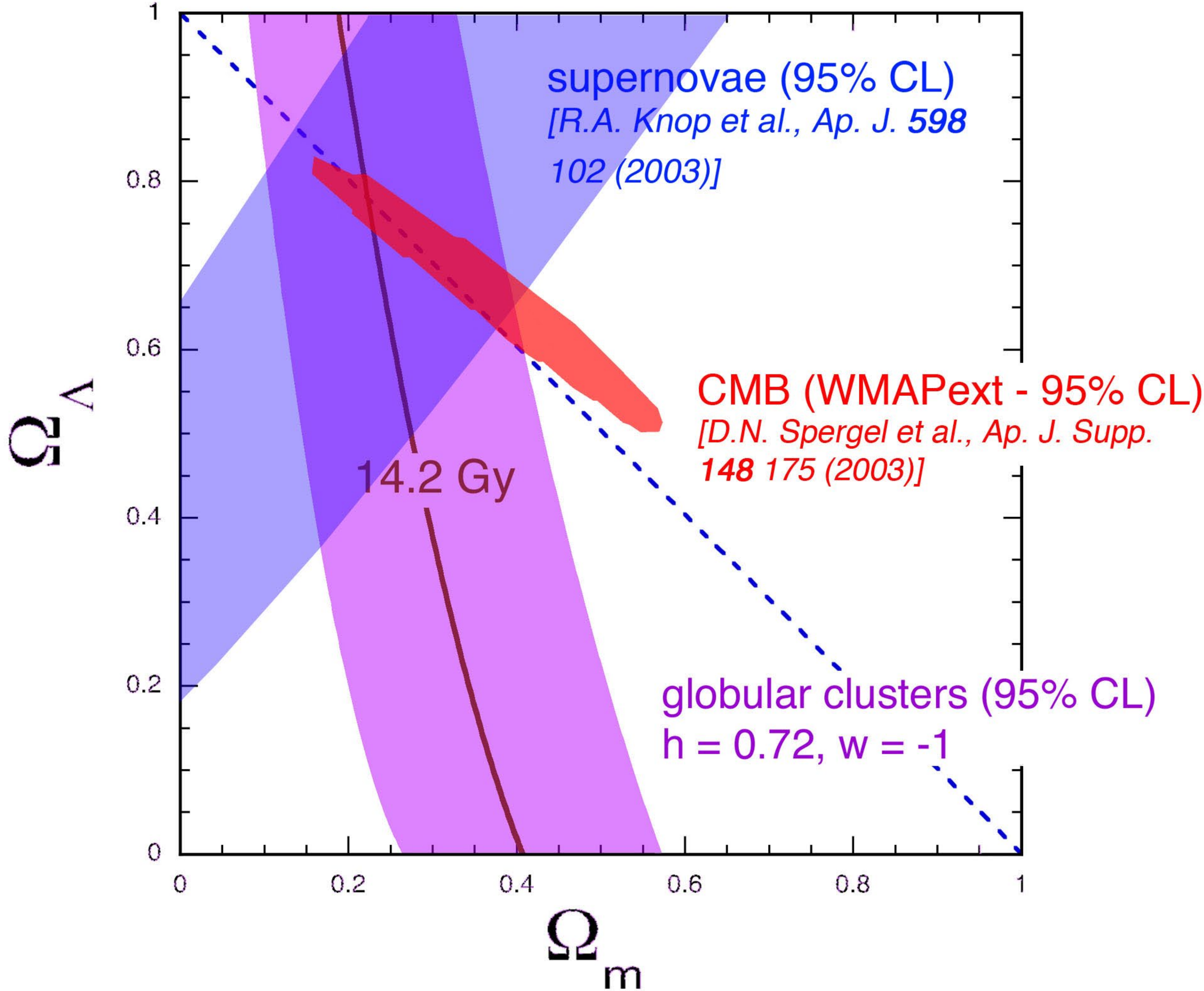

supernovae (95% CL)
[R.A. Knop et al., Ap. J. 598 102 (2003)]
CMB (WMAPext - 95% CL)
[D.N. Spergel et al., Ap. J. Supp. 148 175 (2003)]
14.2 Gy
globular clusters (95% CL)
h = 0.72, w = -1
0
0.2
0.4
0.6
0.8
1
Ω_Λ
Ω_m

Abundance anomalies in globular clusters

Na vs. O

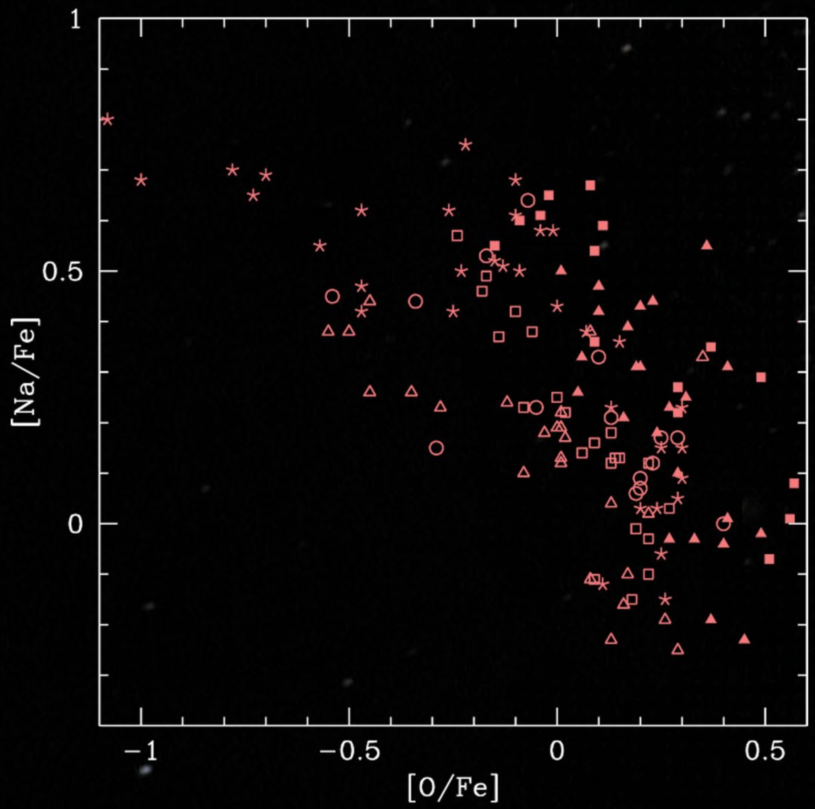

various clusters; see: P. Ventura and F. D'Antona, A&A 457, 995 (2006)

Mg vs. Al

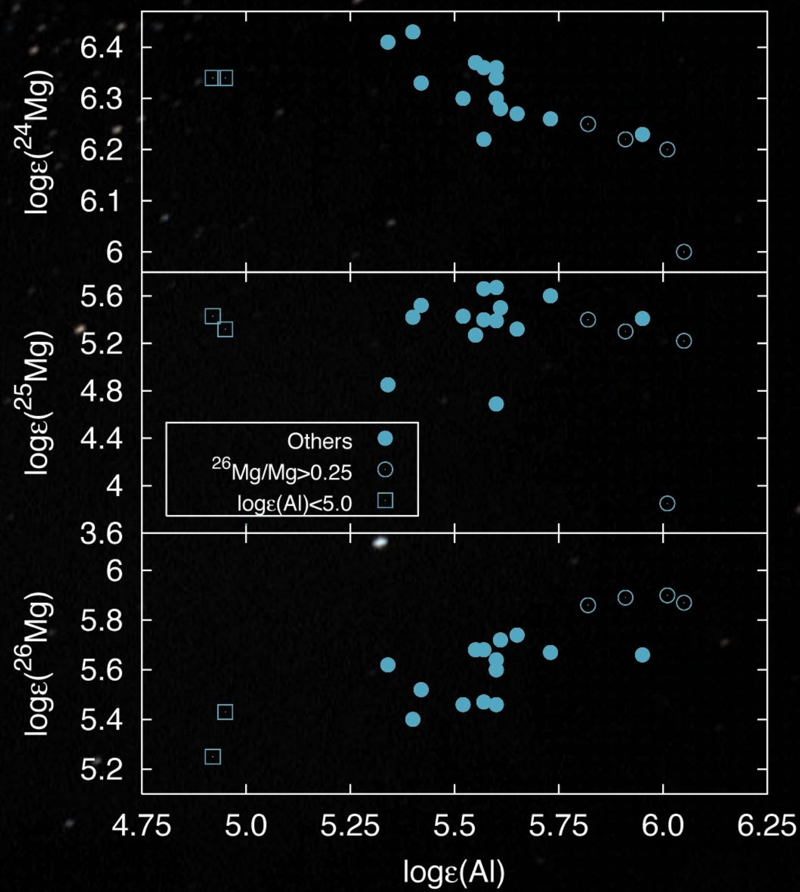

*NGC 6752: D. Yong et al., A&A **402**, 985 (2003)*

Abundance anomalies in globular clusters

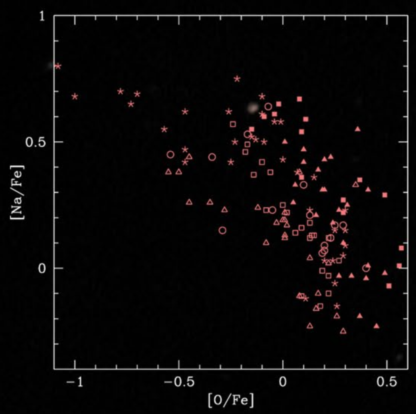

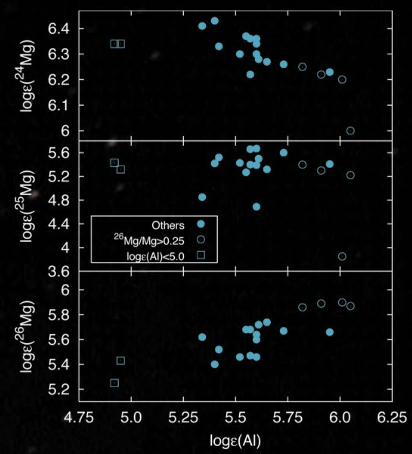

Note range and overall enhancement of Na, Mg and anticorrelation with O, Al

This is observed in clusters, but not in field stars

Neither Na nor Al should be on the surfaces of these stars because the surface radiative zone stops convection

Is this the signature of some “extra” mixing process? If so, what does this imply for evolution and cluster ages?

mixing mechanisms

1. convection

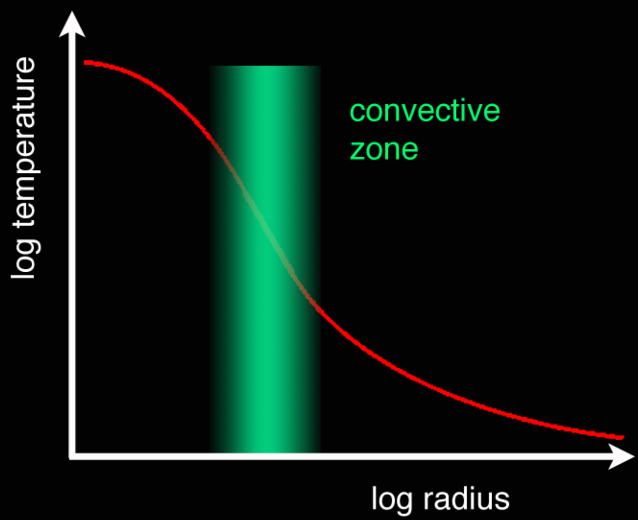

2. rotation (meridional circulation)

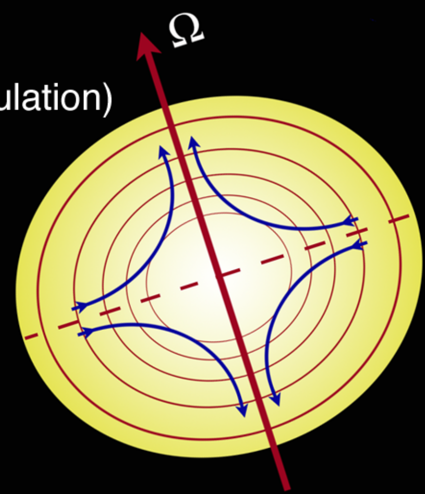

3. gravitational settling

4. diffusion

5. MHD, etc.

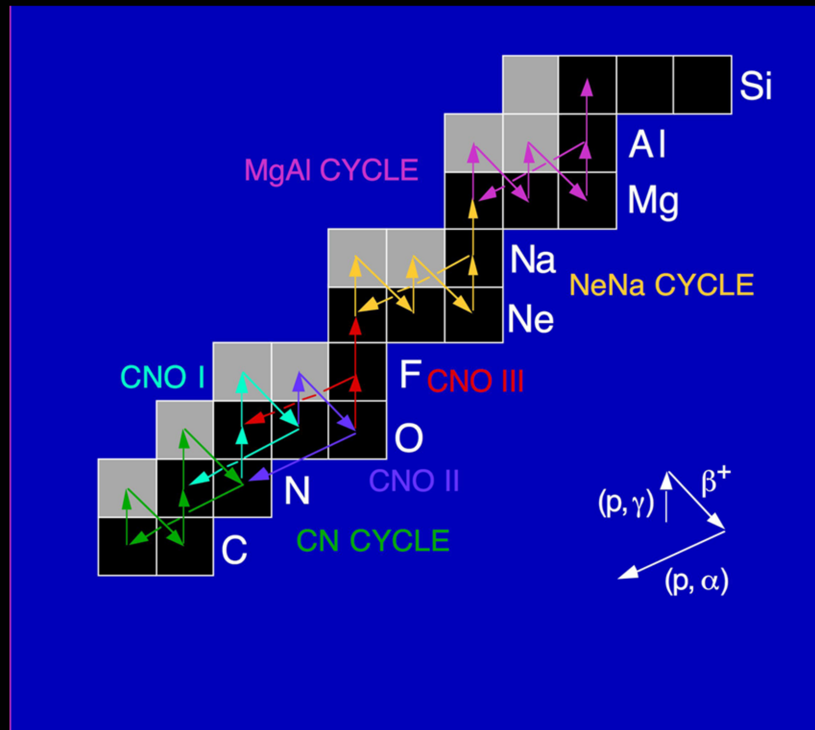

2 clusters with similar [Fe/H] (~-1.6), but note differences in “horizontal branch” (core He burning)

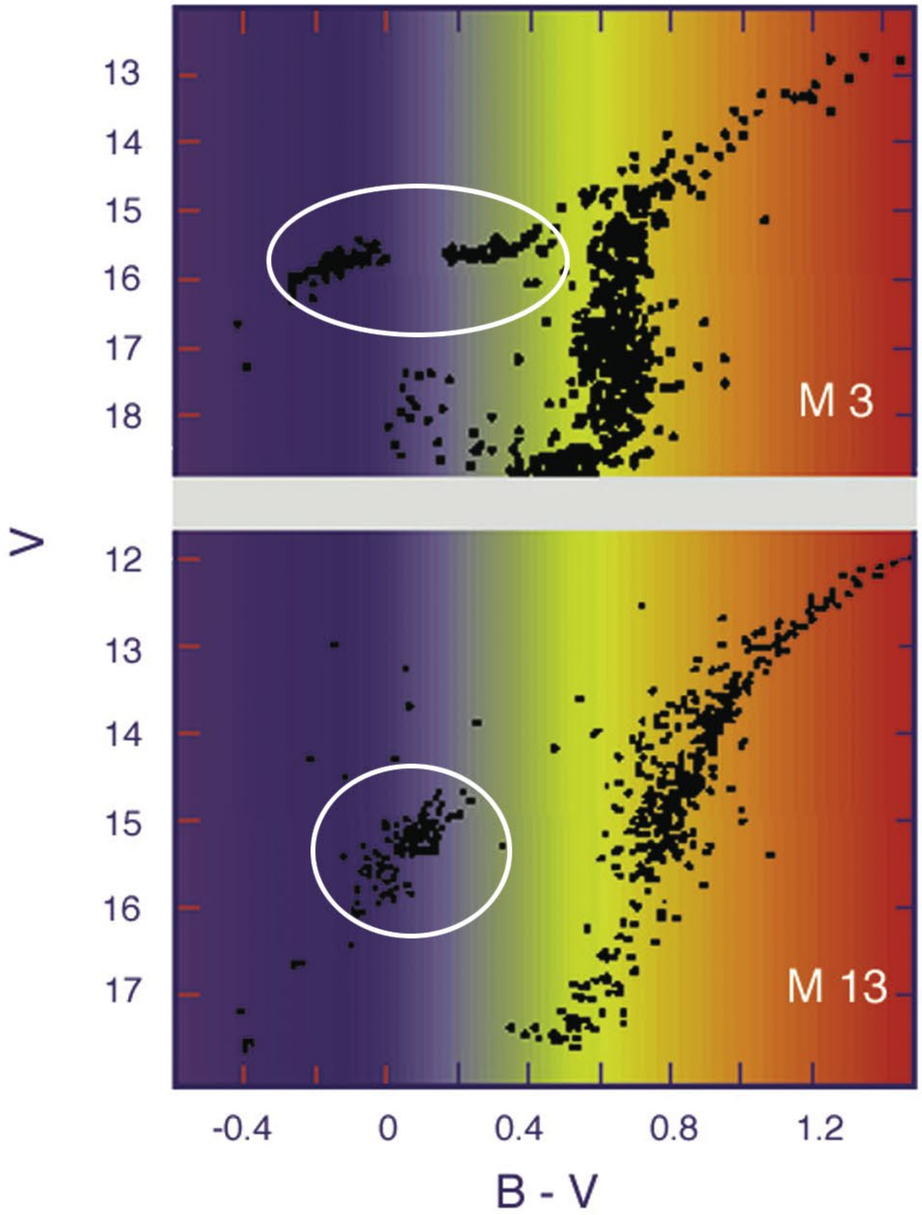

no Al vs. Mg

Al vs. Mg

if mixing brings Al to the surface, it also brings He; He displaces H^- and opacity drops ⟶ envelope shrinks and gets bluer, brighter

overestimate age by 2 Gy?

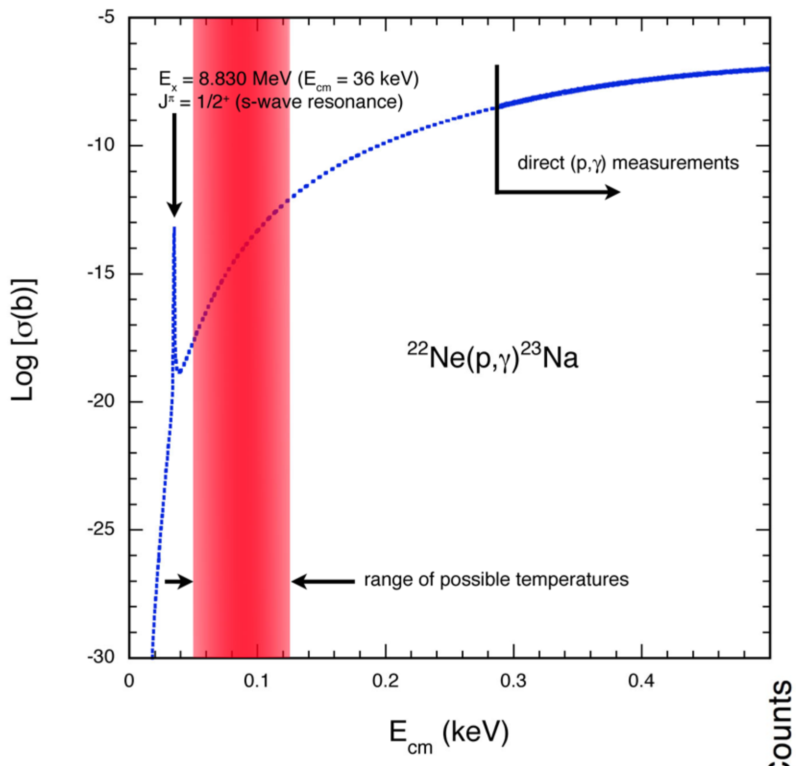

this is a common situation - a direct measurement of the 36-keV resonance would take several million years of beam time

indirect approach

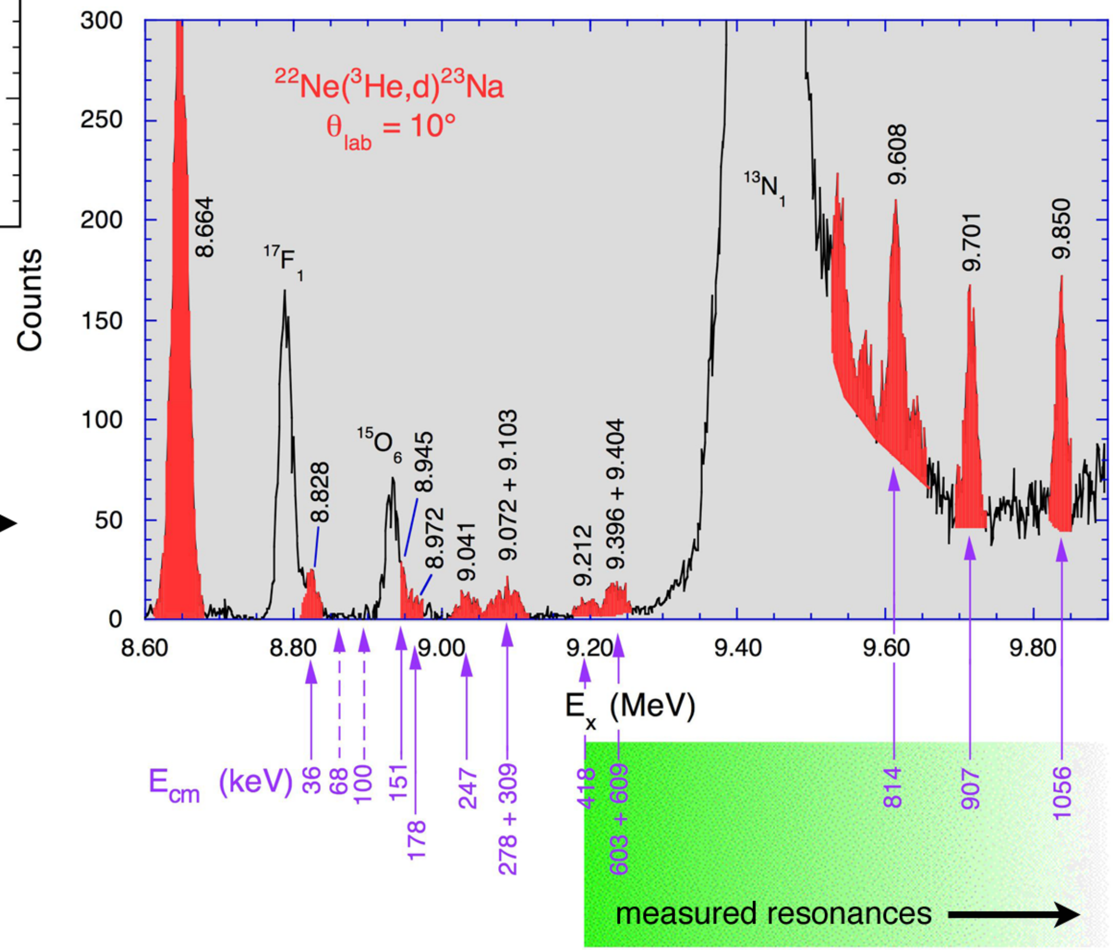

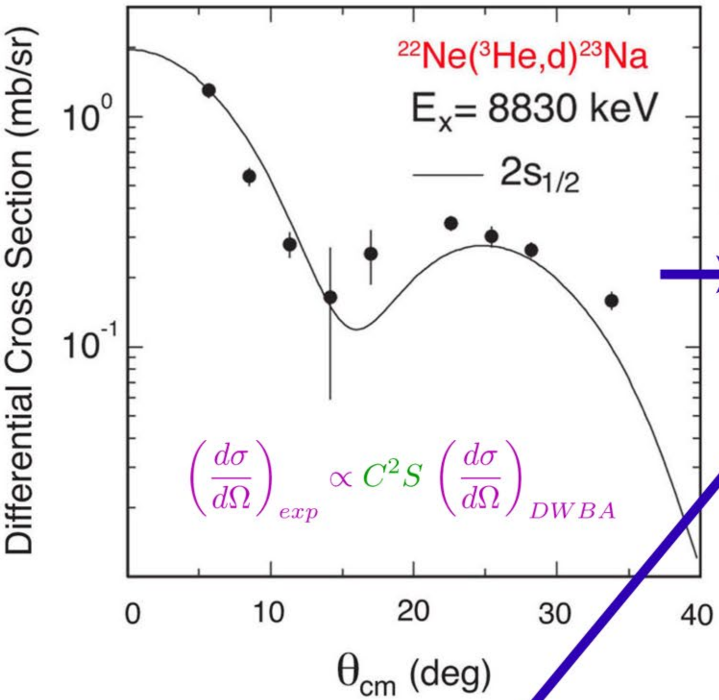

$$\omega\gamma = \omega \frac{\Gamma_p \Gamma_\gamma}{\Gamma} \approx \omega \Gamma_p$$

$$\Gamma_p = 2\, C^2 S\, \gamma_{sp}^2\, P_\ell(E_r)$$

$$C^2S = 0.02$$
$$\rightarrow \;\Gamma_p = 3.6 \times 10^{-15} eV$$

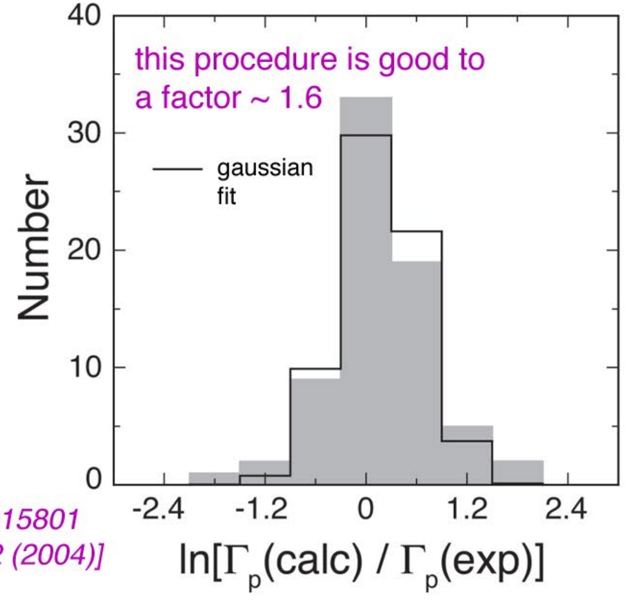

*[S.E. Hale et al., Phys. Rev. **C65**, 015801 (2001) and Phys. Rev. **C70**,045802 (2004)]*

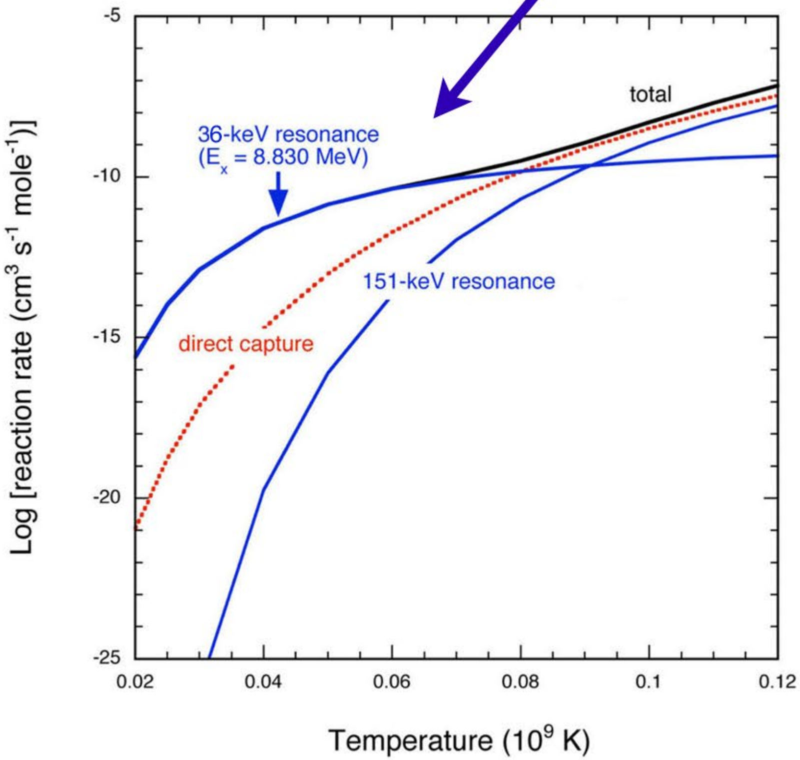

alternately, overlap integral for B ⟶ A + p
can be approximated:

$$I_A^B(r) \approx C_B \frac{W_{-\eta,l+1/2}(2kr)}{r}$$

↑
asymptotic normalization coefficient

(by the way, $C_B = (C^2S)^{1/2}\, b_B$; single-particle radial wavefn

$$R(r) \approx b_B \frac{W_{-\eta,l+1/2}(2kr)}{r}$$)

the procedure for extracting ANCs is less model dependant than for spectroscopic factors, but this largely goes away in the calculation of Γ_p

*[see e.g. A.M. Mukhamedzhanov & R. Tribble, Phys. Rev. **C59**, 3418 (1999) and P.F. Bertone et al., Phys. Rev. **C66**,055804 (2002) for a comparison of the 2 techniques]*

The current picture:

*1. Na vs. O can arise from O ⟶ N in the CN cycle and Ne ⟶ Na in the NeNa cycle IF the rate for the $^{23}Na(p,\alpha)^{20}Ne$ reaction is reduced by a factor of ~4 [see P. Ventura and F. D'Antona, A&A **457**, 995 (2006)].*

2. H-burning in low-mass stars can not produce Mg vs. Al unless our current stellar models are wrong (predicted temperatures are too low).

3. Both effects can arise from environmental pollution - winds from AGB stars.

AGB stars

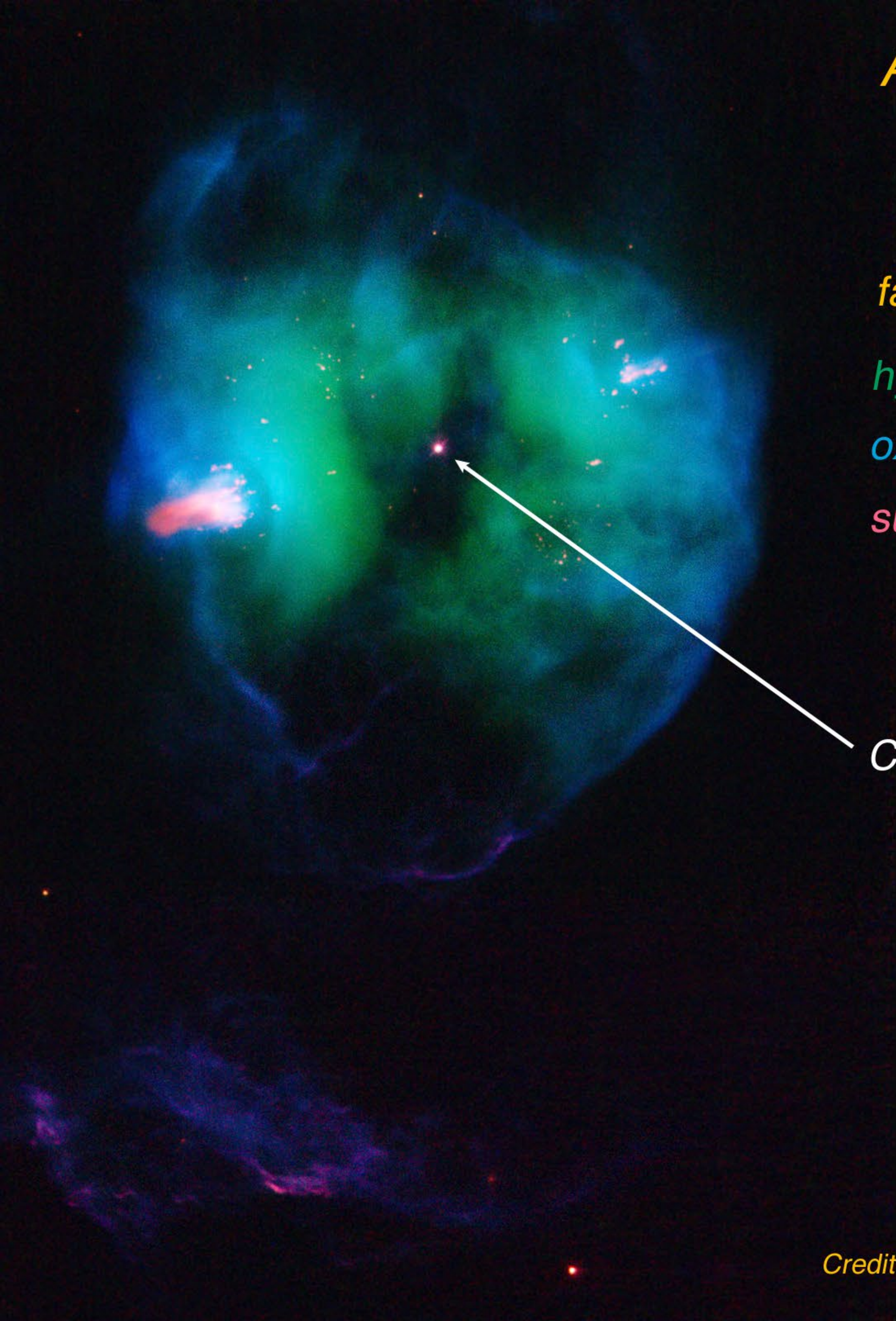

false-color image of NGC 2371:

hydrogen

oxygen

sulfer, nitrogen

C-O core (white dwarf)

Credit: NASA, ESA, and the Hubble Heritage Team (STScI/AURA)

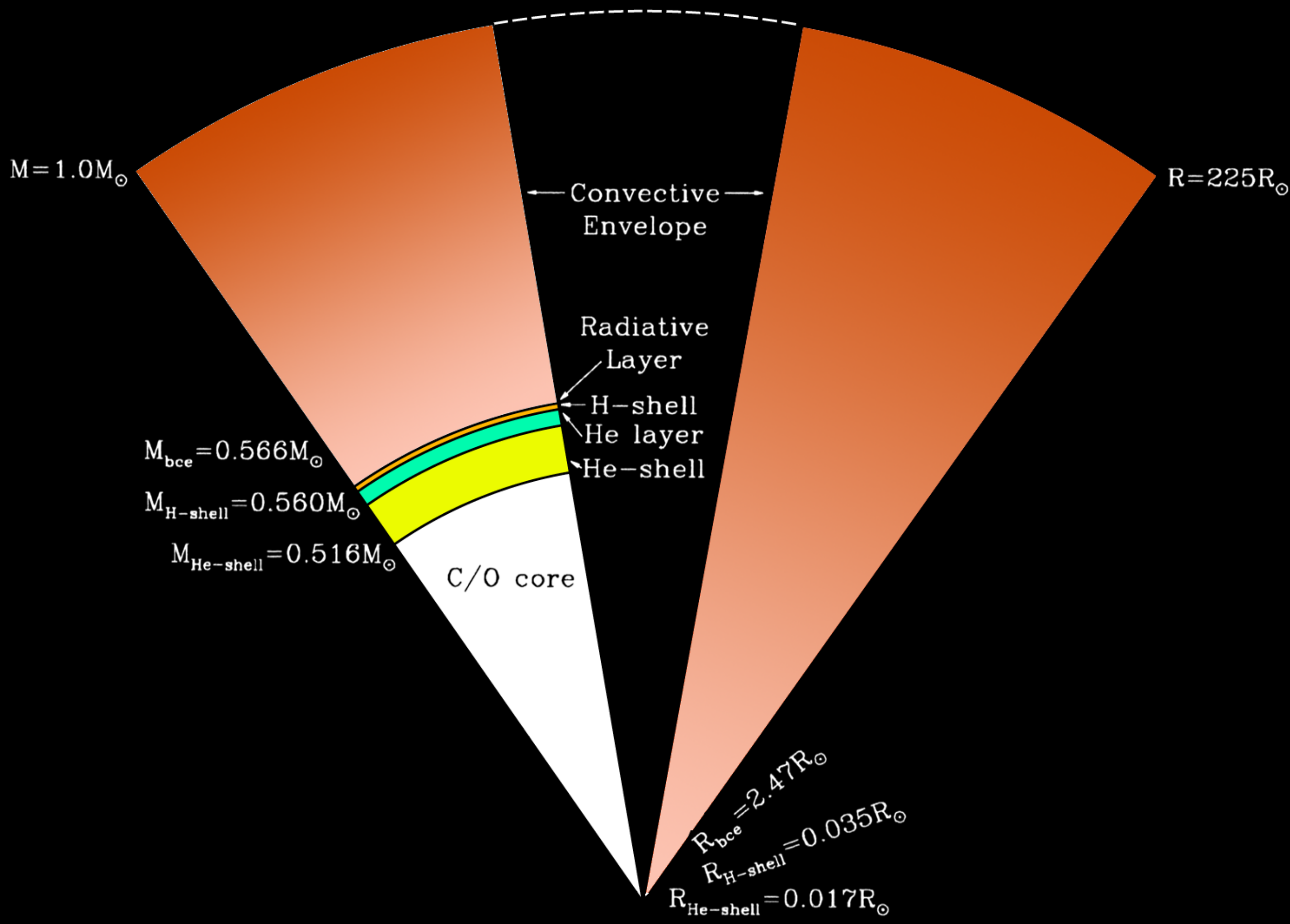

Fig. 2.6. A schematic view of a $1\,M_\odot$ AGB star interior. On the **left**, various regions in the star are plotted against mass fraction, while on the **right** the regions are plotted against radius. M_{bce} is the mass at the base of the convective envelope, while $M_{H-shell}$ and $M_{He-shell}$ are the masses at the middle of the hydrogen- and helium-burning shells, respectively

[adapted from J.C. Lattanzio and P.R. Wood in "Asymptotic Giant Branch Stars", H. J. Habing, Hans Olofsson, ed., Springer (2003)]

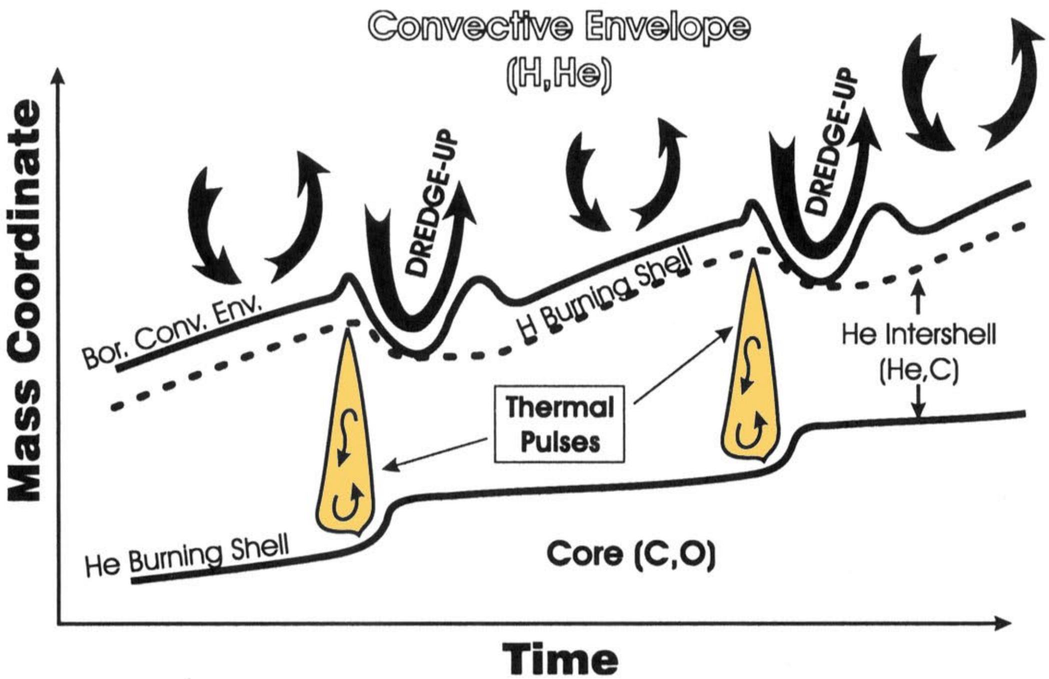

Fig. 1. This sketch illustrates the evolution of the positions of the inner border of the convective envelope, the H-burning shell and the He-burning shell, during the thermally pulsing AGB phase. The convective regions generated by two subsequent thermal pulses are also shown. Note that the temporal developments of thermal pulses and of following TDU episodes are off scale with respect to the interpulse period.

AGB nucleosynthesis (~1-3 $M_\odot$)

1. Interpulse phase, H-burning shell is main source of luminosity:

   H $\rightarrow$ He in CNO cycles; ^{12}C ↓, ^{18}O ↓, ^{13}C ↑, ^{14}N ↑, ^{17}O ↑
   if base of convective envelope reaches H-burning shell, then ^{7}Li, ^{19}F, NeNa and MgAl cycles in "hot-bottom burning"

   Mixing of protons from envelope into intershell;
   $^{12}C(p,\gamma)^{13}N(\beta^+)^{13}C(\alpha,n)^{16}O$,
   n + "Fe" $\rightarrow$ "*s-process*" (main component)

2. Thermal pulse, He-burning shell is main source of luminosity:

   $3\alpha \rightarrow {}^{12}C$, $^{12}C(\alpha,\gamma)^{16}O$
   $^{14}N(\alpha,\gamma)^{18}F(\beta^+)^{18}O(\alpha,\gamma)^{22}Ne(\alpha,n)^{25}Mg$
   n + "Fe" $\rightarrow$ *s-process*

3. Power down: convective envelope reaches into intershell
   "dredge up"

How do we know that this is happening?

SPECTROSCOPIC OBSERVATIONS OF STARS OF CLASS S

Paul W. Merrill
Mount Wilson and Palomar Observatories
Carnegie Institution of Washington
California Institute of Technology

Received February 27, 1952

Lines of *Tc* I, an element believed to have no completely stable isotope, appear to be stronger in the stars with the more dominant S-type characteristics. This fact, together with others, might suggest that S-type stars represent a comparatively transient phase of stellar existence.

*ApJ **116**, 21 (1952)*

enhanced Pb in AGB stars

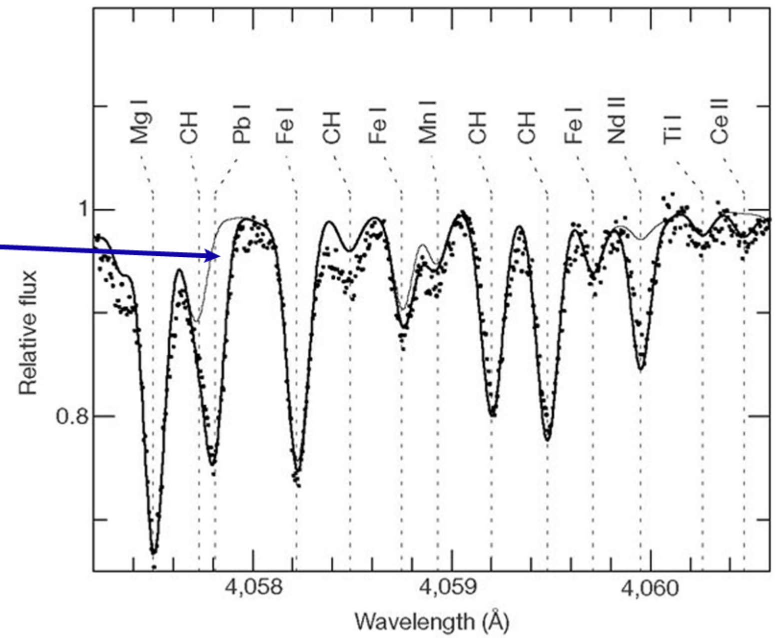

*S. Van Eck, S. Goriely, A. Jorissen and B. Plez, Nature **412**, 793 (2001)*

SiC meteoritic grains

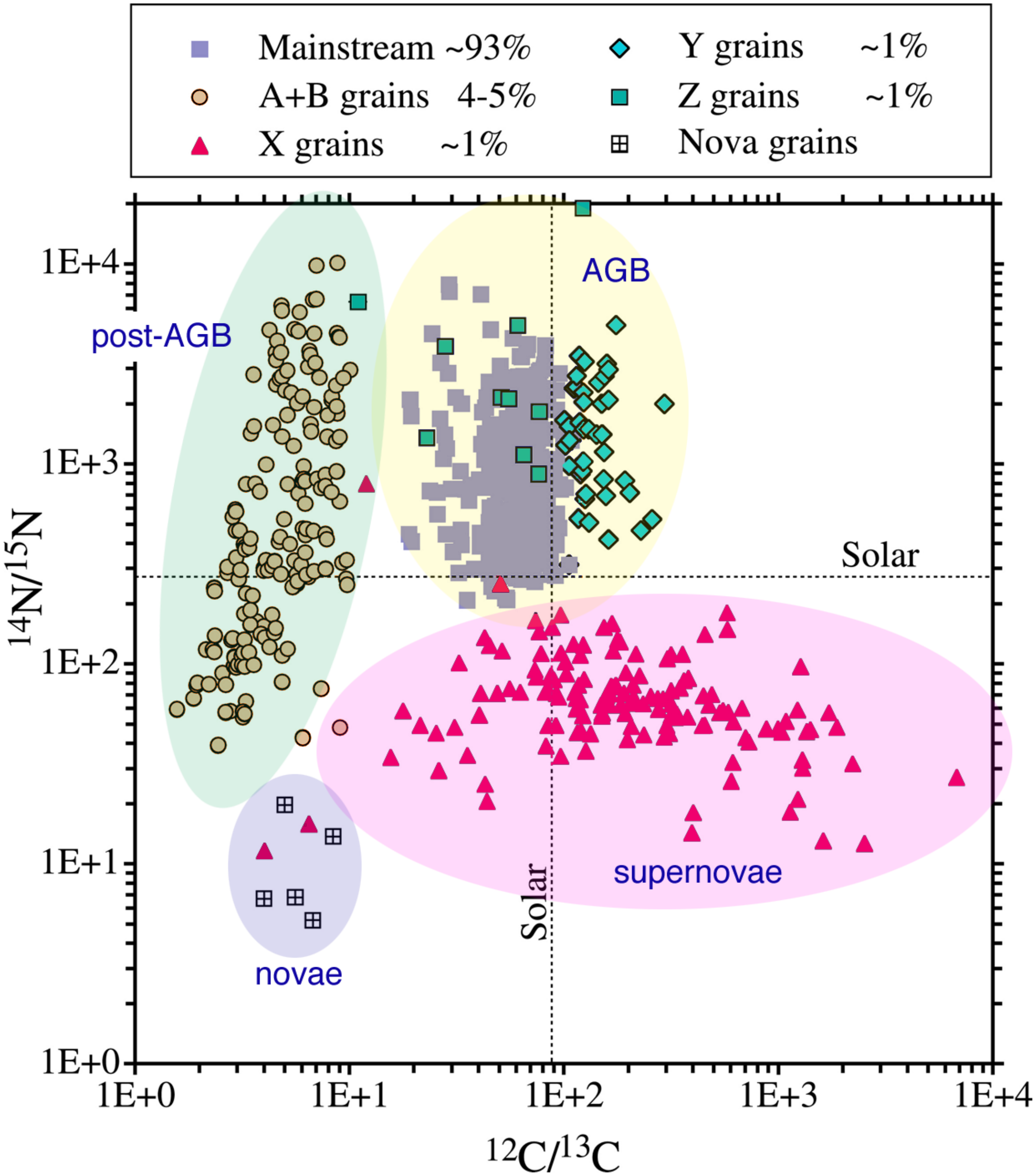

*adapted from E. Zinner et al., Ap J **650**, 350 (2006)*

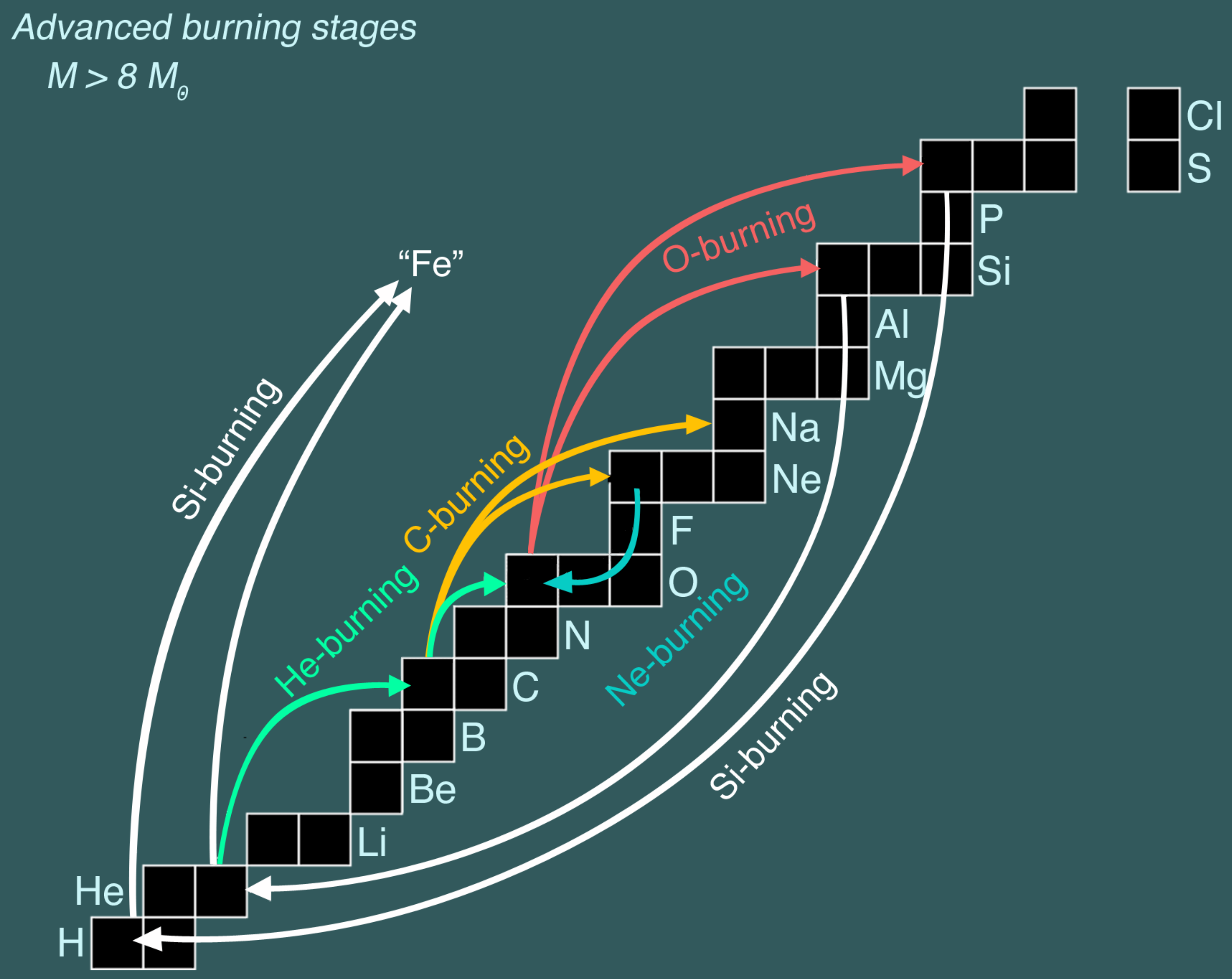

Advanced burning stages
$M > 8\ M_{\odot}$
"Fe"
Si-burning
He-burning
C-burning
O-burning
Ne-burning
Si-burning
H
He
Li
Be
B
C
N
O
F
Ne
Na
Mg
Al
Si
P
S
Cl

elemental distribution
reflects some basic
nuclear properties

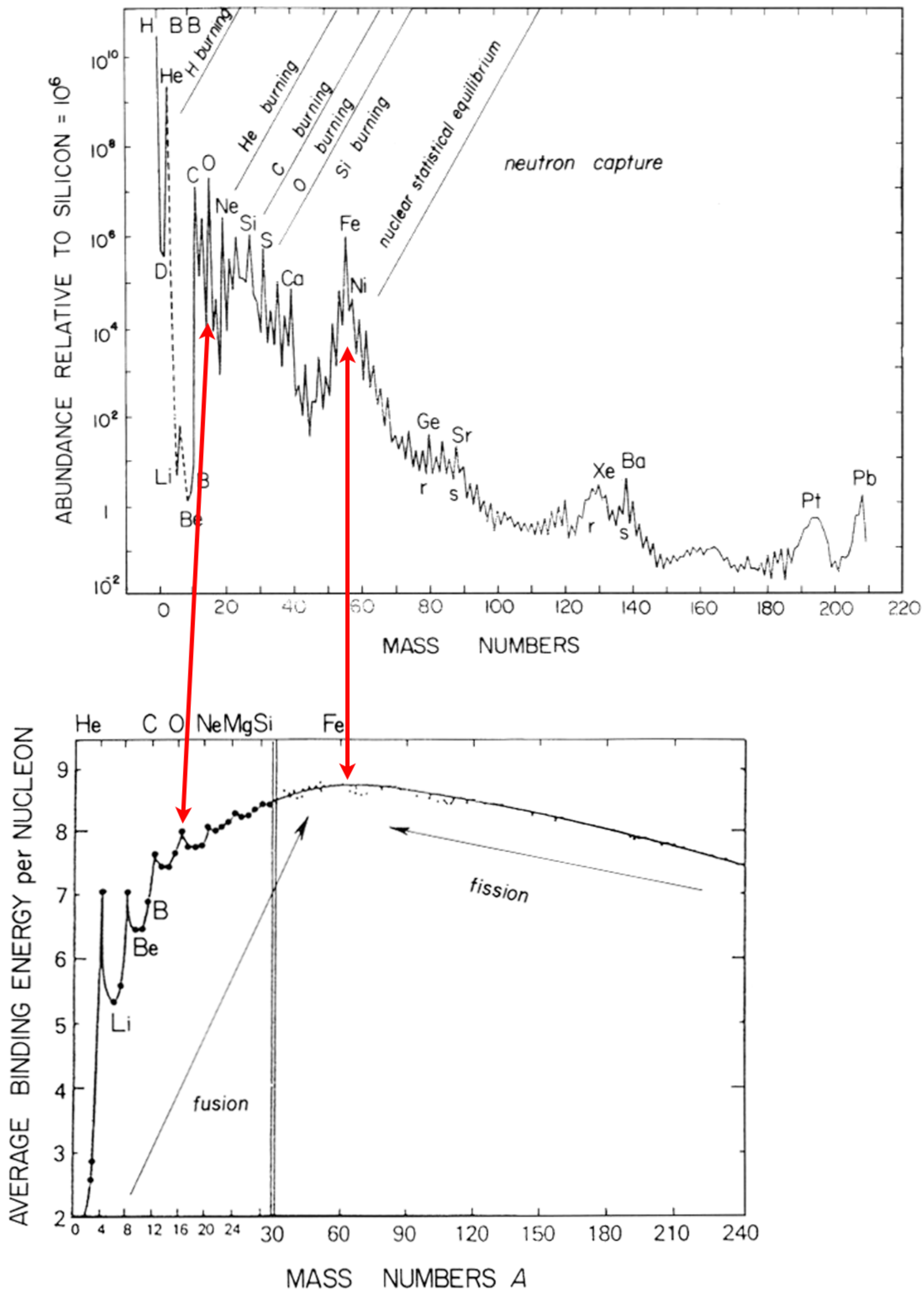

$^{12}C(\alpha,\gamma)^{16}O$

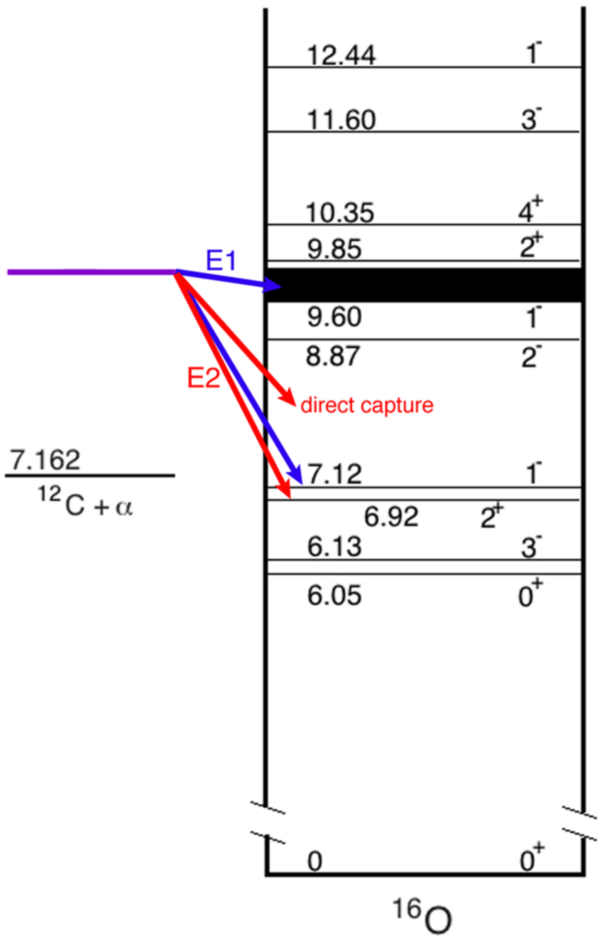

must also include interference with tails of distant 1^- and 2^+ states

recent capture data and R-matrix fits

J. Phys. G: Nucl. Part. Phys. **35** (2008) 014009 F Strieder

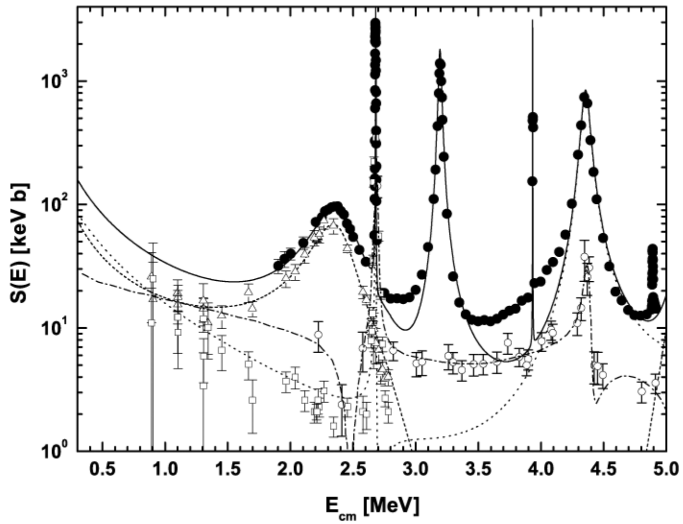

Figure 1. ERNA total S factor data (filled-in circles) [20] for $^{12}C(\alpha,\gamma)^{16}O$ compared with the recent E1 (open triangles) and E2 (open squares) γ-measurements [19] and the $E_x = 6.05$ MeV cascade data (open circles) [21]. The solid line represents the sum of the single amplitudes of an R matrix fit [26] (the dotted and dashed lines are the E1 and E2 amplitudes, respectively). In addition, the R matrix fit of [21] to their cascade data (dotted-dashed line) is shown. The latter component is not included in the sum and might explain the high yield in the ERNA data between the resonances.

[19] Assuncão M *et al* 2006 *Phys. Rev.* C **73** 055801
Fey M 2004 *PhD Thesis* Universität Stuttgart, Germany
[20] Schürmann D *et al* 2005 *Eur. Phys. J.* A **26** 301
[21] Matei C *et al* 2006 *Phys. Rev. Lett.* **97** 242503
[26] Kunz R *et al* 2002 *Astrophys. J.* **567** 643

S(300) = 145 keV b ± ~25%
[L.R. Buchmann and C.A. Barnes, Nucl. Phys. **A 777,** 256 (2006)]

effect of $^{12}C(\alpha,\gamma)$ in massive stars (some examples)

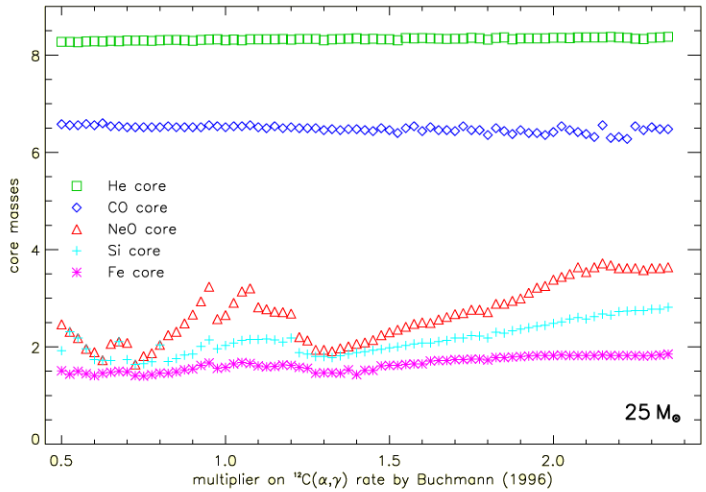

supernovae

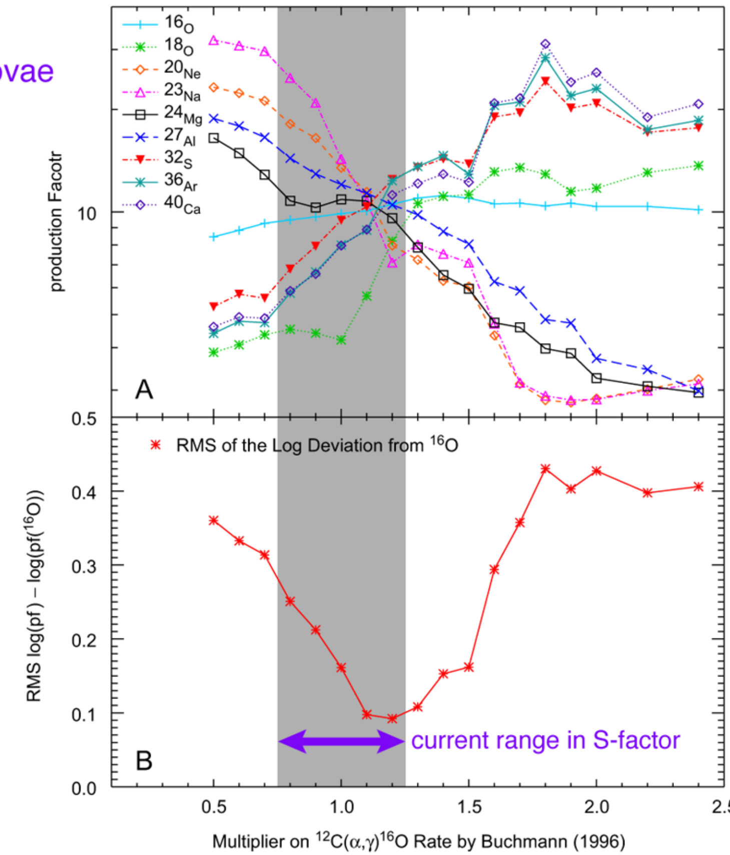

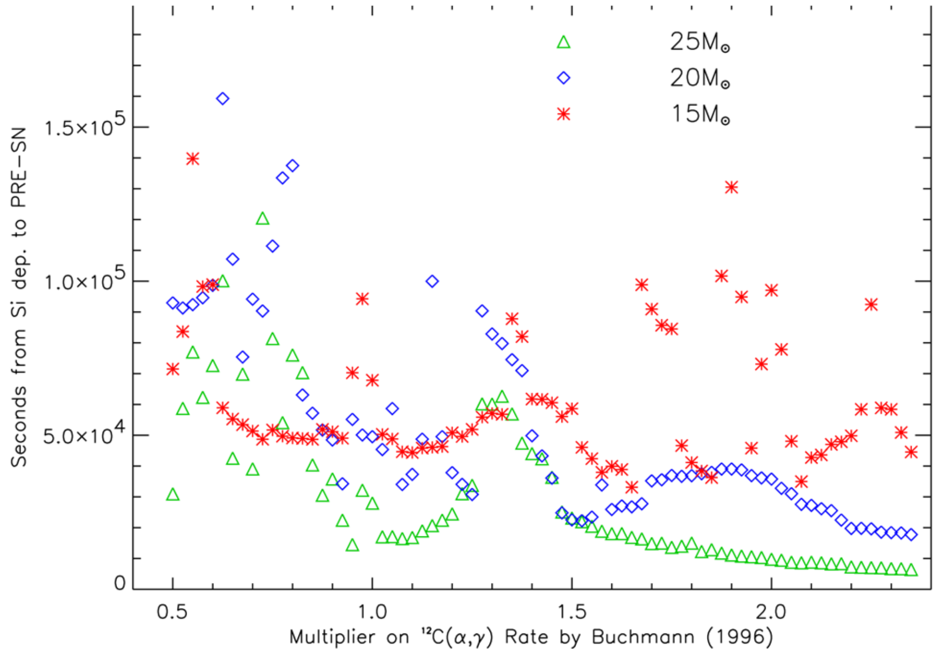

S.E. Woosley and A. Heeger, Phys. Rep. ***442****, 269 (2007)*
and M. Boyse, senior thesis, U.C. Santa Cruz (2002)
(http://www.supersci.org/data/nucleo/12cag/index.html)

also: chemical composition of white dwarfs,
propagation of deflagration front in SNIa, etc.

Carbon burning: $^{12}C + ^{12}C$
$^{12}C + ^{16}O$

$M > 8\ M_{\odot}$, $T_9 \sim 0.85$ or SN Ia, CO white dwarf, $T_9 \sim 2.0$

2 dominant channels

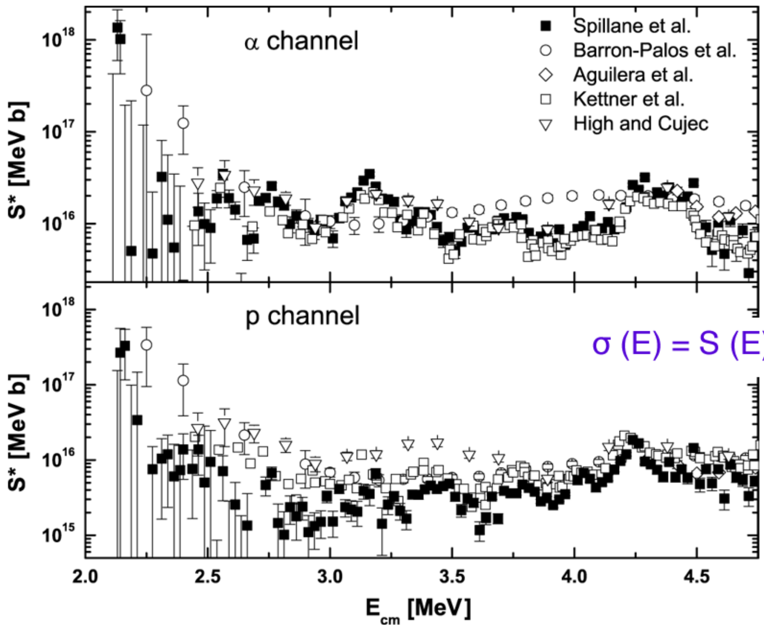

$\sigma(E) = S(E)^{*}\,E^{-1}\exp(-87.21E^{-1/2} - 0.46E)$

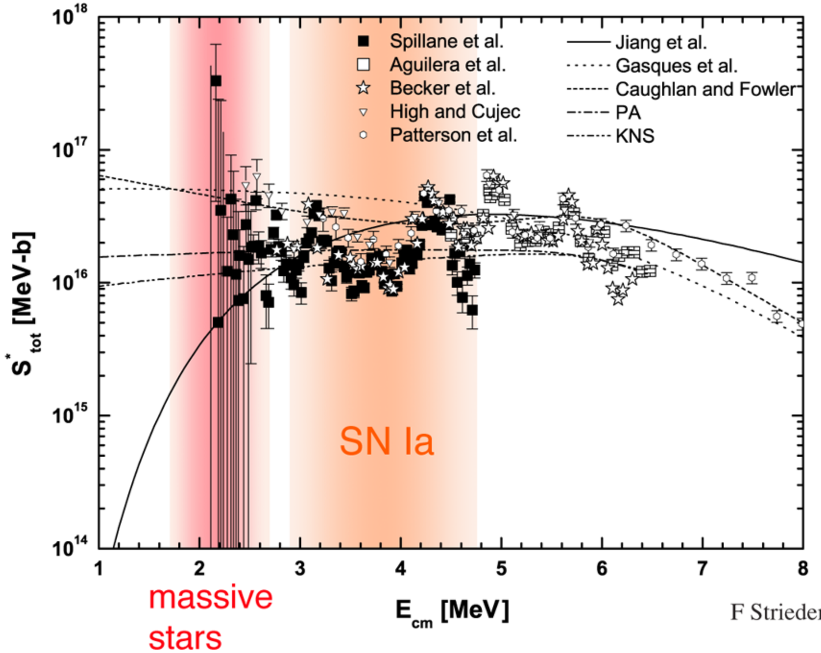

origin of resonant structures is not well understood - quasi-molecular states?

F Strieder J. Phys. G: Nucl. Part. Phys. **35** (2008) 014009

Do we understand the fusion process at low energies?

*[see C.L. Jiang et al., Phys Rev. C **75**, 015803 (2007)]*

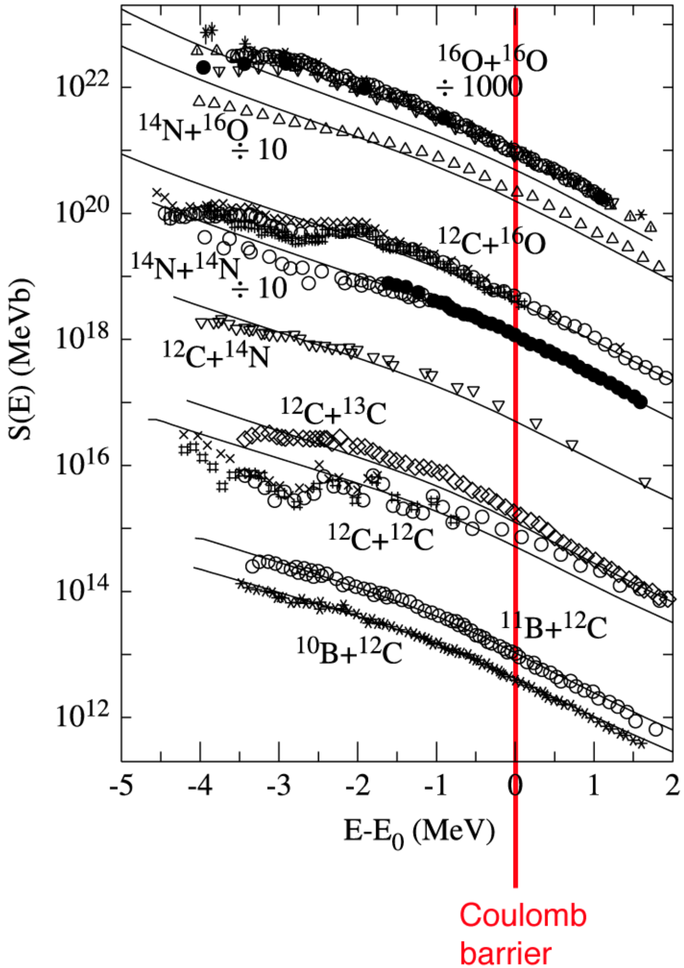

Notice that (optical-model) calculations over-predict the low-energy S-factor.
Short-range repulsive part of N-N interaction gives rise to minimum in energy vs. density at about 0.16 nucleons/fm³ (”saturation density”). This reduces the tunneling probability at low energies. In terms of potentials [see S. Miscu and H. Esbensen,(PRL **96**, 112701 (2006)]:

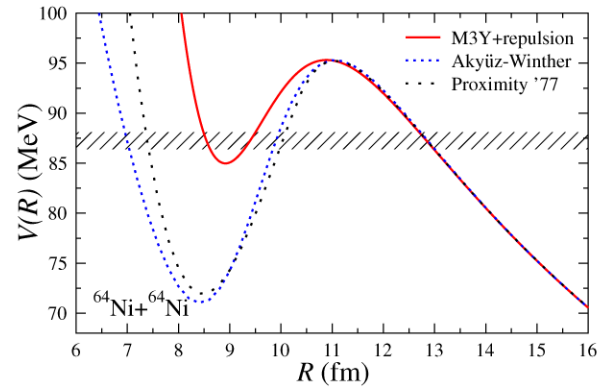

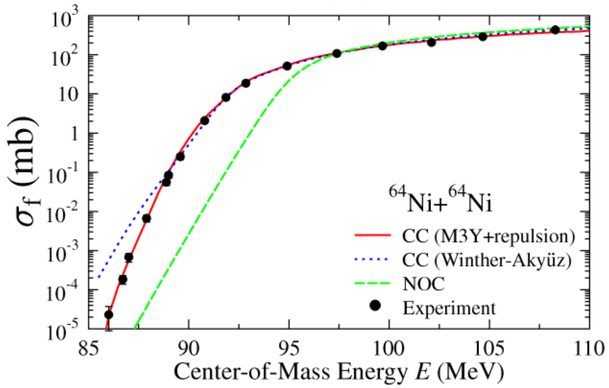

*from C.L. Jiang, Phys. Rev. C**75**, 015803 (2007)*

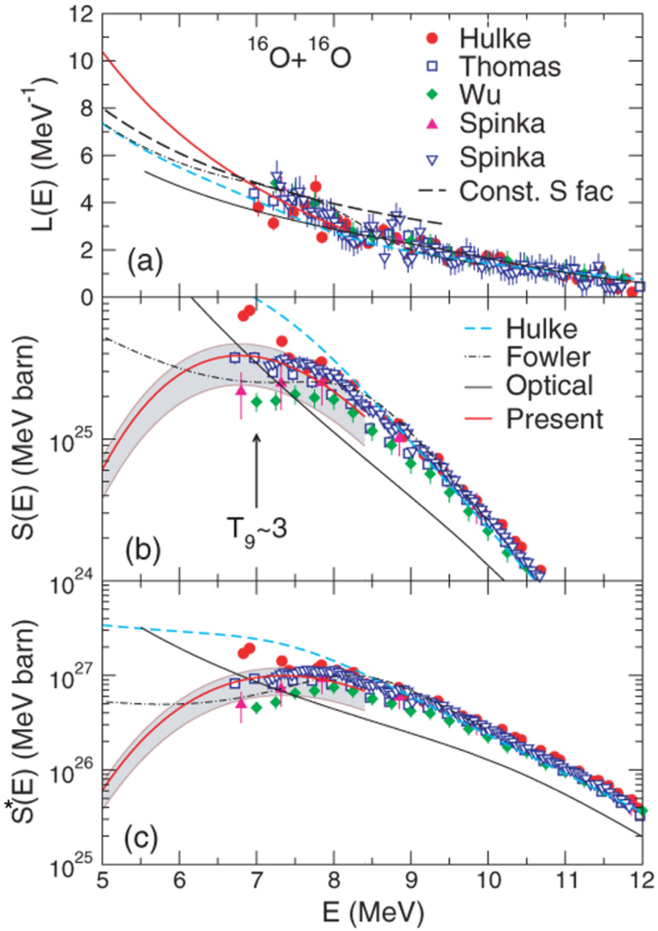

ratio vs. Fowler, Caughlam, Zimmerman compilation (1975)

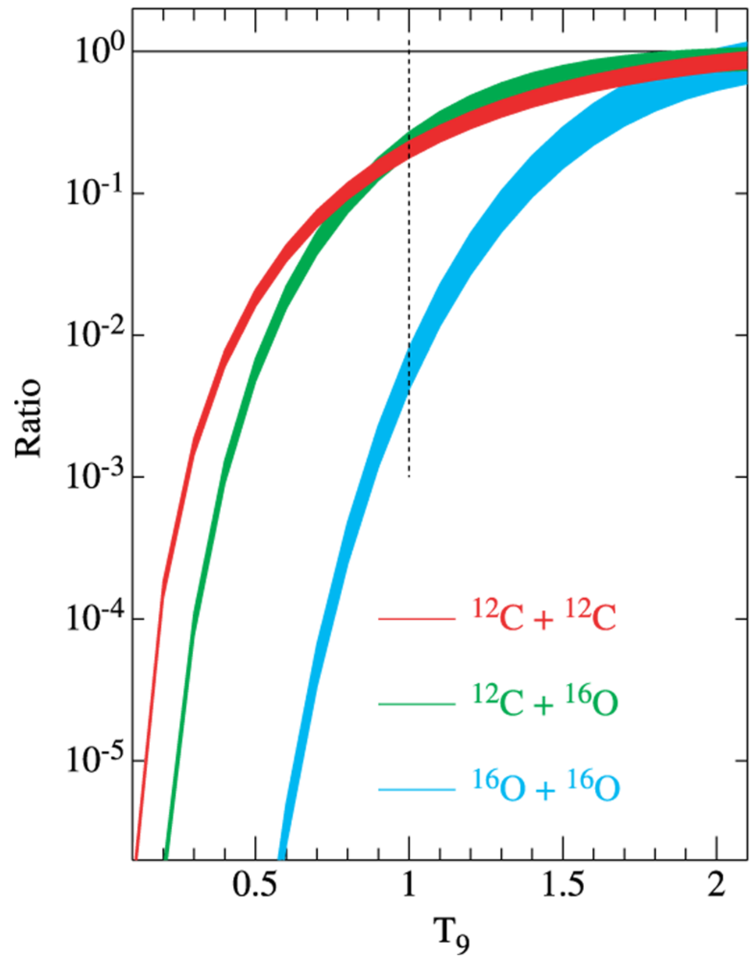

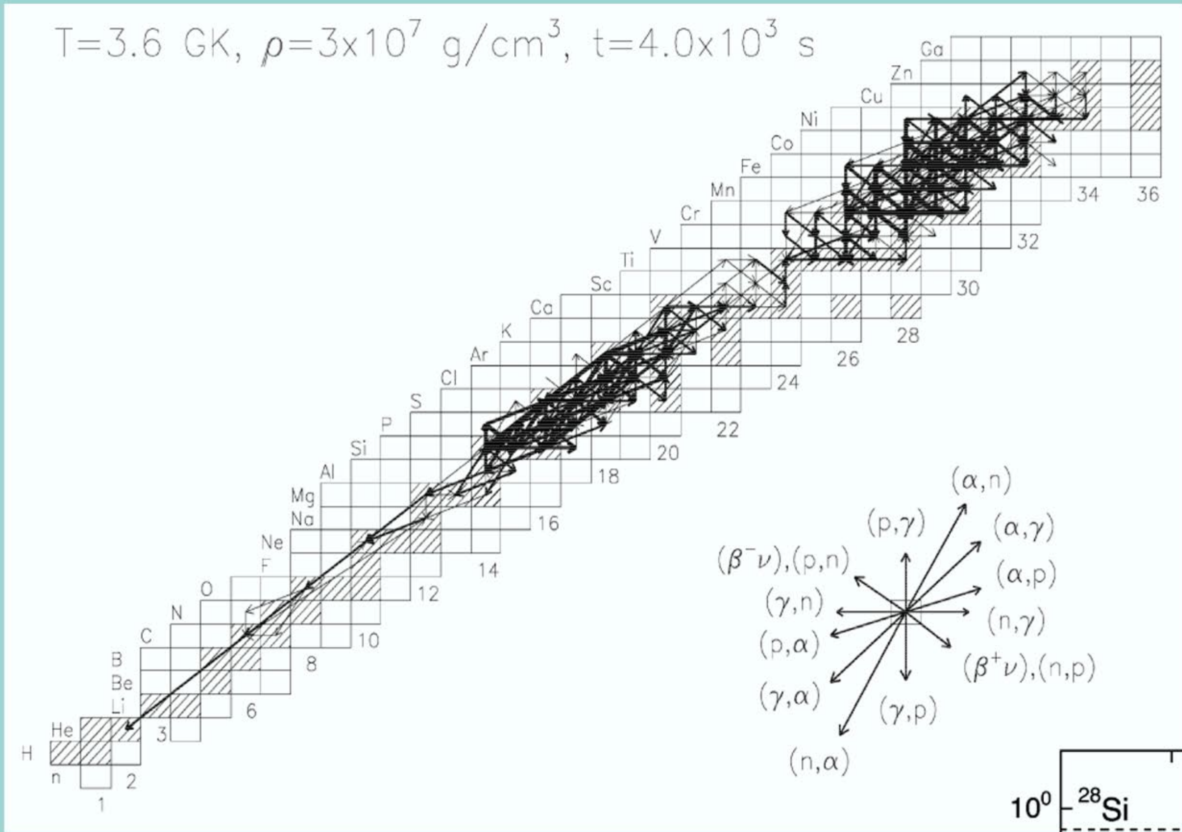

Core Si-burning
25 M⊙

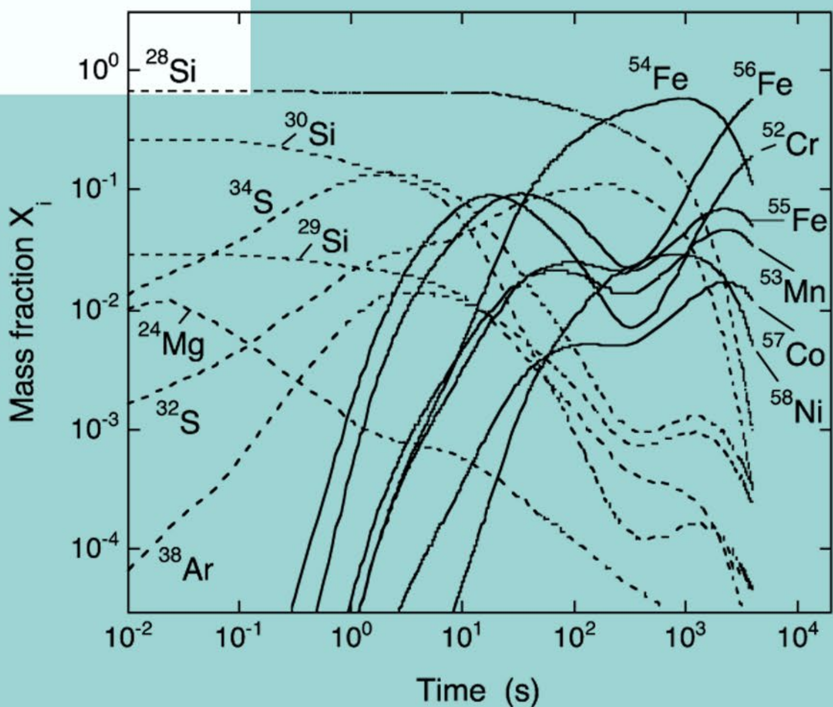

(courtesy of C. Iliadis)

from "Nuclear Physics of Stars", C. Iliadis:

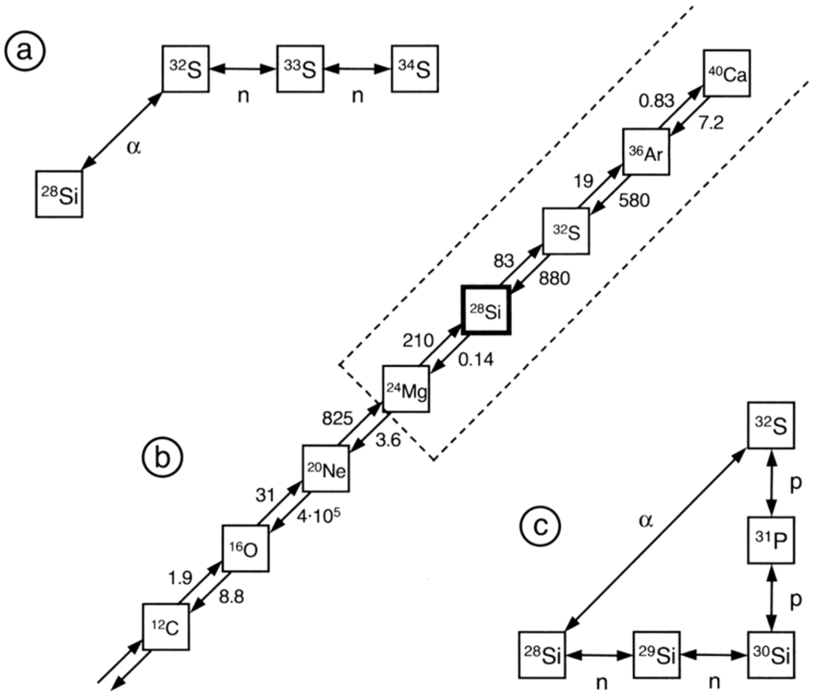

Fig. 5.54 Reaction chains in silicon burning. (a) The reaction chain $^{28}Si \leftrightarrow ^{32}S \leftrightarrow ^{33}S \leftrightarrow ^{34}S$ in equilibrium. (b) $(\alpha,\gamma) \leftrightarrow (\gamma,\alpha)$ reaction links between ^{12}C and ^{40}Ca. The numbers next to the arrows indicate values of the decay constants λ_α and λ_γ (in units of s^{-1}) for (α,γ) and (γ,α) reactions, respectively, assuming a temperature of T = 3.6 GK. The quantity λ_α is calculated by using $\rho = 3\times10^7$ g/cm^3 and $X_\alpha = 10^{-6}$. The latter value is adopted from the network calculation displayed in Fig. 5.52. Nuclides located within the region demarked by the dashed lines are in quasiequilibrium. (c) The closed reaction chain $^{28}Si \leftrightarrow ^{32}S \leftrightarrow ^{31}P \leftrightarrow ^{30}Si \leftrightarrow ^{29}Si \leftrightarrow ^{28}Si$ in equilibrium.

photodisintregation leads to equilibrium

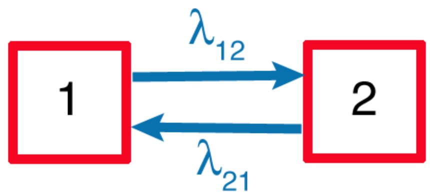

$$\frac{dN_1}{dt} = -N_1\lambda_{12} + N_2\lambda_{21}$$
$$\frac{dN_2}{dt} = -N_2\lambda_{21} + N_1\lambda_{12}$$

$$\frac{d}{dt}\begin{pmatrix} N_1 \\ N_2 \end{pmatrix} = \begin{bmatrix} -\lambda_{12} & \lambda_{21} \\ \lambda_{12} & -\lambda_{21} \end{bmatrix}\begin{pmatrix} N_1 \\ N_2 \end{pmatrix}$$

$$\frac{d}{dt}\begin{pmatrix} N_1 \\ N_2 \end{pmatrix} = \begin{bmatrix} -\lambda_{12} & \lambda_{21} \\ \lambda_{12} & -\lambda_{21} \end{bmatrix}\begin{pmatrix} N_1 \\ N_2 \end{pmatrix}$$

$$\text{suppose at } t = 0, \begin{pmatrix} N_1 \\ N_2 \end{pmatrix} = \begin{pmatrix} 1 \\ 0 \end{pmatrix}, \text{then}$$

$$\begin{pmatrix} N_1(t) \\ N_2(t) \end{pmatrix} = \frac{1}{\lambda_{12}+\lambda_{21}}\begin{pmatrix} \lambda_{21} \\ \lambda_{12} \end{pmatrix} + \frac{1}{\lambda_{12}+\lambda_{21}}\begin{pmatrix} \lambda_{12} \\ -\lambda_{12} \end{pmatrix} e^{-(\lambda_{12}+\lambda_{21})t}$$

$$\text{after a sufficiently long time: } N_1 \longrightarrow \frac{\lambda_{21}}{\lambda_{12}+\lambda_{21}}$$

$$N_2 \longrightarrow \frac{\lambda_{12}}{\lambda_{12}+\lambda_{21}}$$

N_1 and N_2 form a *quasi-equilibrium cluster*

However, note that N_1/N_2 (= $\lambda_{21}/\lambda_{12}$) does not depend on reaction rates! Recall that we already derived

$$\frac{\lambda_{21}}{\lambda_{12}} \propto e^{-Q/kT}$$

When we calculate $\langle\sigma v\rangle$ for a photon-induced reaction, we have to include E_γ= pc and photon statistics. At a given temperature,

$$\lambda_{21} = \frac{8\pi}{h^3c^2}\int_0^\infty \frac{E_\gamma^2}{e^{E_\gamma/kT}-1}\sigma\left(E_\gamma\right)dE_\gamma \quad \text{and}$$

$$\frac{\lambda_{21}}{\lambda_{12}} = \left(\frac{2\pi}{h^2}\right)^{3/2}\frac{(\mu kT)^{3/2}}{N_A}\frac{(2j+1)(2J_1+1)}{2J_2+1}e^{-Q_{12}/kT},$$

where J_1 and J_2 are the spins of nuclei 1 and 2; j is the spin of whatever is interacting with nucleus 1. Note that this depends on the Q-value, not on the cross section. One complication is that we now have to consider the roles of excited states in the transition rates, each of which makes its own contribution to λ_{12} and λ_{21}.

Excited states:

As long as the forward and backward reactions maintain equilibrium, the transition rate has the same form as before, but is weighted by the probability that the state in question is occupied. In other words, the transition rate is multiplied by a *normalized partition function:*

$$G^{norm} = \frac{\sum_i g_i e^{-E_{xi}/kT}}{g_{ground}}, \text{ where } \; g = 2J+1$$

Also, to do this properly, we need to keep track of the number of reacting nuclei, which I'll call N_0. The net reusult is that the abundance ratio N_2/N_1 is replaced by N_2/N_0N_1:

$$0{+}1 \leftrightarrow 2{+}\gamma : \;\; \frac{N_2}{N_0 N_1} = \left(\frac{h^2}{2\pi}\right)^{3/2} \frac{1}{(\mu_{01}kT)^{3/2}} \frac{G_3^{norm}}{G_0^{norm} G_1^{norm}} e^{-Q_{0+1}/kT} \;\; (Saha \text{ equation})$$

Here's an example. Suppose that the initial Si is dissociated into a gas of protons and neutrons, which are re-assembled into heavier nuclei, which are photodisintegrated, etc. so that all forward and backward reactions are in equilibrium. Nucleus Y is made of π protons and ν neutrons, and

$$N_Y = N_p^\pi N_n^\nu \frac{1}{\theta^{A-1}} \left(\frac{m_Y}{m_p^\pi m_n^\nu}\right) \frac{g_Y}{2^A} G_Y^{norm} e^{B_Y/kT}$$

$$\text{where } \; A = \pi + \nu \; \text{ and } \; \theta = (\mu_{01}kT)^{3/2} .$$

This requires multiple applications of the Saha equation - one for each step up to nucleus Y. Notice that the Q-value is replaced by the binding energy of Y (B_Y), wich is just the Q-value for assembling π protons and ν neutrons.

During Si-burning, nucleons and nuclei are re-arranged in favor of maximum binding energy, which depends on T, ρ and Z/N:

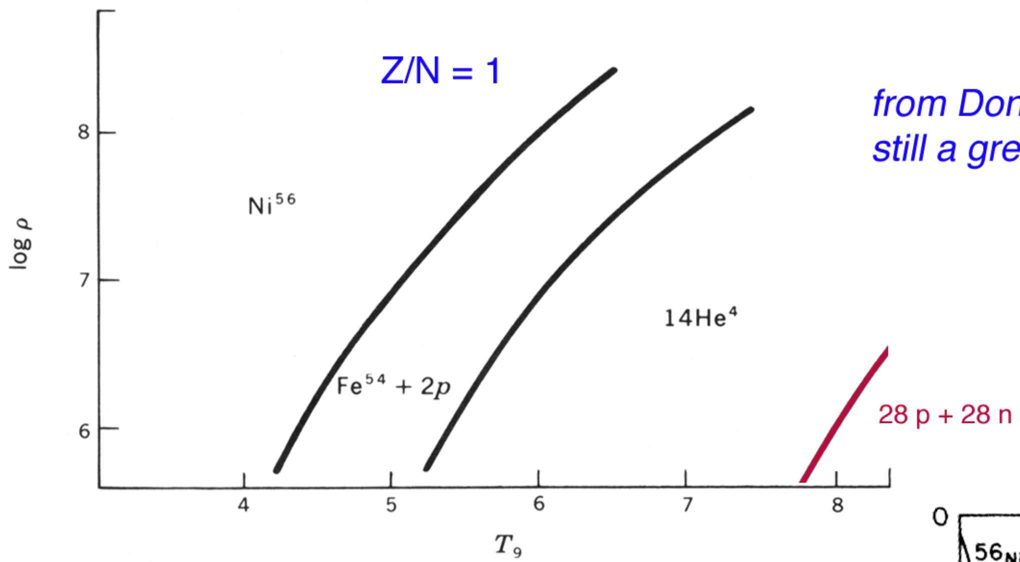

from Don Clayton's book (with modification - still a great resource)

for $T_9 = 3.5$, $\rho = 10^7$ g/cm³ (from Iliadis)

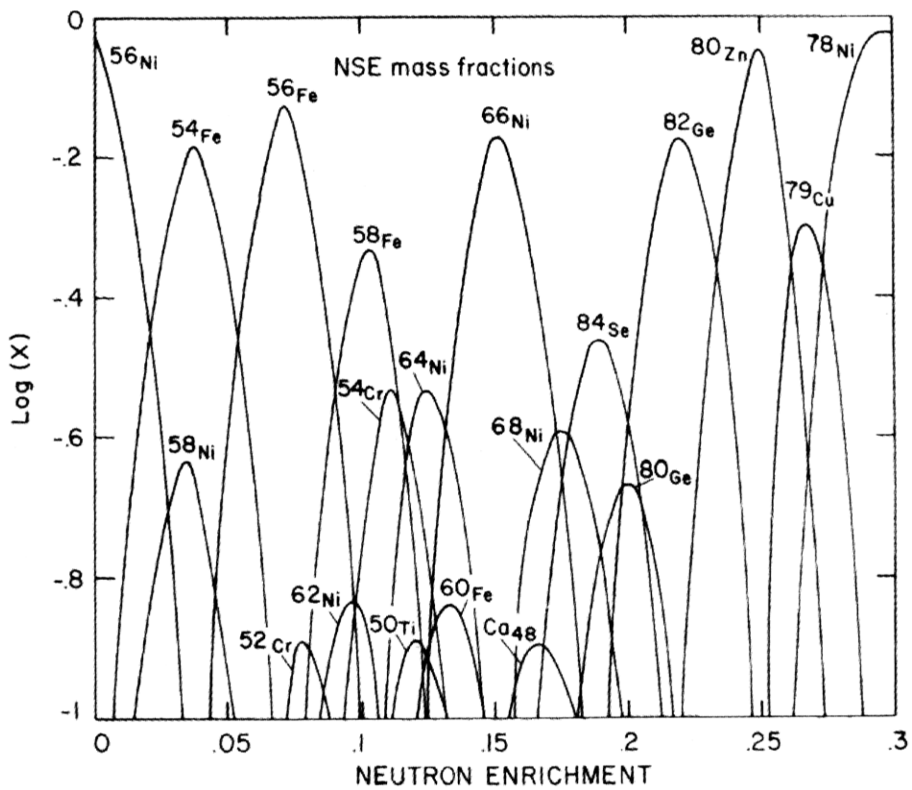

nuclei heavier than Fe

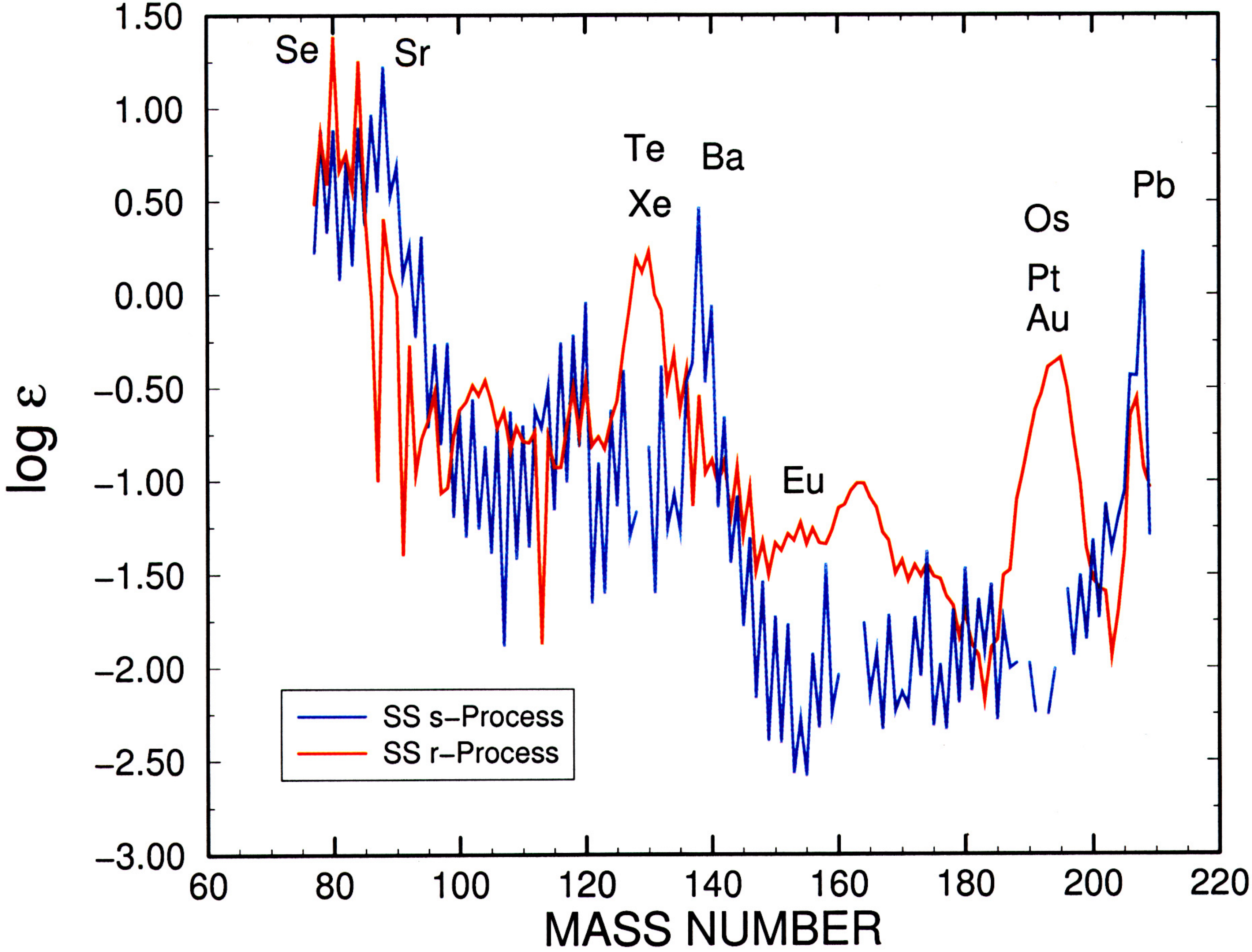

origin of the abundance peaks

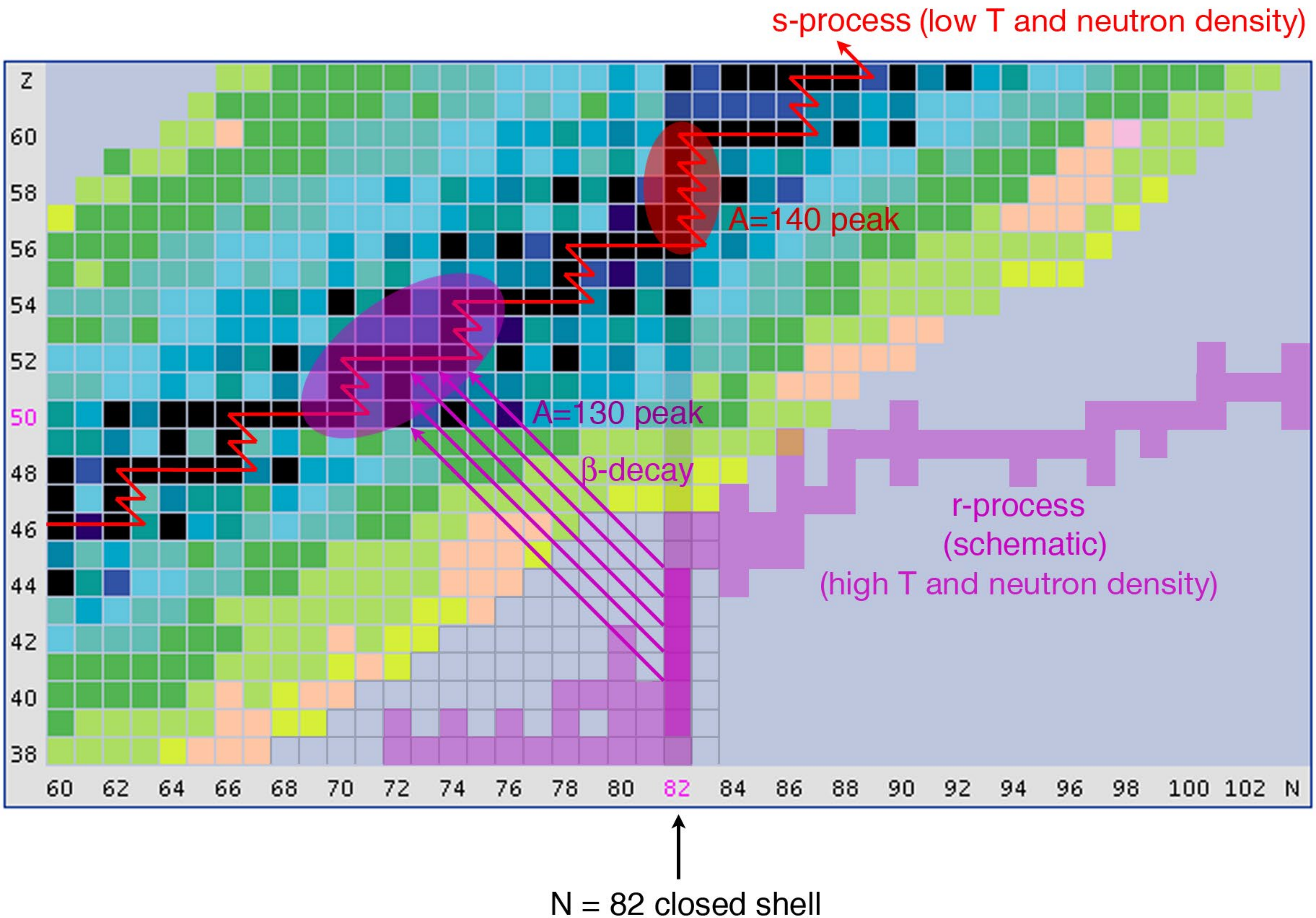

The s-process: T_9 ~0.08 (kT ~ 8 keV), ρ_n ~$10^7/cm^3$, duration ~ 2 x 10^4 y

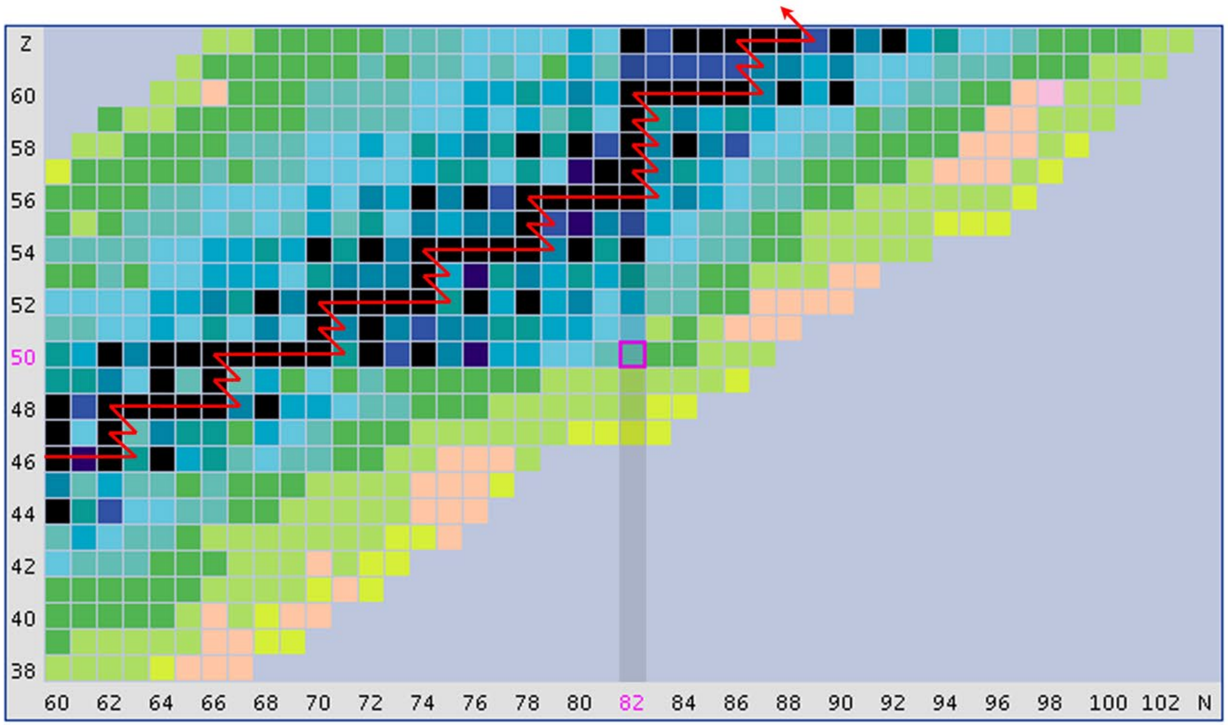

some equations:

$$\frac{dN(A)}{dt} = -N_n N(A)\langle\sigma v\rangle_A + N_n N(A-1)\langle\sigma v\rangle_{A-1}$$

$$N_A\langle\sigma\rangle \equiv \frac{N_A\langle\sigma v\rangle}{v_T} = \frac{1}{v_T} N_A \int_0^\infty v\phi(v)\sigma_n(v)dv$$

$$= \frac{4}{\sqrt{\pi}}\frac{N_A}{v_T^2}\int_0^\infty v\sigma_n(v)\left(\frac{v}{v_T}\right)^2 e^{-(v/v_T)^2}dv$$

$$v_T = \sqrt{\frac{2kT}{\mu}},\ \mu \approx m_n$$

why do this? $\quad$ low-energy, s-wave capture : $\sigma \;\alpha\; P_\ell(E) = kR$ so $\sigma \;\alpha\; \dfrac{1}{v}$

$$\text{higher energies}: \; \sigma \;\alpha\; \frac{1}{v^2} \; \text{(s-waves)}; \;\; \alpha\; v \; \text{(p-waves)}$$

$$\text{so} \; \langle \sigma v \rangle \approx \text{const.} \approx \langle \sigma \rangle v_T$$

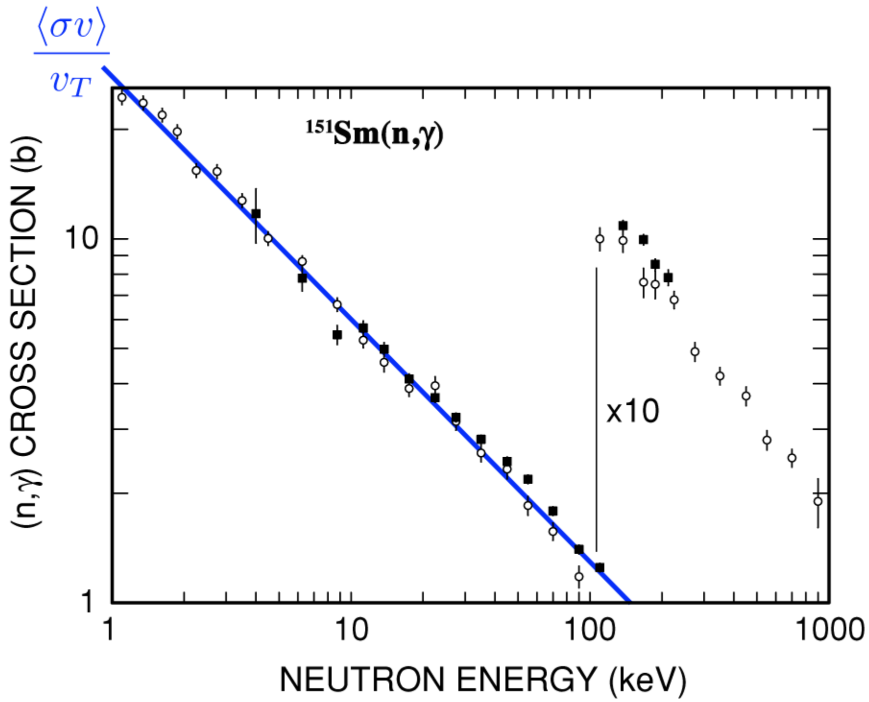

K. Wisshak *et al.*,
Phys. Rev. C **73**, 015802 (2006)

$$\frac{dN(A)}{dt} = v_T N_n(t)[-N(A)\langle\sigma\rangle_A + N(A-1)\langle\sigma\rangle_{A-1}]$$

$$\text{neutron exposure} \;\; \tau = v_T \int N_n(t)dt \;\; \Longrightarrow dt = \frac{d\tau}{v_T N_n(t)}$$

$$\text{so} \;\; \frac{dN(A,\tau)}{d\tau} = -N(A)\langle\sigma\rangle_A + N(A-1)\langle\sigma\rangle_{A-1}$$

$$\frac{dN(A,\tau)}{d\tau} = -N(A)\langle\sigma\rangle_A + N(A-1)\langle\sigma\rangle_{A-1}$$

this is a self-regulating system, i.e. for sufficiently long times:

$$\frac{dN(A,\tau)}{d\tau} \longrightarrow 0 \;\text{ or }\; N(A)\langle\sigma\rangle_A = N(A-1)\langle\sigma\rangle_{A-1}$$

$$\text{"}\textit{local approximation}\text{"}, N\langle\sigma\rangle \approx \text{const.}$$

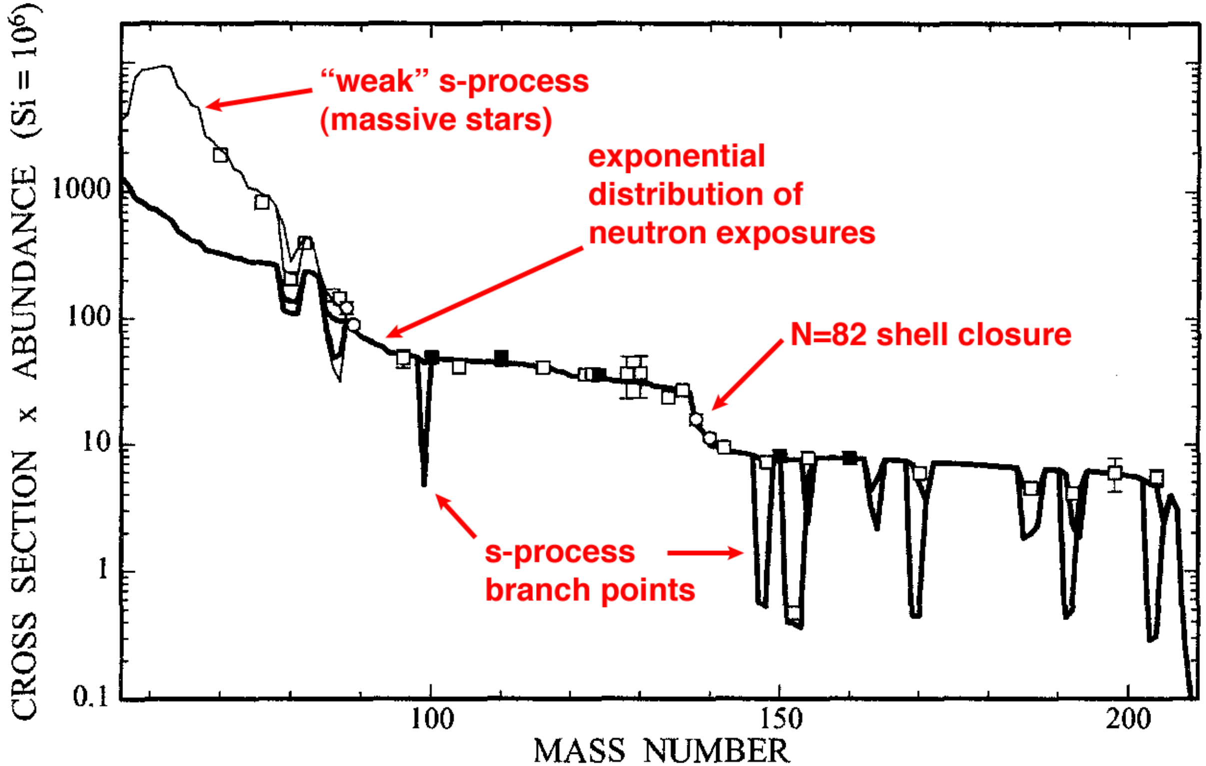

F. Käppeler / Prog. Part. Nucl. Phys. 43 (1999) 419–483 "*s*" implies $\tau_n < \tau_\beta$

e.g. A = 150,
kT = 8 keV,
$v_T = 10^7$ cm/s
$<\sigma> \sim 1$ b

$<\sigma>v_T = 10^{-18}$ cm^3/s

$\tau_n = (N_n<\sigma>v_T)^{-1} = 300$ y

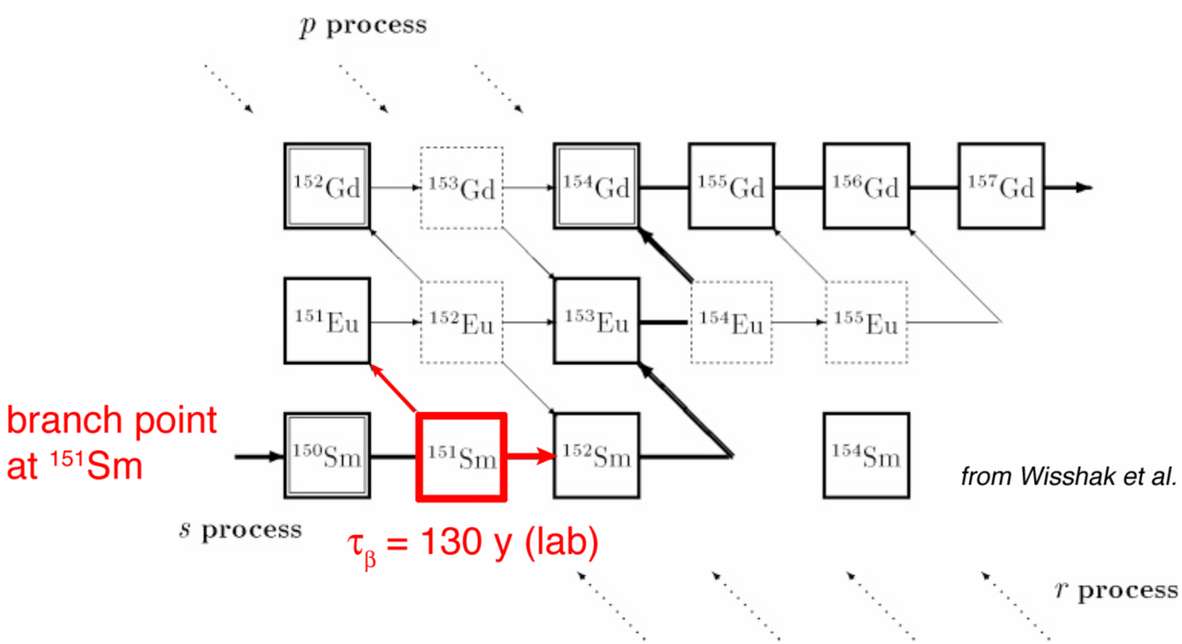

β-decay (temperature dependent)
vs.
n-capture (depends mostly on N_n)

branch points show evidence for activation of the ^{22}Ne n-source during thermal pulses: $T_9 \sim 0.25$-0.3, $\rho_n \sim 10^{10}$/cm^3, duration of ~ 10-20 y

Another reason why the s-process is interesting:

D.L. Lambert and C.A. Prieto, Mon. Not. R. Astron. Soc. **335**, 325 (2002)

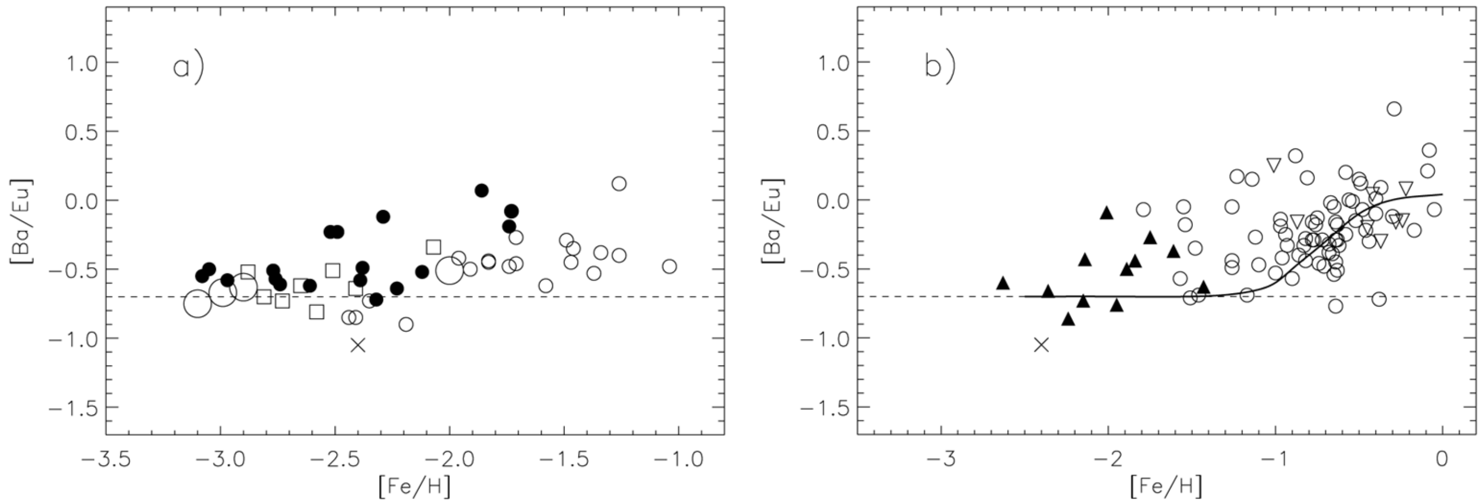

Figure 4. The abundance ratio [Ba/Eu] versus [Fe/H] for a representative sample of metal-poor giants (a) and dwarf/sub-giants (b). HD 140283 is identified by a cross. Symbols are as in Fig. 3 where the four severely r-process enriched giants are shown by large open circles.

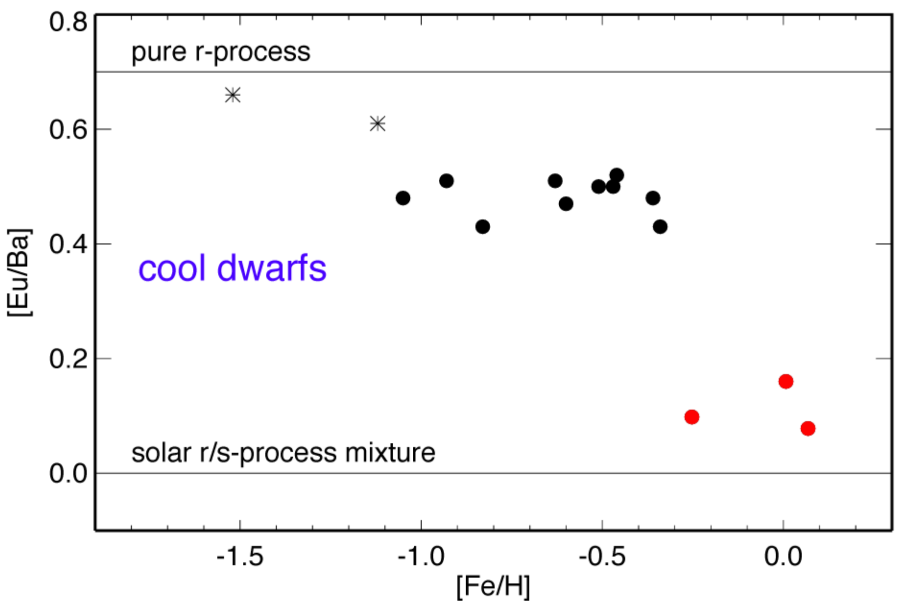

L. Mashonkina and T. Gehren, A&A **364**, 249 (2000) a rough interpretation

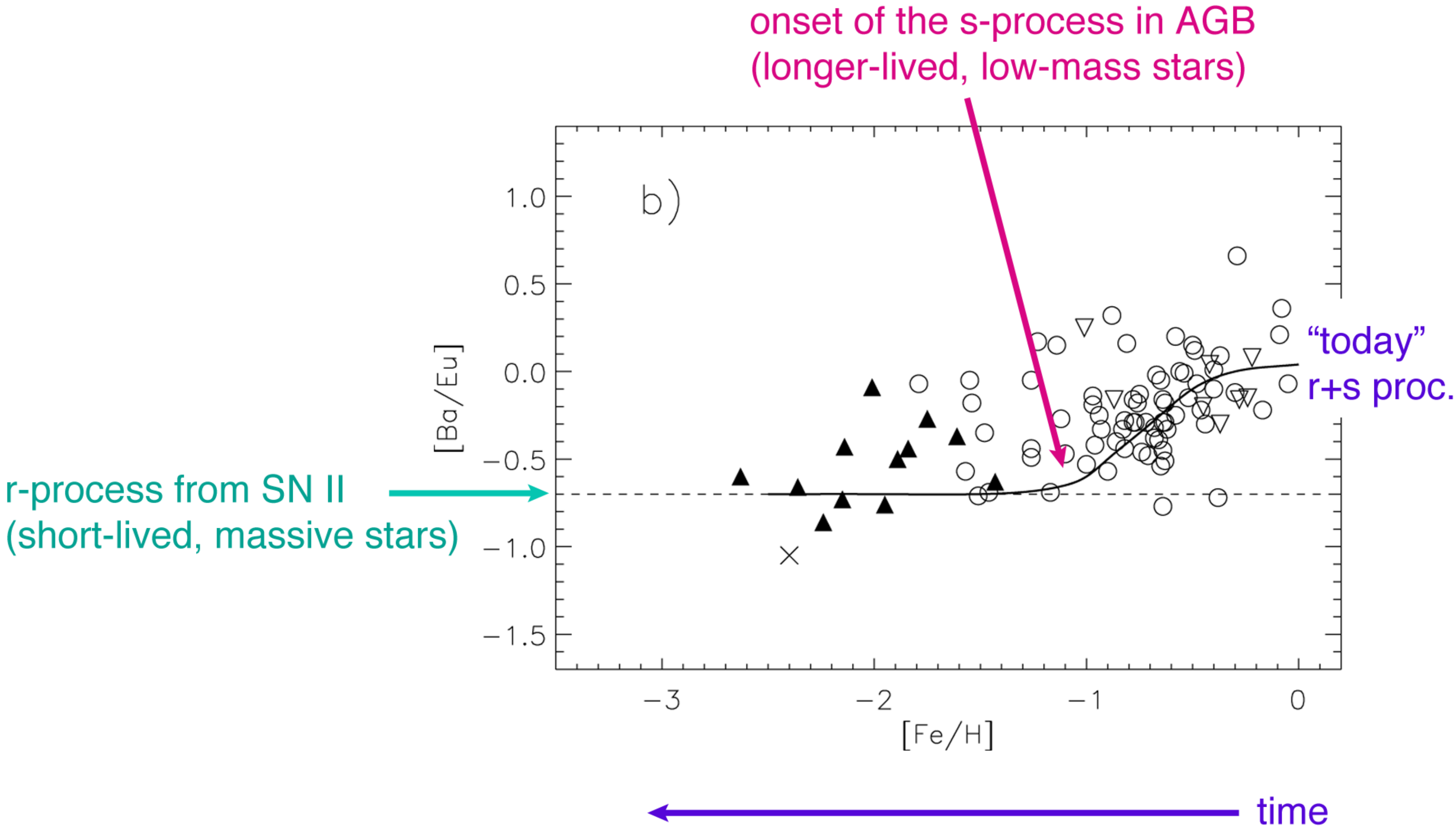

Observations of very metal-poor halo stars

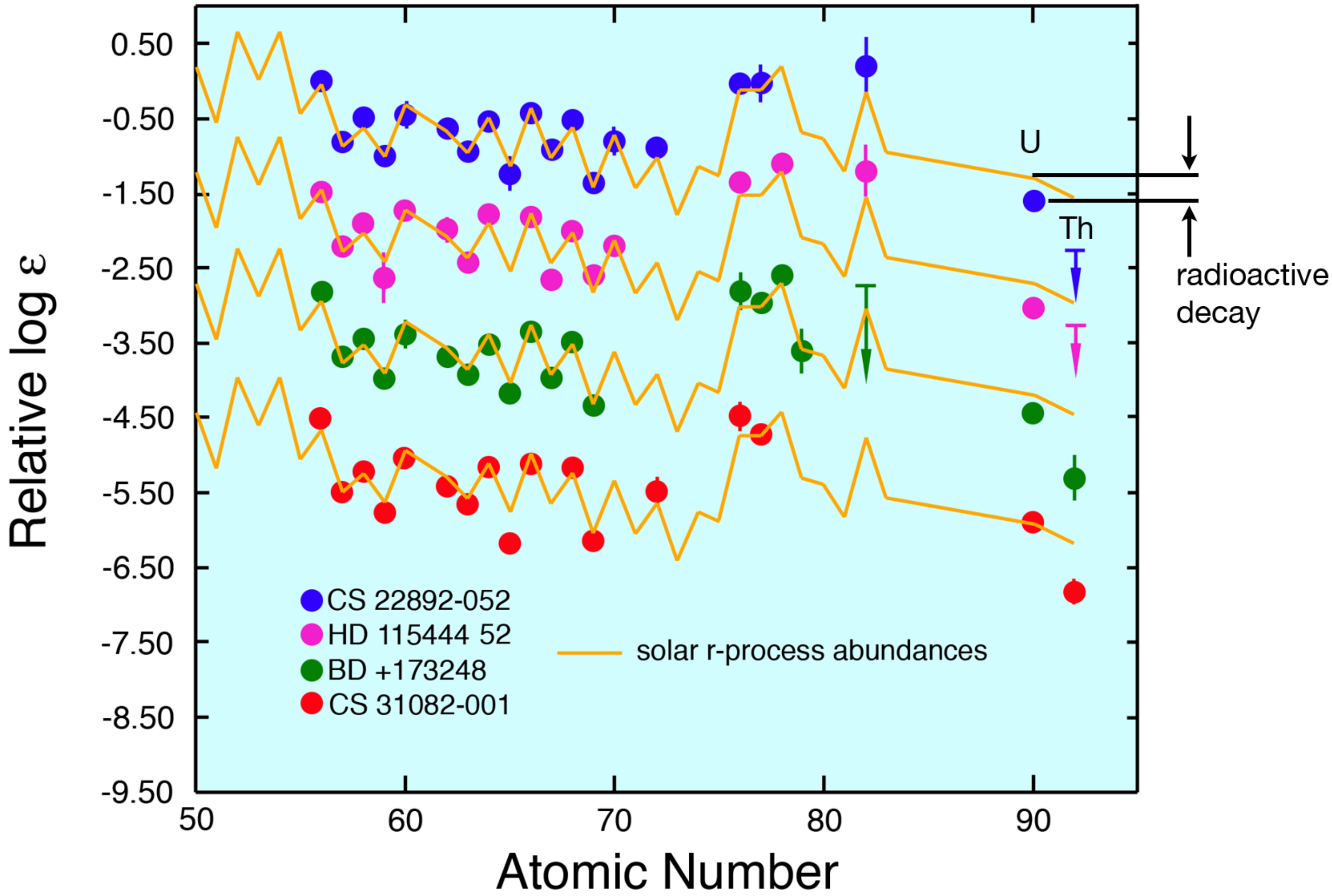

adapted from J.J. Cowan and C. Sneden

Eu-Th ages ~12 - 15 Gy

U-Th age = 14.1 ± 2.4 Gy [CS 31082-001, S. Wanajo *et al.*, Ap. J. **593**, 968 (2003)]

r-process: we need an environment with $T_9 > 1$ and
$\rho_n \sim 10^{22}/cm^3$ (so $\tau_{(n,\gamma)} \sim 100$ ns)

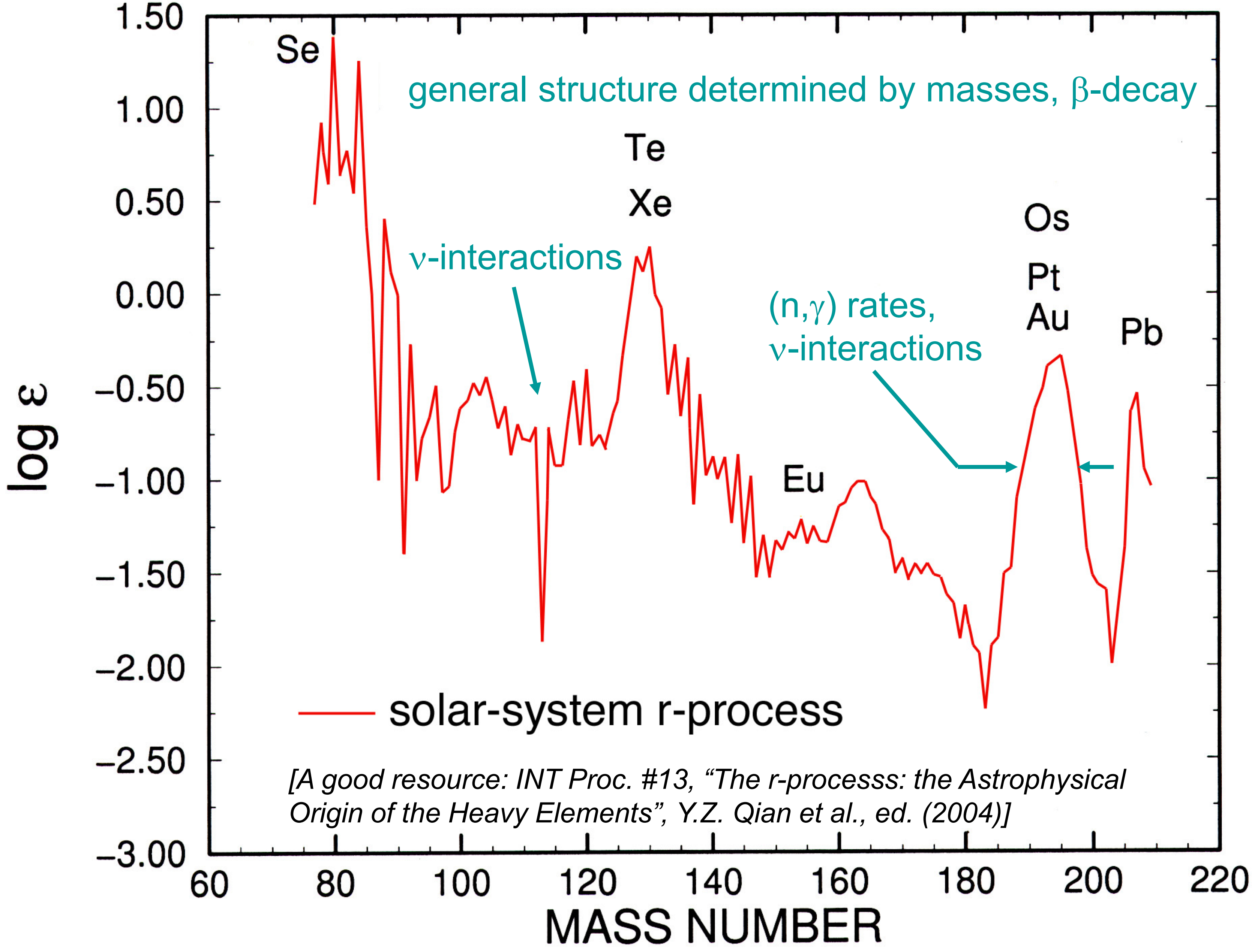

building blocks of the r-process

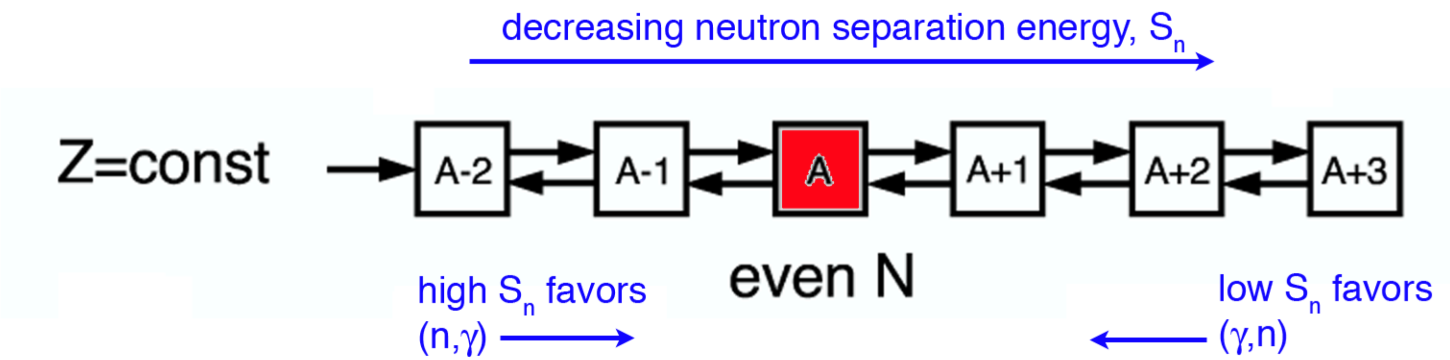

for (n,γ) - (γ,n) equilibrium:

$$\frac{N(Z,A+1)}{N(Z,A)} = n_n \left(\frac{2\pi\hbar^2}{\mu_A kT}\right)^{3/2} \frac{2J_{A+1}+1}{(2J_A+1)(2J_n+1)} \frac{G^{norm}_{A+1}}{G^{norm}_{A}} e^{S_n/kT}$$ (Saha equation)

for $\frac{N(Z,A+1)}{N(Z,A)} = 1: \; S_n(MeV) = \frac{T_9}{11.605}\left[77.8 + 1.5\ln T_9 - \ln n_n(cm^{-3})\right] \simeq 3\,MeV$

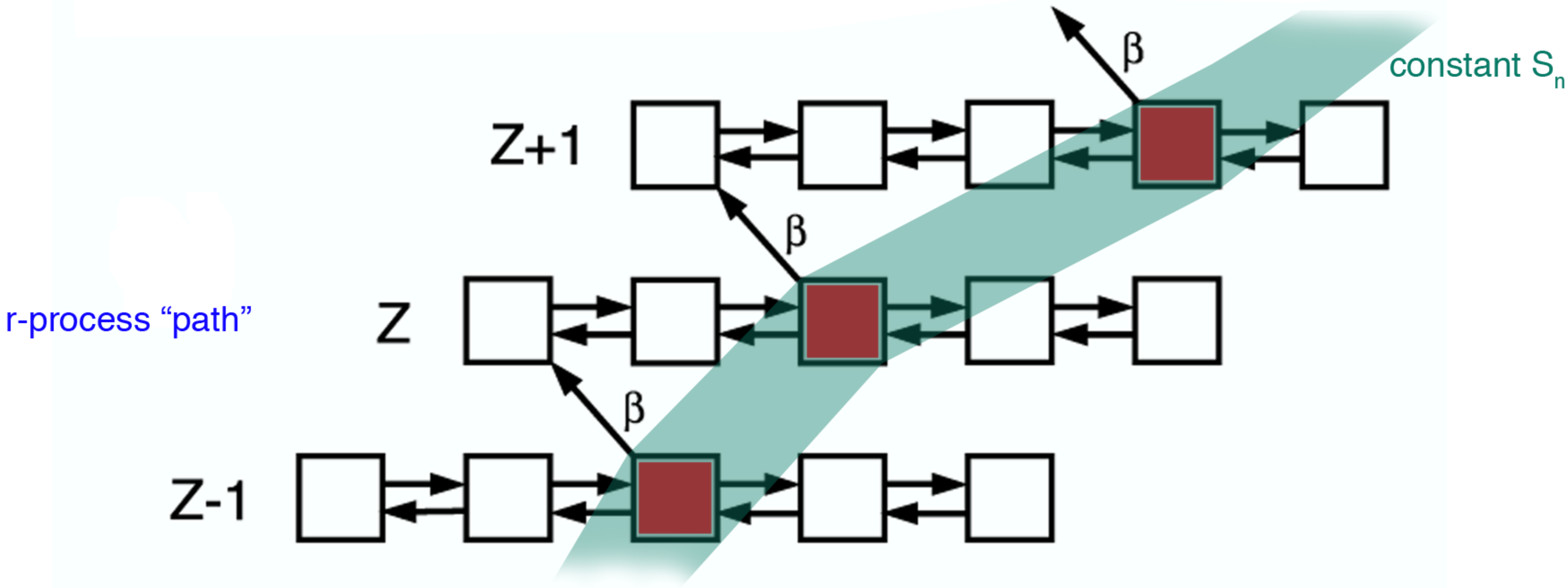

at the closed neutron shells:

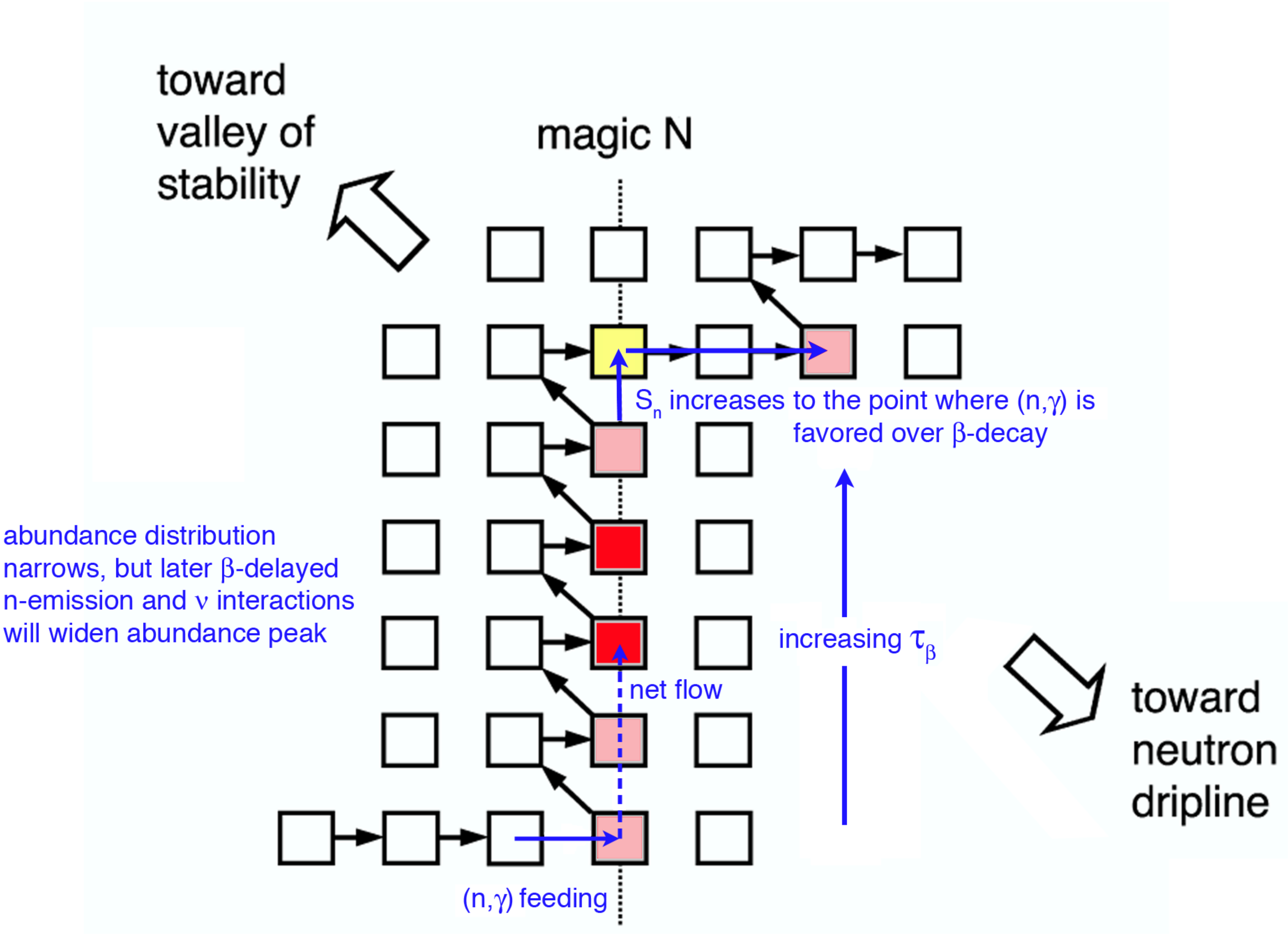

mass flow between isotopic chains: $\frac{dN_Z}{dt} = -\lambda_{\beta(Z)} N_Z + \lambda_{\beta(Z-1)} N_{Z-1}$

which evolves to $\frac{dN_Z}{dt} = 0 \longrightarrow \lambda_{\beta(Z)} N_Z \approx \lambda_{\beta(Z-1)} N_{Z-1}$ or $\lambda_{\beta(Z)} N_Z = const.$

("steady flow approx.")

best-fit parameters for steady flow
[K.L. Kratz et al.]

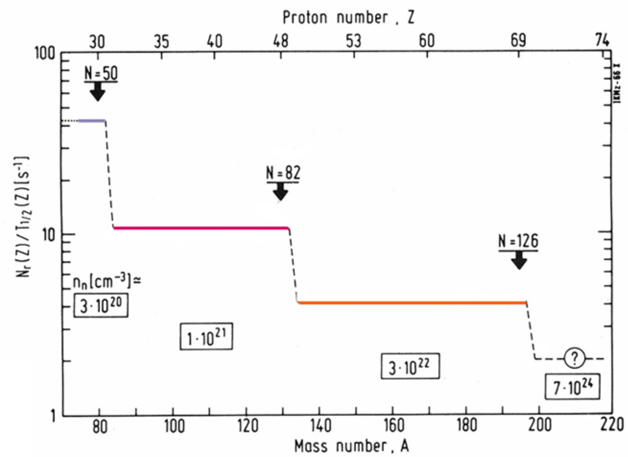

but note mid-shell problems -
nuclear physics or astrophysics?

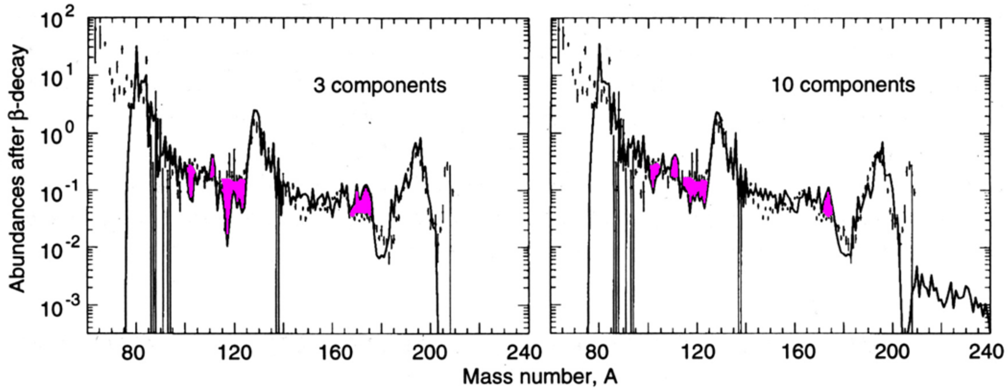

freezeout:

as T, n_n go down, equilibrium shifts to higher S_n, i.e. β-decay goes to higher S_n and (n,γ) cannot push out to lower S_n so a new equilibrium is established at higher S_n and the flow moves closer to stability

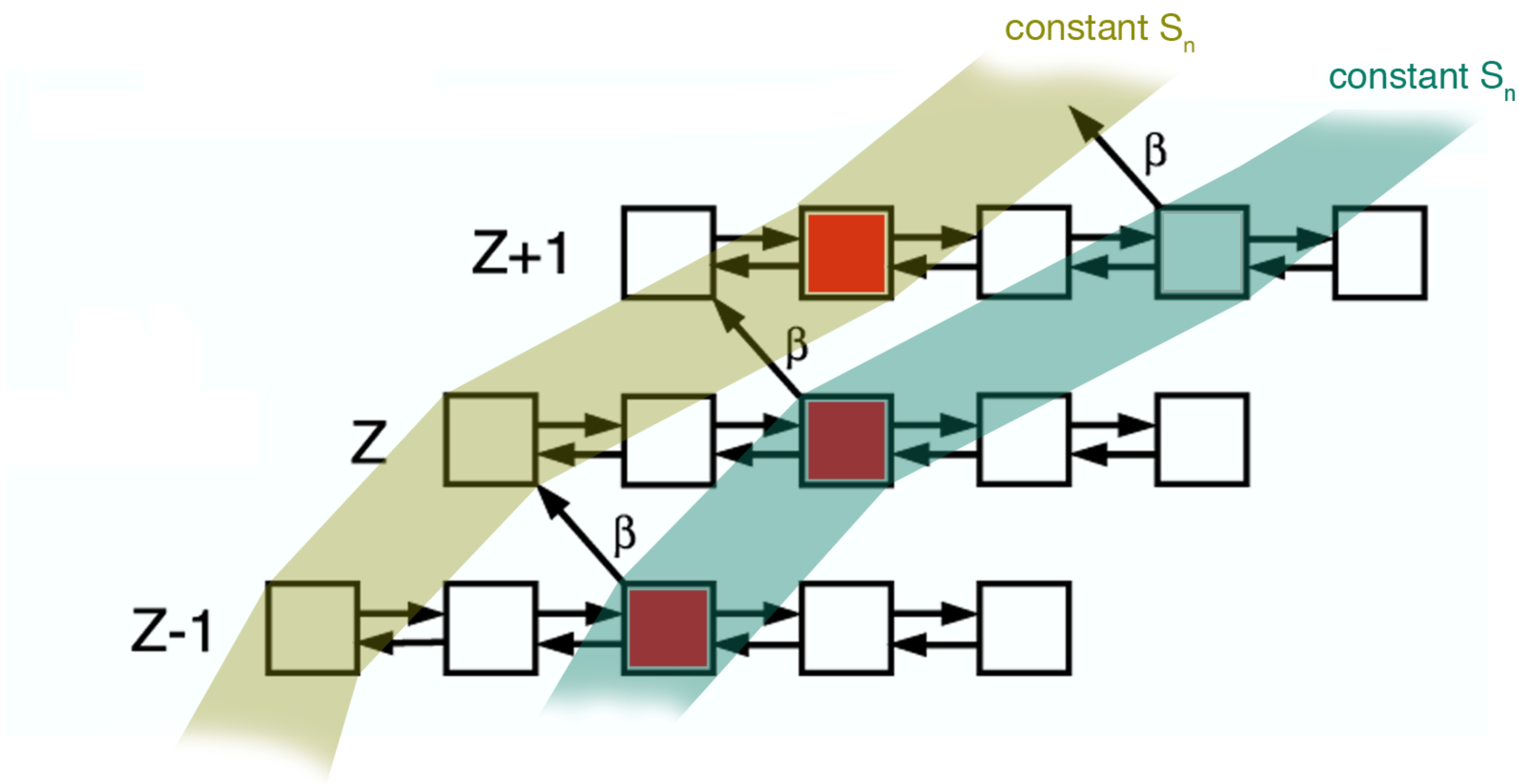

finally, equilibrium breaks down and $\tau_n > \tau_\beta \longrightarrow$ β-decay to stability recap:

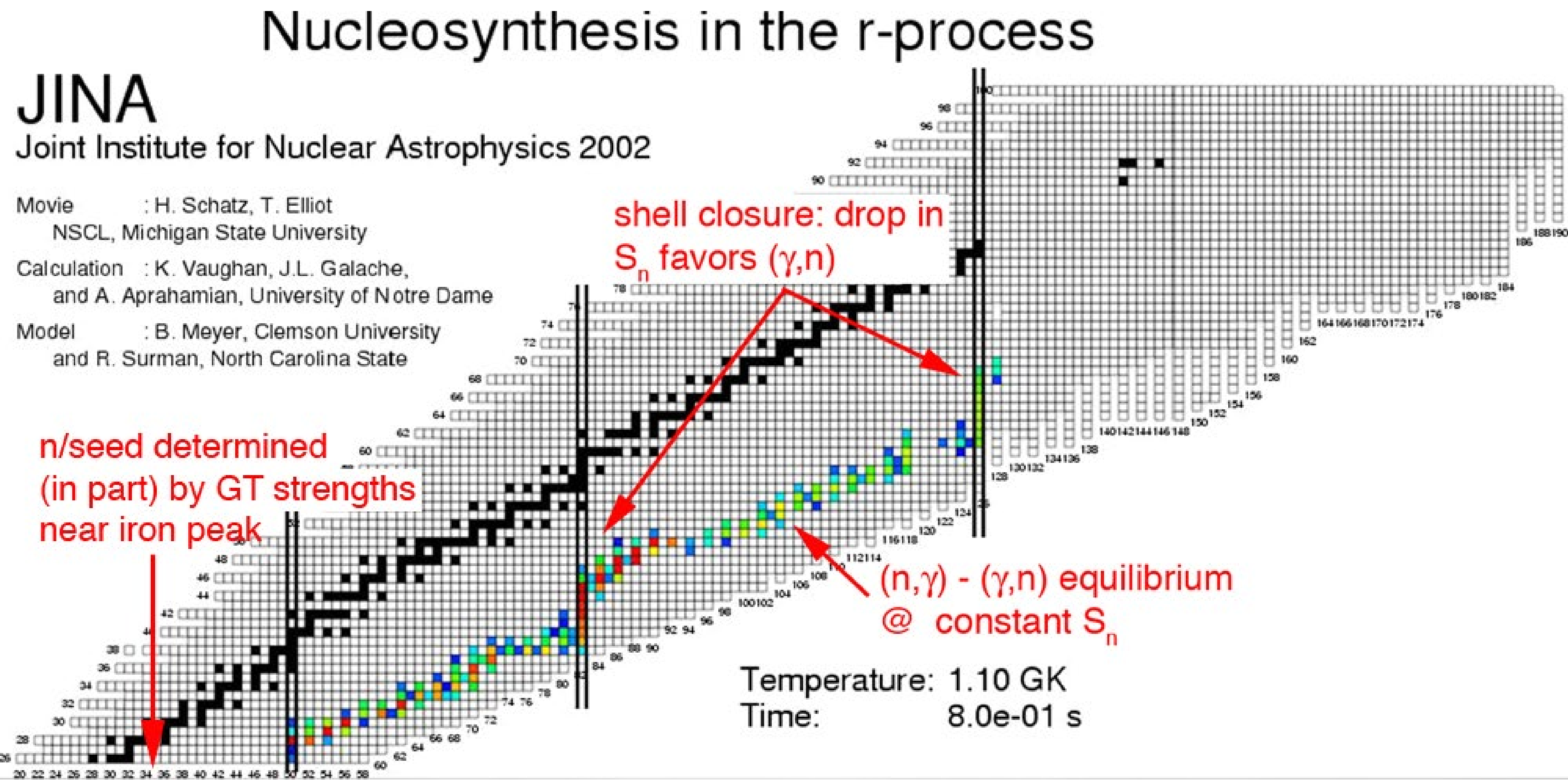
Nucleosynthesis in the r-process
JINA
Joint Institute for Nuclear Astrophysics 2002
Movie : H. Schatz, T. Elliot
NSCL, Michigan State University
Calculation : K. Vaughan, J.L. Galache,
and A. Aprahamian, University of Notre Dame
Model : B. Meyer, Clemson University
and R. Surman, North Carolina State
shell closure: drop in S_n favors (γ,n)
n/seed determined (in part) by GT strengths near iron peak
(n,γ) - (γ,n) equilibrium @ constant S_n
Temperature: 1.10 GK
Time: 8.0e-01 s

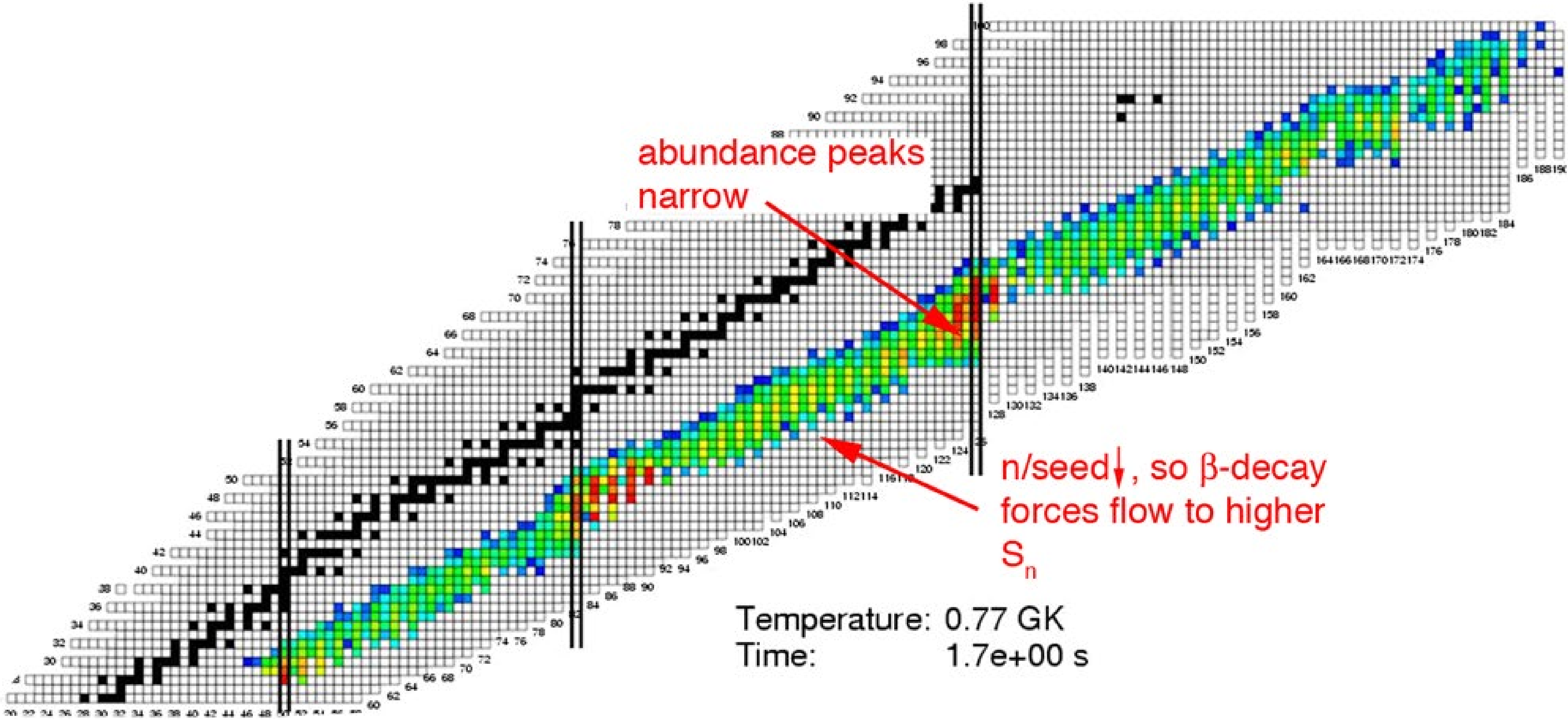
abundance peaks
narrow
n/seed↓, so β-decay
forces flow to higher
S_n
Temperature: 0.77 GK
Time: 1.7e+00 s

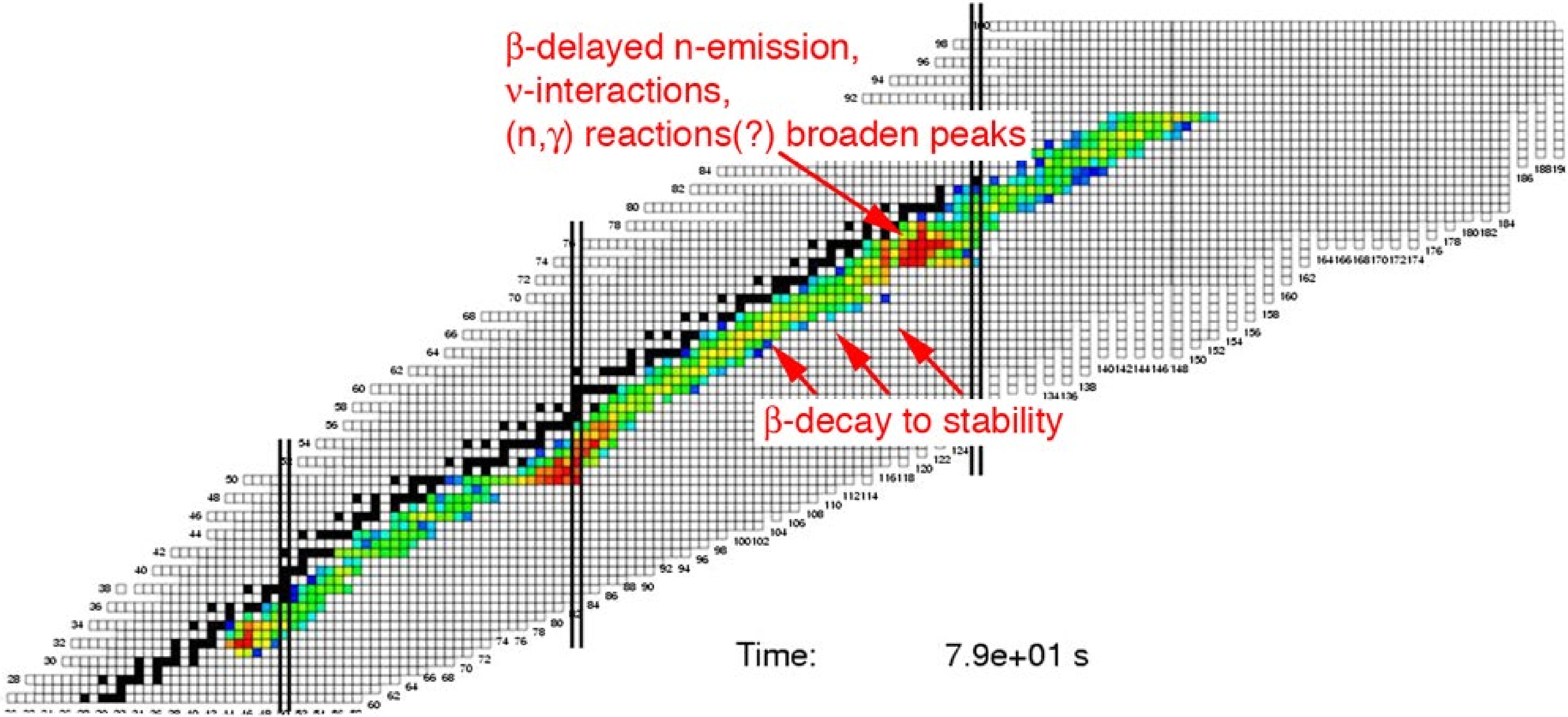
β-delayed n-emission,
ν-interactions,
(n,γ) reactions(?) broaden peaks
β-decay to stability
Time: 7.9e+01 s

So far, this is entirely schematic ***and*** there's been no mention of where this might occur. However, if we want to say something about ages or astrophysics from the abundances, then the nuclear input has to be correct:

For example, calculations with 2 different mass models (which predict S_n and τ_β):

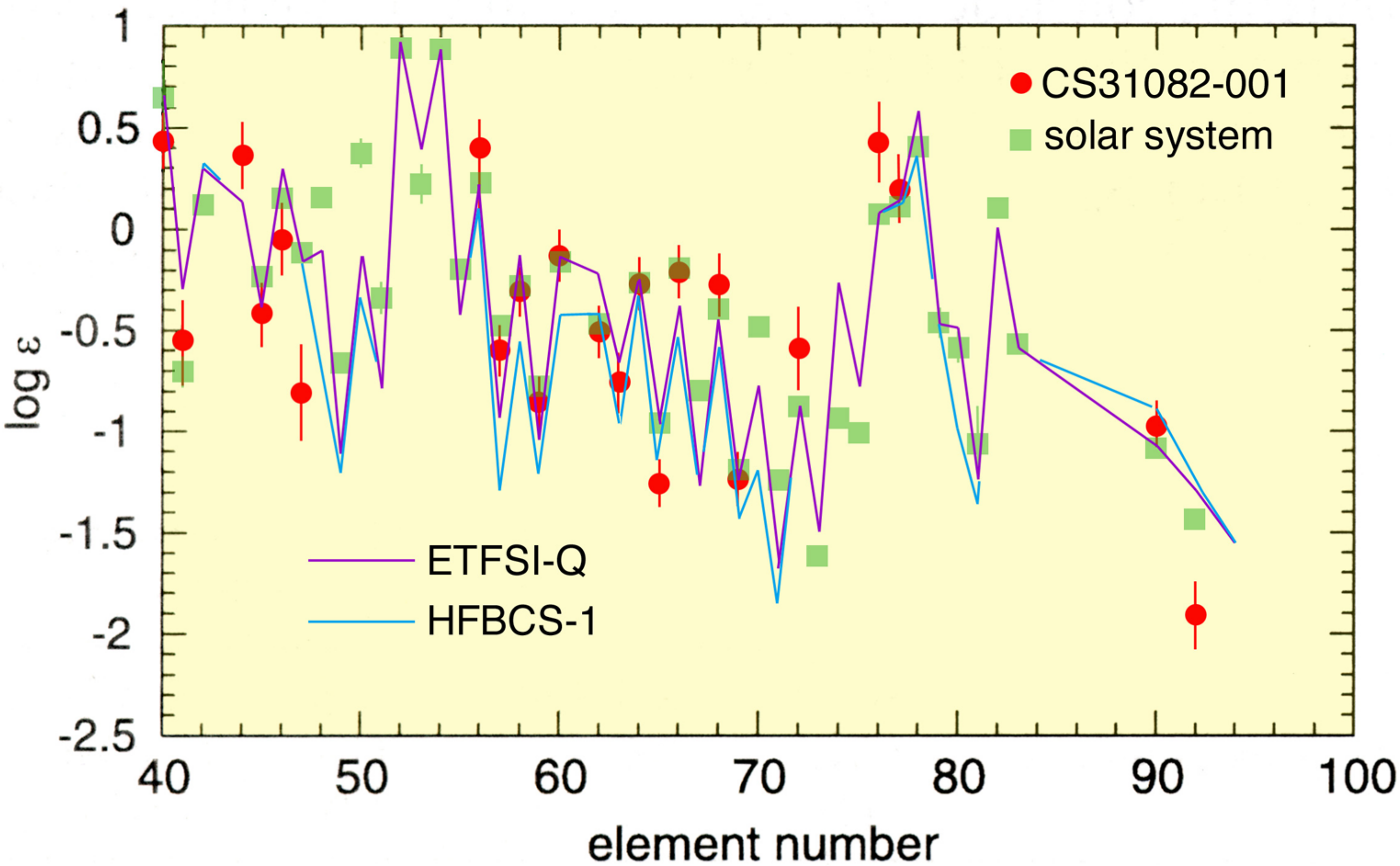

H. Schatz et al. Ap. J. 579, 626 (2002)

mass models

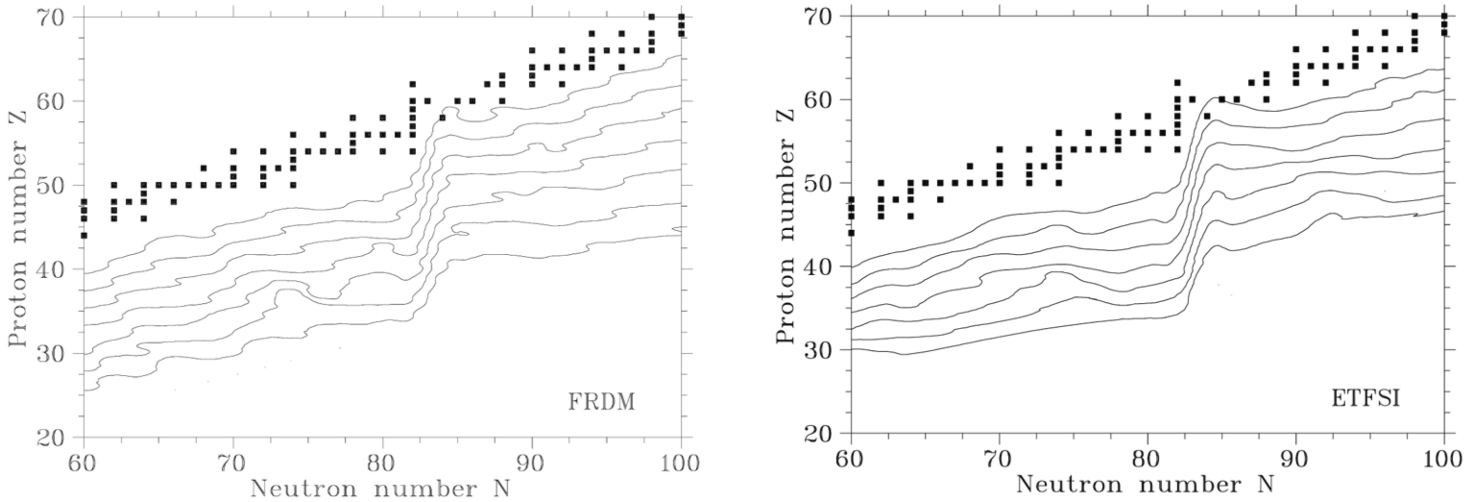

FIG. 1.—Contour plots of constant neutron separation energies in the $80 \leq A \leq 140$ mass region for the FRDM mass model (Möller et al. 1995) and the ETFSI mass model (Aboussir et al. 1995) at $S_n = 1, 2, 3, \ldots, 7$ MeV for even-N isotopes. The saddle point behavior before the shell closure at $N = -82$, causes the deep trough before the peak at $A = 130$ (see upper part of Fig. 3) as the step from the abundance maximum of an isotopic chain Z to $Z + 1$ can cause a large jump in N or equivalently A, leading to a large number of unpopulated mass numbers A.

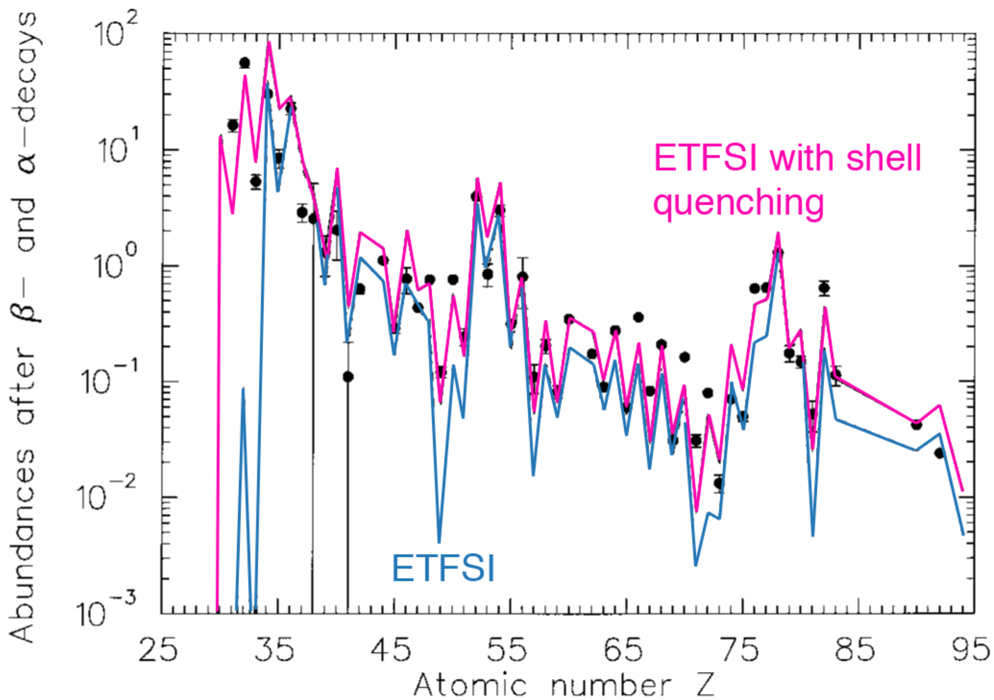

[reducing the shell gap slows (n,γ) vs. (γ,n) and increases τ_β, both of which impede flow out of mid-shell region]

[C. Freiburghaus et al. Ap. J. ***516****, 381 (1999)]*

a fairly typical situation:

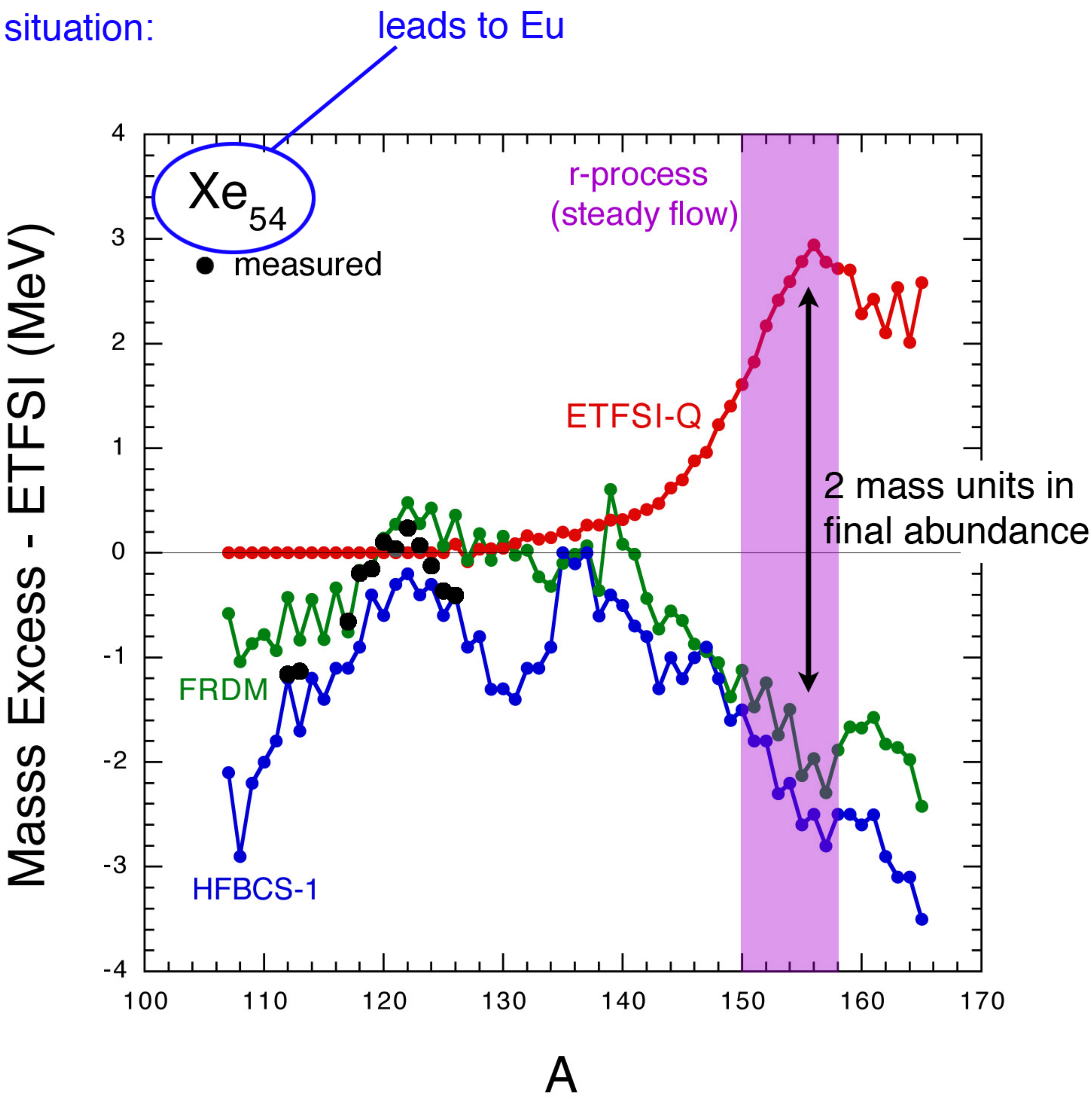

mass measurements of neutron-rich nuclei

[this example from S. Rahaman *et al.*, EPJ Special Topics, **150**, 349 (2007)]

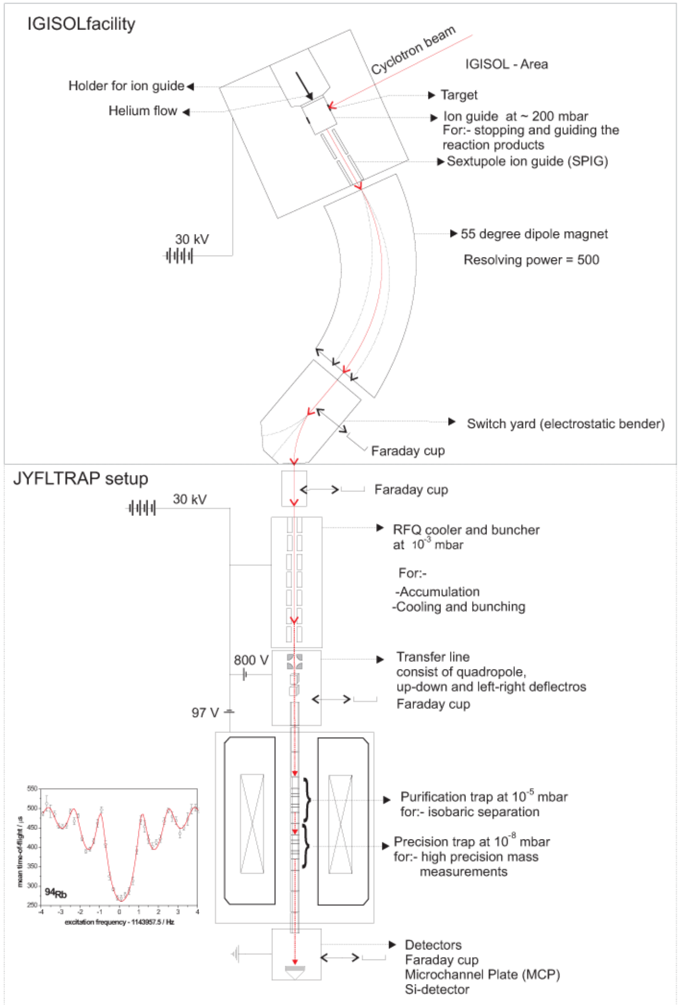

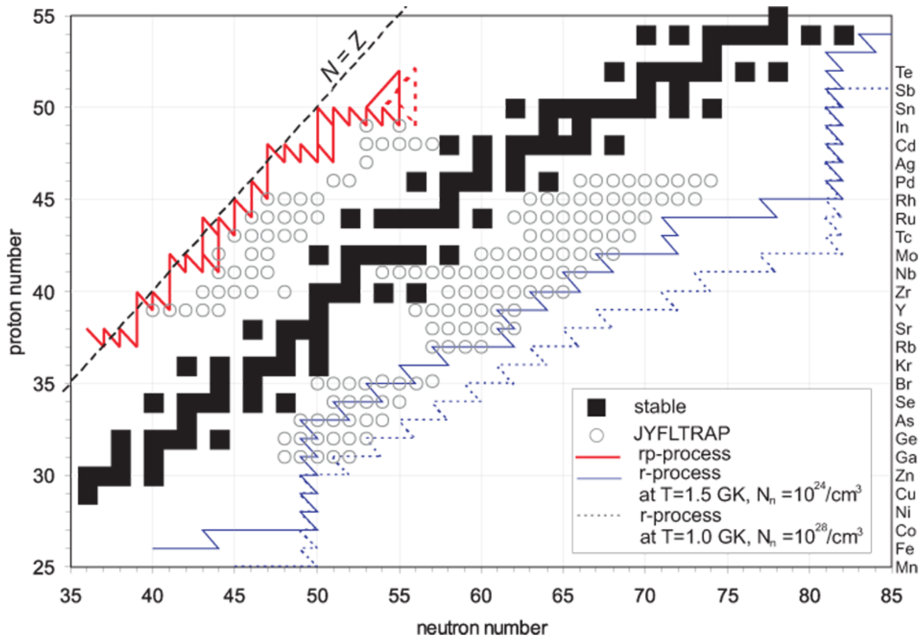

into the N = 50 peak

$^{2}H(^{82}Ge,p)^{83}Ge$

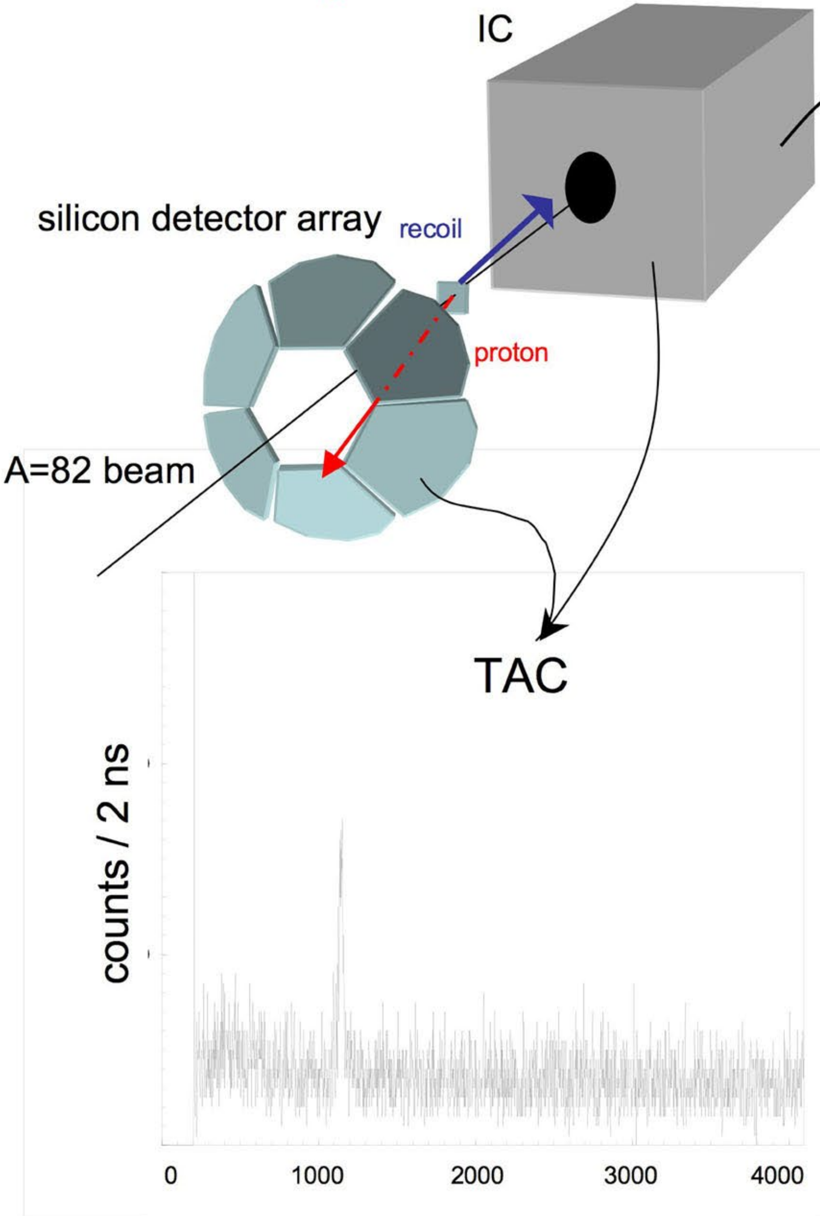

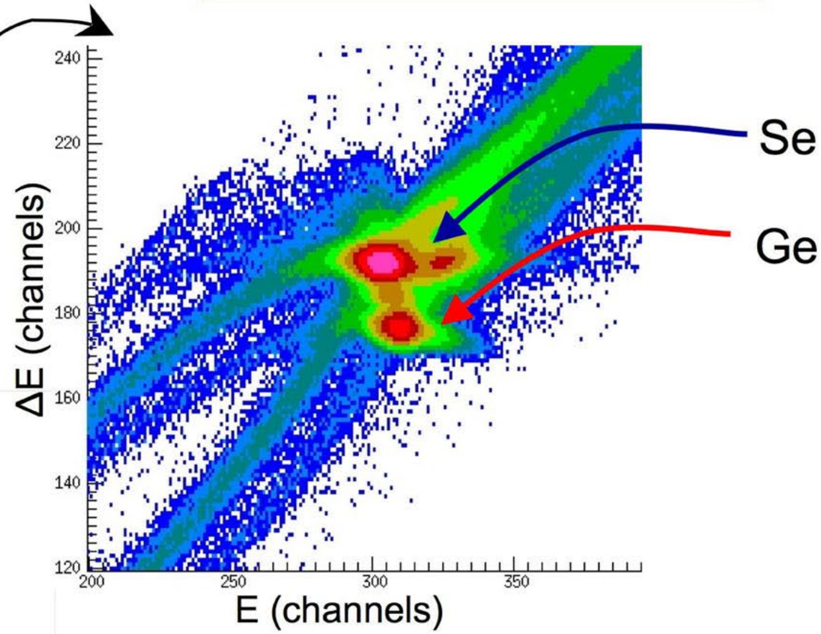

E_{beam} = 330 MeV (4 MeV/u)

430 μg/cm² CD_2 target

Ionization chamber at θ_{lab} = 0° filled with CF_4

SIDAR in lampshade configuration covering θ_{lab} = 105°-150°

coincidence timing between IC and SIDAR

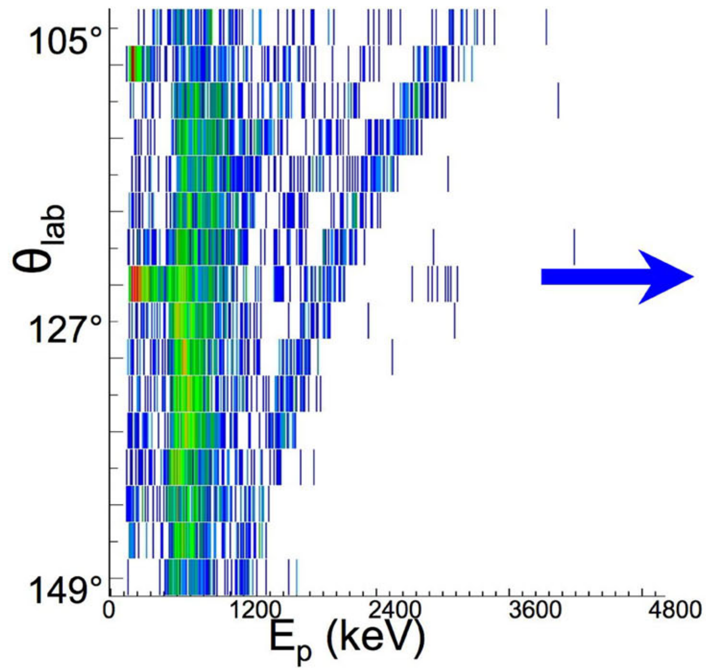

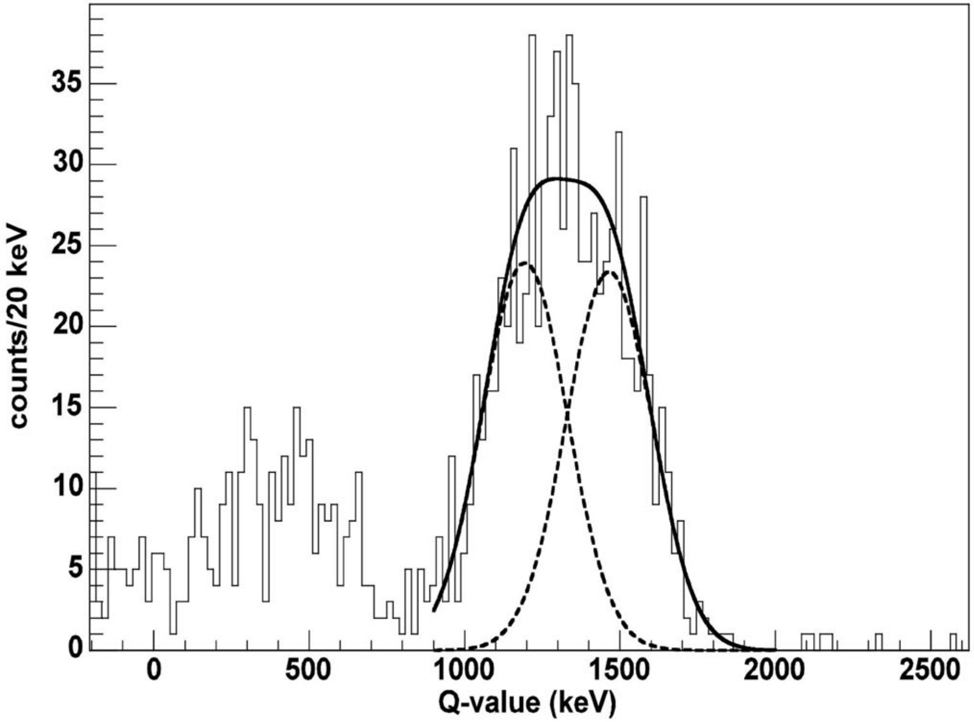

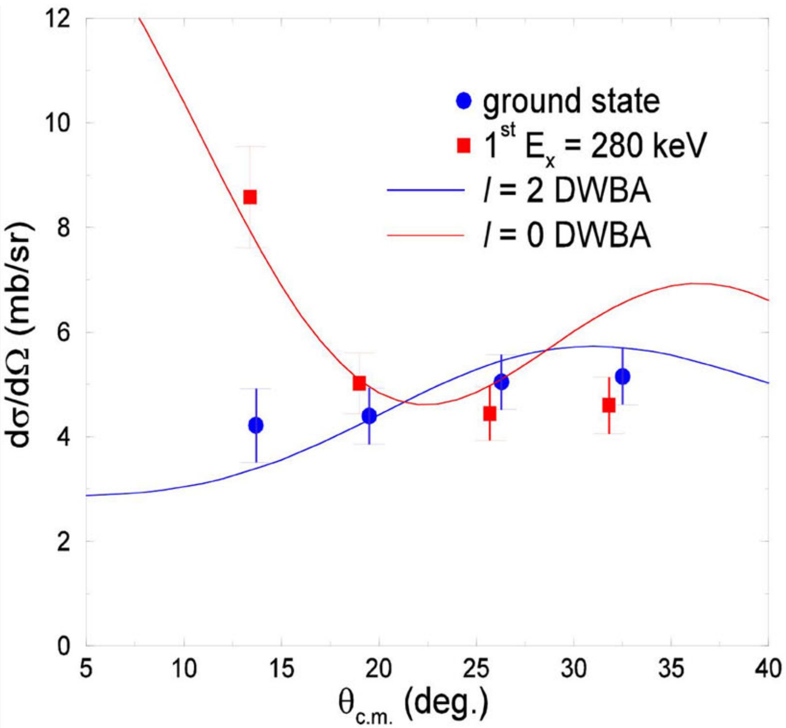

Q = 1.47 (±0.02 stat., ±0.07 sys.) MeV

1st E_x = 280 (± 20 stat.) keV

$S_n(^{83}Ge)$ = 3.69 ± 0.07 MeV

$\Delta(^{83}Ge)$ = – 61.25 ± 0.26 MeV

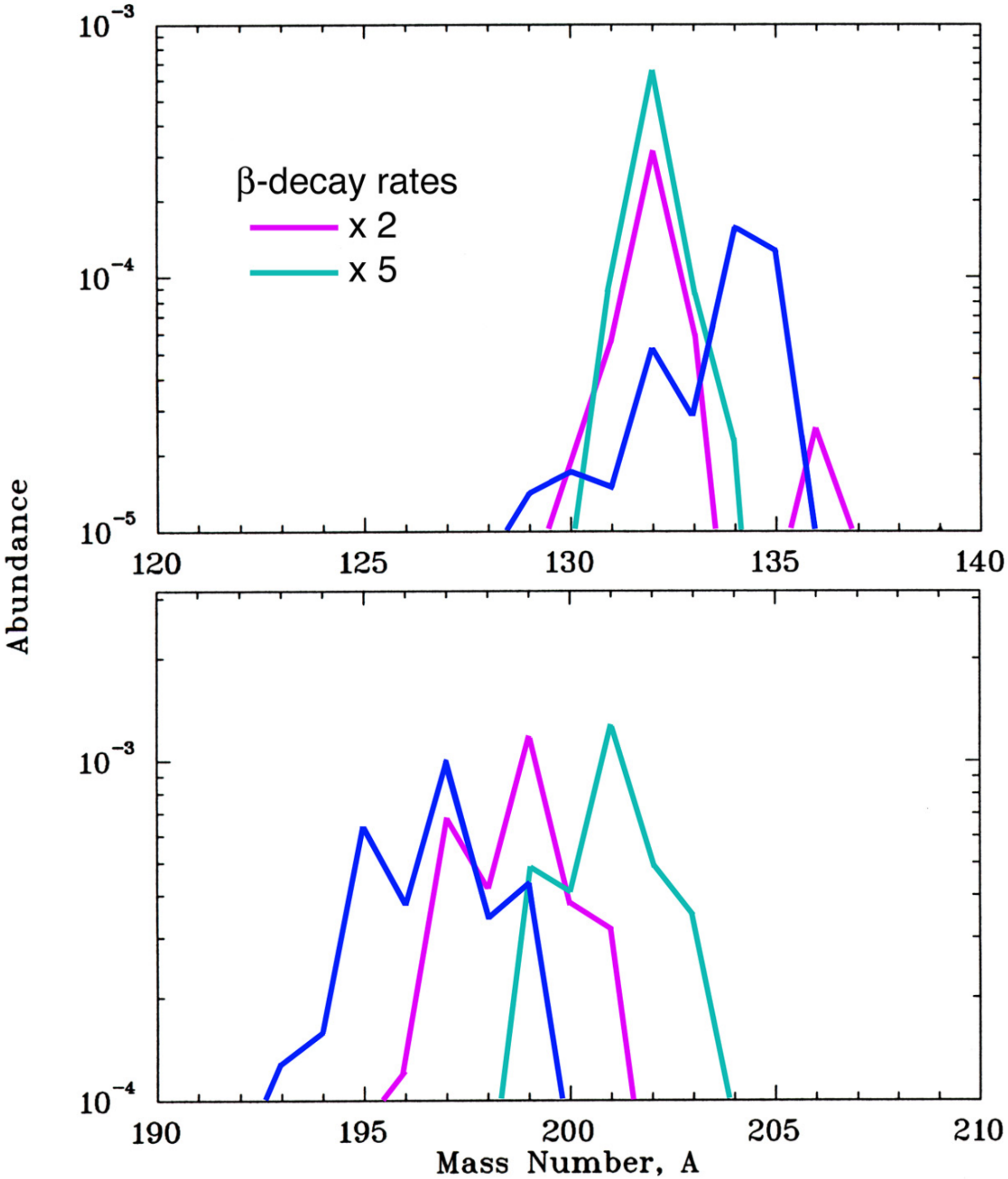

here material moves into N=82 region faster and abundances shift to lower Z

(later on)
β-decay removes neutrons so freezeout occurs at higher T (lower S_n)

B.S. Meyer and J.S. Brown, Ap. J. Supp. ***112****, 199 (1997)*

Effect of n-capture rates

neutron capture can influence the morphology of the abundance peaks, particularly if there are free neutrons at freezeout

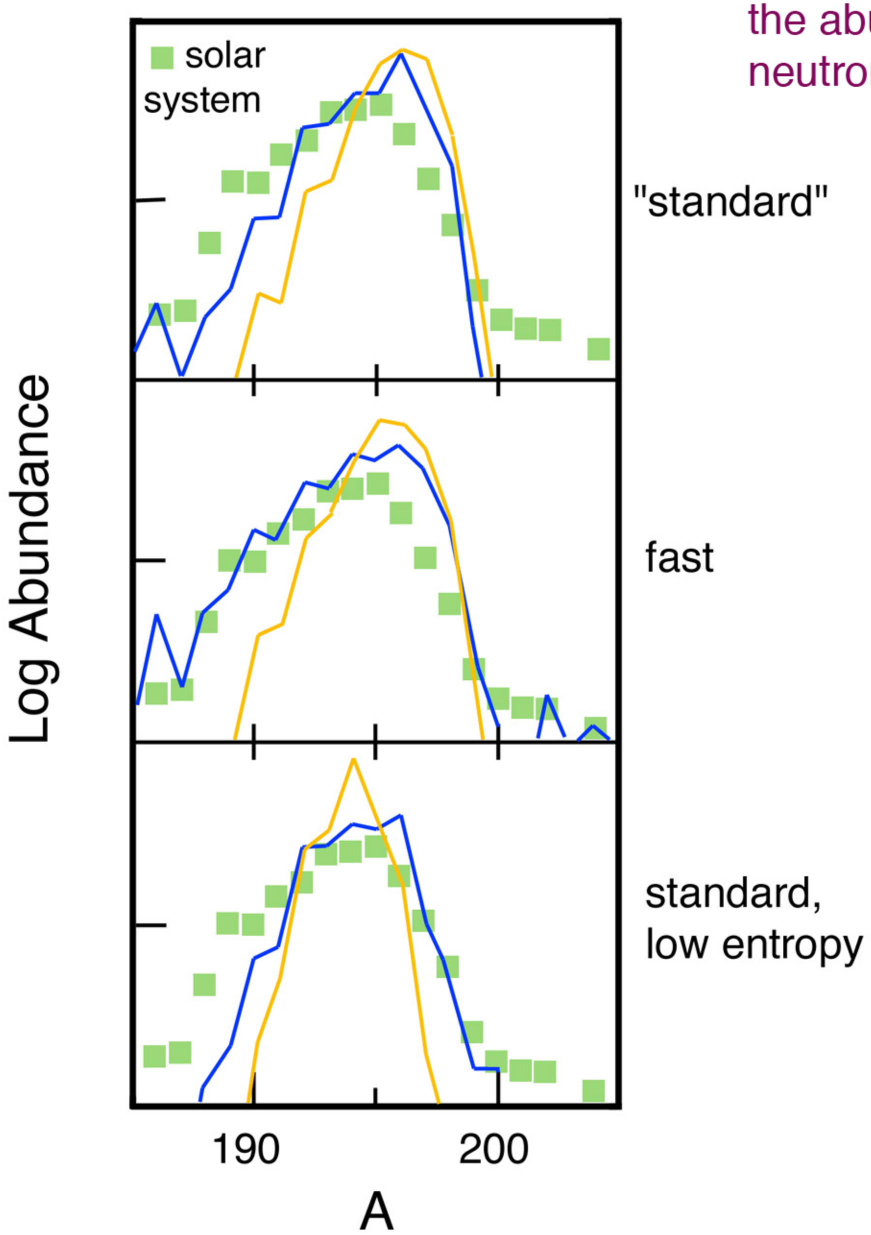

(note that this looks similar to what we saw for β-decay rates - it's very difficult to isolate a single "critical" effect!)

R. Surman and J. Engel, Phys. Rev. ***C64****, 035801 (2001)*

other effects, e.g. late-time (ν,n) reactions

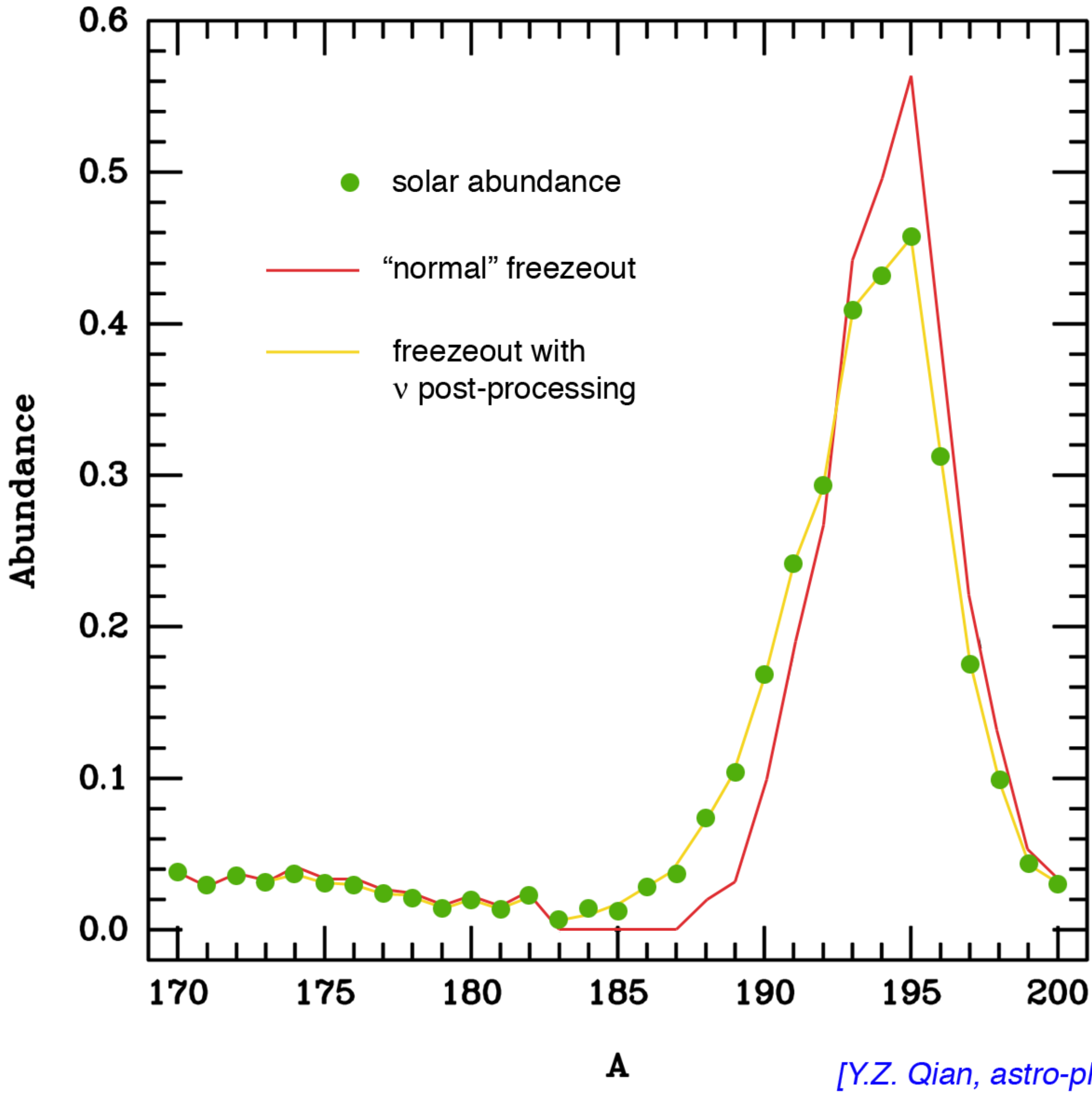

[Y.Z. Qian, astro-ph/0301422 v2 (2003)]

But...

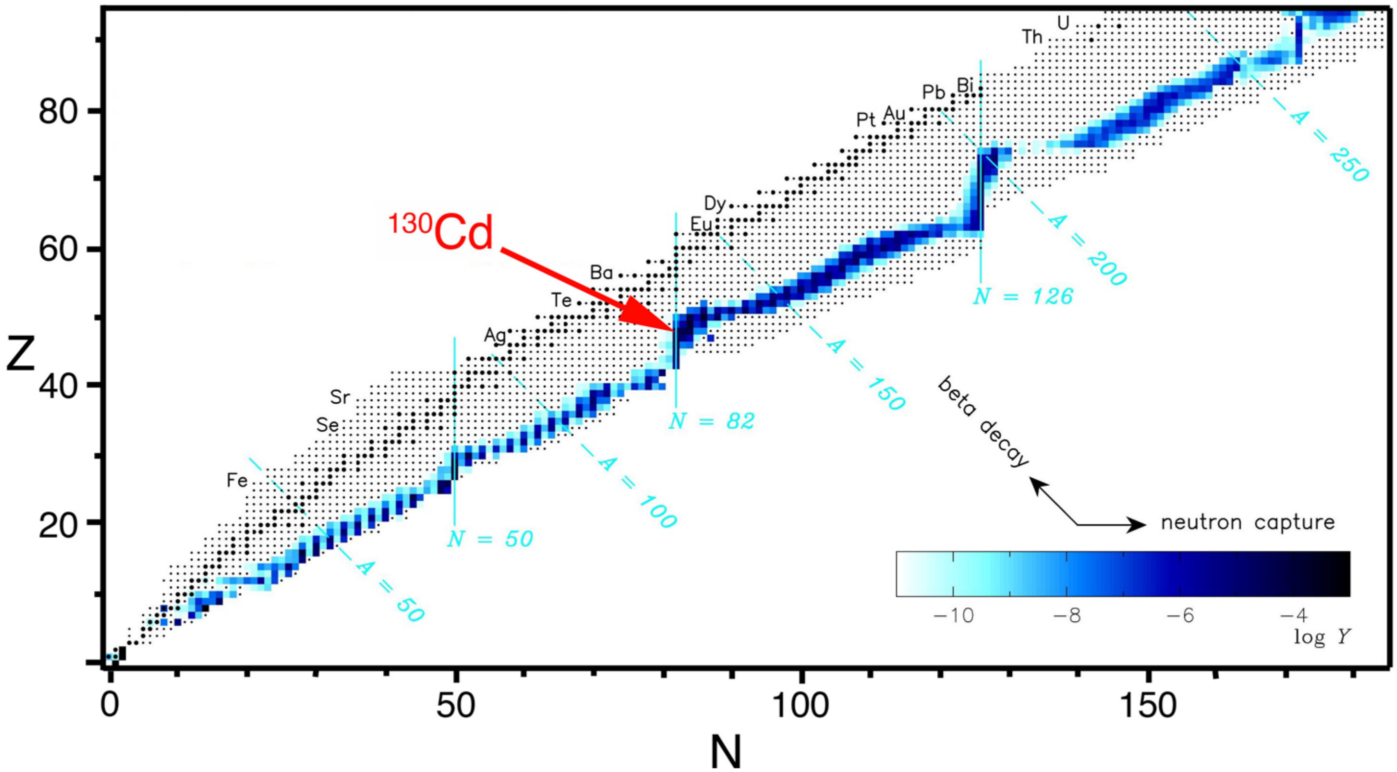

[I. Dillmann et al., Phys. Rev. Lett. **91**, 162503 (2003)]

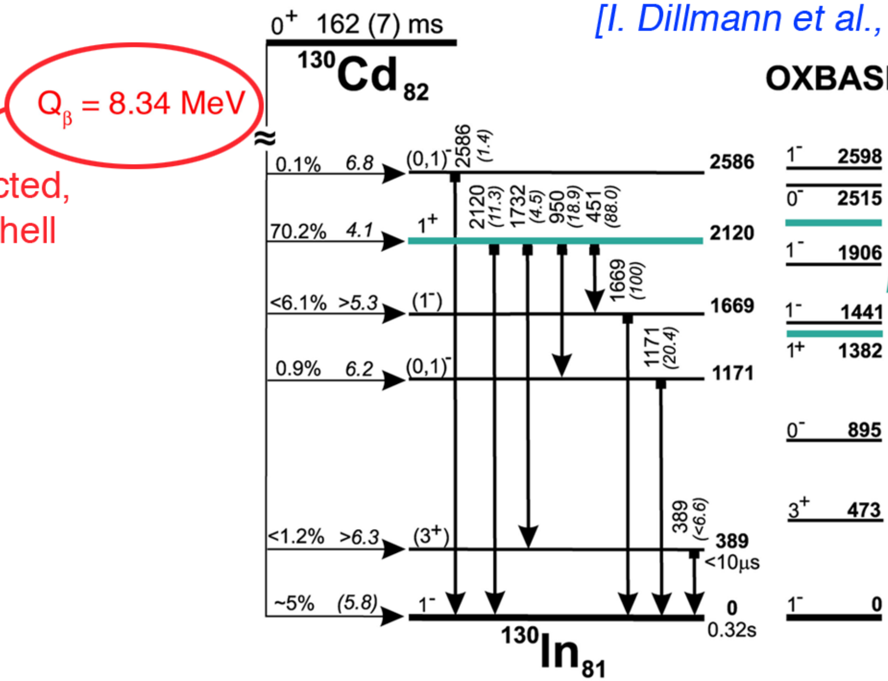

higher than expected, (consistent with shell quenching)

reduce two-body matrix element (B.A. Brown)

$\pi g_{9/2} \times \nu g_{7/2}$ GT resonance must reduce p-n $9_{9/2}g_{7/2} \leftrightarrow g_{9/2}h_{11/2}$ interaction

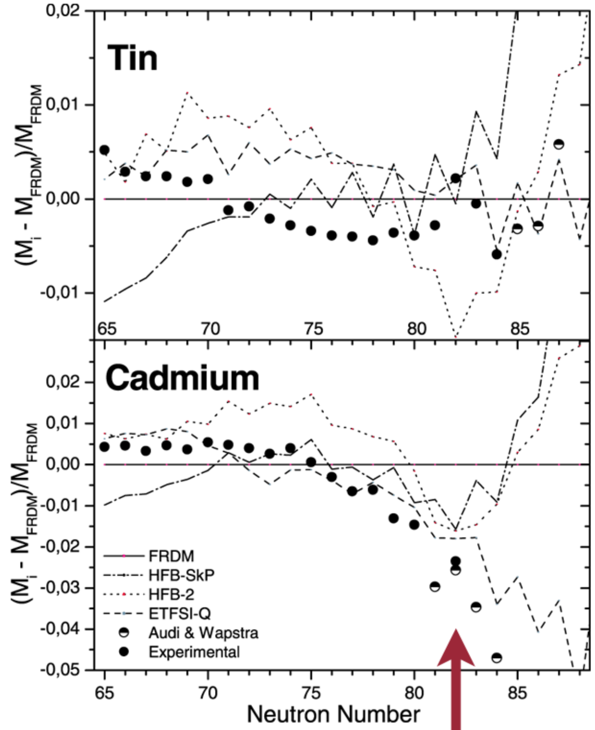

evidence for shell quenching

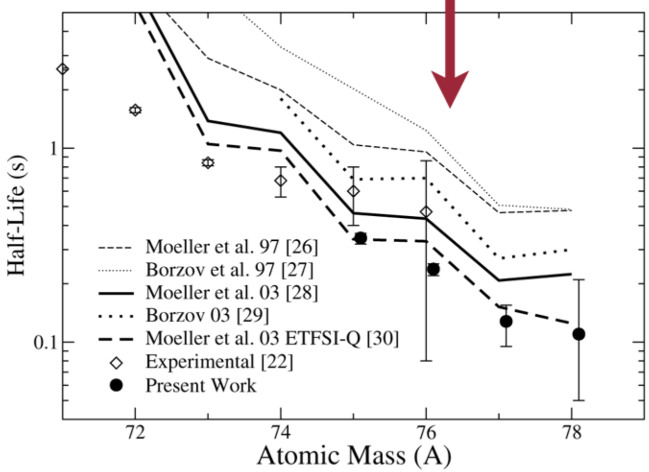

half-life of ^{78}Ni
[P.T. Hosmer et al.,
Phys. Rev. Lett ***94****, 112501 (2005)]*

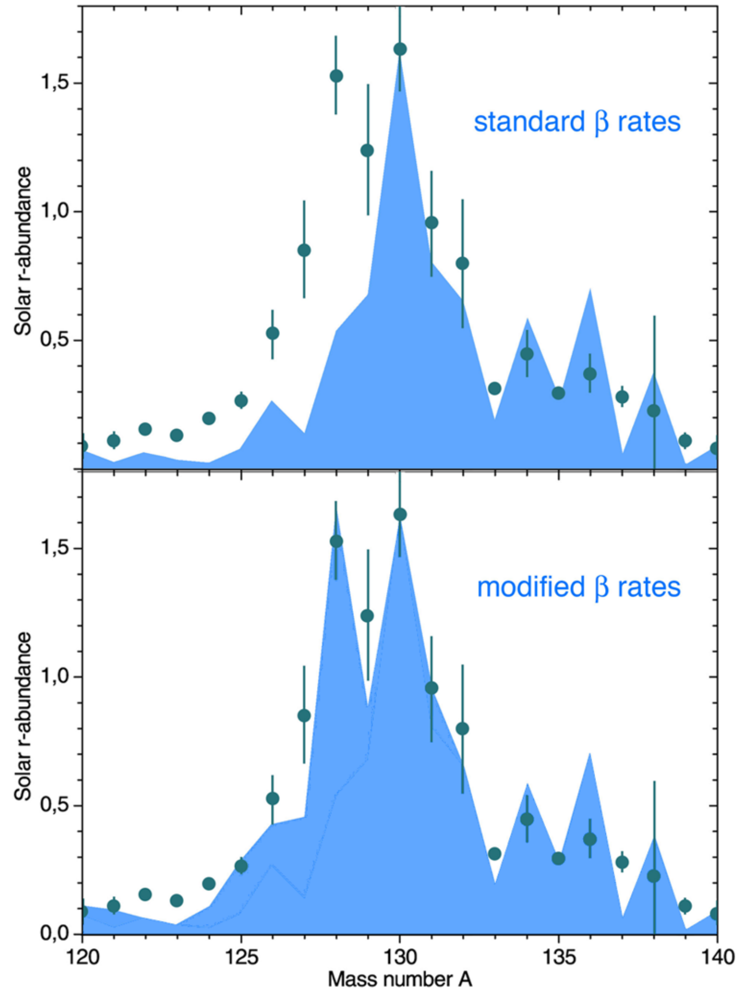

improved nuclear structure
no ν-interactions required

what is the site of the r-process?

In 1995, WalkerGroup/CNI developed an The Envirobranding(r) process for IKEA. The 7200-square-foot space transformed itself every six weeks - from IKEA Sleeps to IKEA Cooks to IKEA Plays, etc. - and all the signage, graphics, merchandise presentations, cabinets, audio, in-store promotions and printed media changed in tandem with product change-outs.

RECIRCULATING AIR HEATERS

Series R Process Air Heaters

- Meets FM, NFPA and IRI Standards
- Fuels Natural or Propane Gas
- Single Pass or Recirculating
- Standard Units Available with the following Specifications
- Static Pressures from –5" WC to 2" WC
- Maximum Outlet Temperatures to 1000°F
- Capacities of 500,000 thru 4,500,000 BTUH

Top: 2.5 MILLION BTUH RECIRCULATING SERIES R PROCESS AIR HEATERS FOR A 5 ZONE PRINTING PRESS.

Bottom: 800,000 BTUH SERIES R PROCESS AIR HEATER WITH CONTROL PANEL SUPPLIED FOR REMOTE MOUNTING.

What is the site of the r-process (where do we find lots of neutrons and high temperatures)?
First of all, is it correct to say ***the*** r-process?

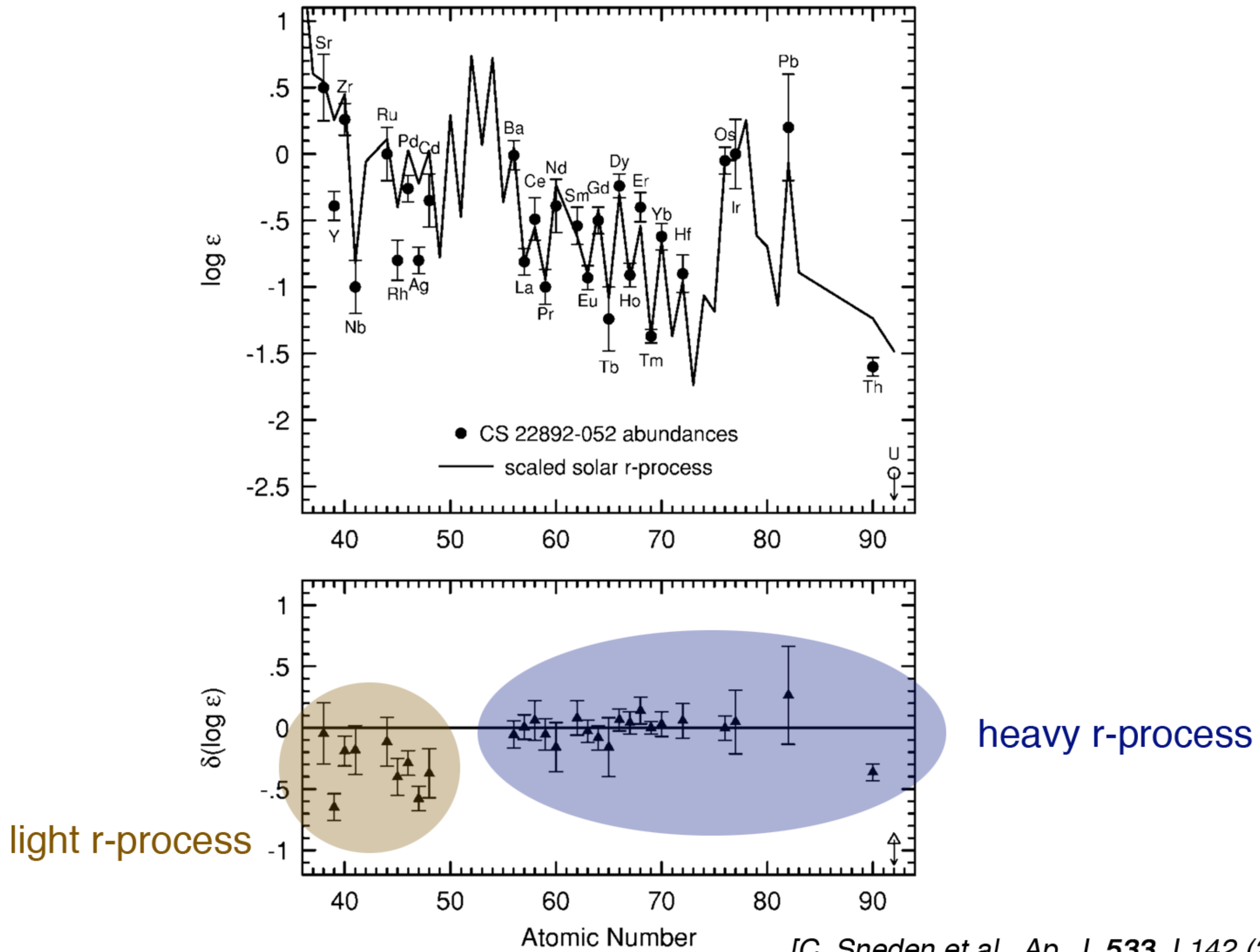

[C. Sneden et al., Ap. J. ***533****, L142 (2000)]*

there is also evidence in meteorite data

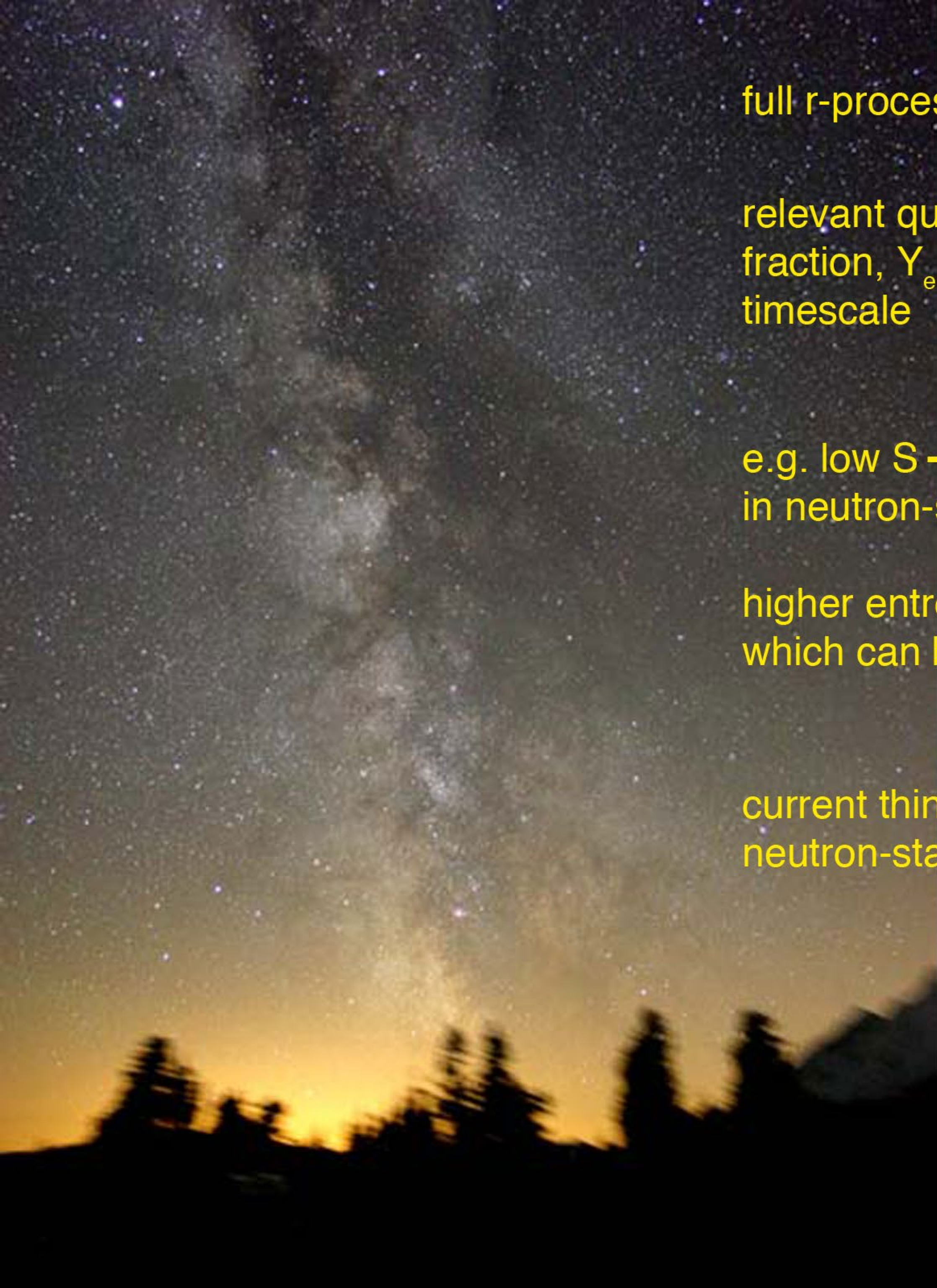

full r-process requires ~150 neutrons/seed

relevant quantities are entropy, S; electron fraction, Y_e (or proton/nucleon) and expansion timescale

e.g. low S $\longrightarrow$ low Y_e, which may be found in neutron-star material

higher entropies can have $Y_e \sim 0.4 - 0.5$, which can be characteristic of supernovae

current thinking: type II supernovae or neutron-star mergers (or both)

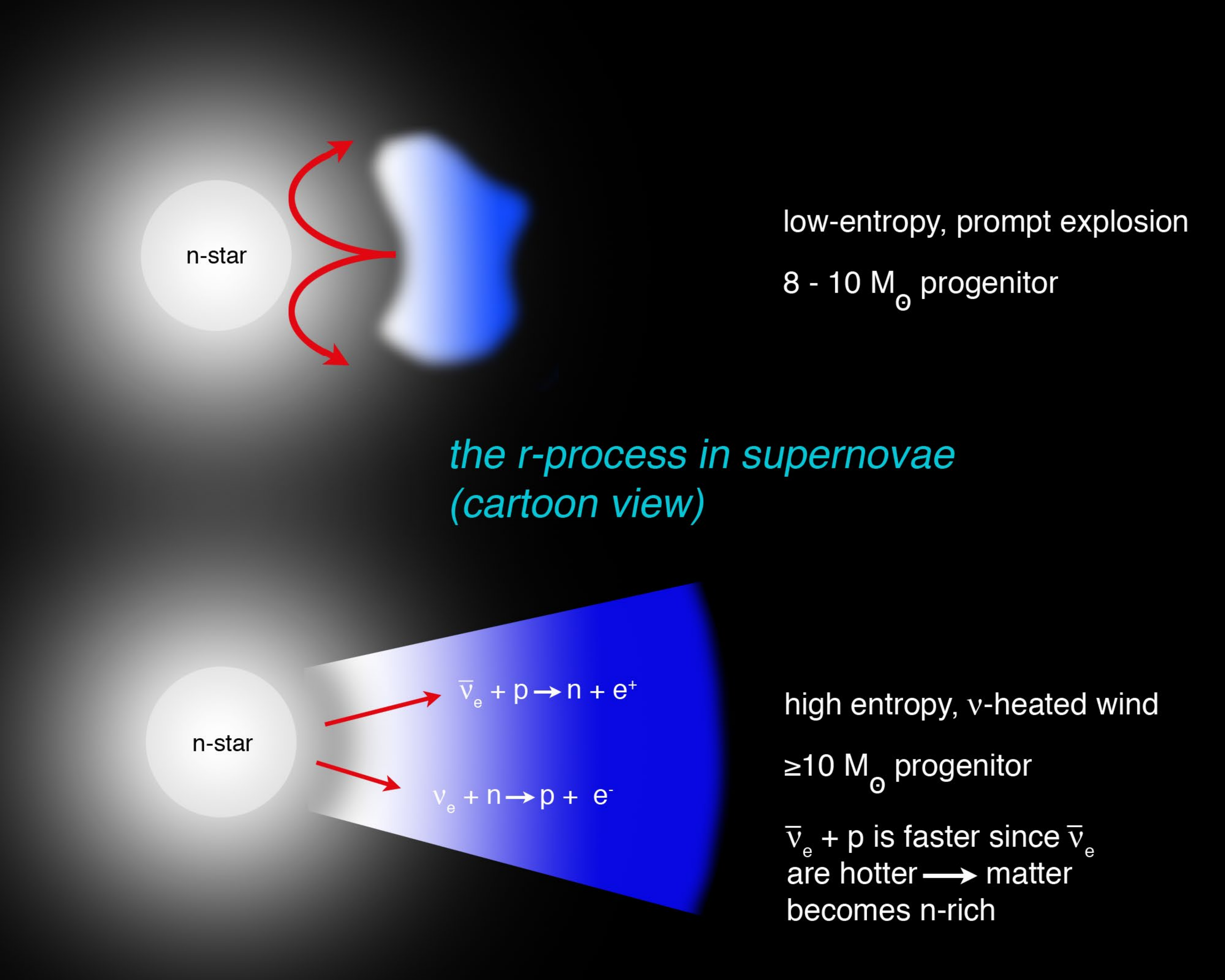
n-star
low-entropy, prompt explosion
8 - 10 $M_\odot$ progenitor
the r-process in supernovae (cartoon view)
n-star
$\bar{\nu}_e + p \rightarrow n + e^+$
$\nu_e + n \rightarrow p + e^-$
high entropy, ν-heated wind
$\geq$10 $M_\odot$ progenitor
$\bar{\nu}_e$ + p is faster since $\bar{\nu}_e$ are hotter $\longrightarrow$ matter becomes n-rich

neutron-star merger:

by Roland Oeschslin (Univ. of Basel, quasar.physik.unibas.ch/~oechslin/pict.html) *observational constraint:*

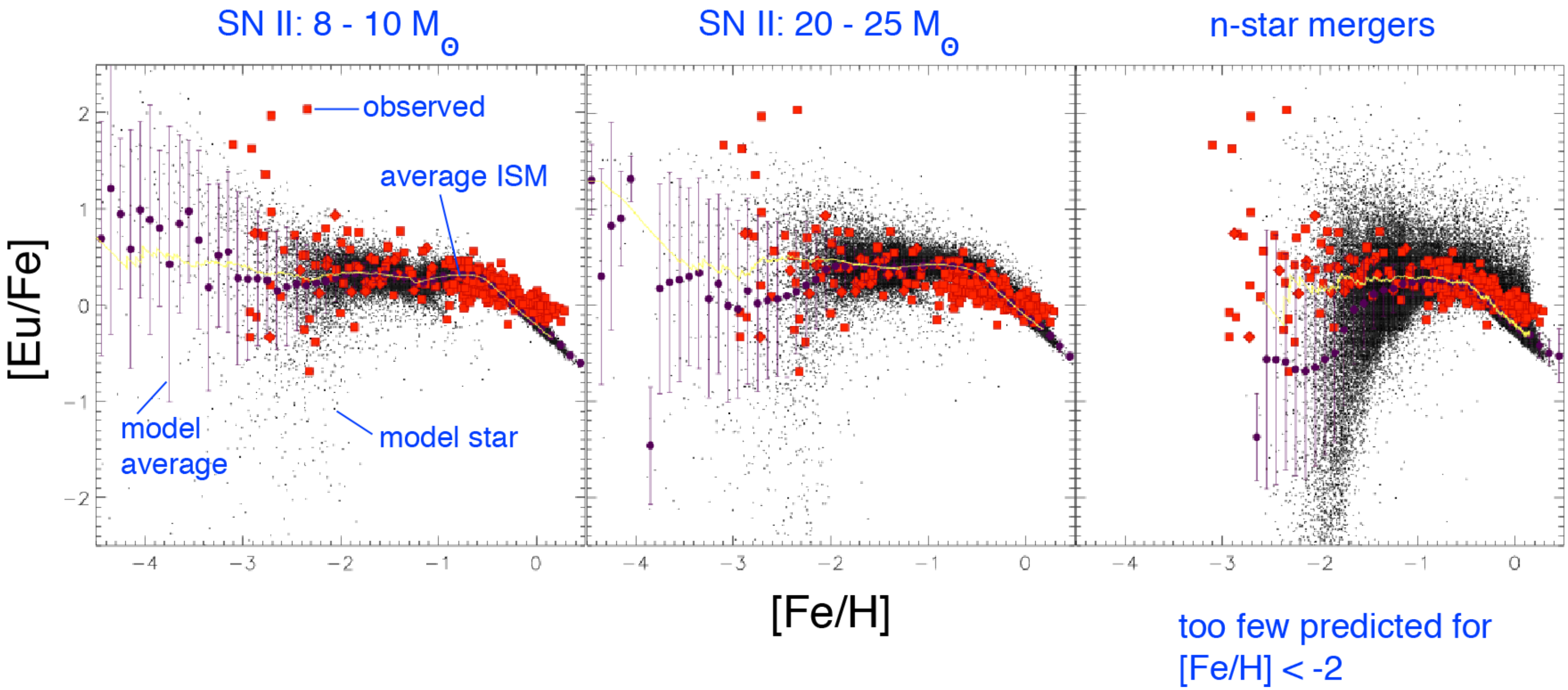

*chemical evolution calculation by D. Argast et al., Astron. Astrophys. **416**, 997 (2004)*

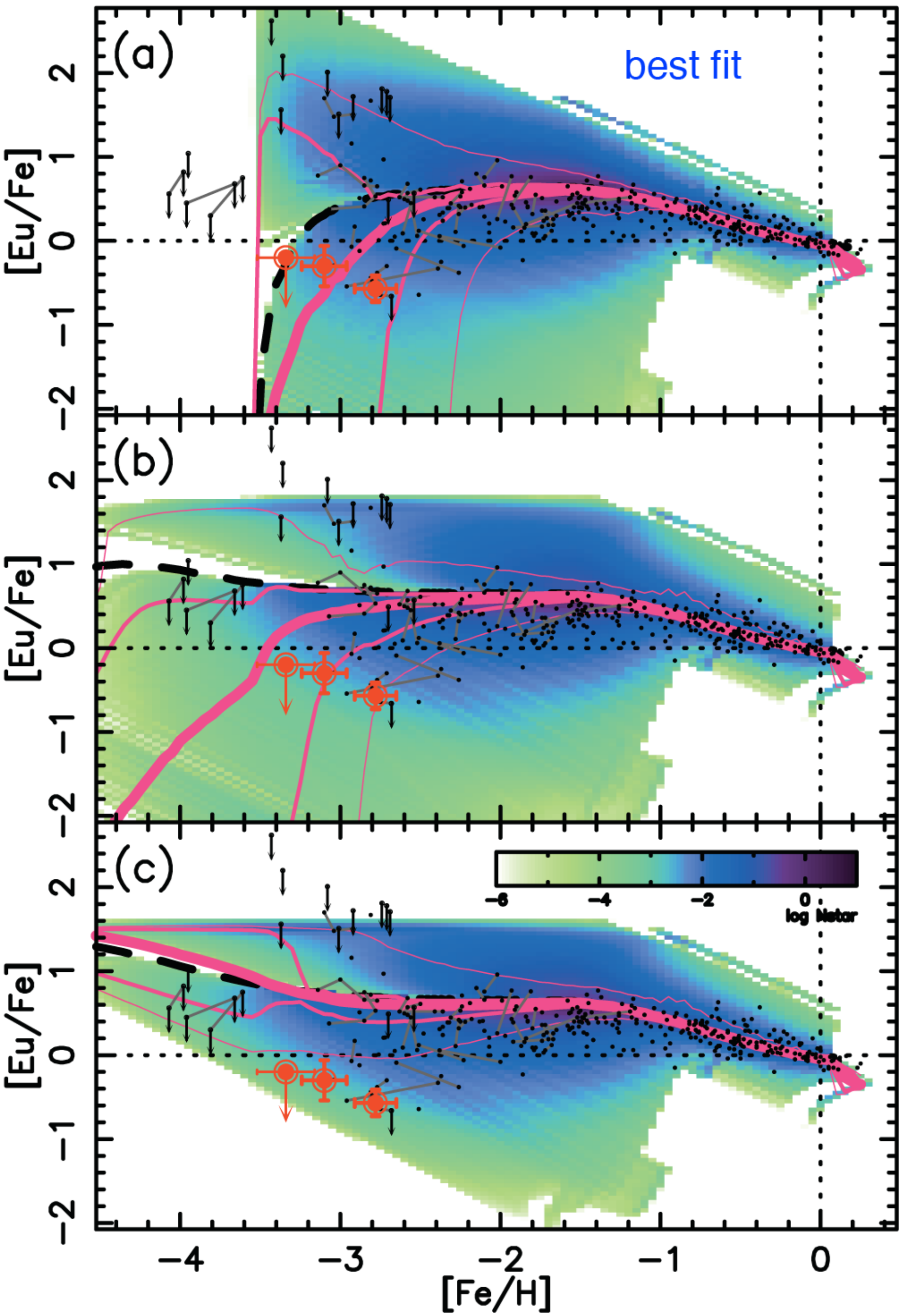

new observations by
Y. Ishimaru et al., Ap. J ***600****, L47 (2004)*

lower masses seem favored

FIG. 2.—Comparison of the observed data with the model predictions. The *r*-process site is assumed to be SNe of (*a*) 8–10 $M_\odot$, (*b*) 20–25 $M_\odot$, and (*c*) greater than 30 $M_\odot$ stars. The predicted number density of stars per unit area is color coded. The average stellar abundance distributions are indicated by heavy lines, with 50% and 90% confidence intervals (*medium and light lines, respectively*). The average abundances of the ISM are denoted by the heavy dashed lines. The current observational data are given by open circles, with others (*filled circles*) taken from Gratton & Sneden (1994), McWilliam et al. (1995), McWilliam (1998), Woolf, Tomkin, & Lambert (1995), Ryan et al. (1996), Shetrone (1996), Sneden et al. (1996), Westin et al. (1998), Burris et al. (2000), Fulbright (2000), Norris, Ryan, & Beers (2001), Johnson (2002), Johnson & Bolte (2002), François et al. (2003), and Honda et al. 2003).

the r-process in a ν-driven wind

*[T.A. Thompson et al., Ap. J. **562**, 887 (2001)]*

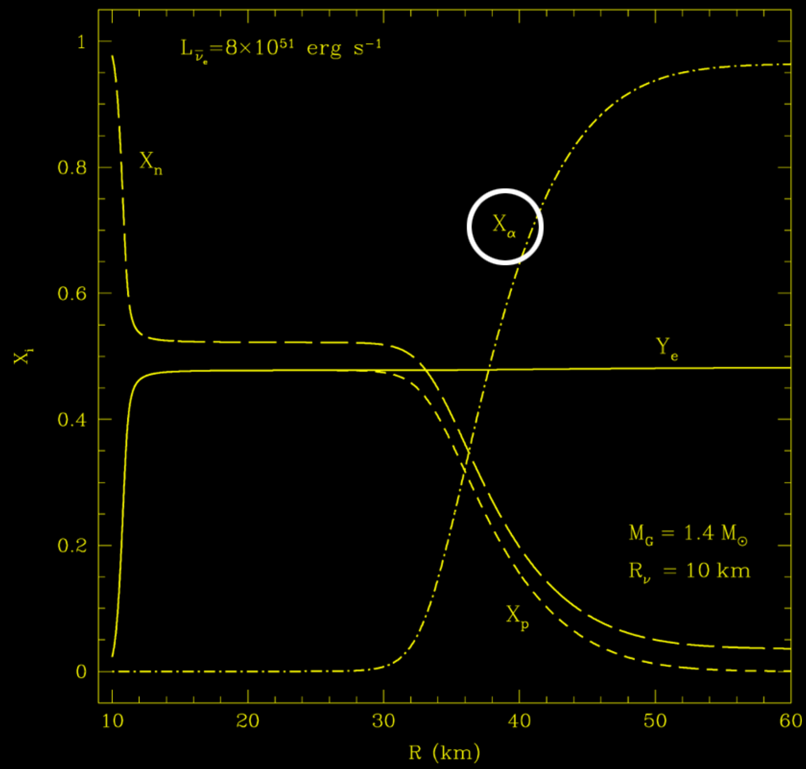

note production of α-particles (generally thought to be bad since the ν-opacity drops and thus n/seed drops)

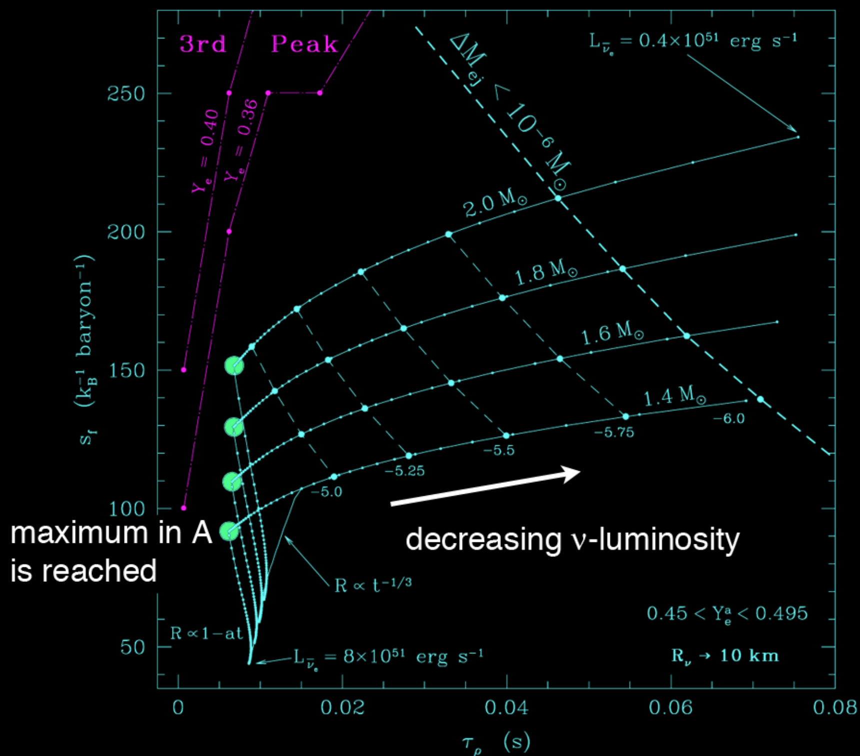

(e-folding time of density at T = 0.5 MeV)

in these calculations, r-process doesn't reach the A = 195 peak (doesn't get beyond A ~ 90 for 1.4 $M_\odot$ model)


Initiatives in
nuclear astrophysics

Experimental initiiatives: a next-generation RIB facility

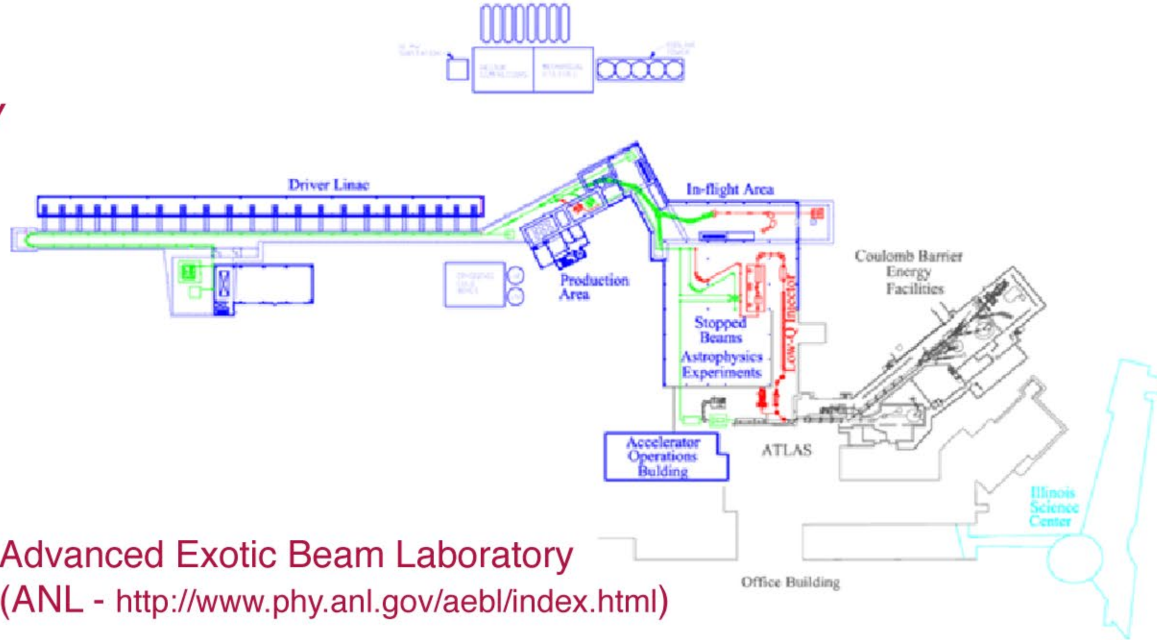

Advanced Exotic Beam Laboratory
(ANL - http://www.phy.anl.gov/aebl/index.html)

both designs feature a 200-MeV, 400 kW driver, stopped, re-accelerated and fast beams

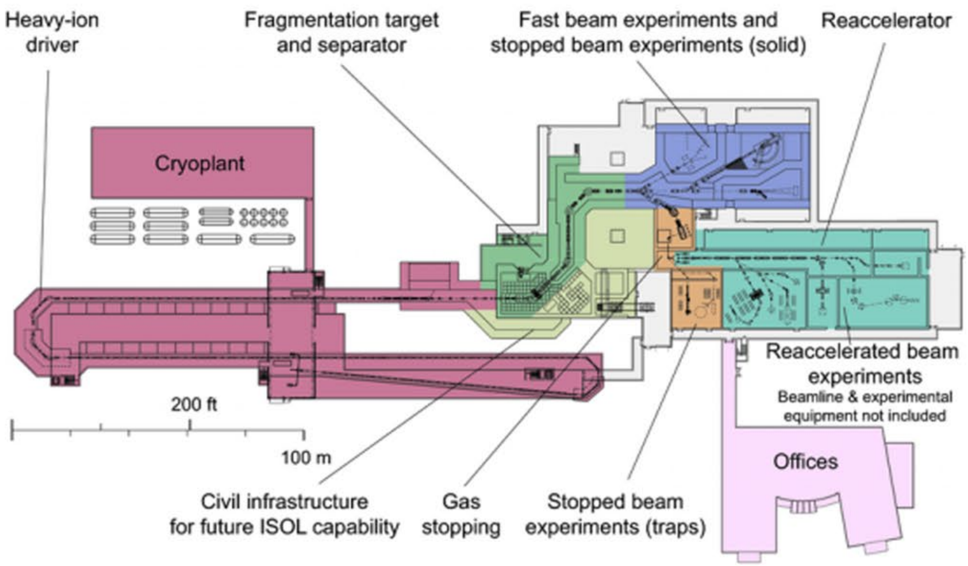

Isotope Science facility
(MSU - http://www.nscl.msu.edu/future/isf/)

projected beam intensities: ISF vs. original RIA

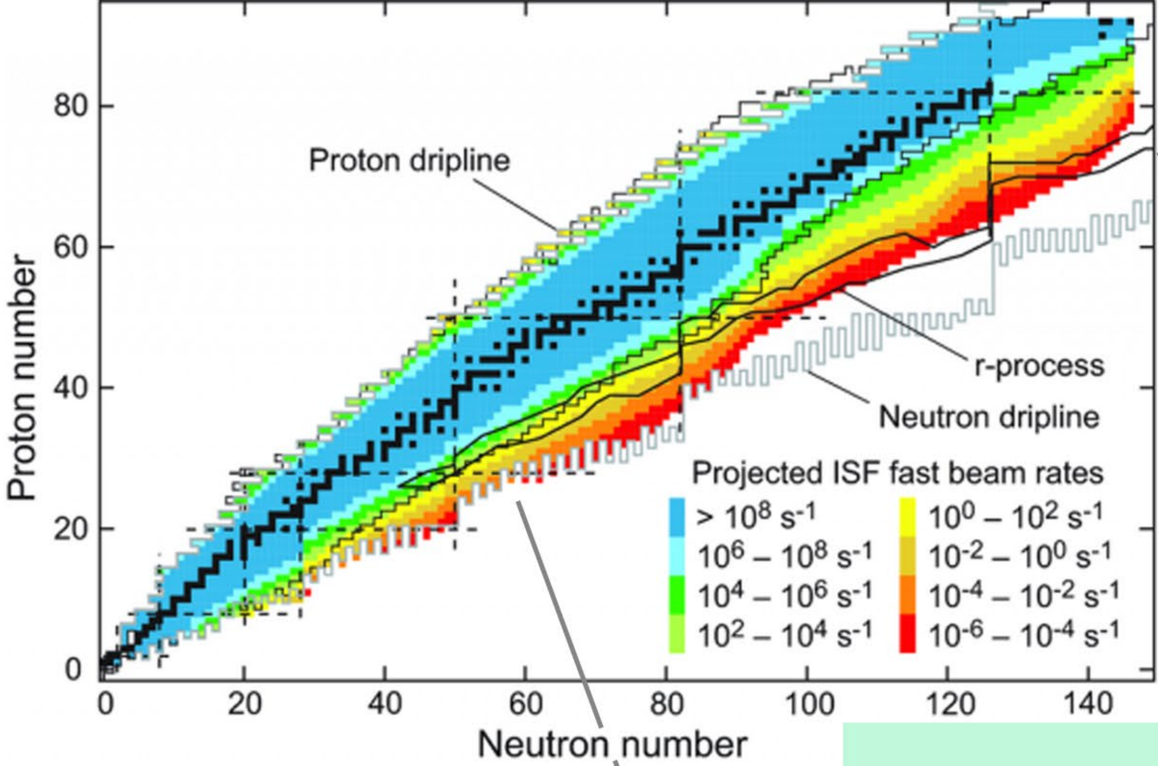

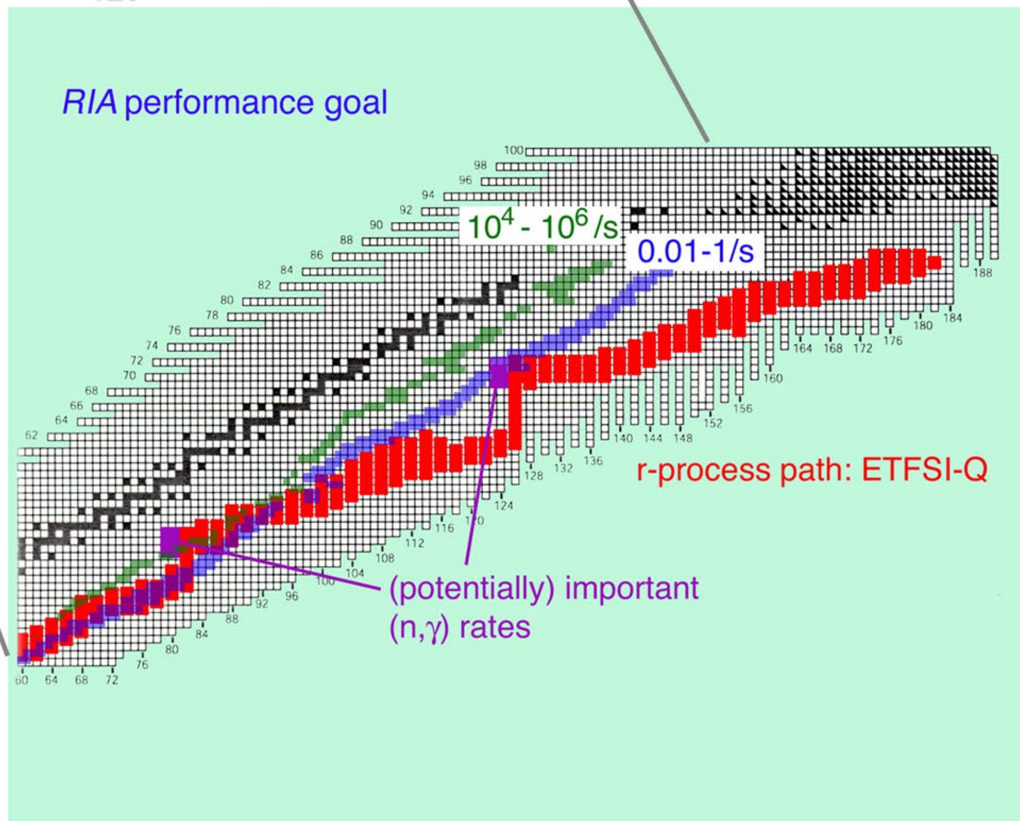

ALNA - Accelerator Laboratory for Nuclear Astrophysics Underground

(from DUSEL science meeting)

Two accelerator based experimental areas

- High current DC accelerator (CLAIRE)
  - A compact, high intensity low energy accelerator for forward kinematics reactions (complementary or expanding on LUNA activities)

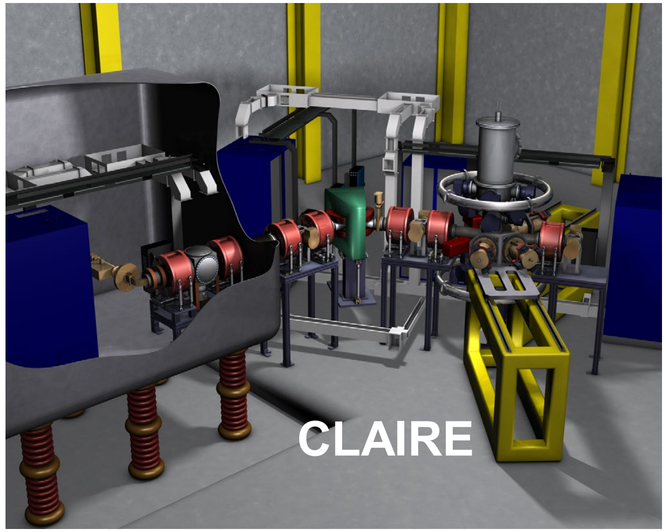

- A high intensity heavy ion accelerator
  - for inverse kinematic reaction and low energy fusion reactions
- Ion sources for both accelerators
  - high intensity 1+ ECR (up to 100mA)
  - Medium intensity n+ ECR (.5mA)

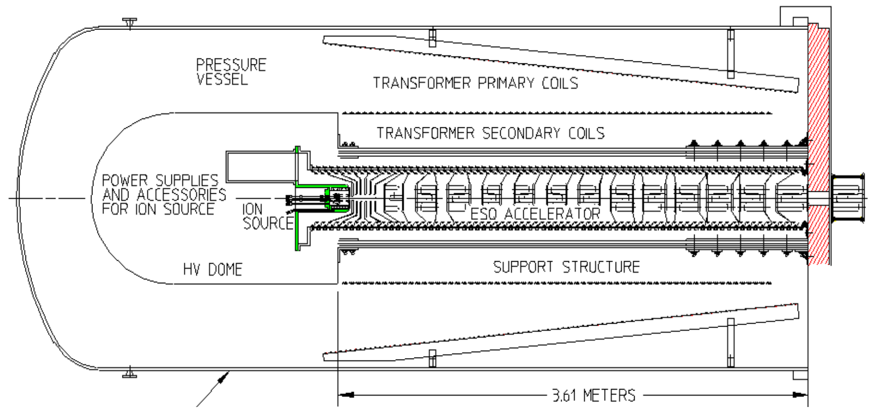

ESQ Dynamitron

- The energy range of both accelerators combined should ideally cover beam energies from as low as 50keV up to 1 MeV/u
- The two accelerators should have an overlap in energy range for comparison between experiments over a common energy.

Large-scale simulations
e.g. Jaguar @ ORNL:
31,000 cores,
263 teraflops

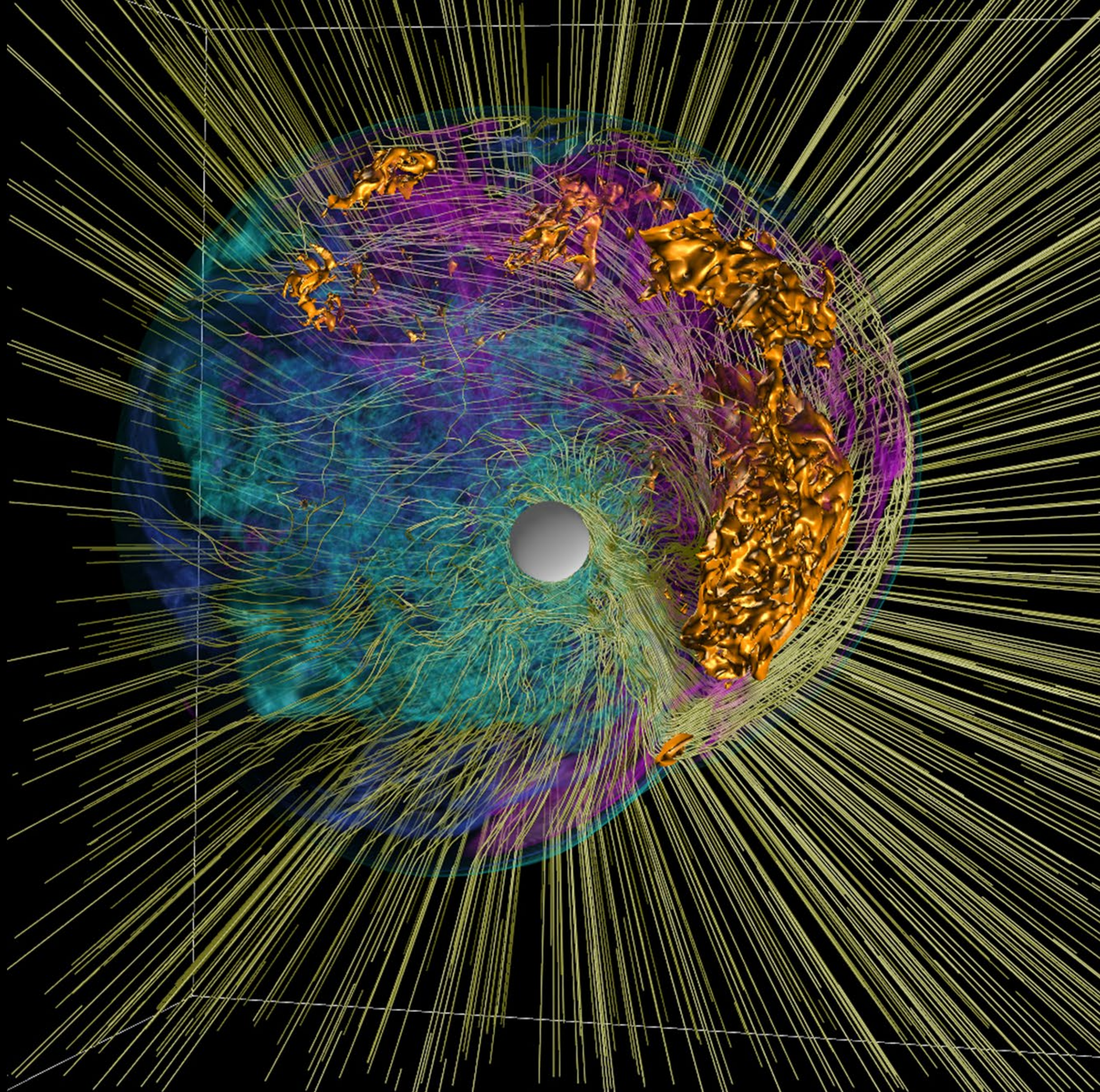

The stream lines in this image show the two counter rotating flows that may be established below the supernova shock wave (the surface in the image) by the instability of the shock in a core collapse supernova explosion. The innermost flow accretes onto the central object, known as theproto-neutron star, spinning it up. This may be the mechanism whereby pulsars (spinning neutron stars) are born. [Blondin and Mezzacappa, Nature 445, 58 (2007)]

It’s a big universe -
what did I leave out?

1. neutrinos in astrophysics and cosmology
2. other links between nucleosynthesis and stellar/galactic evolution
3. novae and x-ray bursts
4. other things that I’ve forgotten about ... start reading!